UNIVERSIDADE DE LISBOA

INSTITUTO SUPERIOR TÉCNICO

Concentrating Solar Power + Desalination Plants (CSP+D): Models and Performance Analysis

Sérgio Miguel Alegria Casimiro

Supervisor: Doctor Paulo Manuel Cadete Ferrão
Co-Supervisor: Doctor Christos Ioakeimidis

Thesis approved in public session to obtain the PhD Degree in Sustainable Energy Systems

Jury final classification: Pass with Merit

Chairperson: Chairman of the IST Scientific Board
Members of the Committee:
Doctor Christos Ioakeimidis
Doctor Paulo Manuel Cadete Ferrão
Doctor Carlos Augusto Santos Silva
Engineer João Augusto Farinha Mendes
Doctor Luís Filipe Moreira Mendes
Doctor Andrea Cipollina

2015

UNIVERSIDADE DE LISBOA

INSTITUTO SUPERIOR TÉCNICO

Concentrating Solar Power + Desalination Plants (CSP+D): Models and Performance Analysis

Sérgio Miguel Alegria Casimiro

Supervisor: Doctor Paulo Manuel Cadete Ferrão
Co-Supervisor: Doctor Christos Ioakeimidis

Thesis approved in public session to obtain the PhD Degree in Sustainable Energy Systems

Jury final classification: Pass with Merit

Chairperson: Chairman of the IST Scientific Board
Members of the Committee:

Doctor Christos Ioakeimidis, Professor, Faculté Polytechnique, Université de Mons, Belgique
Doctor Paulo Manuel Cadete Ferrão, Full Professor of Instituto Superior Técnico, Universidade de Lisboa
Doctor Carlos Augusto Santos Silva, Invited Assistant Professor at Instituto Superior Técnico, Universidade de Lisboa
Engineer João Augusto Farinha Mendes, Principal Researcher, Laboratório Nacional de Energia e Geologia, I.P.
Doctor Luís Filipe Moreira Mendes, Assistant Professor at Instituto Superior Técnico, Universidade de Lisboa
Doctor Andrea Cipollina, Researcher, Università degli Studi di Palermo, Italia

2015

Resumo

Em 2013 a capacidade mundial para produção de água potável através de processos industriais de dessalinização era aproximadamente de 81 milhões de metros cúbicos por dia. Além disso, 9 dos 10 países com maior capacidade instalada para produzir água por dessalinização situam-se em regiões com altos níveis de irradiação solar.

A combinação de centrais Solares Termoeléctricas de Concentração (CSP) e unidades de produção de água potável, poderá ser uma alternativa viável com vista a minimizar a poluição gerada com a cogeração de água e de electricidade.

O trabalho apresentado descreve o desenvolvimento de modelos para a análise termodinâmica deste tipo de centrais em cogeração (em fase de pré-dimensionamento). Foi desenvolvido um novo modelo que descreve o processo de Destilação por Multi-Efeito (MED), tendo sido validado com dados de uma central comercial. Este modelo foi integrado num modelo existente capaz de simular a operação de centrais de CSP. A simulação de centrais de CSP em cogeração com centrais de Osmose Inversa (RO) também foi analisada.

A região de Trapani, na Sicília foi utilizada como caso de estudo. Os resultados da utilização destas novas ferramentas apontam para um potencial bom desempenho térmico de centrais de dessalinização em cogeração com centrais de CSP.

Palavras-chave: Modelo; Dessalinização; CSP; Centrais Solares Termoeléctricas de Concentração; MED; Osmose Inversa; SAM; TRNSYS; ROSA; Simulação; Análise de Exequibilidade.

Abstract

In 2013 the global capacity for water desalination was approximately 81 million cubic meters per day and growing. Moreover, 9 of the top 10 countries in seawater desalination capacity reside in regions of very high solar insolation (most in the Mediterranean Sea or the Middle East).

The combination of Concentrating Solar Power (CSP) and available commercial desalination technologies is one way to offset many of the negative impacts of running desalination plants.

The work presented in this thesis shows the development of new models for the thermodynamic analysis of such systems in cogeneration, suitable for feasibility studies. In particular a new Multi-Effect-Distillation (MED) model was developed and validated against data from a commercial plant. This model was integrated into software capable of simulating the operation of CSP plants. The simulation of CSP plants in cogeneration with Reverse Osmosis (RO) units was also analyzed.

The city of Trapani, Sicily was used as a case study. Detailed data from a commercial MED plant operating in this city, using a thermal vapor compressor (TVC) was used for data comparison and development of the models. The results of these new tools show that desalination units powered by CSP plants can potentially present good performances.

Keywords: Model; Desalination; CSP; Concentrating Solar Thermal; MED; RO; SAM; TRNSYS; Simulation; Feasibility Analysis.

Acknowledgments

This adventure would have not been possible without the support of my parents, to whom I'm deeply grateful for always having been there for me and helping me to the best of their abilities. The same goes for the rest of my family.

I would also like to thank my buddy João Gomes, Gauri Das and Chara Tsoukala for the help they gave me as I went along the PhD journey, for being good listeners, for their comments and for cheering me up when I needed it.

Special thanks goes to my friend João P. Cardoso, who I met at LNEG, and who was a source of inspiration. For always giving me relevant inputs on the many technical and practical issues that arose while doing the thesis. He always found the time to help me and I learned a lot with him.

I am thankful to LNEG as a whole, where I did a large share of my PhD. In particular I am very thankful to Eng. João Farinha Mendes, who accepted me at this institution, and always helped me with a positive attitude during the challenges that had to be overcome. Many other people at LNEG helped me when I needed them: Ricardo Encarnação Coelho, Luís Guerreiro, Margarida Giestas, David Loureiro, Rui Rodrigues, Lúcia Santos, just to name a few.

A significant part of my PhD was also spent at NREL in Golden, Colorado, with the Thermal Systems Group. In fact my PhD is very much based on a software developed by NREL, and this would have not been possible without the help of Dr. Craig Turchi from NREL and Dr. Tzahi Cath from the Colorado School of Mines (CSM). They were always very supportive of my work at NREL and helped me whenever I needed them. Terri Spinuzzi had the patience of a saint, as she guided me through all the necessary bureaucracies, and the arrangements for my stay there. She was the best. Chuck and Guangdong always had a nice word to say, and Mike and Tyler always found time to help me out with code issues. Living in Golden was a true life experience, and my stay there would have not been the same without the good friends I made there: Anna Trendewicz, Carolin Ulbrich, Sarah Coonon, Ash McCullough, Stefan Oosterhout, Ben Lee, Lorenz Haid, and Marco Binnoti.

In Sicily I made two friends that were paramount in the development of the models I am presenting in this thesis: Andrea Cipollina from UNIPA and Carmelo Mineo from Sicilacque S.p.A. Without professor Andrea and Eng. Mineo I would probably have not been able to visit an operational large scale commercial MED plant. Their help enabled me to really understand the functioning of this type of plants. Looking back I am amazed how Eng. Mineo, the plant manager, found the time to show me the plant and explain to me the details of its operation within three full days (!), and for that I am deeply thankful. It was a great experience to have been so well received in Sicily.

I also had to contact steam ejector manufacturers to accomplish part of the work in my thesis, and I'm thankful for the help given by Eng. Heinrich-Arend Kroemer from Koerting Hannover A.G., who helped me understand how these were dimensioned for the purposes I needed, providing me the necessary information. A large part of my thesis would have not been possible to make without his time and inputs.

I also made other technical visits to desalination and power plants while doing this thesis, which were very important to accomplish the work, and for that I'm thankful to Eng. Pedro Roque from the EDP Ribatejo CCGT power plant. The same goes to the researchers at PSA, Spain, who were very helpful during my visit to their installations with the EU SFERA program (Diego-César Alarcón-Padilla and Patricia Palenzuela in particular).

During the last part of my PhD the help of Filipe Marques from IST was very important to accomplish the task of obtaining new performance curves for the Rankine cycle using genetic algorithms. Filipe was very supportive, and even though he was near the end of his own PhD studies, he still managed to find the time to help me and I am very thankful for that.

My supervisors, professors Christos Ioakimidis and Paulo Ferrão from IST / MIT Portugal Program were very important to accomplish the work I am presenting, with their helpful comments and guidance, as well as professors Steve Connors and David Marks from MIT.

I could not pass without mentioning the persons I met while in Boston, that made part of the "MIT experience", and without whom life during that year would have not been as interesting as it was: Nuno Clímaco, Ana Gonçalves, Ana Laura, João Pita, Alda Metrass, Joana Abreu, Ivo Caixeiro, Gustavo Haydt, Hanna Gerbelová, Dan Livinghood, Way Ling, Daniel Wiesmann, Pedro Fazenda, Vasco Granadeiro and Jan Kokol.

During the very last part of this work I had the invaluable help of Hebah Bukhari that kindly and patiently reviewed various parts of my thesis for grammar, typos and all kind of formatting issues.

Finally, this work would have not been possible without the financial support of the following institutions to which I am very thankful: the Portuguese National Science Foundation (FCT) through the financial support of the MIT Portugal Program (the program through which I worked on my PhD) and scholarship funding SFRH/BD/44969/2008; the Luso-American Foundation (FLAD) through the FLAD Seed Fund for Portugal/NREL Networking Advancement; NREL; and the EU seventh framework program through both the Scientific and Technological Alliance for Guaranteeing the European Excellence in Concentrating Solar Thermal Energy (STAGE-STE) project with contract number 609 837 and the Solar Facilities for the European Research Area (SFERA) project.

Acronyms

Abbreviations

BPE	Boiling Point Elevation
CCGT	Combined Cycle Gas Turbine
CIEMAT	Spanish Research Center for Energy, Environment and Technology
CPC	Compound Parabolic Concentrator
CSIRO	Australian Commonwealth Scientific and Research Organization
CSP	Concentrating Solar Power
DAE	Dry Air Equivalent
DEAHP	Double Effect Absorption Heat Pump
DEEP	Desalination Economic Evaluation Program
DLR	German Aerospace Center
DNI	Direct Normal Radiation
EDP	Energias de Portugal
EES	Engineering Equation Solver
EU	European Commission
FF	Forward Feed
FLAD	Fundação Luso-Americana para o Desenvolvimento
GHG	Greenhouse Gases
GOR	Gained Output Ratio
GUI	Graphical User Interface
HEI	Heat Exchange Institute
HFF	Hollow Fine Fiber
HT	High Temperature
HTX	Heat Exchanger
IAEA	International Atomic Energy Agency
IEA	International Energy Agency
IGCC	Integrated Gasification Combined Cycle
IST	Instituto Superior Técnico
LNEG	Laboratório Nacional de Energia e Geologia, I.P.
LT	Low Temperature
MED	Multi-Effect Distillation
MENA	Middle East and North Africa
MSF	Multi Stage Flash
MVC	Mechanical Vapor Compression
NCG	Non-Condensable Gases
NEA	Non Equilibrium Allowance

NPSHr	Net Positive Suction Head required
NREL	National Renewable Energy Laboratory
P	Parallel Feed
PR	Performance Ratio
PSA	Plataforma Solar de Almeria
PV	Photovoltaic
RO	Reverse Osmosis
ROSA	Reverse Osmosis System Analysis
SAM	System Advisor Model
SDS	Solar Desalination System
STAGE-STE	Scientific and Technological Alliance for Guaranteeing the European Excellence in Concentrating Solar Thermal Energy
SW	Spiral Wound
SWCC	Once-Through Seawater Condenser
TDP	Thermal Desalination Processes
TorayDS2	Toray Design System
TRNSYS	TRaNsient SYstem Simulation
TVC	Thermal Vapor Compressors
Winflows	Membrane System Design Software
WRA	The Desalination Feasibility Cost Planning Model

Variable naming conventions

A	Area	m^2
B	Brine mass flow rate	kg/s
C_p	Specific heat at constant pressure	J/(kg.ºC)
D	Distillate mass flow	kg/s
Eta_ND	Normalized cycle efficiency	-
g	Gravity	m/s^2
h'	Specific enthalpy (liquid phase)	kJ/kg
h''	Specific enthalpy (vapor phase)	kJ/kg
Head	Total head	m
M	Mass flow	kg/s
M_dot_j_ND	Normalized mass flow from extraction “j”	-
M_dot_k_ND	Normalized mass flow from extraction “k”	-
moles	Number of moles	mol
MM	Molecular weight	kg/kmol
MTD	Mean temperature difference	ºC
n	Number of effects in a MED system	-

P	Pressure	Pa
P_cond	Condenser pressure	Pa
Q	Thermal load	kW
Q_ND	Normalized heat input to the cycle	-
Qual_s	Quality of steam outlet from low-pressure turbine	%
T	Temperature	ºC
Ts_out	Temperature of steam outlet from low-pressure turbine	ºC
u	Velocity	m/s
U	Overall heat transfer coefficient	W/(m^2.ºC)
UA	Thermal conductance	W/ºC
V	Mass flow of vapor	kg/s
W	Entrainment	-
z	Elevation	m
Δ	Difference	-
ρ	Density	kg/m^3
γ	Molar Fraction	-
χ	Steam quality	%

Variable subscript convention

b	Brine
BPE	Boiling Point Elevation
c	Compressed
cf	Correction factor
cw	Cooling water
d	Distillate
DAE	Dry air equivalent
ds / desuper	Desuperheater
e	Entrained
Ej_2	Steam ejector number two
flash	Flashing process
H_2O	Water
htx	Heat transfer
loss	Temperature loss
m	Motive steam
NCG	Non-condensable gases
out	Output

r	Ratio
remain	Remaining
s	Steam
sat	Saturated
sub	Subcooled
super	Superheated
super_ratio	Steam superheating ratio
T	Total
TVC	Thermal vapor compressor
v	Vapor

Annex 8 also contains a detailed list with the variable names, corresponding units and description that are part of the new computer code developed in this work.

Index

List of Figures

List of Tables

1. Introduction

1.1 Motivation

Water scarcity has been a problem for many regions around the world, causing various economic, social, and environmental impacts. Technological developments, the need for clean water, and the growing concerns about water supply availability in different areas of the world, amongst other economic, political and social issues have justified investments in different types of desalination technologies powered by different energy sources. Desalination processes require intensive energy consumption, making energy security and market fluctuations in fuel prices important issues to be considered when deciding whether or not to install a specific type of desalination system in any given place.

Fresh water is increasingly becoming an asset facing valorization in many parts of the world. In fact figures from 2014 show that 748 million people worldwide are reliant on unimproved drinking water sources [1].

In 2013 the global capacity of water desalination was approximately 85 million cubic meters per day and growing [2]. Moreover, 9 of the top 10 countries in seawater desalination capacity (by total installed capacity since 1945) reside in regions of very high solar insolation, with many being on the Mediterranean Sea or in the Middle East [3]. The need for potable water mainly in arid, sunny regions of the world has led to the development of large thermal and membrane desalination plants. Multi-Effect Distillation (MED), Multi Stage Flash (MSF), and Reverse Osmosis (RO) are the technologies that dominate what is today a mature and conservative desalination market [2], that is forecasted to become a $21 billion industry by 2019 [4], and to triple by 2030 the current level of contracted installed capacity per year [5].

Combining desalination technologies with sustainable energy sources (non-carbon emitting) is one way to offset many of the negative impacts of running desalination plants. Concentrating Solar Power (CSP) is one of such clean technologies that could perform well when integrated with the energy intensive desalination processes [6], as it is highly dispatchable. CSP can provide both thermal and electrical power in large scale (including for base-load production), and is one of the few renewable energy technologies that can reliably and economically store energy to produce at a constant output (using thermal storage) even when its main resource — solar energy — is insufficient. Other solar technologies, namely photovoltaic (PV) panels, cannot economically provide power at a constant output with a significant degree of independence from the solar resource availability, and cannot shift its production in time to match demand [6]. Despite the many advantages that PV technologies can offer versus CSP, only with more efficient energy storage systems [7], PV could become dispatchable. Several CSP plants have been deployed in particular since 2008 using different configurations, and although the CSP market is not consolidated, the first generation of CSP

plants using parabolic trough solar collectors is already considered to be a mature technology [8], followed by the central receiver technology which is transitioning into commercial maturity.

Producing fresh water and electricity using solar power instead of fossil fuels, also makes sense when taking into account the global consensus of specialist of different areas that anthropogenic emissions of greenhouse gases (GHG) are starting to have negative impacts on the global climate [9]. The International Energy Agency (IEA) forecasts that *circa* 7000 GW of electrical generation capacity will need to be built to meet global demand by 2040 [10]. The EIA also forecasts up to 11% (~5000 TWh) of the electric demand to be met by CSP by 2050 [11], which may translate into potential investment opportunities to implement solar powered water desalination.

Currently there are no commercial CSP plants operating in direct cogeneration with desalination units, and very few experimental projects were actually built. Though, the cogeneration of water and electricity using commercial desalination units powered by fossil fueled thermal power plants is not a novelty, particularly in the Middle East region [2]. Currently powering desalination plants using the CSP technologies represent a challenge regarding optimization of the installed power and energy storage, operating schedules, and technologies to be chosen. Also, depending on the price of water and electricity in a determined region, it may be more profitable to favor the water production instead of electricity or vice versa, depending on the time of the day and time of the year [12]. This implies different economic outcomes for similar options.

Because of the untapped potential of using a much needed reliable renewable solar energy technology that is capable of a baseload production profile to power energy intensive desalination plants, this work is focused in obtaining a technical tool that would allow an easier analysis of such cogeneration projects.

1.1.1 Potential sites for CSP

As CSP plants convert direct solar radiation into electricity radiation, the majority of the locations suitable for its installation are placed in the so-called “Sunbelt” region. As it can be seen in Figure 1, according to satellite data for Direct Normal Radiation (DNI), the German Aerospace Center (DLR) assessed the areas of the world with the highest potential to power these plants. As a rule of thumb it is considered that at least 1800 - 2000 kWh/m^2 a year are needed in order for a CSP plant to be economically competitive, being the best sites the ones that receive more than 2800 kWh/m^2 a year [6], [13]. These reference DNI values were set for typical CSP plant performances, but in practice are very site specific. From this analysis the largest areas in the world that are appropriate to install CSP are located in Northern and Southern parts of Africa, the Middle East, Northeast part of India, Australia, Southwest parts

of both North and South America, which predominantly overlaps with the arid parts of the world.

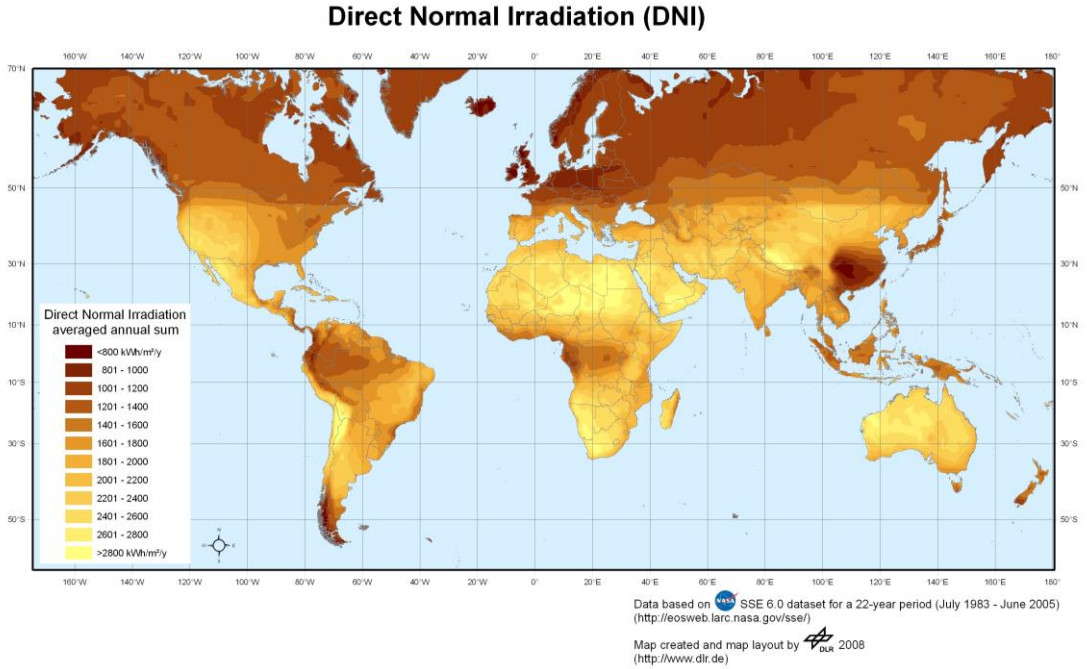

Figure 1 - Global Direct Normal Irradiance [14].

1.1.2 Potential sites for Desalination

Coastal zones, in the Sunbelt regions of the world near high population agglomerates represent the locations with the highest potential for the installation of CSP plants combined with desalination. Prime examples of such zones are the countries of the Middle East and North Africa (MENA), where the largest desalination markets exist [6]. Comparing Figure 1 and Figure 2 it can be seen that most of the areas where CSP has the greatest potential (Figure 1) also correspond to the areas of water shortage (Figure 2) where desalination may have a role to play.

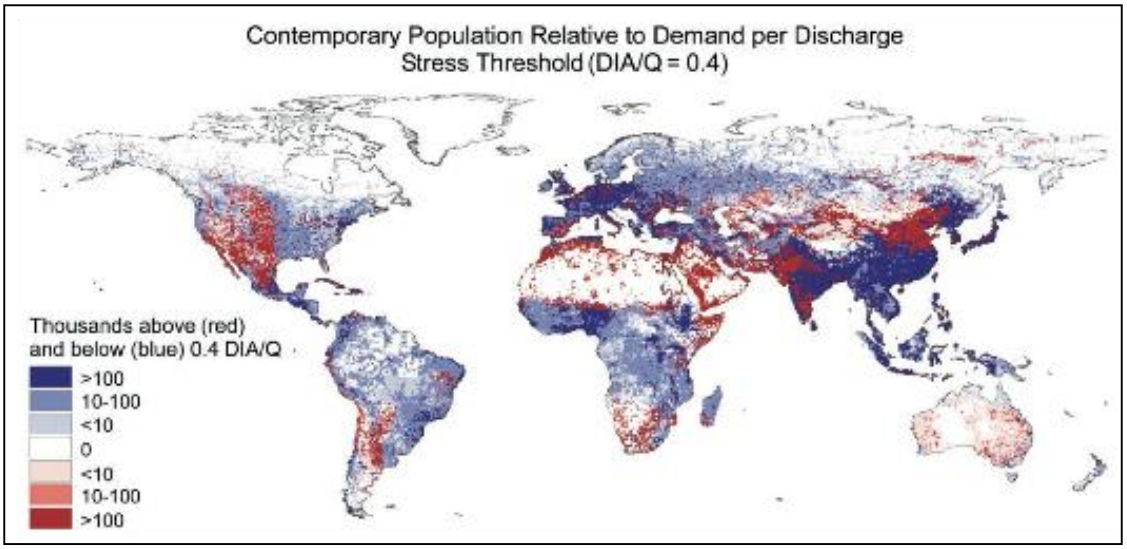

Figure 2 - Distribution of population with respect to relative water demand defined as the ratio of water withdrawal or water use to discharge. Domestic, Industrial, and Agricultural (DIA) sectors per Mean annual surface and subsurface (shallow aquifer) runoff, accumulated as river discharge (Q) is assumed to constitute the sustainable water supply to which local human populations have access [15].

1.2 Statement of the Problem

Today the production of fresh water and electricity using desalination plants powered by CSP present poses significant questions both in technical and economic terms, regardless of the selected type of CSP or desalination technology. In particular the selection of RO versus MED (the two most energy efficient desalination technologies commercially established) can have different outcomes for similar projects depending on the location. Currently there is no single tool available (commercial or freeware) that quickly and easily allows a first technical-economic evaluation for such investments with the required degree of accuracy.

To fully access the performance of investments using desalination plants powered by CSP, both the technical and economic aspects need to be considered, and both can be very complex. This type of information is also difficult to access, requiring classified information from the companies that have the know-how of designing, building and operating these plants. Two paths presented as valid to conduct this research: the first, focusing on the physical operation of these machines; and the second, on the economics behind it. It was decided to favor the physical analysis in order to formulate a deeper understanding of the physical constraints of implementing and operating these plants, in such a manner that would allow for potential future upgrades addressing economical and financial issues of the new models.

When analyzing the cogeneration using CSP to power a MED system versus RO, the integration of MED plants with CSP appears to be the most complex theoretical case to analyze. Operating a MED system powered by CSP requires an intrinsic physical integration, as both are thermal systems. On the other hand, as RO uses electricity and not thermal energy, it does not even require to be installed near the CSP plant or to be directly connected to it. Therefore, it was given priority to the physical simulation of CSP+MED, although work was done to perform the analysis of CSP+RO for a comparative case-study with CSP+MED.

The research questions addressed in this work are:

RQ1: Is it thermodynamically feasible to cogenerate water and electricity with CSP using MED and RO desalination plants?

RQ2: Can physical, semi-empirical, or empirical models be used to support findings on this matter?

RQ3: Which desalination technology is better suited to work in a system powered by a specific type of CSP plant?

RQ4: What is the optimum configuration for a CSP+D plant scheme for a particular case-study and can that configuration be possibly used in other case studies also?

1.3 Objectives

The first objective of this work is to obtain a tool applicable to a feasibility study that can simulate the physical performance of a CSP plant powering a MED unit for the cogeneration of fresh water and electricity. This tool should be capable of simulating these plants in cogeneration with a degree of accuracy that allows the user to run a simulation during pre-design stage, without the need of an extensive list of inputs. The second objective is to obtain information regarding the operation of an RO system powered by CSP, for a comparative case-study. The third objective is to analyze a case-study for a location where a real commercial desalination plant operates, and compare it with the theoretical physical performance of both a MED and a RO systems powered by a CSP plants.

1st Objective: CSP+MED model development

Much of the work done consisted of in upgrading a model previously developed by the US National Renewable Energy Laboratory (NREL). The model is able to perform technical-economic analysis to CSP plants: the System Advisor Model (SAM) is one of the most widely used software packages for the analysis of CSP plants. The upgrade added to SAM the capability of simulating the operation of a MED plant in cogeneration with CSP. The goal of this work shared the same strategy as SAM's: the desalination upgrade is not intended to be used for the design phase of a project in order to test a specific design, but rather instead it is intended to represent the performance of a given technology [16]. Also, the aim of integrating the MED model into SAM was to make it possible to upgrade it later on to include an economic and financial evaluation. Most of the MED plants operating commercially follow a parallel feed (P) configuration, while many of the experimental ones were built using a forward feed configuration (FF). To boost performance, several commercial MED plants are fitted with Thermal Vapor Compressors (TVC) [2], [12]. Because of this, the new models were developed to be able to simulate plants using these configurations.

To integrate the MED add-on into the CSP computer code in SAM, the following goals were set:

MED - Main physical process:

- Develop a simple model for a MED-FF plant (steady-state);
- Develop a detailed model for a MED-P plant (steady-state);
- Develop a detailed model for a MED-FF plant (steady-state);
- Write the developed MED models into computer code;
- Validate the MED models with data from real plants.

MED - Auxiliary processes and Controller:

- Develop a simple model for a TVC (steady-state);

- Develop a simple model for the removal of Non-Condensable Gases (NCG) using steam ejectors (steady-state);
- Develop a simple model for the water pumping to and from the MED and/or the CSP plants (steady-state);
- Develop a controller model for the MED plant;
- Develop a user friendly error message system, and set operational boundaries;
- Write the developed auxiliary and controller models into computer code;
- Integrate the developed auxiliary and controller models into the MED computer code;
- Validate the auxiliary and controller computer models with data from real plants.

Rankine cycle:

- Obtain performance curves describing the operation of a Rankine cycle with the necessary steam extractions to power a MED plant (steady-state), for high and low temperature input steam;
- Integrate the new performance curves into the Rankine cycle used in SAM;
- Validate the new performance curves;
- Integrate MED controller into the Rankine cycle code used in SAM;
- Develop a simple model for the operation of a Once-Through Seawater Condenser (SWCC) (steady-state);
- Upgrade Wet-Cooling code in SAM to assume the usage of seawater instead of fresh water;
- Develop a user friendly error message system, and set operational boundaries;
- Validate the upgraded Rankine cycle, the new cooling systems, and the cogeneration operation as a whole.

2nd Objective: CSP+RO model integration

The second objective is to gather existing tools capable of simulating CSP and RO plants and determine a strategy to combine them in such a way that they could be used as tools for the simulation of a CSP+RO system in a case study. When analyzing the RO system powered by CSP, the aim was not to create a tool applicable to a pre-feasibility study, but instead, the aim was to use currently available software.

3rd Objective: Case study analysis

The aim of the third objective is to compare data from a location where CSP and desalination can be used, using information from a real desalination plant, and data from the simulations using the CSP+MED model added to SAM, and the CSP+RO study using available software. Another goal was to validate the desalination models developed and used to simulate the MED and RO systems with the data from real MED and RO plants.

1.4 Methodology

The methodologies used in each phase of this thesis are presented below according to the objectives previously set.

1st Objective: CSP+MED model development

To achieve the first objective, the adopted methodology is to identify the best available models that could be used to simulate the physical performance of a CSP plant and a MED unit for a pre-design stage analysis, and to upgrade them as required, namely:

- CSP plants:
  Some models and corresponding software are able to simulate the performance of a CSP technology during pre-design stage [17], e.g. SAM, TRNSYS, Greenius and Insel. From these, the most widely used is SAM (which uses TRNSYS software), and it was the one selected to be used as the tool to integrate the rest of the models and computer code developed in this work for MED plants. SAM is also freeware, it is well documented, much of its core code is available, regularly updated, and can perform one-year technical-economic simulations (with hourly resolution) for the main CSP technologies available.

- MED plants:
  Several models and software are available in the literature, though none of them match either the pretended accuracy for a pre-design stage of a MED plant, and/or their algorithm/code was not available to be integrated with SAM. It was therefore decided to develop a MED model and a corresponding computer code that could be integrated into SAM's CSP block.

Several models and sub-models were developed to create the MED add-on in SAM.

- Simple MED-FF plant model (steady-state):
  - What exists: A simple steady-state model from H.T. El-Dessouky and H.M. Ettouney [18], is able to calculate the performance of a MED-FF plant, using a few inputs with some degree of accuracy, though it is necessary that the user knows the overall heat transfer coefficient (U) that should be usedfor the down-condenser and in each one of the cells (or effects) of the MED plant. This model is also described in [18] with a flaw. This model uses as input strategy the amount of distillate that is aimed at being produced, and not the amount of steam that is available.

- What was done: This model was upgraded by correcting the flaw that was identified in [18]; changing the algorithm so that it could be used to accept the mass of steam as an input and not an output; adding a correction factor to the overall heat load input to account for the actual losses in the system using data from a test campaign with an experimental MED-FF plant at Plataforma Solar de Almeria (PSA), Spain, and so validating the model.

- Detailed MED-P and MED-FF plant models (steady-state):
  - What exists: The equations used to build detailed steady-state MED models for parallel and forward feed configurations are described in the literature (e.g. [18]), but at the time this model started to be built none had the algorithm thoroughly explained to be easily replicated.
  - What was done: A new detailed steady-state MED model was created based on the experience of trying to build other detailed MED models (steady-state and dynamic) available in the literature. This new model describes in detail both the flashing of brine and distillate when they enter the different chambers within the MED unit. It assumes a preset efficiency for the heat transfer across the effects. The configuration of a real commercial plant was used as base to build the model and adapt to different sub-configurations. The model was built so that it could be integrated with other auxiliary models necessary to simulate the operation of an entire MED plant.

- Simple model for steam ejectors (steady-state):
  - What existed: There are published models that can be used to simulate the operation of a steam ejector, though most of them require detailed information as inputs, which will not be available during pre-design stage assessments. Some simple models are also available as the one described in [18], that use semi-empirical data, but when their output is compared to real data from commercial MED plants, their results were too far off.
  - What was done: A new empirical model was developed to estimate the performance of steam ejectors for MED plants, namely for a TVC, and two-stage NCG steam ejectors. These models were created using information provided by steam ejector manufacturers that operate on the desalination market.

- MED plant controller:
  - What existed: The controlling process of MED plants can be simulated with proprietary software like the one from GSE Systems^{tm} [19], but its code and exact strategy are not freely available.

- What was done: The specificity of the MED code written for SAM implied that the MED controller had to be adaptable to SAM, and for that a new controller model was developed.

- Model for auxiliary water pumping to and from the plants, SWCC and Upgrade Wet-Cooling code in SAM:
  - What existed: There is abundant information in the literature about the ruling fundamentals, equations, and models describing the pumping process required for installations as the CSP and the MED plants. The same was also true for the fundamentals when using saltwater with wet-cooling processes and once-through cooling systems.
  - What was done: The ruling fundamentals and equations for water pumping, once-through cooling systems and wet-cooling using saltwater were applied to the code used in the SAM.

- Rankine cycle performance curves using intermediate steam extractions for cogeneration processes:
  - What existed: There are abundant sources of information available in the literature and several models exist that can be used to simulate the performance of Rankine cycle under different conditions using different components.
  - What was done: SAM uses performance curves that describe the Rankine cycle operation, using steam at a “high” temperature (~510ºC) for central receiver towers, “low” temperature (~372ºC) for parabolic troughs and linear Fresnel, and organic Rankine cycles. These curves were calculated for “high” and “low” temperature steam, using two physical models developed using the software Engineering Equation Solver (EES): one for the design, and the other for the off-design simulations of the Rankine cycle (steady-state conditions). These EES models were initially built by NREL [20] using crucial inputs taken from proprietary software like IPSEpro^{tm}, that are normally used to design power plants amongst other industrial installations. In order to enable the comparison of results using a CSP plant working with or without a MED unit in SAM, it was decided to perform a major upgrade to the same cycle described initially in EES, and assume in that model two extra steam extractions powering the MED plant. The adaptation of the EES model was done by a researcher from Laboratório Nacional de Engenharia e Geologia, I.P. (LNEG) in Portugal by engineer João P. Cardoso [21]. Using this updated version of the EES models, it was possible to extract a database of ~50 000 points of operation that included design and off-design conditions of the Rankine cycle (this was a shared effort between the author of this work and

engineer João P. Cardoso). With the aid of a model using genetic algorithms running in Matlab environment [21] developed at Instituto Superior Técnico (IST), Lisbon, Portugal by engineer Filipe Marques, the necessary mathematical correlations describing the operation of the Rankine cycle were computed (this was done by the author of this work, with the guidance of the developer of the genetic algorithm code, engineer Filipe Marques). These correlations describing a Rankine cycle with and without intermediate steam extractions were then merged into SAM.

2nd Objective: CSP+RO model integration

To achieve the objective of simulating a RO system powered by CSP for a case-study, it was decided to use freeware software that is made available by the main RO membrane producers [22], [23]. This work was conducted through the joint work and supervision of a Master's student (Mahran Abdelkarim Ahmed) in the context of his internship at LNEG between July and December 2014.

- What existed: No software is available that can simulate the operation of a CSP plant powering an RO system for a yearly simulation for pre-design stage. However, several software packages were already built and made freely available, that are able to simulate independently the CSP and the RO systems. CSP+RO systems do not need such a high level of integration as CSP+MED, as RO uses electricity instead of thermal energy. Therefore, it was possible to easily simulate the operation of CSP+RO with unrelated software, unlike CSP+MED. Several software is made available to simulate and/or dimension the performance of a RO system for both design and/or off-design conditions, e.g. Reverse Osmosis System Analysis (ROSA) from Dow Chemical Company, Toray Design System (TorayDS2) from Toray Industries, The Membrane System Design Software (Winflows) from General Electric, or IMSDesign from Hydranautics.

- What was done: The ROSA software from Dow Chemical Company was selected to be used in this work, as it revealed to be both accurate [22] and one of the easiest software to use. SAM was used to simulate the CSP plant powering a theoretical RO system. A location was chosen for the case study (see third objective). The net electric CSP output was calculated using SAM, whereas ROSA was used to dimension and calculate the RO plants output under the different conditions it would find throughout the year. Data from the CSP and the RO system was combined using a simple controlling strategy applied in Microsoft Excel, to determine when the RO plant would operate

and how much electricity would remain from the total net electric CSP output after deducting the RO consumption.

3rd Objective: Case study analysis

To achieve this objective it was necessary to obtain detailed information about a real desalination plant to use as reference, in a location where both CSP and desalination processes would be necessary and logical to use.

- What existed: Design and operational data from existing MED and RO plants are insufficient in the literature to define a complete reference for a case study (especially for MED plants). Some information was available in the literature though, regarding a specific TVC-MED-P plant in the Southern Italian city of Trapani, West Sicily.
- What was done: Data from real desalination and electric thermal power plants was obtained through technical field visits to both experimental and commercial plants. Real data was complemented with data available in the literature. Visits were conducted to different MED, RO, CSP, fuel oil, and combined cycle thermal plants. The location of Trapani (Sicily, Italy) was used as a reference for the case study presented in this work, as it was possible to obtain detailed information from the commercial TVC-MED-P plant operating near Trapani. The information available on the literature regarding this plant was used as a complement. This data was also used to validate the detailed MED, steam ejector and auxiliary pumping models.

1.5 Publications

The work described along the chapters in this thesis resulted in a number of publications, which included conference presentations, proceedings, and journal papers. The most relevant are:

- **Paper I** –*Experimental Validation of MED Forward Feed Steady-State Model* by Sérgio Casimiro, Diego-César Alarcón-Padilla, Christos Ioakimidis and João Farinha Mendes published in the Energy Procedia publications by Elsevier [24], 2014.

  The work presented in this paper involved using real data gathered from the operation of the experimental plant at PSA, which was conducted by PSA staff lead by the researcher Diego-César Alarcón-Padilla. The data analysis, the adaptation and development of the model, and its validation was conducted by the author of this work, with the supervision and helpful comments of the co-authors. The author of this thesis completed 80% of the work presented in Paper I.

- **Paper II** – *MED Parallel System Powered by Concentrating Solar Power (CSP). Model and Case Study: Trapani, Sicily* by Sérgio Casimiro, João Cardoso, J. Farinha Mendes, Carmelo Mineo and Andrea Cipollina published in the Desalination and Water Treatment journal [25], 2014.

  The research in this paper was conducted by the author of this work, with the supervision and helpful comments of the co-authors. The author of this thesis completed more than 95% of the work presented in Paper II.

- **Paper III** – *Modeling Multi Effect Distillation Powered by CSP in TRNSYS* by Sérgio Casimiro, João Cardoso, Diego-César Alarcón-Padilla, Craig Turchi, Christos Ioakimidis and João Farinha Mendes, published in the Energy Procedia publications by Elsevier [26], 2014.

  The work presented in this paper was conducted by the author of this work, with the supervision and helpful comments of the co-authors. The author of this thesis completed more than 95% of the work presented in Paper III.

- **Paper IV** – *Reverse Osmosis Powered by Concentrating Solar Power (CSP): A Case Study for Trapani, Sicily* by Mahran K.A. Ahmed, João P. Cardoso, J. Farinha Mendes and Sérgio Casimiro published in the Desalination and Water Treatment journal [27], 2015.

  This work is a follow-up of the work previously conducted for the CSP+MED integration by the author of this thesis, and it was conducted through the joint work and supervision of a Master's student (Mahran Abdelkarim Ahmed) in the context of his internship at LNEG between July and December 2014. Helpful comments were given from the other co-authors. The author of this thesis completed 30% of the work presented in Paper IV.

- **Paper V** – *Performance Curves of Rankine Cycles for Solar Co-Generation of Water and Electricity* by João P. Cardoso, Filipe Marques, Sérgio Casimiro. This is paper is in preparation, near completion.

  This paper describes the work conducted to create the new Rankine cycle performance curves in cogeneration with an MED plant, which included upgrading the existing EES code originally developed by NREL, and calculating the mathematical splines describing the cycle's performance using a genetic algorithm. The author of this work completed roughly one third of the work presented in Paper V.

1.6 Structure of the Thesis

The thesis is organized in the following structure:

- **Introduction**: In this chapter, the author explains the inspirations and motivations behind this work, the problems he addresses, and the questions he attempts to answer.

- **Literature review**: This chapter explains the main CSP and desalination technologies and their main technical characteristics,in addition to pointing out the pros and cons of using them in different situations according to the available literature. Also, this chapter reviews the models/software available to simulate CSP and desalination technologies. The desalination area was emphasized throughout the literature review.

- **Models Development and Validation**: Here the models developed in this work are described in detail, how they were designed and coded, namely: the development of the MED models and the necessary auxiliary processes, the integration of the MED models in SAM to simulate CSP+MED, and the use of ROSA in combination with SAM to simulate CSP+RO.

- **Case-Study**: This section presents a case study where the physical performance of a simulated CSP+MED system is analyzed versus a simulated CSP+RO, using as reference the data from the real TVC-MED-P commercial plant in the city of Trapani, Sicily, Italy.

- **Conclusions and Future Work**: These sections present the overall achievements and answers to the research questions, together with proposalsfor future research topics.

Table 1 identifies the sections related to the work done regarding model development/integration and case study analysis in the mentioned papers above. It also provides a short summary of each one of these sections along with the corresponding papers to which they relate.

Table 1 – Chapters of this thesis and corresponding papers in which they are described.

Section	Paper	Main Purpose
3.1	I	New simple MED-FF physical model description and validation
3.2	II	New detailed MED physical model description and validation
3.3	II	New auxiliary steam ejector empirical model description
3.4	-	New auxiliary pumping physical model description
4.1	III	General description of the new solar desalination add-on to SAM
4.2	III	Strategy used for MED plant dimensioning with SAM
4.3	III	Strategy used for the CSP-MED controller in SAM
4.4	V	Description of the original and new performance curves used in SAM, describing the Rankine cycle performance when using dedicated intermediate steam extractions for the MED processes
4.5	-	Description of the original and upgraded Rankine cycle subroutine in SAM
5	IV	Description of algorithm used to integrate existing CSP+RO models (SAM+ROSA)
6.1	II	Case study analysis using CSP+MED models
6.2	IV	Case study analysis using CSP+RO models
6.3	IV	Case study analysis comparing CSP+RO with CSP+MED
6.4	II & IV	Comparison of results from the simulated CSP+MED and CSP+RO systems with the real output from the commercial MED plant in Trapani

2. Literature Review

2.1 Desalination: Technologies Overview

The commercially proven desalination technologies for large-scale water production can be grouped into two sections:

- Distillation processes: MSF and MED
- Membrane processes: RO

Hybrid desalination processes can also be theoretically implemented combining the evaporation and membrane plants working next to each other. Much of the progression obtained in the learning curve establishing the current commercial desalination technologies was obtain in particular due to the large investments in desalination projects made in the Middle East region at least since the 1970's.

Thermal desalination systems use thermal energy to produce fresh water from the sea or from brackish water sources. Thermal desalination systems produce distillate using phase change (liquid to vapor). Only water molecules pass to the vapor phase, leaving all other constituents in the liquid that did not evaporate. Contamination of the distillate produced with dissolved salts is negligible (~100 ppm for total dissolved solids) [28].

Membrane processes use pressure to force water molecules through thin selective membranes. There are different types of membranes available with different characteristics. They differ in thickness, mechanical strength, pressurization capacity, working life, pH stability, and selectivity and efficiency to remove solutes [29]. Some are used for pre-treatments, like micro and ultra-filtration with larger pores, that help reduce loads on processes as RO that have more restrictive membranes. The RO process uses high-pressure water pumps to force saltwater against selective membranes. Other membrane processes use other techniques, for instance, membrane distillation that only allows vapor to flow across the membranes using hydrophobic membranes. However, RO clearly dominates the membrane desalination market.

2.1.1 MED

MED accounted for 7% of the total installed desalination capacity worldwide by technology in 2014 [2]. MED technology can have several different vertical or horizontal configurations. The MED process uses a series of interconnected shell-and-tube heat exchangers (also commonly called evaporators, cells or effects), where the vapor formed in one effect powers the next [18]. A series of effects connected to each other is called a MED train. Each group of

heat transfer tubes inside each effect is called a tube bundle. The space outside the tube bundle is called the shell side, and the space inside tubes of the tube bundle is called the tube side. At the end of the MED train, connected to the last effect is a condenser, normally called the down-condenser. The general configuration of a MED effect is presented in Figure 3 and in Figure 4.

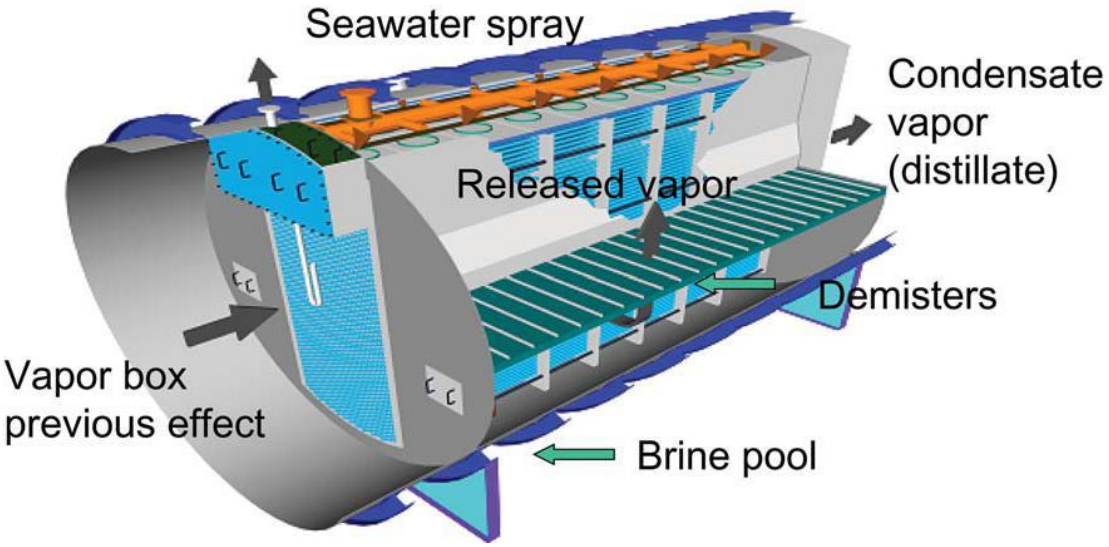

Figure 3 – General schematic of a MED effect, obtained from [30].

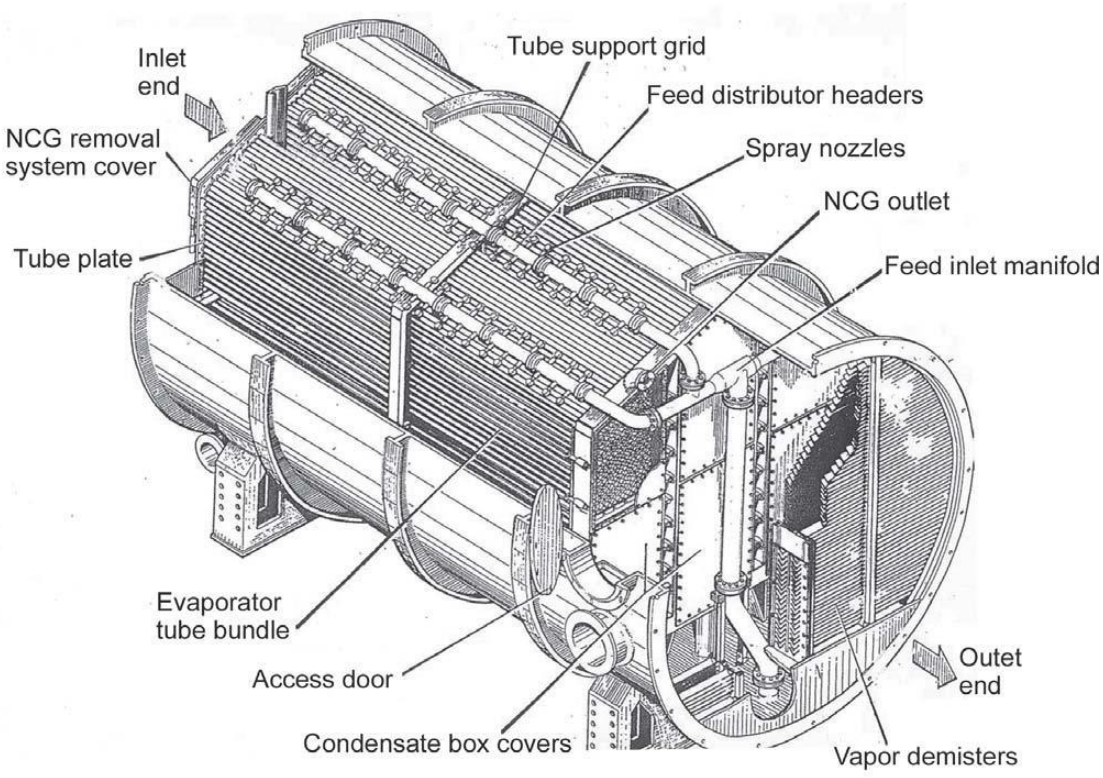

Figure 4 – General schematic of a MED effect, obtained from [31].

The MED system works by operating the effects at a consecutively decreasing level of pressure (and temperature), from the first (hot) to the last (cold). In these effects the salt water is sprayed on the shell side of the tube bundle and it flows downwards by gravity. The vapor formed in the previous evaporator is directed and condensed on the tube side of the tube bundle of the next effect. As the saltwater is sprayed over the tube bundle, it creates a water layer thick enough to cover the entire external surface of these tubes and prevents the occurrence of dry patches (that can lead to permanent salt deposition on the tubes outer surface). At the bottom of the tube bundle a brine pool collects the remaining salt water, from where brine is routed normally into the next effect. There are seven main different types of masses flowing throughout the MED process:

1. Brine: concentrated salt water;
2. Cooling water: salt water that is used in the cooling process at the down-condenser;
3. Distillate: fresh water produced with a negligible salt concentration;
4. Feedwater: preheated salt water entering the effects with the same salt concentration than the intake salt water entering the plant;
5. Motive steam: steam entering the first effect;
6. Non-Condensable Gases: Dissolved gases in the feedwater that are released during the evaporation/flashing processes and that are not possible to be condensed at the temperatures that the MED plant operates;
7. Water vapor: saturated vapor produced inside each effect.

Apart from these flows, anti-scalents and anti-foaming agents can also be used to control and improve the performance of the MED process [28]. Heating steam is introduced inside the tube bundles of the first effect. As salt water cools the tubes externally, the vapor inside the tubes will condense (releasing mostly latent heat, and some sensible heat especially if condensed to a temperature slightly below the saturation). Heat transfer will take place through the tube wall. The salt water will warm up until pressures reach equilibrium on the shell side. As part of the salt water evaporates while dripping down the tubes, its salt concentration increases (as salt evaporation/carry-over together with the vapor formed is almost negligible). This concentrated salt water, called brine, is collected at the bottom of each effect. The vapor produced in each effect is routed into the tube bundle of the next (colder) effect, being condensed inside these tubes, and allowing the replication of the condensation/evaporation process. As each effect is at a lower pressure than its predecessor, the vapor produced outside the tubes (released through the evaporation of the salt water) is at a lower temperature than the heating vapor inside the tube bundle [18]. This is a critical condition for the operation of this type of machines, in order to maximize the evaporation rate with the same amount of energy.

Depending on the configuration of the MED plant, the salt water flowing on the shell side of tube bundles:

- Can be released in all effects at the same temperature and mass flows (parallel configuration) having been preheated only during one stage, when passing through the final condenser;
- Can be preheated between effects as it is pumped into them. The feedwater can be released with this configuration at an equal rate in all effects (parallel configuration), or it can be totally directed to the first effect (forward feed configuration). If forward feed is the case, then the brine is transported across the plant due to the pressure difference between effects, and sprayed on top of the tube bundle of the next effect (with the aid of pumps if these pressure differences are not enough to overcome gravity and other pressure losses). The forward feed configuration means that the brine concentration increases downstream as the water flows from one effect to the other. With a parallel configuration the brine concentration in all effects increases slightly towards to the effect. The parallel configuration is typical in commercial MED plants, and the forward feed was found to be used only with experimental plants.
- A backwards configuration is also possible. In this case, the feed water enters the last effect and the brine flows from the coldest to the hottest effect. This configuration is not common, as the brine will reach its highest concentration inside the hottest effect, meaning that the risk of permanent deposition of calcium sulfates in the tube bundle is also higher in case the plant is not properly operated.

The main schematics of these three MED configurations are shown in Figure 5.

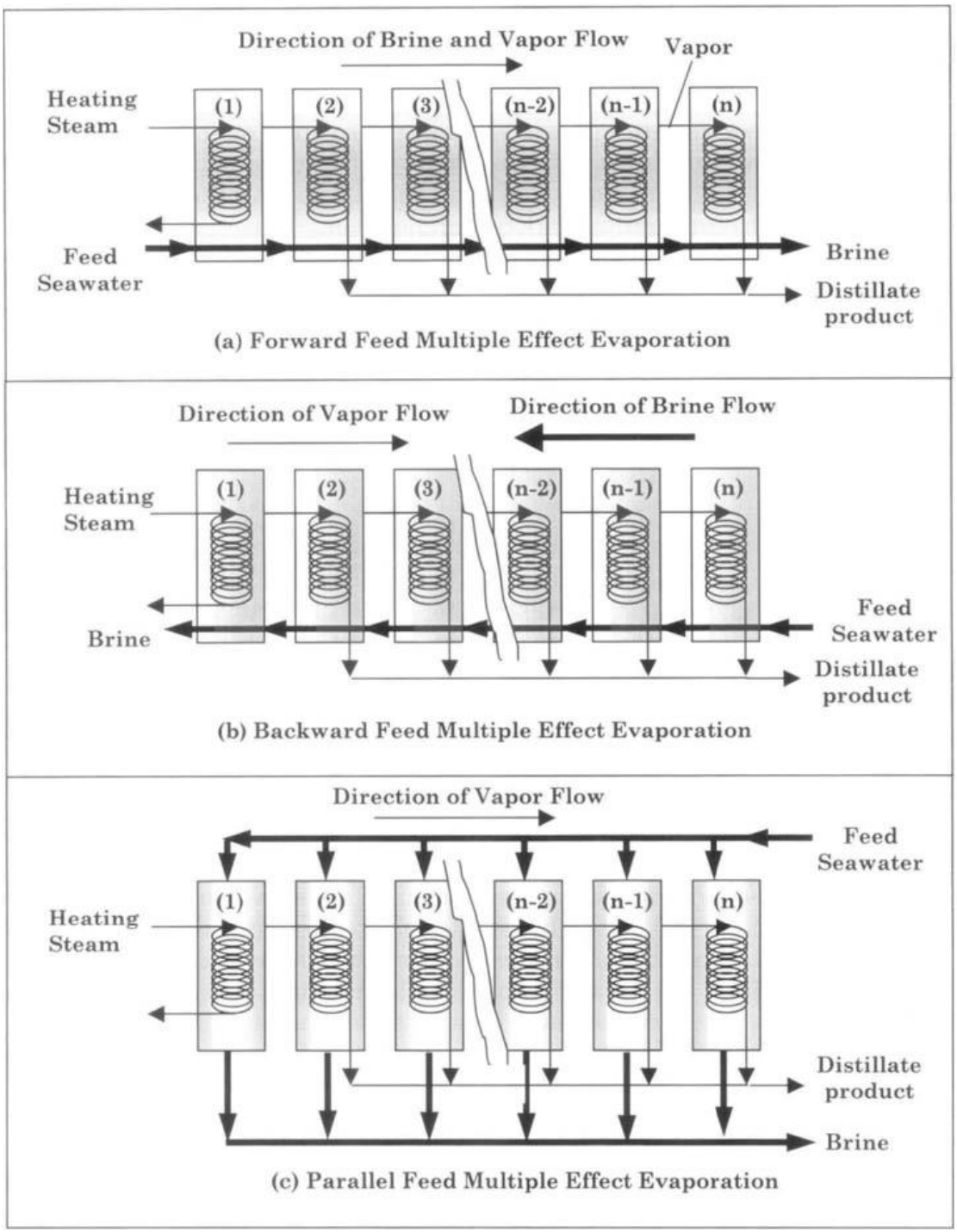

Figure 5 – General schematics of MED configurations, obtained from [18]: Forward Feed, Backwards and Parallel.

The vapor formed in the last effect is also condensed using a final shell-and-tube heat exchanger, but in this case the vapor flows on the shell side of the tube bundle, and the salt water flows on the tube side. The pressure gradient that exists between effects in the MED plant is maintained at the bottom by the down-condenser, setting the pressure at which the last effect will operate. The more energy the condenser dissipates, the lower the vapor pressure will be inside the last effect. The lower the pressure in the last effect, the lower its

operational temperature will be. This pressure/temperature drop will then cascade upstream, as this will also force the vapor formed in the previous effect (n-1) to condense at a higher rate, reducing the pressure of the previous effect, and lowering its temperature (this condensation happens in the tube side of the tube bundle in the last effect, n). This phenomenon replicates across each effect of the MED plant until reaching the first one, which is limited at the top by the temperature of the heat source powering the plant. The heat source is normally saturated steam, though, other sources of heat can also be used (e.g. the experimental plant at PSA uses hot water powering the first effect). The shell side pressure achieved in the condenser is also dependent on the seawater temperature that acts as the cooling medium. The operational temperatures and pressure gradients in this type of plants is therefore dependent and delimited at the top by the temperature powering the first effect and at the bottom by the seawater temperature, which define the main driving force for heat transfer.

The condenser (also called the down-condenser) provides normally the initial preheat of the feedwater flowing into the plant to be fed to the effects. Some plants are designed to use all of the preheated water when leaving the condenser, while others are only designed to use part of it. Normally the ones using all of the preheated water from the condenser use thermal vapor compression to increase the MED plant efficiency and reduce the amount of vapor to be dealt with by the down-condenser (at the cost of using motive steam at higher pressures). This means that plants that do not use all of the preheated feedwater will have to dump large amounts of energy back to the sea and spend more energy pumping water per amount of distillate produced. On the other hand, these plants also probably use motive steam at much lower pressures, requiring less energy to operate the first effect.

The MED process includes a second physical phenomenon, called flashing that produces vapor. The flashing process occurs when a liquid is subject to a lower pressure than its saturation pressure. Under these conditions the saturation temperature of the liquid decreases, and suddenly it passes from a saturated to a superheated condition [32]. Unlike other evaporation processes where energy is supplied to the liquid from the outside, in the flashing process the energy for the vapor production comes from within the liquid, being transformed into latent heat as vapor is created with this process. Depending on the MED process configuration, some of the flows inside the effects will flash. When water enters each effect it will be at a higher pressure than the vapor pressure inside the shell side. As a result, part of this water will immediately flash producing vapor. This flashing process is not as relevant as the evaporation in the MED processes (unlike MSF), but depending on the type of plant configuration it can have a relevant role by aiding in the vapor production, especially in the last effects when using parallel configuration, or in the first effects (excluding the very first) if using forward feed configuration. Flashing can occur mainly inside the distillate boxes, or when brine from the previous effect enters the main chamber of the next effect [18].

At present MED plants operate at top brine temperatures between 55ºC and 70ºC to limit

scale formation and corrosion, allowing the use of low-grade waste heat if coupled to a steam cycle power plant, obtaining a better performance than MSF. Also, standard condensing turbines may be used instead of back-pressure turbines [6]. MED systems can be combined with heat input between stages from several sources, including mechanical (MVC) or thermal vapor compression (TVC). TVC-MED systems may have thermal performance ratios up to 17, while the combination of MED with a heat-absorption heat pump could reach a ratio of 21 [6]. Without TVC a MED plant can have a heat consumption of 53-108 kWh_t/m^3 of distillate produced (190-390 kJ/kg) in the form of process steam at less than 0.35 bar withdrawn from the steam turbine, with a specific electricity consumption of 1.5-2.5 kWh_e/m^3 (for pumping and control) [6].

In comparison to RO plants, the energy consumption of MED and MSF plants tends to be less affected by feedwater quality. The quality of the produced water is extremely high (<10 ppm total dissolved solids), making it too pure to be drinkable. Therefore salts are added to the distillate to make it suitable for human consumption.

The performance ratio of a MED plant is approximately equal to the number of effects minus 1 or 2. The maximum number of effects can rise up to 16, having each effect a lower pressure than its predecessor to compensate, as the temperature decreases along the chain of effects.

The MED is based on heat transfer, causing thermodynamic losses during different steps of the process. The most relevant thermodynamic losses are the Boiling Point Elevation (BPE), the Non Equilibrium Allowance (NEA), and the pressure losses as vapor flows through the different paths it must cross (including losses to the exterior) [18].

MED plants also require auxiliary systems to run. In particular, to eject non-condensable gases, and remove from the last effect part of the vapor produced in case the plant is fitted with a thermal vapor compressor. These two systems, in particular, are normally run on MED plants using steam ejectors. Also, pumping systems are required to remove the condensate from the first effect back into its original source (e.g. Rankine cycle boiler), remove brine and distillate from the last effect and down-condenser respectively, collect saltwater into the down-condenser, and return brine and excess cooling water back into the sea.

Steam ejectors operate by using energy contained in high-pressure steam. They transfer it to lower pressure vapor or gas, producing a mixed discharge stream of intermediate pressure [33]. Conventional steam ejectors do not have moving parts. A conventional ejector has a diffuser (from where compressed gases are exhausted), a suction chamber (where the low-pressure fluid is drawn into), and the nozzle (where the high pressure steam flows through just before entering into contact with a low-pressure zone) [34]. During partial load operation, in real plants, the operators can eventually close the entrance where the low-pressure gas is drawn into the ejector, and in this case the TVC would operate just as a

normal steam pipe [35].

There are three systems in a MED plant that make the use of steam ejectors as auxiliary systems, namely:

1) *Compression of vapor entering the first effect*
   A thermal vapor compressor is typically a large steam ejector that connects an effect down the line of the MED train to the first effect, and it is used to compress vapor entering into the first effect. It is used to improve the MED plant efficiency, as it recycles low-pressure vapor produced in the last effects to be used again in the first effect. When using a TVC, less motive steam is required to to power the MED plant, but it requires steam at higher pressures (higher specific enthalpy). Using a TVC also impacts the operation of the down-condenser, as less vapor will reach it. Less vapor, means less cooling water and less energy to drive the pumping systems. The TVC reduces the total heat load that is required to be dissipated inside the down-condenser [18].

2) *Removal of NCG*
   Multi-stage ejector systems are normally used in commercial MED plants to remove non-condensable gases. In many of them, the NCG venting system uses two-steam ejectors in series (2 stage system) [18], [36], [28].

3) *Initial vacuum creation across effects during startup*
   The ejector used to create the initial vacuum in the system is called the hogging ejector [37].

2.1.2 MSF

The MSF technology has provided a well-proven operational feedback since the 1950's in large-scale industrial operations- using a compact modular construction. It was used for both small and large-scale installations in the past, but now it can be only used competitively for in large-scale installations [12]. In 2014, MSF represented 21% of the total installed desalination capacity worldwide [2]. MSF runs several stages, where the evaporation and condensation steps are coupled with each other in such a way that the latent heat of evaporation is reused to preheat the incoming water [38]. After the pre-heating, the incoming feed water is heated to its maximum temperature in the brine heater, by condensing saturated steam from a heat source (normally the cold end of a steam cycle power plant).

In each stage only a small amount of brine is converted to vapor. Depending on the pressure used, when the hot water enters each stage with a lower pressure than the previous,

it will cause the saltwater to boil very quickly, almost exploding or “flashing” into vapor, reaching a dynamic equilibrium.

MSF is considered a mature technology, and has benefited from improvements coming out from the experience of running several large installations for several years. The first version of MSF consisted of a long tube configuration with an acid dosing scale control system. In this configuration the tube bundle (that crosses each stage partition in a straight line) has the flashing brine flowing parallel to it. The plant efficiency can be improved by increasing the number of stages, but these expansions are limited by both the tube extension and stage.

Scaling was one of the main issues (especially in the first plants of this type) related to the hot brine temperature, while handling and safety problems were associated with the acid based scale control. Sponge ball cleaning systems and specific anti-scaling chemical products, gradually solved the problem, and this was the reason why MSF gained popularity over MED for a long time, being MED a more complex configuration only used in small installations in remote locations during this development era.

In the cross-flow configuration the brine tube bundle is generally located in the middle of the flash chamber, and water boxes external to the vessel connect each stage tube bundle. This improved configuration allowed for steady increases of plant sizes over the years up to today’s maximum of around ~3 800 m^3 per hour [12].

Large MSF units are often coupled with steam or gas turbine plants for better usage of the fuel energy. The steam produced by the power plants is expanded through a turbine to produce electricity, and the low / moderate temperature steam leaving the turbine is then used to drive the MSF plant with its condensation. The higher the exhaust temperature of the steam from the low-pressure turbine of the power plant, the higher the cutback on the Rankine cycle performance and consequently, the net electrical output is lower, but more energy is left to power the desalination process and increase the fresh water production [6].

MSF plants use steam at 90-120ºC at around 2.5 to 3 bar minimum. As a condensing steam turbine works typically at 35-40ºC (though this is dependent on the type of cooling process used), the reduction of power generation of a steam cycle power plant can be considerable. MSF plants are less efficient than other distillation processes accounting energy consumption and capital costs, namely compared with MED. Though, its installations present very long lifespans (between 30 and 40 years), high reliability, with low service factor and relatively low chemical costs. A typical MSF plant has a heat requirement of 69-92 kWh_t/m^3 of distillate produced (250-330 kJ/kg), and an electricity consumption in the order of 3-5 kWh_e/m^3. A cogeneration with such figures would imply a net electrical output reduction equivalent to 6-8 kWh_e/m^3 of clean water produced. A typical performance ratio (ratio between produced water and input heat) of a MSF plant is in the range of 7 to 9 [12]. While MSF is a

quite robust system, it can be specially suited when the feed water produces low quality due to high salinity, temperature or contamination.

2.1.3 RO

RO accounts for 65% of the total installed desalination capacity worldwide by technology in 2014 [2]. Reverse Osmosis works by exerting pressure over a special membrane, opposite to what happens with distillation methods where thermal energy is the key factor for the separation of fresh water from seawater or brackish water. The RO membranes act as a barrier between two phases allowing selective crossing of one or more type of fluids mixtures, from one phase to the other. RO reverses the natural process of solvent transportation from a region of lower solute to a region of higher solute when separated by a semi-permeable membrane.

Pressure, concentration, and chemical potential are the three types of driving forces that can be applied for membrane separation [39]. Normally industrial processes use pressure driven RO, powered by electrical engines that pump the seawater or brackish water through a series of semi-permeable membranes.

The external pressure used in RO is applied to the high solute concentrated water, causing the solvent to migrate through the membrane against the osmotic pressure caused by the difference in concentration, which if let alone would force water to flow to the opposite direction through the membrane.

Some membranes reject up to 99% of all ionic solids, organic molecules and organisms, excluding all particles lighter than 100 to 300 Daltons [29]. There are two types of membranes that can be used in RO processes: Hollow Fine Fiber (HFF) and Spiral Wound (SW). The product water from RO processes is not as pure as in distillation processes. RO can produce water normally in the range of 10 to 500 ppm of total dissolved solids, but the normal range is between 200 and 500 ppm. The higher the salinity of the feedwater the more energy is necessary to force water through the RO membranes. So, using brackish water as feedwater will tend to use less energy than seawater, and because of that RO is often the preferred method to use with brackish water. In this situation lower pressures are required to drive the O process comparatively with cases using feedwater with higher salt content [6].

The operating pressures used for brackish water systems range from 10-15 bar and seawater systems from 50-80 bar. Osmotic pressure of seawater is about 25 bar, for a salinity of 35 g/kg. To power RO units, 4-7 kWh_e/m^3 are required depending on the plant size and energy recovery systems used [40].

RO started to be deployed in the 1970's, and has been increasing its efficiency ever since, and as a result it has become the technology of choice wherever there is the need for a

stand-alone desalination plant, specially due to the introduction of pressure recovery mechanical systems.

2.1.4 Hybrid Systems

Hybrid systems contain both thermal and membrane desalination processes. This combination can be quite suitable for improving a matching requirement between water and power. For example, countries in the Gulf region in the Middle East face an unusual electricity demand profile with a peak during summer time (by the usage of air-conditioners), which drops 30-40% during the rest of the year [12]. Contrary to this, water demand keeps almost constant throughout the year. As there is a power-water imbalance during a large part of the year, running the thermal desalination plants only on steam resulting from the production of electricity will cause lack of energy to produce the sufficient amount of water. The result is that power plants keep burning fuel just to produce steam for the desalination plants, increasing the marginal price of water during the off-peak periods, as each kJ of steam is being paid in a larger share by water production only, with a reduced electricity production "subsidizing" each m^3 of water with low-grade waste steam.

Having a combination of desalination units that use both thermal energy (MSF or MED) and electricity (RO), can reduce the overall energy requirements and operating costs for water production and electricity generation in such situations.

If hybrid systems are fully integrated (meaning the plants are planned from day one to work together) the RO operating costs can be reduced by supplying some of the thermal desalination plant outlet water to the RO unit. This can allow the raising of temperature of the feed water of the RO (increasing its performance), and the reduction of both operating and construction costs by common post treatment. Also, the low-pressure steam from the thermal desalination plant can be used to de-aerate the feedwater to the RO plant to minimize corrosion and reduce residual chlorine [12], and brine discharge from the RO plant can be combined with the brine recycle in the thermal desalination unit (brine from the RO plant will be more concentrated than the brine produced by the thermal desalination plants).

This combination of desalination technologies can also benefit the RO plant, as only a single stage system can be used (water passing only once-through the membranes), maintaining long membrane life, by blending the RO product water with high purity distilled water from the thermal desalination unit. Also this combination adds flexibility to respond economically to the variation in power demand in places like the Middle East.

2.1.5 Key Players

For several decades, desalination has been studied and commercially implemented with success, leading to the existence of several companies operating in the desalination market,

including large corporations like Veolia, Doosan, VA Tech Wabag, Dow Chemical Company, and Toray [2]. Also several research groups from various institutions do work in desalination (e.g. the Spanish Plataforma Solar de Almería or the French Alternative Energies and Atomic Energy Commission).

2.2 CSP: Technologies Overview

There are four main types of CSP Technologies nowadays as seen in Figure 6: parabolic troughs, solar towers or central receivers, linear Fresnel, and parabolic dishes. The different CSP technologies are at different stages of development.

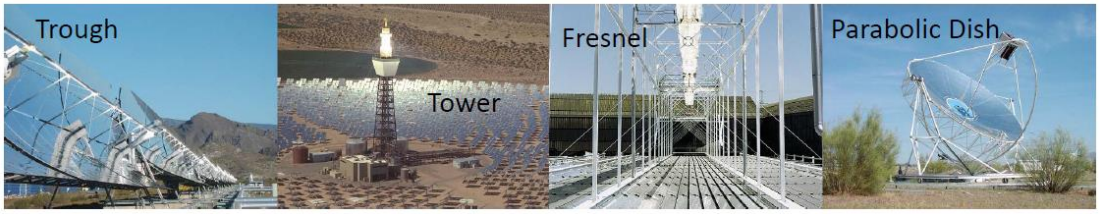

Figure 6 - Images representing the four main types of CSP technologies [41].

Most CSP technologies produce electricity in a similar way to conventional power plants. The typical configuration of CSP plants using parabolic troughs, central receivers, and linear Fresnel mirrors use steam to drive a turbine that is connected to a generator producing an electric current. The main difference is that the energy to boil the water instead of coming from the burning of fossil fuels comes from solar radiation [6], where mirrors are used to concentrate the solar energy into a working fluid. Heat storage systems, typically using molten salts or pressurized steam, can be used to increase the working hours of CSP plants beyond the hours of the day where the sun shines over the plant and/or shift production in time to match the demand. Using oils, the common heat transfer fluid used in CSP plants, creates a barrier to achieve the steam temperatures that steam turbines conventionally use as input in other thermal power plants. These oils degrade above ~400ºC, being this the temperature limit used. Molten salts and pressurized water allow higher maximum operating temperatures, namely, 550ºC and 500ºC, respectively [42]. Though, molten salts solidify at ~220 ºC (conventional solar salt: 60% $NaNO_3$, 40% KNO_3), meaning that this is the limit from which the energy from the solar field can be extracted [43], [44]. The size of the solar field can be measured not only in total area, but in relation to the installed capacity of the power block. The solar multiple is the solar field aperture area expressed as a multiple of the aperture area required to operate the power cycle at nominal capacity [20]. The aperture area is the total solar energy collection area of the solar field in square meters, and for example, it is less than the total mirror surface area in the case of parabolic troughs, as the mirrors are curved, with a parabolic shape.

Most of the CSP plants make use of a Rankine cycle. To operate this cycle, it is necessary to use cooling devices, in order to condensate the exhaust steam from the low-pressure turbine. The most efficient cooling options use water, which can be very scarce in the areas where the DNI values are higher. There are two main types of cooling options used with CSP plants, namely, wet cooling and dry cooling. Wet cooling uses water evaporation to

enhance the cooling system's performance, and make use of the wet bulb temperature, but it also requires require large amounts of water. On the other hand dry cooling only uses air fans and does not require water to cool down the system, but it can only make use of the dry bulb temperature, and so, using it will normally imply a cut back on the cycle's performance [20], [45].

As CSP plants operate similarly to conventional thermal power plants, there is the possibility of using fossil fuels in combination with solar heating to generate power in the plant, which can also help to produce reliable peak-load supply, even during less sunny days (with the exception of the parabolic dish technology which many times use stirling engines). This has been done up to now typically using a backup boiler, though in some cases CSP circuits have been used as secondary system to aid in the steam generation of thermal power plants [46]. Theoretically it can also be used to power gas turbines as the ones used in combined cycles [42].

2.2.1 Parabolic Troughs

CSP plants using parabolic troughs are the most mature CSP technology. Through plants form the bulk of commercial plants currently installed [47]. These systems consist of parallel rows of reflecting mirrors (e.g. 100 m long), curbed as a parabola in one dimension (e.g. 6 m across), so that all the light that hits the mirrors is reflected into the same line (in this case the absorber). These absorbers, placed inside an evacuated glass envelope, are covered with a selective coating allowing high levels of energy to pass into the working fluid that runs inside the tube that at the same time does not allow the outflow of energy into the surrounding environment. The result is that only a small amount of infra-red radiation is emitted by these pipes. The troughs are usually designed to track the sun along one axis, predominantly north-south [13]. This configuration is used to increase the performance of the solar field during the morning and afternoon, aiming to match the demand profile. Using this orientation with a one-axis tracking, the cosine effect originates some energy loss during the middle of the day [48]. The cosine effect refers to the losses originated by the mirrors not being aligned with the normal to the incident solar rays [49]. The apparent area of a mirror reflecting off-axis is reduced as seen from the sun, according to the cosine of the incidence angle [50]. The working fluid can be steam, synthetic oil, or molten salts, though, parabolic plants generally use oil, as the investment hasn't been done to operate one using molten salts directly through the glass receivers. As most of these plants use synthetic oil, their maximum operating temperature is ~400ºC [11]. Currently trough plants concentration factor is between 60-80 times [51]. Peak solar to electricity conversion efficiency is between 14-20%, annual solar to electricity efficiency conversion between 11-16% [52].

2.2.2 Linear Fresnel

Linear Fresnel plants are very similar in concept to the parabolic troughs, being the major difference the way that the reflecting mirrors are mounted. Instead of parabolic mirrors as in the trough system, long flat or slightly curved mirrors are mounted near each other to reflect the sun's ray onto a downward–facing linear fixed receiver like a Fresnel lens [42]. The main advantage of such linear systems is the lower costs, as mirrors are easier to manufacture and space usage is smaller. As the concentration factor is lower than in troughs (this mirrors as a whole do not perform as well as parabolic mirrors), lower temperatures are achieved with the fluid passing through the receivers, reaching ~250/300ºC [42]. These lower maximum temperatures imply lower efficiencies of the Rankine cycle receiving energy from the solar field, but this means that less expensive materials can be used. Due to this lower temperatures, these facilitates also use water as the working fluid for direct steam generation, eliminating costs by not having to re-circulate other heat transfer fluids and not having heat exchangers, as the steam produced inside the absorbers goes directly into the Rankine cycle. Linear Fresnel plants concentration factor is between 60-80 times [51]. Peak solar to electricity conversion efficiency is ~18%, and annual solar to electricity efficiency conversion is ~13% [52]. Tough, recent advances in this technology – new conceptual design at the optical level of the solar field [53] and even at commercial level [54] – are improving it for the operation above 500ºC in combination with the usage of molten salts, allowing the reduction of the LCOE. Improvements on the optical aspects of Fresnel like the CLFR-EM and the LFR SMS XX concepts using an improved primary and secondary design which can achieve an optical efficiency in the range 70-72% and concentration values in the range of 50 up to 74 [55], compares to the geometric concentration of 26 that is achieved by parabolic trough collectors. This increase in the optical performance makes it possible for Fresnel collectors to achieve high flux and high temperatures, albeit a lower overall efficiency. This improvement could imply that, for a system using molten salts up to 550ºC, a cost of 11cEuro/kWh_e can be theoretically achievable in the south of Europe [56]. A lower cost would even be possible for locations like north of Chile, parts of Africa, Australia and North America.

2.2.3 Solar Tower or Central Receiver

This configuration of CSP technology consists on a central receiver mounted at the top of a tower that receives concentrated sunlight reflected by an array of heliostats. At the top of the tower a working fluid absorbs the radiation that is converted into steam. Operating temperatures reach 800ºC to over 1000ºC, and because of that it can theoretically be used with a gas turbine. This option increases the efficiency at which the heat is converted into electricity, reducing costs of thermal storage [11]. To date, the heat transfer fluid in this type of CSP plants consisted in water/steam, molten salt and air. Existing power plants of this sort are in the range of the MW's. Solar towers plants concentration factor is between 600-1000 times [51]. Peak solar to electricity conversion efficiency is between 23-35%, and annual solar to electricity efficiency conversion between 7-20% [52]. This technology has the potential to

surpass parabolic and Fresnel plants as it allows higher operating temperatures, at acceptable costs.

2.2.4 Dish-Stirling or Parabolic Dish

This technology concentrates the sunlight into a receiver that is at the focal point of the dish. A fluid or gas is heated to approximately 750 ºC. The entire apparatus tracks the sun. Most dishes use an independent small piston or Stirling engine, or a micro turbine to generate electricity, which eliminates the need for a heat transfer fluid and a cooling water system [51]. Dishes offer the highest solar to electric conversion performance, though their installation costs are still quite high, and not much investment has been made on this technology comparatively to troughs and towers. Though, theoretically technically this CSP dish technology can compete more easily with PV models as dishes they have a compact size comparatively with troughs and tower system, and are more modular. Each dish normally is limited in size being its output in the order of the kW. Parabolic Dishes concentration factor is between 600-1000 times [51]. Peak solar to electricity conversion efficiency is between ~30%, and annual solar to electricity efficiency conversion between 12-25% [52]. Until now it lags behind all the other three main CSP technologies [42].

2.2.5 Key Players

Large private corporations invest in CSP technology (e.g. Abengoa, BrightSource, Flabeg, Schott) [8]. International bodies like the International Energy Agency or the European Commission (EU) have issued reports on CSP as being an option to help reducing climate change. Several research institutes around the globe have dedicated groups working on this topic also, as the German “DLR”, the “Spanish Research Center for Energy, Environment and Technology” (CIEMAT), NREL or the Australian Commonwealth Scientific and Research Organization (CSIRO) are examples. Dedicated cooperative networks and organizations to the advancement of CSP also exist, as it is the case of SolarPACES sponsored by the EIA.

2.3 CSP+D: Physical Performance Overview

When combining CSP with a desalination technology the most important design parameters may differ significantly from site to site, so there is no standard optimum configuration [6]. The most important parameters are the different nominal performances of the solar field (determined by the latitude that defines the nominal solar incidence angle) and the salinity of the water to be desalted which has a big impact on the performance of RO units, something that does happen with thermal desalination technologies. Ambient temperature, relative humidity have also a role to play on the decision of the technologies to choose (impacting mainly on steam pressure obtained at the Rankine cycle condenser, and in some extent heat losses to the surroundings), but not as important as nominal solar irradiance and seawater salinity.

Comparing both MED and MSF, it is clear that MED has a lower cost and it is more efficient regarding electricity and thermal energy consumption, as it requires steam at lower pressure, and having less impact on the electric production cutback. Comparing MED with RO, at the first glance, RO might be considered as the preferred one, due to the relative lower cost and primary energy consumption [12]. Though, if MED is coupled to a CSP power plant the analysis may change. The MED plant will replace the cost of a condensation unit of the steam cycle and will use waste heat from the electrical power generation, as part of the steam that it requires to operate. In this case the steam that is taken from the electrical production should be accounted as primary energy used for desalination, as the remaining can be considered free waste heat that the power plant would reject anyway [6].

Most studies comparing RO with thermal desalination, consider RO a better choice, though analyzing the combination of CSP and desalination, this opinion changes. From the detailed study executed in 2007 by the Institute of Technical Thermodynamics, from the DLR [6], CSP+MED may have a slight advantage over CSP+RO. From their analysis on the performance of CSP+MED versus CSP+RO in 7 locations in the Middle East and North Africa (MENA) region, CSP+MED had between 4 and 11% better performance than CSP+RO. Similar conclusions were taken from another study also performed by the DLR [57]. Tough, other reports have a contradictory opinion, mentioning the better performance of CSP+RO compared with CSP+MED [58].

Depending on the location where the plants are needed, the optimum combination may vary. In general the feasibility analysis of combination of CSP and desalination technologies is in an early stage, with no plants operating up to now like that. There is no definitive answer on which would be the best option, and accounting the state of the art at the moment it would be premature to choose one solution over the other as a standard.

2.3.1 Projects: High Temperature Solar + Desalination

Not many real experiments were made to test the actual performance of CSP plants and desalination technologies combined. At the PSA, two relevant projects took place were MED and RO systems were tested. These projects consisted in using solar energy systems similar to the ones that could be used in CSP plants, to power different types of desalination systems. They were called the Aquasol and the Powersol projects respectively, and were executed during the last decade. It is important to notice that the PSA is one of the leading research locations worldwide for the development of CSP technologies.

Aquasol project

The Aquasol project started in 2002 with a duration of 4 years. Its main objective was to develop MED desalination technology that could be powered by solar energy [59]. The development of an improved Double Effect Absorption Heat Pump (DEAHP), and the reduction to zero of brine discharge were also in the to-do-list.

A 500 m^2 Compound Parabolic Concentrator (CPC) solar collector field, two water storage tanks, and a MED together with a DEAHP using H_2O-LiBr were erected and operated, and subsystems have been modeled to estimate system behavior and develop control techniques for maintaining optimal operating conditions [60]. Results showed that plant specific consumption was in the order of 60 to 70 kWh per m^3 in the solar only mode, and 35 to 40 kWh per m^3 when using the DEAHP (fossil fuel mode only). During the testing was concluded that very reduced thermal losses were happening during operation or at night from the thermal storage system, allowing a simple and flexible operation of the MED plant both with when powered by the solar field or with gas and the DEAHP.

Powersol project

The Powersol project started in 2007 and was assigned to last roughly 3 years. Its objective was to develop for rural communities a shaft power generation technology based on solar heat thermodynamic cycle using low to medium temperatures able to power an RO unit. In this project mechanical energy could be used to directly produce electricity or power an RO unit.

A full technical and economic evaluation of the these technologies was made, the solar heated thermodynamic cycle was modeled, and three solar collectors prototypes to operate at 80ºC , 100-150ºC, and 200-250ºC were developed and constructed (using static flat plate collectors, static CPC and a sun-tracking parabolic trough collector).

Aqaba Hotel & Resort AYLA OASIS project

The DLR study of 2007 on the usage of CSP to power desalination technologies, analyzed the feasibility of a specific case-study: the Aqaba Hotel & Resort AYLA OASIS project. This study was made by a Jordanian/German consortium to assess the economic and technical feasibility of an integrated usage of 10 MW of power to produce, 10 000 m^3 per day of desalted water using RO and 40 MW of cooling for the Ayla Oasis Hotel Resort in Aqaba, Jordan. This project assumed the installation of a linear Fresnel concentrating collector field, with a flat Fresnel structure and the usage of gas boiler to provide steam to a steam turbine. This project aimed to prevent the hotel from buying energy and water from the public grid, to operate compression chillers installed on its rooftop. Additional electricity capacity would need to be installed, equivalent to a natural gas consumption of 85 MW, to produce electricity and fresh water.

The project consisted on the usage of absorption chillers for base-load operation during the holiday season, and compression chillers to be used during the peaking and intermittent demand [6]. The cold water produced by both type of chillers would flow in a cold water district grid connecting the power plant and the different hotel users. According to the DLR study, the usage of such system would require less 35% of fuel input. Better efficiency of combined generation and the solar fuel saver.

The project consists on an installed capacity of 56 MW using natural gas and 14 MW solar, producing a total of 67 MW. From the 67 MW produced, 15 MW corresponded to electric power, 5 MW were used in compression chillers, and 10 MW used as electricity in the local grid. The remaining 52 MW produced in the form of steam at 100 ºC were used for powering an absorption chiller (24 MW input), and an RO desalination plant (28 MW input). The absorption chillers would convert the 24 MW input in 18 MW thermal, and the compression chillers would convert the 5 MW input to 22 MW thermal. The project is currently under construction.

2.3.2 Key Players

One of the most developed groups studying CSP and desalination is based around the PSA in Spain, in collaboration with CIEMAT. Other research groups around the word are now starting to devote time and money to this topic, e.g. governmental institutions like The Cyprus Institute, or private companies like Doosan. Projects around the world start to be announced on CSP+D, namely in the Arab countries where solar resources are immense, and lack of fresh water is a major hurdle.

Low temperature solar thermal desalination is a topic that has been quite explored for decades, but desalination powered by CSP plants has not received much attention and has

only started to become relevant in the last few years. Most of the locations were CSP has been developed are concentrated in two areas of the globe: Southern west part of the USA and South of Spain [11].

Main gaps identified: From the technology overview conducted on the desalination and CSP technologies it is possible to verify that several desalination and CSP plants have been built around the world. Many desalination plants also operate in cogeneration with thermal power plants, which use the same power cycles installed in CSP plants. Though, more research needs to be conducted on the coupling of CSP with desalination processes for cogeneration of fresh water and electricity, as not enough data exists to understand how these two types of plant would behave in cogeneration.

2.4 Desalination: Simulation Tools

2.4.1 MED Software Packages

From the literature research several software packages were found that could simulate the economic and/or the physical performance of thermal desalination plants. These tools can be separated in three different groups. In the first group are the models used for pre-design analysis, e.g. the Desalination Economic Evaluation Program (DEEP) developed by the International Atomic Energy Agency (IAEA) [61], the Thermal Desalination Processes (TDP) developed at the Kuwait University [18], the Solar Desalination System (SDS) developed by by the Suez Canal University and Seville University [62], the WTCost© Model developed in partnership with the U.S. Bureau of Reclamation [63]. In the second group are the programs built for detailed design of a particular configuration of a plant, e.g. IPSEpro developed by the SimTech group [64]. The third group consists of the tools built for training of desalination plant crews, e.g. GSE Systems' JPro developed by GSE Systems [65].

Main gaps identified: Although at least one software package was found during this literature research that is capable of simulating desalination processes for pre-design stage in cogeneration with CSP plants (SDS), its source code was not freely available. This model is also not regularly used by other entities as a reference for evaluation of MED systems, contrary to what happens with SAM, which is a reference for pre-design assessment of CSP plants.

2.4.2 MED Models

There are several models in the literature that are described as being able to simulate MED processes as some are described in [66] and [67]. Most are described for steady-state conditions, while only a few attempt dynamic simulation. The models developed by H.T. El-Dessouky and H.M. Ettouney [18] stand out as being one of the most cited and used as reference to build customized versions for steady-state MED models by other authors. Very few dynamic MED models have been published until ~2010, being the one published by Narmine Aly [66] one of the most cited (although it presents several glitches on the mathematical equations presented). Though, very recently new journal articles have been published with more detailed information describing dynamic models [68], [69].

The models from H.T. El-Dessouky and H.M. Ettouney are based on commonly available equations applicable to heat transfer, that can be found in many sources, e.g. [70], [71], [72]. These models from these two authors are nonetheless very useful to get introduced into the thermal desalination topic, as they have also algorithms described in some detail for different MED configurations, including forward feed, parallel configuration and backward feed. They also provide information regarding the simulation of MED plants using a TVC, and information about MED using mechanical vapor compression. From the comparative information available

in the literature, the forward feed and parallel configurations present as being the most interesting as they present a better performance. In fact experimental plants normally follow a forward feed configuration, while commercial plants follow a parallel configuration.

Regarding the MED steady-state models, there are two types described in the literature that vary in the degree of complexity. The first type is simpler, providing a general overview of the performance for a given plant, and have value specially if faced as a learning path to develop more complex models. The second type present a higher level of detail, describing the main thermodynamic phenomenon's affecting the heat transfer process, and can potentially be used during pre-design stage to describe with the required degree of detail the performance of a MED plant.

Simple models:

The most cited model falling in this category is described in [18]. This simple model is described for the MED forward feed configuration only. It assumes equal thermal loads in each effect (which in reality can very significantly on a MED plant), and only accounts for the evaporation process using latent heat transfer. The flashing of distillate and brine are neglected, as it is the sensible heat transfer. The assumptions of this simple model are:

- Constant specific heat, C_p, for the seawater at different temperatures and concentrations
- Constant thermodynamic losses
- Constant heat transfer area
- The vapor flashing is not directly accounted inside the effects
- Feed seawater enters all effects at saturation temperature (except in the first effect, and this energy loss is accounted)
- Equal thermal loads between effects
- Vapors are salt free
- The difference between the condensation and evaporation temperatures are equal to the driving force for heat transfer in each effect
- Saturated steam powering the first effect
- Constant energy losses to the surrounding

The algorithm to apply this simple model is described in detail, and is based on the predefinition of the overall heat transfer coefficients applicable throughout the several effects. The convergence criterion is defined by the variation on the heat transfer area calculated for each cell (for which a tolerance is set). The convergence occurs through an effect of damped harmonic oscillation. The top and bottom temperatures are predefined, as the steam inlet temperature into the first effect and the vapor temperature at the last effect are preset, respectively. As the heat load is set to be equal across effects and the convergence criterion

is set for equal heat transfer areas, the only variables left to change freely during the iteration process are the operating vapor temperatures used by the intermediate effects. During the iteration process the temperature differences between effects are constantly recalculated in each loop, until equal heat transfer areas are obtained between effects. The other inputs necessary to run this simple model are the salinities of the intake water and feedwater, the pretended salinity of the brine produced, and the total mass of distillate that it is expected to be produced by the plant.

This model sets as an input the outlet brine salinity, which in practice bounds the heat load that is possible to extract from the feedwater that enters each effect, and the corresponding evaporation ratios. For example, the higher the salinity, the more energy is possible to transfer into the next effect, as more vapor will be created (and more concentrated will be the brine). The main outputs of this model are the brine and distillate flow rates, brine concentration produced in each effect, heat transfer area required in each effect, intermediate temperature profile across the effects, and total mass of steam required to power the MED plant.

Although the algorithm presented in [18] is correct when is presented in its generic form, the example shown of its application (which is used by most researchers when developing their own version of such model) has a flaw. The description of the iteration process during the recalculation of the intermediate temperature profile across effects is not entirely correct. During the iteration process all the new intermediate temperatures are recalculated using the temperature difference previously calculated for the first effect, instead of the temperature difference that has been calculated previously for each of the corresponding effects.

Detailed models:

There are a few authors presenting detailed steady-state models for MED processes, though the most cited are H.T. El-Dessouky and H.M. Ettouney, which are described in [18] and [73]. These two authors present detailed models for the MED forward feed, parallel and backwards configurations. In particular they describe the routing of the different mass flows of distillate, brine and vapor through the main components of a MED plant, although generically they might not match exactly the commercial MED plant configurations of different manufacturers (there are many different configurations possible in reality). The heat transfer processes are described in detail, in particular describing the evaporation and flashing of distillate and brine. Both the latent and sensible heat are accounted for during heat transfer processes, heat capacity, density, thermal conductivity, and viscosity. The model also describes the main thermodynamic losses in detail: the boiling point elevation of saltwater (the higher the salinity the more pronounced this phenomenon is), the non-equilibrium allowance (the longer the masses of water stay in a given chamber the smaller theoretically this phenomenon), the

impact on the saturation temperature depression of pressure losses associated with the vapor flow through the demister, the transmission lines, and vapor condensation inside the horizontal tubes (main tube bundle of each effect). It assumes equal heat transfer areas between effects (the standard practice in the industry), energy losses of brine and distillate flowing through the connecting tubes according to their velocity and material of the tubes, and the impact of the non-condensable gases on the heat transfer coefficient of both the evaporators and feedwater preheaters. It neglects the thermal losses to the surroundings, assumes that the vapor produced is salt free and that the heat exchange efficiency is constant across the different heat exchangers simulated. It also assumes an average temperature between inlet and outlet of each stream when calculating proprieties of the streams inside the different effect's chambers. Both the simple and the detailed models do not account steam consumption to eject NCG, but describe the operation of a MED plant with a TVC if pretended.

When these models are described only the ruling equations characterizing the heat transfer process are presented, while the algorithms to implement them are not explicitly revealed. Some of these models are presented together with diagrams describing in a generic form their algorithms, but without enough detail to understand exactly how it does actually operates. Input variables, parameters required and intermediate loops necessary to reach equilibriums inside the main iterative block are normally not well indicated. In particular, the detailed models from H.T. El-Dessouky and H.M. Ettouney mentions that the highly nonlinear equations that form their models are solved by a modified fixed point iteration technique that the same authors developed for a similar model applied to MSF plants [74]. Though, the journal article that describes the solver applied by these authors also has several glitches regarding the equations presented, adding to the fact that some are not well described regarding their origin or description of the variables that they actually use, becoming very hard to understand how to actually implement such mentioned solver.
The models developed by H.T. El-Dessouky and H.M. Ettouney make use of detailed equations to calculate the overall heat transfer coefficient in each effect and down-condenser, instead of using splines to estimate it, though, again the algorithm they use is not easily understandable. The same strategy is also used by other authors (e.g. [75]) that also developed detailed models (where the solution algorithms are also only described using generic diagrams).

From these detailed MED models and possibly experimental data, H.T. El-Dessouky and H.M. Ettouney developed splines to describe the overall heat transfer coefficient applicable to all the effects and down-condenser ([18], [73]), which have been used frequently by other researchers to calculate this parameters in their own MED models (e.g. [36], [67], [76]). These splines are theoretically applicable to any of effect or down-condenser (one single equation applicable to effect 1 to n, and another equation for the down-condenser), using only as input

the operational vapor temperature of the heat exchanger being addressed. The development of splines to calculate the overall heat transfer coefficient was not exclusively performed by H.T. El-Dessouky and H.M. Ettouney, as other researchers did similar work (e.g. [77], [78]). There were also other researchers that used their own experimental facilities (as it happened at PSA in Spain) to obtained dedicated splines for the overall heat transfer coefficient of each individual effect ([79], [80]). These researchers calculated a spline for each effect in particular, instead of a spline that could be theoretically used for any of the effects of a MED plant.

Detailed inputs are required to calculate: the overall heat transfer coefficient without using splines; the pressure losses across the different paths of the vapor through the MED plant; and the pressure losses of the brine as it flows through the connection tubes. In particular it is necessary information regarding sizing of individual components, which are normally not available during pre-design stage (e.g. shell diameter of each effect, type of material used, length of the tubes used for the heat transfer, diameter of tubes used for connection tubes between effects, pretended velocities of different mass flows at nominal conditions).

Main gaps identified: Several authors have published books and journal articles referring the development of models that can be applied to simulate the MED process. In most cases these sources present the ruling equations used in each of the models, though few present the actual algorithm used to model the MED process, and without this information it is not possible a strait forward replication of such models by other researchers. Also some of these models make use of detailed inputs that are not available during pre-design stage (e.g. shell diameter of the evaporators, tube length), to calculate the overall heat transfer coefficient, and pressure losses of the different mass flows inside the MED plant.

2.4.3 Steam Ejectors Models

Although steam ejectors used in MED plants can be categorized as auxiliary devices, they can have a critical impact on the overall energy consumption of the plant, especially the TVC. The NCG steam ejectors consume much less steam, but nonetheless they still can represent a significant percentage of the steam consumption (e.g. ~6% [28]). As their operation is intrinsically connected to the operation of the MED process and the power source providing the whole plant motive steam (e.g. the Rankine cycle), they cannot be neglected when simulating the operation of the MED.

There are a few models in the literature that describe the operation of steam ejectors, though many of them require detailed inputs to be run (e.g. [81], [82]). In particular they require inputs that are only available during design stage, e.g. the pretended gas velocities through different sections, diameter of intake, or diffuser and nozzle efficiencies. Few models were found that could describe the operation steam ejectors using few inputs and still return

outputs with enough quality for a pre-design stage analysis, namely using only information regarding the pressures and mass flows used (assuming optimum configuration designs under those conditions).

Only two models were found in the literature that could fit this criteria described in [18] and [82]. These semi-empirical models presented by El-Dessouky are based on data gathered from several ejector manufacturers that evolved from previous works performed by other authors.

One of these empirical models is based on data and methods presented by Robert Power in [83]. In this semi-empirical model the curves used in the calculations represent smoothed data from several sources. This semi-empirical model uses data for steam ejectors using compression ratios up to ~4, which is below the ratios found at least in the only commercial TVC plant to which it was possible to have extensive access to detailed data during this work (gathered through a technical visit and from the literature): the Trapani TVC-MED parallel plant [28]. According to the author the method is most accurate for motive steam pressures above ~5.2 barg, and agrees with manufacturer's data within 10% over the best-fit range. El-Dessouky mentions that the correlations are valid between 35 bar and 1 bar, entrainment ratios entrainment ratios below 0.25, compression ratios bigger than 1.81 and temperatures above 10 ºC [18]. The outputs of this semi-empirical model when compared with data gathered from ejector manufacturers during this work (Koerting A.G. and Kinetic Therm), shown deviations between ~ –25% and ~ -50% for the majority of the data points available.

The other semi-empirical model is based on three sets of design data gather from different steam ejector manufacturers and data from the literature. The main output is the entrainment ratio (ratio between the mass of entrained gas and motive steam). The model requires inputs for the operating pressures, and uses a set of constants that change according to the compression ratio that is aimed (ratio between the discharge and entrainment pressure). Compression ratios above 1.8 sets the model for choked flow, and below 1.8 sets the model for un-choked flow. Using the output for the entrainment ratio, the model allows an easy calculation of the areas necessary for the nozzle outlet and diffuser. The outputs of this semi-empirical model when compared with data gathered from ejector manufacturers during this work (Koerting A.G. and Kinetic Therm), shown deviations of more than 100% for many of the data points available.

Main gaps identified: Most steam ejector models applicable to MED plants require detailed inputs that are not available during pre-design stage. Only two semi-empirical steam ejector models were found that could potentially be used having only inputs for the operational pressures and mass flows. Though, the outputs from such models do not match the data obtained from ejector manufacturers that was gathered during this work. The semi-empirical

model that return better results when compared with real ejector data (based on Power's data [83]), was also developed using ejector data with compression ratios up to ~4, and from the data obtained from real plants in this work, at least some of them operate steam ejectors at much higher compression ratios (~8/9 [28]).

2.4.4 RO Software Packages

Similarly to thermal desalination, several software packages are available to simulate RO processes. These computer programs found during this literature research were built to perform simulations during design stage. Some of them allow the simulation of CSP in cogeneration with RO processes, e.g. IPSEpro, or the Solar Desalination System developed by the Suez Canal University and Seville University [62]. These in particular are either proprietary, and/or the source code was not available freely.

The remaining software packages found that are capable of simulating RO processes, are not capable of assuming the operation of RO plants powered by CSP. Though, contrary to thermal desalination processes, several RO membrane manufacturers made available detailed simulation tools that are free to access and use [22]. The software released by these companies is updated regularly, well documented and used frequently by many RO plant designers, operators and consultants. The main drawback is that although detailed documentation is available, only the ruling equations used to construct the models used by these software packages are described in their manuals. The actual algorithms are not presented, neither the source code. Examples of such software are the Reverse Osmosis System Analysis (ROSA) program developed by the Dow Chemical Company [39], Toray Design System (TorayDS2) from Toray Industries, the Membrane System Design Software (Winflows) from General Electric, or IMSDesign from Hydranautics. Other software found on during the literature review was developed by university research groups as the Solar Desalination System (SDS) developed by by the Suez Canal University and Seville University [62], the WTCost© Model developed in partnership with the U.S. Bureau of Reclamation [63], or the The Desalination Feasibility Cost Planning Model (WRA RO Model) developed by the Water Resources Associates [84].

Main gaps identified: The software found to be freely available to be used and capable to simulate the RO process and return reliable results is not able to simulate the operation of RO plants in cogeneration with CSP.

2.5 CSP: Simulation Tools

Several models and software packages have been built to describe the functioning of CSP power plants. Some of these models can evaluate the performance of only part of the CSP plant, as for example the power cycle, or the central receiver performance individually [17]. Other models do a more complete analysis of the whole power plant, allowing the simulation of different type of technologies.

Two kinds of computer programs dominate today as tools for the simulation of CSP systems. The first are codes that come along with predefined types of CSP technologies, were the user specifies a relative small number of parameters. Normally with these programs it is possible to easily execute parametric and sensitivity studies for operation periods of one year for example. [85]. This first group of programs for CSP analysis is designed to be used during pre-design stage, when the generic performance of a technology is assessed, and not the performance of a specific configuration of a particular technology [16] (e.g. SAM developed by NREL, and Greenius, or INSEL, these two last developed by the DLR). The second group of software consists of detailed simulation tools. They normally use specific libraries describing each of the components within a CSP plant, and are used for detailed design after the selection of which type of technology to be used has already been done, and require much more detailed information to run (e.g. IPSEpro). They can be used for parametric and sensitivity analysis, but only with the aid of an external tool.

From the analysis made during this work to the software capable of simulating CSP plants for pre-design stage, SAM presented as being the most versatile, up-to-date, well documented, and free to use.

System Advisor Model (SAM)

SAM was built by NREL and the Sandia National Laboratories, both from the US Department of Energy. This model allows users to analyze the physical and economic impact on a plant when changing variations of physical and financial parameters. Today the latest version of SAM allows the evaluation not only of CSP plants, but also PV and generic fossil fuel plants. The model also allows the user to perform parametric and sensitivity analysis to the results. Detailed outputs include the system efficiencies, net and gross electrical production, levelized costs of electricity, return on investment, system capital and operation and maintenance costs [86]. The primary goal of the model is to enable the user to conduct a complex sensitivity analysis, with multiple cases for a single project during pre-design stage.

Until recently, SAM used a technical performance engine to calculate on an hourly base the performance of CSP plants, based in TRNSYS, a tool designed to simulate the transient performance of thermal energy systems, which runs in the background. The hourly output values of the plant are calculated and added to obtain the system’s annual electric energy

output [20]. This value is passed afterwards to the cost, incentive, and financial modules to calculate the annual cash flows, levelized cost of energy, amongst other metrics.

The user does not need to know how to work with TRNSYS as SAM has a graphical user interface (GUI). Physical parameters can be defined within SAM's GUI (e.g. the pretended installed capacity, the location for the plant, the type of mirrors and their efficiency, or the cooling technology used).

TRNSYS

The TRaNsient SYstem Simulation (TRNSYS) is a flexible tool designed for the simulation of transient performance of thermal energy systems. TRNSYS was initially developed through a collaboration between the University of Wisconsin (through the Madison Solar Energy Lab) and the University of Colorado Solar Energy Applications Lab [87]. The program exists for more than 35 years, being its source of success its open and modular structure. TRNSYS uses Fortran language, a widely used programming language since the 1950's when it was first created. Because of the extensive existing content and existing validation of individual components, TRNSYS was chosen as the performance engine for SAM until recently [86].

This model has its own GUI (although it is not used in SAM), allowing drag-and-drop arrangements and editing of components icons. Also post-processing through the GUI and reporting is available [17]. In TRNSYS the component represent a physical process or feature in the system, and can be added and developed as needed. A text based input file is read by the components, providing a solution of algebraic or differential equations as output. TRNSYS has the ability to use two types of methods for solving coupled system of algebraic and differential equations: the "successive substitution" method and the "Powell's" method [87]. There are several components available, namely 80 standard components, and add-on libraries offering over 300 other components Lab. Specific processes can be modeled for subcomponents of the total system, and total system performance analysis can also be performed [17]. TRNSYS is a reference tool in many studies made both on solar thermal as it was noticed during this literature review.

It is important to mention that there is a library created in TRNSYS for the simulation of CSP plants, developed through an international collaboration agreement and released freely to the public by the SolarPaces organization [88]. Though comparatively to SAM, the models included on the STEC library are not as detailed.

Main gaps identified: None of the models found are capable of simulating CSP plant during pre-design stage working in cogeneration with desalination processes. These models also do

not have the option of simulating the operation of a CSP plant using a once-trough seawater cooling circuit instead of wet or dry-cooling.

3. MED Models: Development and Validation

This chapter presents the development and validation of the following models:

1. A simple physical MED model for forward feed configuration;
2. A detailed physical MED model for parallel and forward configuration;
3. A simple empirical steam ejector model (auxiliary process);
4. A simple physical pumping model (auxiliary process);

Two MED models were developed in this work for the simulation of MED plants: the first was based on the simple MED forward feed model developed by H.T. El-Dessouky and H.M. Ettouney, which acted as a learning path to develop a second more complex and detailed MED model. The MED detailed model was developed for two main configurations – parallel and forward feed, and because of that, two subchapters were devoted to describe each in detail. The main auxiliary systems were modeled to simulate the energy consumption when running a MED system, namely: steam ejectors (applicable to the TVC and NCG removal); and pumps related to the intake of feedwater, outlet of brine and storage of distillate.

The validation of these models was performed using data available in the literature and gathered during visits to real plants.

These models were developed aiming the integration in SAM (that is able to simulate the operation of CSP plants). As CSP plants have inherently a higher degree of irregularity of its operation when compared with conventional fossil fuel power plants, their daily operation will probably require some degree of throttling and/or standby and shutdown procedures of the power cycle. Due to the potential small startup times for MED plants from hot standbys (ranging from ~30 minutes to one hour), it was considered that a steady-state model could return good results, especially if the MED plant could be downsized compared with the CSP plant installed capacity (in order to operate the MED plant more frequently near design conditions). SAM uses a time resolution of one hour (although it can be set for a higher resolution), matching the weather data that is available from popular sources (e.g. Meteonorm, or Energy Plus from the US Department of Energy). Real MED plants opearte using a fine equilibrium of pressures set in cascade between all the effects. The throttling of MED plants is possible: between 20-110% of the heat load entering the plant when using a MED low temperature configuration and 50-110% when using a TVC-MED configuration (information gathered informally from SIDEM – own by Veolia corporation and one of the leading firms designing and building commercial MED plants for more than 40 years). Although MED plants can operate in part load within a large range it is recommended to perform throttling slowly, so that it is possible to maintain the dynamic equilibrium of cascading pressures between effects (which is critical for a continuous operation of the process). Although the effects are directly connected to each other, the gas phase of one

effect is not directly connected to the gas phase of the following effect. The pressure equilibrium in each effect is set according to the evaporation rate that is achieved in the previous effect and the condensation rate of that same vapor inside the tube bundles (as it flows across the plant). This is obtained pumping more or less feedwater through the tube side inside each effect, and throttling the amount of motive steam input into the plant, to achieve a balance between condensation and evaporation across the effects.

The operation of MED plants with steam ejectors adds a degree of complexity, as these systems are required to operate in equilibrium with the MED process. In this work the steam ejectors were modeled for steady-state conditions for the same reasons presented before for MED models. Also, it would probably be very difficult to obtain from the ejector manufacturer's more detailed information describing the ejectors operation at part load operation (note that the data obtained in this work from one of the leading steam ejector manufacturer is referent to different ejectors, all at design conditions, and does not refer to part load operation of the same ejector).

3.1 MED – Simple MED Model

3.1.1 General Description

This model is based on the work presented by El-Dessouky and H.T. Ettouney in [18]. The MED simple model has relevance mainly for academic purposes. Despite of all the simplifying assumptions that it uses, this simple model allows an easy path to the understanding of the physical processes inside MED plants, and it is a good starting point for the development of more complex models. Only a small number of basic inputs referring to the operation of the MED plant are required to run this model versus more complex ones. This feature might be interesting in case absolutely no information is available, and/or the user does not have a deep knowledge regarding the design and operation of MED plants.

As mentioned, this simple MED model makes several assumptions that limit the accuracy of its results, especially because of: 1) the assumption that the feedwater will always reach the first effect in saturated conditions, 2) no energy losses occur to the surroundings, and 3) all effects have equal thermal loads. The algorithm describing the way the model reaches convergence is described in the literature, section 2.4.2.

It is important to note that this model is only applicable to MED plants with forward feed configuration, while most commercial plants use a parallel configuration. The inputs to this model refer to the inlet and outlet temperatures entering the system, the mass flow of motive steam, the overall heat transfer coefficient for the first effect and its rate of decrease across subsequent effects. The main outputs are referent to the total mass flow rate of feedwater and cooling water used; total mass flow rate of distillate and brine produced; and brine temperatures inside intermediate MED effects.

3.1.2 MED Forward Feed: Mathematical Model and Algorithm

The simple MED-FF model is a modification of the model described in [18]. The original model uses the mass of distillate output from the plant as an input and the mass of motive steam required as an output. On the other hand, the model described in this work uses the mass of motive steam as input and the mass of feedwater as output, allowing its use with SAM for the simulations considering the cogeneration with CSP plants.

The main parameters, inputs and outputs necessary from the adapted model are presented in Table 2.

Table 2 - Inputs, parameters and outputs from the mathematical simple MED-FF model.

Parameters	Inputs	Outputs	
n	M_s	A_c	Q_c
T_n	T_s	A_e	T_i

$T_{BPE\ loss}$	T_{sw}	B_i	T_{vi}
T_f	X_{sw}	D_i	U_c
Tol	$Q_{extra\ loss}$	M_{sw}	X_n
U	$\Delta T_{preheat\ loss\ (1st\ effect)}$	M_d	
X_b	U_reduction	GOR	

Comparing the model used in this work to the simple MED model from [5] in which this work was based on, the main differences lies on: 1) the usage of the mass of distillate (M_d) as an output and the mass of steam (M_s) as an input; 2) accounting the losses to the surroundings; and 3) accounting the energy losses with the feedwater preheating inside the first effect. The main equations considered to model the MED system in this work are described below.

$$B_n = \frac{X_f}{X_n - X_f} \times M_d \tag{1}$$

$$Q_1 = Q_2 = \cdots = Q_{n-1} = Q_n \tag{2}$$

$$\Delta T = \Delta T_s - T_n = \Delta T_1 + \Delta T_2 + \cdots + \Delta T_{n-1} + \Delta T_n \tag{3}$$

$$\Delta T_1 = \frac{\Delta T_t}{U_1 \times \sum_{i=1}^{n} \frac{1}{U_i}} \tag{4}$$

$$\Delta T_i = \Delta T_1 \times \frac{U_1}{U_i} \tag{5}$$

$$T_i = \Delta T_{i-1} - \Delta T_1 \times \frac{U_1}{U_i} \tag{6}$$

$$D_i = D_1 \times \frac{\lambda_{v_1}}{\lambda_{v_i}} \tag{7}$$

$$M_d = D_1 + D_1 \times \frac{\lambda_{v_1}}{\lambda_{v_2}} + \cdots + D_1 \times \frac{\lambda_{v_1}}{\lambda_{v_{n-1}}} + D_1 \times \frac{\lambda_{v_1}}{\lambda_{v_n}} \tag{8}$$

$$D_1 = \frac{M_d}{1 + \lambda_{v_1}\left(\frac{1}{\lambda_{v_2}} + \cdots + \frac{1}{\lambda_{v_{n-1}}} + \frac{1}{\lambda_{v_n}}\right)} \tag{9}$$

$$B_1 = M_f - D_1 \tag{10}$$

$$B_i = B_{i-1} - D_i \tag{11}$$

$$X_i = \frac{X_{i-1} \times B_{i-1}}{B_i} \tag{12}$$

$$A_i = \frac{D_i \times \lambda_i}{U_i \times \left(\Delta T_i - \Delta T_{bpe\ loss}\right)} \tag{13}$$

3.1.3 Model Calibration and Validation

MED plant at PSA

The MED forward feed desalination plant at PSA was used to validate and calibrate this model. This plant dates back from 1987, and it was made by ENTROPIE [68], [69], [80], [89]. It has 14 effects in vertically stacked. Originally its heat source was low-pressure saturated steam, but in 2005 it was remodeled and now it uses hot water as heat transfer media from a two tank system with 24 m^3 capacity that can be powered by several sources. The heat source used to validate this model was a solar field with 252 CPC panels made by the Portuguese company AO SOL, with a total surface area of 500 m^2, providing hot water to the tanks.

Using the data from the MED plant at PSA

To test the mathematical model described in this section, the MED plant was operated near nominal steady-state conditions, in an experimental campaign during July 2012 at PSA. The access to this MED-FF plant was possible through the EU funded program Solar Facilities for the European Research Area (SFERA). The data used for the validation process is shown in Table 2, and corresponds to the average of 20 minutes of operation for the mentioned plant.

Table 3 - Design specifications of the MED plant at PSA.

	Design values ([68], [69], [80], [89] and direct contact with the plant operator)	**Experimental values**	
		Average Value obtained after 20m in steady-state operation	**Standard Deviation**
Number of effects	14	-	-
Feed seawater flow rate, m^3/h	8	7.99	0.18%
Brine flow rate from the last effect, m^3/h	5	5.59	2.5%
Hot water flow rate, L/s	12	11.941	0.26%
Total distillate output, m^3/h	3	2.39	5.84%
Cooling seawater flow rate at 25ºC, m^3/h	20	22.74 (at 27.2ºC)	0.26%
Heat source energy consumption, kW	200	193	2.00%
Performance ratio	>9	8.01	6.1%
Vacuum system	Hydro-ejectors (seawater at 3 bars)	-	-
Inlet/outlet hot water temperature, ºC	74.0 / 70.0	75.1 / 71.3	0.12% / 0.14%
Brine temperature (on first cell), ºC	68	69.3	0.12%
Feed and cooling seawater temperature at outlet of the condenser, ºC	33	34.7	1.23%
Heat transfer Areas used per effects, m^2	(1^{st}): 24.26 (2^{nd} -14^{th}): 26.28 Pre-heater: 5.0 Condenser: 18.3	-	-

Effects are numbered assuming that the first is the one receiving hot water from the tank's system. The measured versus the calculated temperature profiles across the MED plant during 20 minutes of steady-state operation can be observed in Figure 7.

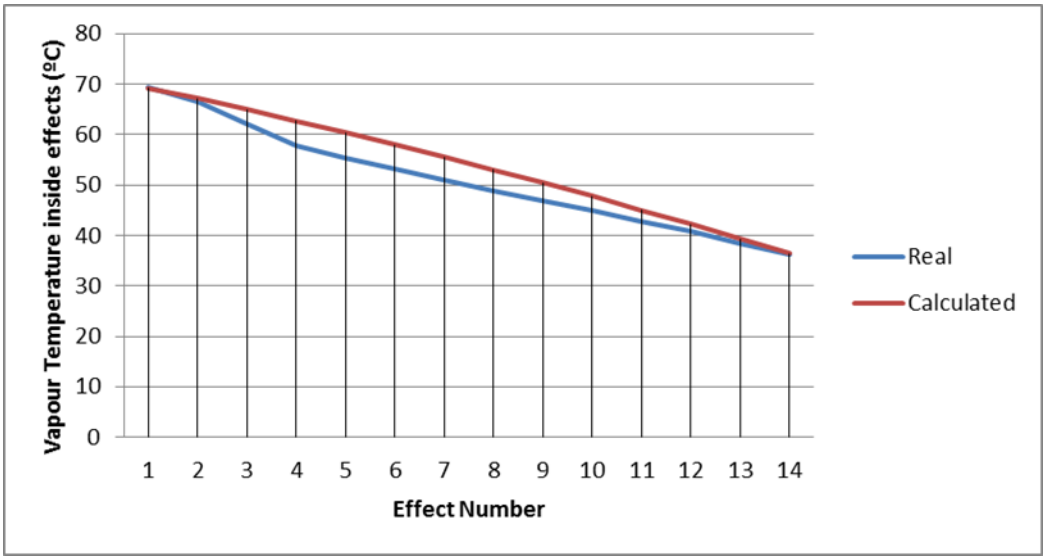

Figure 7 - Real and calculated temperature profile inside MED effects (vapor temperature ºC) at PSA.

The temperature of the preheated feedwater measured in the first effect was in average 67.69ºC, with a standard deviation of 0.58%. The U values used in the model for the MED plant at PSA were obtained using equations from [89] and [80]. Their values ranged from 2.55 kW/m^2.ºC in the second effect to 1.62 kW/m^2.ºC in the last one. The tolerance used to reach equilibrium in the model was 10^{-4}.

Calculated temperatures from both the first and last effects show a good match with the real values. The individual averages for the values measured within the 20 minutes of operation taken into account had a standard deviation percentage below 1.17 %, with the exception of the distillate mass produced that presented a standard deviation of 5.84 %. Also the operational temperatures calculated for intermediate effects presented a noticeable deviation compared to the real ones, though it is very likely that the thermodynamic losses in the first effects were higher than the average value used as input to the mathematical model. These deviations between real versus calculated temperature values go from nearly zero at the extremes, up to a maximum of 8.9 % for the sixth effect at the middle.

No flow meters were available to measure mass flows between intermediate effects. In the intermediate effects only pressure could be measured and only in those effects corresponding to an even number in their counting from top to bottom. Saturated vapor pressure conditions were assumed during operation, and an average for the temperature readings was made between the adjacent effects to calculate the temperature inside the

effects with no readings. As the MED plant at PSA is powered by hot water and not by saturated steam, the mathematical model had to be adjusted to account this.

The original model from [18] also assumes that feedwater enters all effects at saturated conditions, which was not the case for the first effect in this plant. Preheated water enters the first effect at a temperature bellow saturation conditions, although it suffers preheating not only in the down-condenser, but also as it crosses the preheaters of each effect on its way up. Both the mass flows and inlet/outlet temperatures of the fluids passing through the heat exchanger in the first effect could be measured. To assume a more realistic estimation of the heat load input accounting the original mathematical model from [18], extra energy losses were accounted, and subtracted from the overall heat input. These were: 1) the sensible heat actually transferred to the feedwater in the first effect to reach saturated conditions; and 2) an average of extra losses per effect in the MED plant (that in reality are likely to occur mainly in the first effects internally and to the surroundings of the plant). These extra losses per effect will likely be higher in the first effects, as higher temperature differential exists in relation to the ambient air, and also internally higher pressure losses are likely to occur in these first effects due to higher mass flow rates (in the demister, transmission lines, condensation inside horizontal tubes, and inefficiency on the preheaters). The last effects probably produce less distillate as they receive less energy than their predecessors.

The thermal load transferred from the hot water into the plant was in average 193 kW. The heat lost in the first effect to make the feedwater reach saturation temperature was 19 kW (~10%). 174 kW remain to power the evaporation process. If this value is used as input to the mathematical model, the model will oversize both the heat transfer areas and mass flow rates output of the plant by ~50%.

The original mathematical model from [18] assumes perfect conditions, in which all the effects receive the same heat flow, but in reality extra losses occur apart from the average thermodynamic losses initially defined in the model (mainly the BPE). In order to obtain correct values for the heat transfer areas used and distillate mass produced, the original model from [18] requires the usage of 111.5 kW as heat input, instead of 193 kW. Using the heat transfer areas calculated by the model as reference (calculated values versus real data), it was possible to estimate the losses that were not being accounted. The extra losses in the MED process at PSA are assumed therefore to be 62.5 kW (174 - 111.5 kW), equivalent to an average loss per effect of 2.3 % of the bulk energy it would theoretically receive: 193 kW.

Using as input to the model the energy that the MED plant effectively used in the evaporation process (111.5 kW), the calculated average value for the heat transfer areas was 27.64 m^2 per effect, 5.7 % higher than the average for the real areas used in the plant. The distillate mass flow rate calculated was 2.31 m^3/h, ~1 % lower than the experimental data (this variation is below the standard deviation percentage of the experimental data for this variable).

This model is dependent on the accuracy of the overall heat transfer coefficients, as MED plants are formed mostly by heat exchangers. Their value has a strong impact on the calculated heat transfer areas. In this particular case of the experimental MED plant at PSA, detailed formulas to calculate this variable were available, which enabled to maintain accuracy when analyzing this existing plant. The results obtained with the adjustments made with real plant info return interesting results, but it is important to stress that these calculated correction factors are very specific for the MED-FF plant at PSA. Having this into consideration the calculated results show a good correlation relations with the real values, namely, for the top and lower operating temperatures (less than 1% deviation in the first and last effects), mass flows of distillate produced (less than 1% deviation) and heat transfer areas (5.7% deviation). On the other hand the temperature profile of the intermediate effects shown to diverge more, reaching a deviation of 9% on effect number 6. Overall, the model suggests a good correlation between heat transfer areas required and mass flow rate of distillate produced.

3.2 MED – Detailed MED Model

3.2.1 General Description

The model describes the mass and heat flow across the several effects of a MED plant in steady-state conditions taking into account both the evaporation and the flashing of brine and distillate when they enter the different chambers within the MED unit. The model is capable of simulating the operation of a MED system with Forward Feed (FF) or Parallel (P) configuration (with or without cross-flow), predicting the operation of a plant coupled with a TVC or just using steam at low-pressure and temperature (e.g. provided by the exhaust of a condensing steam turbine) to feed the first effect. In the current version of this model, the TVC only entrains vapor from the last effect. Section 3.2.2 describes the MED-Parallel model in detail, and section 3.2.3 the MED-Forward Feed model. Section 3.2.4 presents the validation results.

The main inputs to the model reflect the temperature profile, namely: the top and bottom operating temperatures, the characteristics of the steam and seawater entering the plant (temperature and salinity), the number of effects and the salinity of brine produced in the first effect. The main outputs are: the flow rates and salinities of the different streams flowing within the MED plant along the several stages, the heat load inside the effects and preheaters, the mass flow of steam used to operate the Non-Condensable Gases (NCG) ejectors, the mass of entrained vapor from the last effect if a TVC is assumed to exist, the intermediate temperatures used inside the: distillate boxes, shell side of the effects and mass flows leaving the plant.

The model does not include detailed calculations for pressure losses during the vapor flow in the demisters, vapor transmission lines and vapor condensation inside the tube bundles. The user can set a fixed percentage for thermal energy losses that is applied to each effect. A similar user defined input was also set for the vapor temperature output from each effect. As the model does not calculate in detail heat losses and subcooling during heat transfer in the tube bundles, these variables were introduced in the code so that the user could have some degree of control over these expected losses when simulating a MED plant. The quality of the distillate produced by the MED plant is also considered to be completely salt free by this model. This model can also simulate the operation at steady-state of steam ejectors and auxiliary electric pumps by calling a steam ejector model and a pumping model developed in parallel with the MED detailed model. These two models are described in sections 3.3 and 3.4, respectively.

The physical model is capable of simulating several sub configurations available for MED units, and has been validated with real data from at least three MED plants using different configurations.

For simulations considering the operation of a TVC, the user can define the TVC discharge saturated temperature, or set the model to use the maximum or minimum possible compression ratios that are feasible accounting the remaining characteristics also set for the plant. If the MED plant does not use a TVC it is considered as being a Low Temperature (LT) plant, as it normally will receive steam from the Rankine cycle at low-pressures (~70/60 °C saturated steam). The operation of a two-stage steam ejector system for the removal of Non-Condensable Gases (NCG) can also be simulated. The user can define the location of the intercondensers connected to this auxiliary system across the effects. The model calculates how much motive steam will be necessary to operate the NCG steam ejectors. The code also simulates the operation of plate heat exchangers for pre-heating feedwater entering the down-condenser using the warmer brine and distillate produced by the plant. The model assumes an equally distributed temperature difference between effects, as it is industry practice, and the user has the ability to set the feedwater preheater's positioning across effects. Table 4 presents the list of main configurations possible to be defined for the MED detailed model.

Table 4 – Possible configurations available in the current version of the detailed MED model

Configurations	Options available
Plant configuration:	1. MED-P Low Temp; 2. TVC-MED-P; 3. MED-FF Low Temp; 4. TVC-MED-FF;
TVC strategy:	1. TVC uses the lowest possible compression ratio* ; 2. TVC saturated discharge temperature is user defined; 3. TVC uses the highest possible compression ratio* ; *(calculated by the model);
Steam ejector's model for the entrainment ratio:	1. Empirical model using ratios obtained from steam ejector manufacturer; 2. Empirical model adapted from the work of Robert Power described in [83] and [90]; 3. Semi-empirical model adapted from the work of El-Dessouky [91];
Cross-flow of distillate:	1. No distillate flashes, distillate is not routed between effects; 2. Distillate flashes and flows between effects;
Preheaters configuration:	1. No preheaters; 2. Preheaters between every effect (with NCG steam jet ejectors); 3. Preheaters between every 2 effects (with NCG steam jet ejectors); 4. Preheaters between every effect (without NCG steam jet ejectors); 5. Preheaters between every 2 effects (without NCG steam jet ejectors);
Location of the preheaters powered by the NCG venting system:	1. Number of the effect from where it is assumed that the external preheating of the feedwater will be supported by NCG steam extraction;
Preheaters with plate heat exchangers:	2. The plate heat exchangers are not present; 3. The plate heat exchangers are present;

Figure 8 shows a simplified diagram describing the algorithm used in the MED detailed model (which embeds the steam jet ejector model and the pumping model). More information can be found in Annex 1 where a very detailed diagram is available, together with a list of the main inputs and outputs into the model.

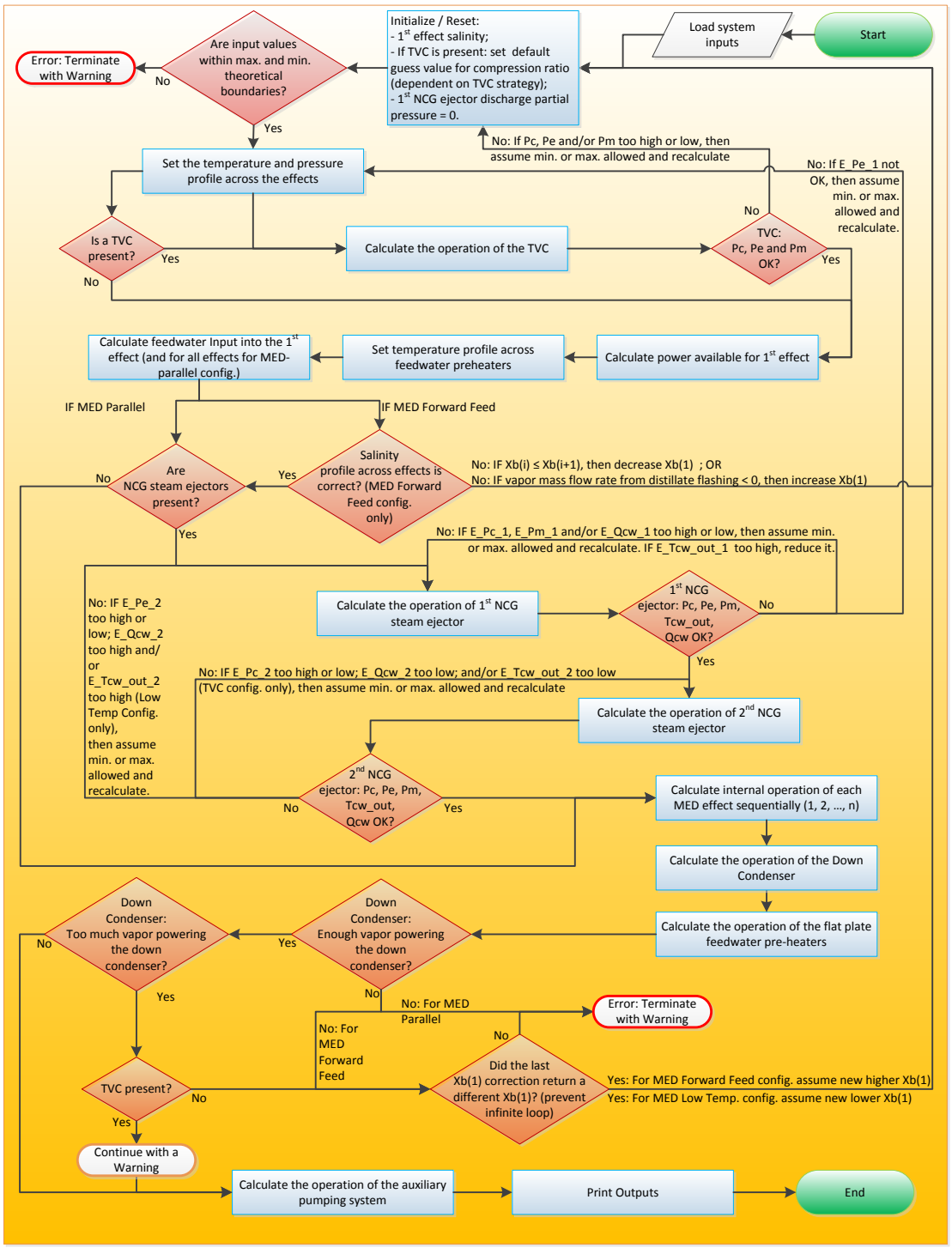

Figure 8 - General overview of the control flow diagram for the detailed MED model

After the inputs are set, the MED detail model operates by predefining the temperature profile across the effects. With this information the operation of the TVC is predicted, in case one is assumed to be present. Knowing the mass flow rate, temperature and pressure of the steam powering the first effect, the model then calculates the heat load powering it. With this value it is possible to calculate the mass of feedwater entering the MED system, in particular the first effect (as the salinity of the brine produced in the first effect is an input given to the model). The mass flow rate of feedwater entering the effects and the temperature profile across effects is then used to calculate the operation of the NCG steam ejectors (in case they are assumed to be installed). With this information a loop is run sequentially from the first to the last effect, calculating how much distillate and brine is produced inside each one. The output of each effect is used as input to the next, until reaching the last one that provides the inputs necessary to calculate the operation of both the down-condenser and the flat plate feedwater preheaters. Finally the operation of the electric pumps is assessed by the model before printing results and ending calculations.

3.2.2 MED Parallel Feed: Mathematical Model and Algorithm

A scheme with the bulk of the MED process considered for the parallel feed configuration in this detailed model is shown in Figure 9 when using a TVC, and in Figure 10 when using a low temperature configuration.

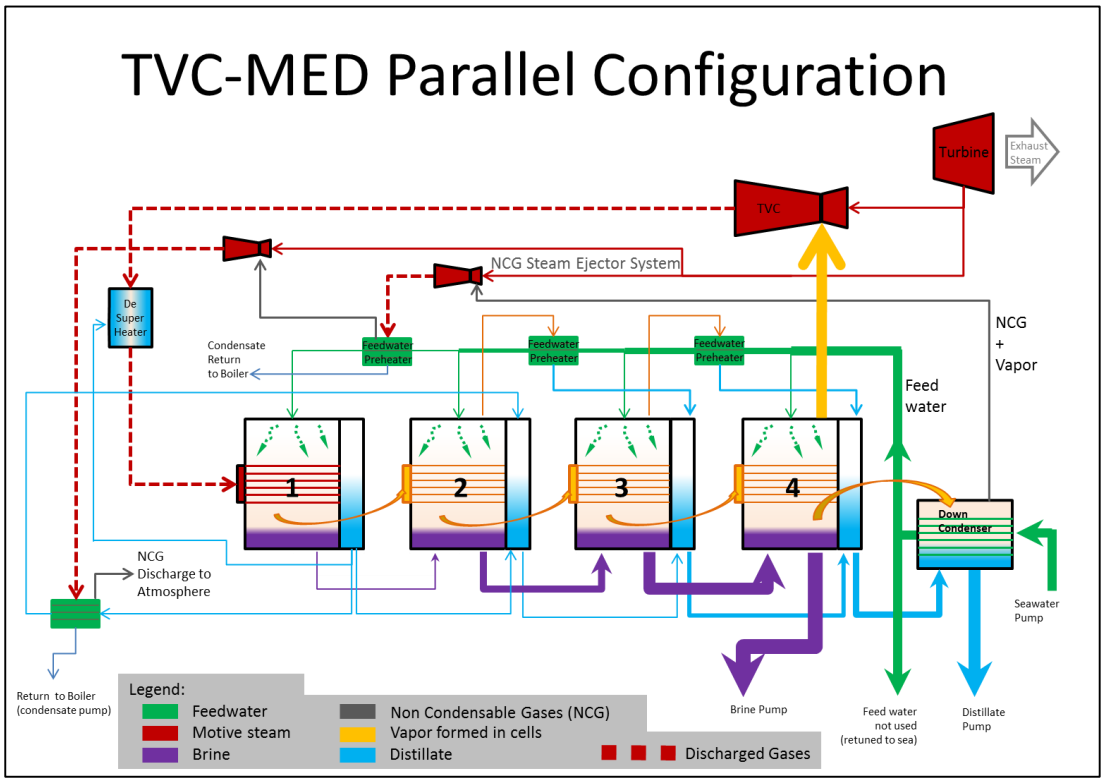

Figure 9 - TVC-MED Parallel generic configuration considered in the MED detailed model.

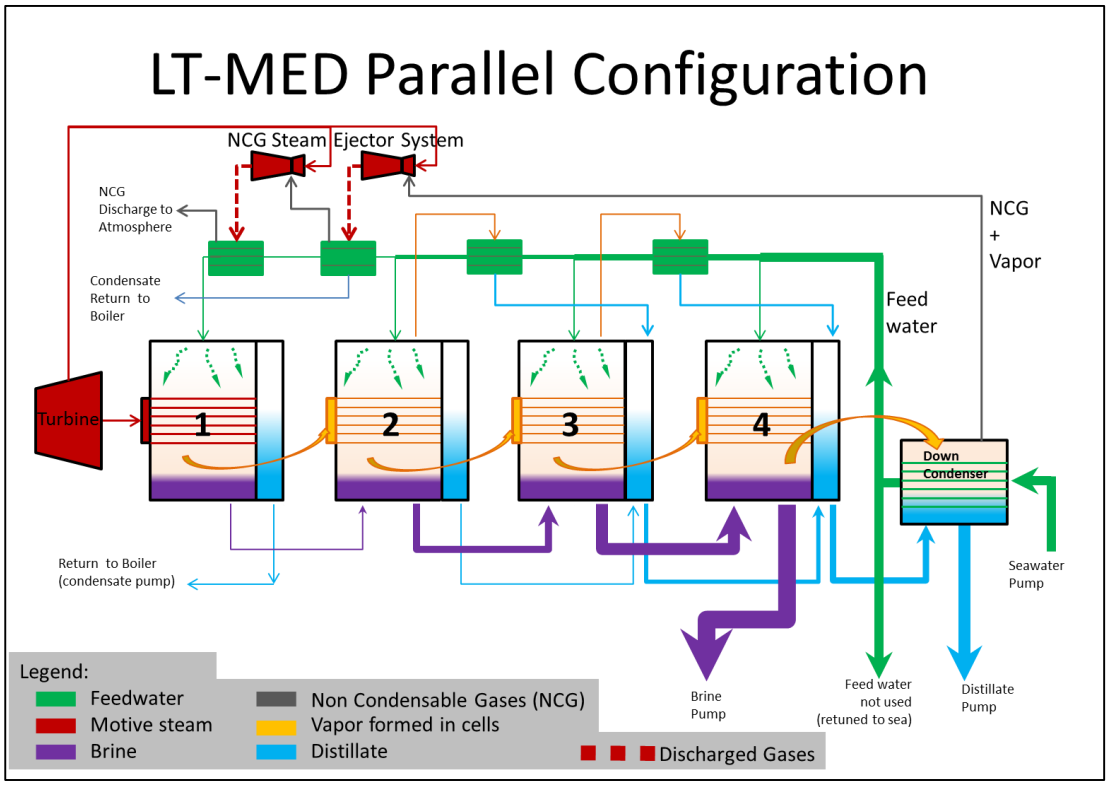

Figure 10 - LT-MED Parallel generic configuration considered in the MED detailed model.

A comprehensive diagram of the algorithm used in the MED detailed model with parallel configuration is presented in Annex 1 where the calculation steps are described in depth.

The calculations start by setting the temperature and pressure profile used to run the model. This is done assuming an equal difference between vapor temperature of adjacent effects, knowing the top and bottom operating temperatures and the number of effects (in this work, subscripts next to variables refer to the number of effects, e.g. $T_{f\ (1:2)}$ refers to the feedwater temperature that enters effects 1 to 2).

Code block 1:

```
Delta_Tv = (Tv(1) - Tv(n)) / (n-1)
```

The boiling temperatures are calculated using the vapor temperature in each effect and the corresponding Boiling Point Elevation (BPE). The BPE is estimated assuming the salinity of brine in all the effects in the plant to be equal to the salinity in the first one (this assumption is only done for the calculation of the BPE, as the salinity of the brine (X_b) in this model is actually calculated for each effect). This is an approximation, as at this stage of calculations, the salt balance for each effect is not known. In practice using a MED parallel configuration

the variability of X_b will be relatively small across effects and between the first and the last effect (~1 wt%), which means that the variation of T_b using a correct X_b versus this approximation with $X_{b\ (1)}$ will be around 0.12 ºC, and it is assumed to be negligible for the calculation of the BPE in this model.

Code block 2:

```
Tb(i) = Tv(i) + BPE_Tv_fun(Tv(i), Xb(1))
```

This model allows the user to define the configuration of the preheaters throughout the plant. The user can define if the preheaters are placed between every effect or between every two effects. The user can also define if the last feedwater preheater (the hottest) is powered by a NCG steam ejection system. It is always assumed that there are no preheaters between effects that receive feedwater preheated by the intercondensers of the Non-Condensable Gases (NCG) steam jet ejectors system. The user defines the temperature difference between the feedwater entering the last effect and its vapor temperature. The temperature profile of the feedwater across effects is then calculated in all effects assuming they will have this same temperature difference between the feedwater and the vapor temperature.

Code block 3:

```
Tf_eph(i) = Tb(i) - Delta_Tf_iph
```

The user can also define that no preheaters are installed, being only considered the existence of a down-condenser. In this case, all effects receive feedwater at the same temperature (meaning that the feedwater temperature for all effects will be the temperature that the user set for the outlet of the down-condenser).

The first effect is the hottest, and has the highest potential for work compared with the remaining effects (in case the plant is assumed to have preheaters attached to every effect). The transfer of energy into the first effect considers the passage of both sensible and latent heat from the steam entering its heat transfer tube bundle.

Code block 4:

```
Q(1) = Ms * (Hs_super - Hs_sub)
```

For the remaining effects only latent heat transfer is considered, meaning that it is assumed that the steam enters at saturated conditions and that no subcooling of distillate takes place. In this MED detailed parallel model not all the heat flowing into each effect is used directly in the evaporation process. Depending on the preheaters configuration throughout the plant, the heat load powering an effect may actually be higher than the

previous one that operates at higher temperature. Such can happen for example if the preheaters are positioned between every two effects.

This MED parallel model assumes that the vapor formation inside the effects occurs due to the physical processes of evaporation and flashing. These take place on the external surface of the heat exchanger tubes (in the shell side of each evaporator), on the brine pool, and inside the distillate boxes. Using a parallel configuration the last effects lose more energy preheating the feedwater (externally) then the first ones, as they need to preheat not only the feedwater they will use, but also the entire amount of feedwater flowing into the first effects.

Code block 5:

```
Q_eph(i) < Q_eph(i+1), for effects with an external feedwater preheater attached.
```

Most of the heat load powering each effect is the result of the mass of vapor that was not used in the previous effect to preheat the feedwater (internally, and externally if a preheater receives vapor from the previous effect).

Code block 6:

```
Q_iph(i) = F(i) * Delta_H_iph(i)

Delta_H_iph(i) = Hb_Tb(i) - Hf_Tf(i)

Q_eph(i) = SUM(F(1:i)) * Delta_H_eph(i)

Delta_H_eph(i) = Hf_Tf_eph(i) - Hf_Tf_eph(i+1)
```

To partially compensate these losses with feedwater preheating, the masses of brine and distillate produced in each effect are routed into the subsequent effect for flashing (if a crossflow configuration is used). As the masses of brine and distillate enter the next effect, part of them will flash and create more vapor.

Code block 7:

```
D_enter_next(i) = D(i), assuming cross-flow of distillate for effects that do not have to route condensate back into the boiler

D(i) = V(i-1) + D_enter_next(i-1), assuming cross-flow of distillate

B(i) = B_evap(i) + B_b_flash_remain(i), assuming cross-flow of brine

B_b_flash_remain(i) = B(i-1) - V_b_flash(i), assuming cross-flow of brine
```

The energy released during the flashing process is equal to the enthalpy decrease of the flashing solution (namely the brine or distillate). This energy is released mainly by the water molecules near the liquid surface, as they overcome the surrounding hydrostatic pressure and surface tension, decreasing the liquid temperature [32], [92]. This energy release is equal to the latent heat necessary to evaporate water at the saturation temperature at which the vapor will be formed in the chamber.

Code block 8:

```
V_d_flash(i) = D_enter_next(i-1) * (Hd_out(i-1) - Hd_d_flash_remain(i)) / LHv_d_flash(i)

Qd_flash(i) = V_d_flash(i) * (Hv_d_flash(i) - Hd_Tv_out(i-1) )

V_b_flash(i) = B(i-1) * (Hb_Tb_out(i-1) - Hb_b_flash_remain(i) ) / LHv_b_flash(i)

Qv_b_flash(i) = V_b_flash(i) * LHv_b_flash(i)
```

As the liquid does not release energy equally across its depth during the time it flows through the chamber where flash occurs, a temperature gradient will be established and a Non Equilibrium Allowance (NEA) will take place, meaning that the temperature at which the water mass will leave the chamber will actually be above the saturation temperature at which the chamber operates.

Code block 9:

```
Delta_T_d_NEA(i) = 33d0 * (Td_out(i-1) - Tv_out(i-1))**(0.55d0) / Tv_out(i-1)

Tv_d_flash(i) = Tv_out(i-1) + Delta_T_d_NEA(i)

Delta_T_b_NEA(i) = 33d0 * (Tb_out(i-1) - Tb(i))**(0.55d0) / Tv(i)

Tb_b_flash(i) = Tb(i) + Delta_T_b_NEA(i)
```

Each MED effect is assumed to have a tube bundle with two passes as shown in Figure 11. The first pass receives the saturated vapor from the previous effect and its outlet leads directly into the distillate box where the condensed steam flows together with the NCG. Inside the distillate box the condensed steam mixes with the distillate routed from the previous effect. The later flashes and produces vapor. This flashed vapor together with the NCG then flow through the second pass of tubes in the main tube bundle. It is important to note that the first and second passes of the tube bundle are not assumed to be physically connected to each other with a continuous tube loop. The open space inside the distillate box allow the fluids to mix and the gases to enter the second pass (similarly to what happens in real plants).

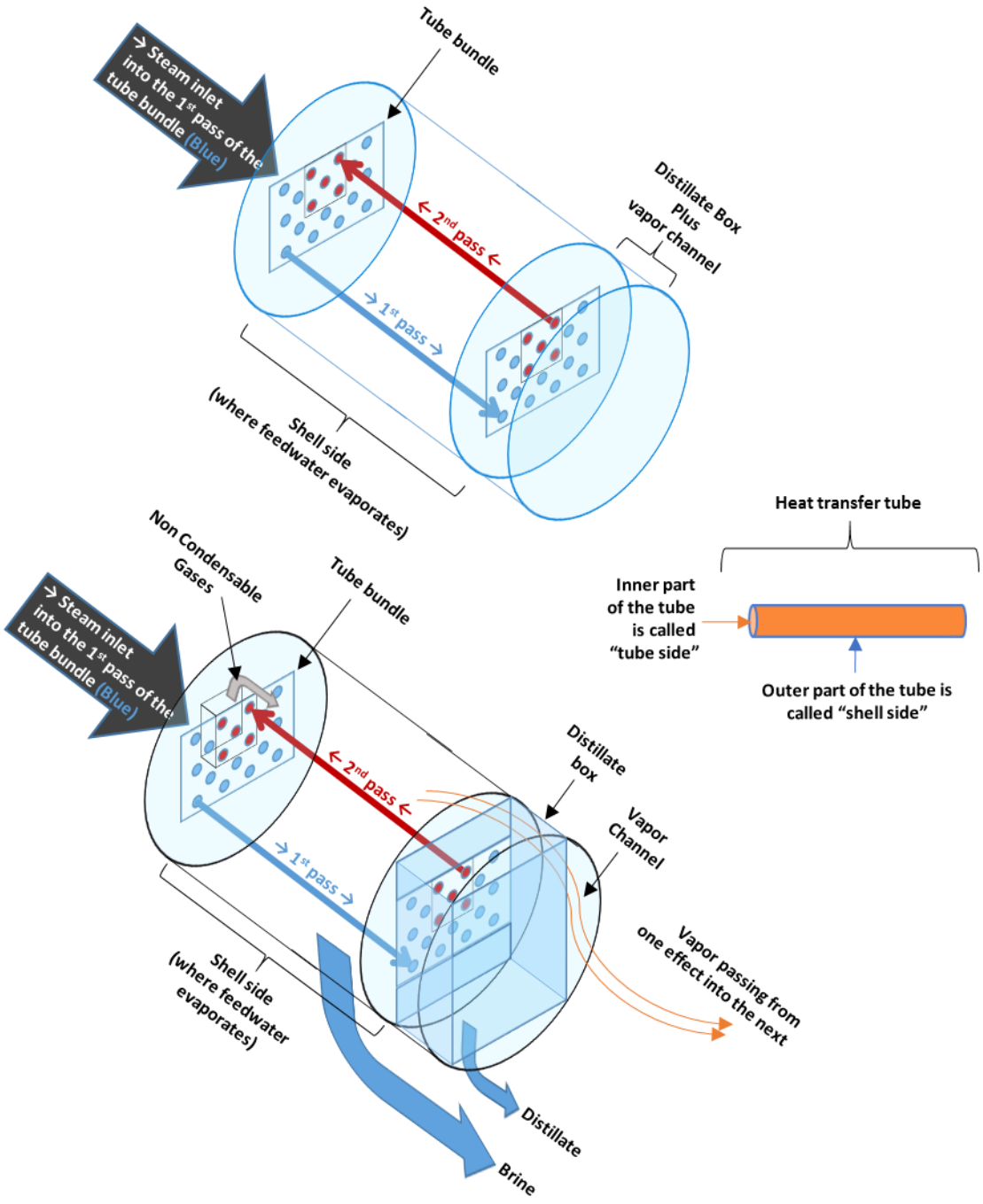

Figure 11 - Diagram with the configuration assumed for the main tube bundle inside the MED effects for the MED detailed model.

It is assumed that all the vapor formed by flash of distillate in the distillate box (Tv_d_flash(i)) is condensed as it flows through the second pass of the tubes leading to the shell side of the same effect, and that the condensation inside those tubes takes place at a pressure defined by the saturation temperature of the vapor entering the distillate box. This vapor formed by flash is assumed to be superheated, as it was formed at Tv_d_flash(i) at a pressure defined by the saturated temperature outlet from the previous effect (Tv_out(i-1)). At

the end of the second pass the model assumes that only NCG pass into the shell side of the current effect (passing from P(i-1) to P(i)) where the evaporation process takes place. It is assumed that all the vapor passing inside the first and second passes is always fully condensed in each effect. The NCG entering the shell side are assumed to follow again a similar path than in the previous effect, moving into the next effect together with the vapor and NCG produced on the shell side of the current effect. The calculation of the amount of NCG uses an input set by the user that defines the concentration of NCG in the seawater. A safety factor is also used to overestimate the amount of NCG dissolved in the water as it is industry practice (these gases can create a major hurdle during the operation of MED plants, as they block the heat transfer if not removed).

Code block 10:

```
E_M_NCG_1 = F_Total * (E_mass_concentr_NCG / (1E3*DENS_sw_fun(Tf_eph(n), Xsw))) * (1 + E_mass_safe_NCG)
```

The temperature of brine and distillate outputs actually leaving each effect are different than the temperature of the brine and distillate produced by the evaporation process and vapor condensation outside and inside the tube bundle, respectively. These differences are a result of thermodynamic losses (being the NEA and BPE the ones accounted by this model). In case a cross-flow of these masses is set by the user, the model makes a mass balance to calculate the temperature outlet from each distillate box and brine pool.

Code block 11:

```
Td_out(i) = ( V(i-1) * Hd_Tv_out(i-1) + D_d_flash_remain(i) * Hd_d_flash_remain(i) + V_d_flash(i) * Hd_Tv_out(i-1)) /  ((V(i-1) * Hd_Tv_out(i-1) / Tv_out(i-1)) + (D_d_flash_remain(i) * Hd_d_flash_remain(i)  / Tv_d_flash(i)    )  +  (V_d_flash(i)       * Hd_Tv_out(i-1) / Tv_out(i-1)) ), for a typical effect with no condensate returning back to the boiler;

Tb_out(i) = ( B_evap(i) * Hb_Tb(i)  +  B_b_flash_remain(i) * Hb_b_flash_remain(i) ) / ((B_evap(i) * Hb_Tb(i) / Tb(i)) + (B_b_flash_remain(i) * Hb_b_flash_remain(i) / Tb_b_flash(i))), assuming cross-flow of brine;
```

More energy is drained from colder effects to preheat the feedwater (inside the feedwater preheaters) than from upstream effects, due to the reduction of feed water flow rate being pre-heated from the last to the first effects. However, since the brine and distillate increase their volume as they move along the stages, the heat load from flashing also increases (although it does not compensate totally the energy used for preheating the feedwater). The vapor formed by the brine flash is assumed to add up to the vapor formed by evaporation of the feedwater in each effect.

Code block 12:

```
V(i) = V_evap(i) + V_b_flash(i)
```

The calculation of the superheated part of the vapor formed by brine flashing could be used for the feedwater preheating inside the effect. Though this only accounts for 0.0132% of the total heat load in the last effect for the Trapani simulations. This percentage is even smaller for other effects. This calculation was removed from the model because of the small impact it has on the overall performance of the MED plant, and because the calculation of this parameter implies a very precise knowledge of the exact T_b and X_b in each effect (the latter one is obtained in this model after the calculation of the heat load in each effect).

After the first effect, the heat load passing into each effect is assumed to correspond to the latent heat released by the vapor condensation inside the heat transfer tube bundle.

Code block 13:

```
Q(i) = Qv_remain_out(i-1) + Qd_flash(i)

Qv_remain_out(i) = (V_evap_remain(i) + V_b_flash(i) + V_f_flash(i)) * LHv_Tv_out(i)

Qv(i) = Qv_evap(i) + Qv_b_flash(i) + Qv_f_flash(i)
```

The operation of a TVC and the NCG steam ejection system can be assessed with the MED detailed model. Section 3.3 describes in detail the model used for steam ejectors as part of the MED detailed model, which incorporates a database describing the performance of steam ejectors for different pressures of motive steam, entrainment and discharged gases obtained from one of the main manufacturers of steam ejectors for MED plants

The pressure inside of the distillate box is defined in this model by the temperature of the steam being condensed inside the heat transfer tube bundle. This pressure is equal to the pressure inside the previous effects minus the average pressure loss predefined when the vapor crosses the tube bundles. The user can set an average temperature loss of the steam entering the tube bundles, and from that value a pressure loss is calculated assuming saturated conditions.

Code block 14:

```
Tv_out(i) = Tv(i) - Tv_Loss

water_TQ_fun (Tv_out(i), 1d0, pres = P_out(i))
```

The distillate boxes collect distillate from different sources, namely: the intercondensers from the NCG ejection system, the outlet from the main tube bundles, and the previous effect

distillate box. When entering the distillate boxes these mass flows will be at different temperatures and pressures, and so flashing will occur. Most of this flashing will be related to the distillate flowing from the previous effect, but a small amount will be from the condensate returning from the NCG ejection system intercondensers into some of the first effects (that are immediately downstream of these intercondensers).

Code block 15:

```
Delta_T_d_NEA_Ej_1 = 33d0 * (E_Tc_Vap_1_ref - Tv_out(i-1))**(0.55d0) / Tv_out(i-1)

Tv_d_flash_Ej_1 = Tv_out(i-1) + Delta_T_d_NEA_Ej_1

Qd_flash_Ej_1 = V_d_flash_Ej_1 * (Hv_d_flash_Ej_1 - Hd_Tv_out(i-1) )

Qd_flash(i) = Qd_flash(i) + Qd_flash_Ej_1
```

Code block 16:

```
Delta_T_d_NEA_Ej_2 = 33d0 * (E_Tc_Vap_2 - Tv_out(i-1))**(0.55d0) / Tv_out(i-1)

Tv_d_flash_Ej_2 = Tv_out(i-1) + Delta_T_d_NEA_Ej_2

Qd_flash_Ej_2 = V_d_flash_Ej_2 * (Hv_d_flash_Ej_2 - Hd_Tv_out(i-1) )

Qd_flash(i) = Qd_flash(i) + Qd_flash_Ej_2
```

The salinity of the brine produced in the first effect is an input. This input is necessary to define the evaporation ratio and to calculate how much energy is transferred into subsequent effects. The mass flow of feedwater entering each effect is considered to be equal to the flow rate necessary to enter the first effect (in order to guarantee equal wetting areas in all effects, especially during part load operation, as the heat transfer areas will be equal across effects in most industrial MED plants).

The salinity profile throughout the effects is calculated having into account the heat flow entering each effect and the mass flow of feedwater. The effects will have different heat loads, but a similar inlet feedwater mass flow rate. Thus, the evaporation ratio and brine salinity in each effect will also differ. From the second effect onwards, the brine salinity of the previous effect is used as guess value to calculate the evaporation ratio. Then, using a small iterative loop for each effect, if the heat flow coming from the previous effect is higher than the one required to reach the initial guess value for the evaporation ratio a higher brine salinity is set. If the heat flow coming from the previous effect is lower, a lower brine salinity is set. The loop runs until the equilibrium is reached: the heat flow entering the effect matches the energy required to evaporate the feedwater with the new (recalculated) evaporation ratio.

Code block 17:

```
D(i) = F(i) * (Xb(i) - Xf) / Xb(i)

Q(i) = F(i) * ( Delta_H_iph(i) + LHv_evap(i) * (Xb(i)-Xf)/Xb(i) )
```

The model calculates the heat transfer area used in each effect and in the down-condenser as a sub-product after all the remaining calculations have been performed. It is assumed that the entire amount of energy entering each effect is actually used for water production (excluding the temperature and percentage of energy losses per effect that the user can predefine at the start of the simulation). It is assumed that the heat transfer area is the same for all effects, and that it is calculated from the heat load powering the last effect (note that $Q_1 > Q_n$).

The heat transfer areas are calculated from the heat flux into the last effect because in reality the remaining effects have a higher degree of subcooling of the distillate formed, reaching its minimum in the last one. The splines obtained from the literature to calculate the overall heat transfer coefficient also seem to work better when using information from the last effect, and it is assumed that this is because they do not assume the process of sensible heat transfer [18] (results from the simulations versus the three real plants used in this work, section 3.2.4, indicate that).

Code block 18:

```
U(n) = 1D-3 * ( DBLE(1939.4) + 1.40562*Tb(n) - 0.0207525*(Tb(n)**2) +
0.0023186*(Tb(n)**3) )

Ae = Q(n) / (  U(n) * (Tv_out(n-1) - Tb(n))  )
```

Code block 19:

```
Udc = 1D-3 * ( DBLE(1617.5) + DBLE(0.1537)*Tv_out(n) + DBLE(0.1825)*(Tv_out(n)**2) -
DBLE(0.00008026)*(Tv_out(n)**3) )

LMTD_dc = (Tf_dc_out - pre_Tsw_out) / DLOG ((Tv_out(n) - pre_Tsw_out)/(Tv_out(n) -
Tf_dc_out)), for plants configured with a flat plate feedwaters heaters

Adc = Qdc_Vapor / (Udc * LMTD_dc)
```

The MED detailed model also accounts the consumption of the main pumping systems of a MED plant, namely: seawater intake up to both the MED and SWCC condensers, seawater inside the MED down-condenser, seawater inside the SWCC condenser, brine between MED effects (if necessary) plus brine extraction from last effect, brine/cooling water outlet from the CSP+MED/SWCC system back to the sea, condensate return back to the Rankine cycle, and

distillate into storage reservoir. A detailed description of the pumping model is described in section 3.4.

More information on the MED model is available in Annex 1, where the main calculation steps are indicated in detail.

3.2.3 MED Forward Feed: Mathematical Model and Algorithm

A scheme with the bulk of the MED process considered for the Forward feed configuration in this detailed model is shown in Figure 12 when using a TVC, and in Figure 13 when using a low temperature configuration.

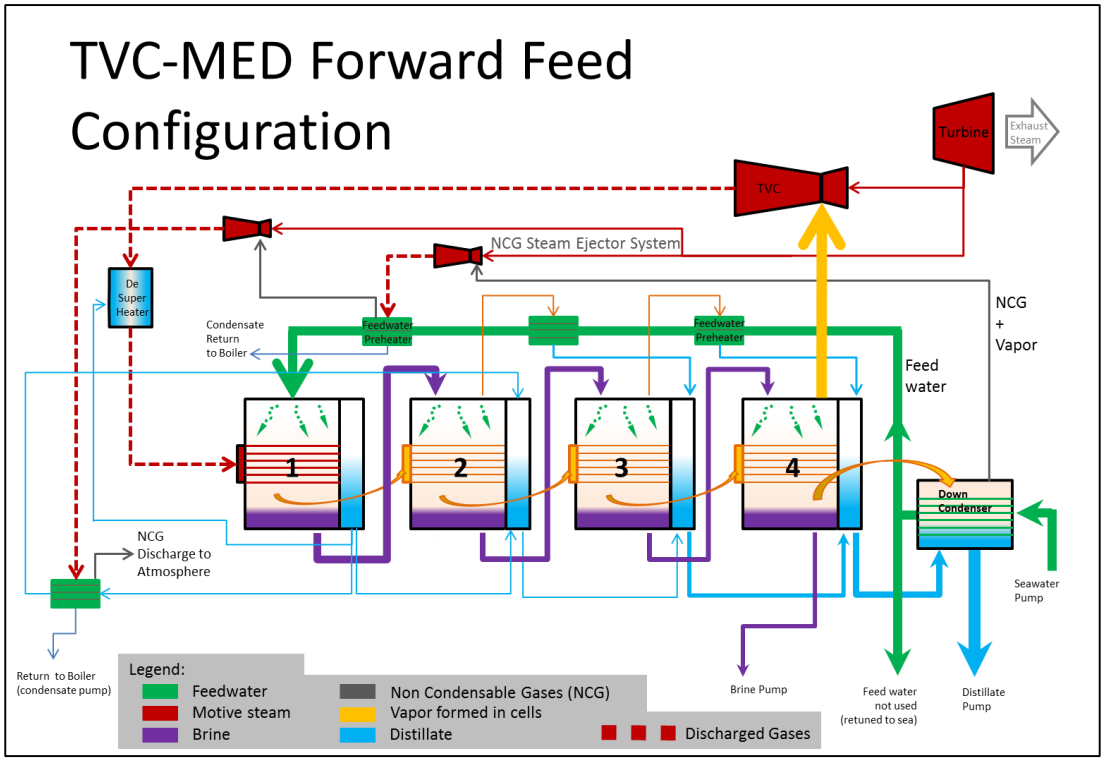

Figure 12 - TVC-MED Forward Feed generic configuration considered in the MED detailed model.

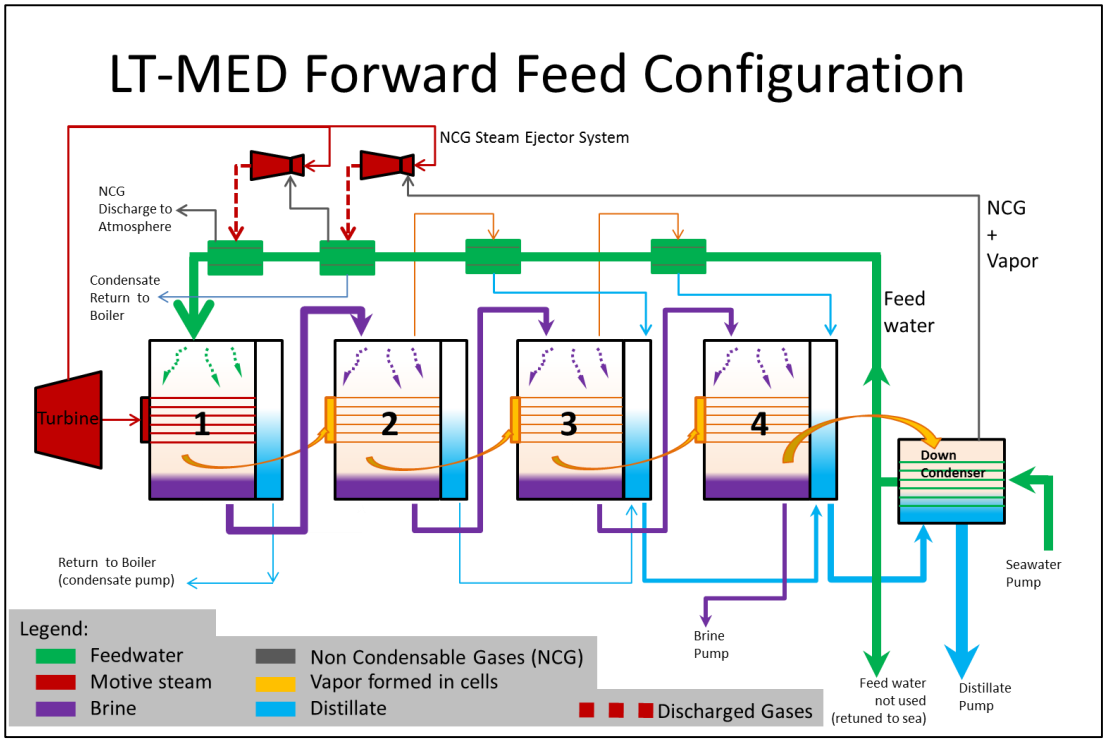

Figure 13 - LT-MED Forward Feed generic configuration considered in the MED detailed model.

The MED Forward feed detailed model was developed as an upgrade to the MED parallel detailed model described previously in section 3.2.2. This subchapter presents only the main differences between these two versions. A comprehensive diagram of the algorithm used for the MED detailed model with forward feed configuration is presented in Annex 1 where the calculation steps are described in depth. The forward feed and parallel configurations differ mainly in the way the feedwater, and brine move through the plant. In both configurations the feedwater tube normally crosses the entire plant from the down-condenser up to the first effect. The distillate flow is similar between these two configurations.

Feedwater main tube

Attached to the feedwater main tube there are normally feedwater preheaters along the way collecting energy from the effects (condensing part of the steam produced in the effects that is routed to the preheaters). This energy is used to gradually preheat the feedwater along its path up to the first effect. In the parallel configuration, each effect receives feedwater directly from the feedwater tube, while in the forward-feed configuration all the feedwater that passed through the down-condenser enters the first effect. This means that in the parallel configuration the amount of feedwater being preheated by each preheater is less than the amount of feedwater preheated in the previous preheater. With such configuration the mass flow of feedwater at the end of the main feedwater pipe is much smaller than the total mass

flow that entered it. This implies that preheaters near the first effect will receive much less feedwater (and so use less energy from the first effects) to preheat than the first preheaters connected to the last effects. On the other hand with the forward feed configuration all the feedwater preheaters will be required to transfer energy to the same amount of water.

Brine/Feedwater

In the parallel configuration as the feedwater entering each effect comes straight out of the feedwater main tube, the brine transfer between effects is not mandatory (although is normally done, to increase the systems efficiency, as it allows the flash of this mass of water as it enters the next effect at lower pressure). Brine in the parallel configuration moves between the brine pool of one effect and the brine pool of the next effect (driven only by pressure difference) where it mixes with the brine produced in this next effect. In parallel configuration the feedwater always enters the effects slightly subcooled, and extra energy is required to preheat it before it starts evaporating. In the forward feed configuration all the feedwater that enters the plant passes through the first effect, entering it slightly subcooled. The brine produced in each effect is passed into the next effect, being sprayed at the top of the of tube bundle. In principle this brine flow is driven by pressure difference only between effects, although pumps may be required in some units. Each effect receives the brine produced in the previous one, which is at a higher pressure, and because of that as the brine enters each effect some flashing will occur. The operation of steam ejectors is calculated in the same way in both the forward feed and parallel models.

Overview of the mathematical model and algorithm

The total amount of feedwater entering the MED effects is calculated accounting only the heat load that goes into the first effect.

Code block 20:

```
F_total = Q(1) / ( Delta_H_iph(1)   +   LHv_evap(1) * (Xb(1)-Xf(1))/Xb(1) )
```

The predefinition of the feedwater temperature entering effects 2 to n is set to be equal to the temperature of the brine produced in the previous effect.

Code block 21:

```
Tf(i) = Tb(i-1)
```

The mass flow of feedwater entering each of the effects 2 to n is set to be equal to the mass flow of brine produced in the previous effect.

Code block 22:

```
F(i) = B(i-1)
```

The vapor production inside the first effect of a parallel and forward feed plant happens similarly. The calculations for subsequent effects (2 to n) are different though. In the forward feed configuration the salinity of feedwater entering each effect is set equal to the salinity of the brine produced in the previous one. In this model it was decided to name the mass of saltwater entering each effect is as feedwater, although it is in practice the mass flow of brine produced in the previous effect (for effects 2 to n). This was done to avoid confusions between the different mass flows described in the model, as the model was upgraded.

Code block 23:

```
Xf(i) = Xb(i-1)
```

In effects 2 to n, the feedwater enters each effect above the saturation pressure and flashes immediately. The amount of vapor produced with the flashing process is calculated using an iterative block. A guess value is used during the calculations of each effect for the salinity of the brine resulting from the flashing process. This guess value is set to be equal to the salinity of the brine produced in the previous effect. As vapor is produced, the salinity of the brine can only increase, and the iterative block is based on this idea.

Code block 24:

```
Xf_f_flash_remain(i) = Xf(i)
```

The actual iterative block is based on a system of three equations, relating: the mass flow of vapor produced with flash when the feedwater enters the effect; the latent heat at the operational vapor temperature of the effect; the mass flow of feedwater entering the effect, its specific enthalpy and salinity; the enthalpy of the feedwater remaining after the flashing effect and its salinity.

Code block 25:

```
V_f_flash(i) * LHv_evap(i) = F(i) * (Hf_Tf(i) - Hf_f_flash_remain(i))
F_flash_remain(i) = F(i) - V_f_flash(i)
Xf_flash_remain(i) * F_flash_remain(i) = F(i) * Xf(i)
```

The unknown variables in this system of equations are: the salinity of the feedwater remaining after the flashing effect and the corresponding mass flow of vapor produced. This iteration block runs by increasing progressively the salinity of the feedwater remaining after flashing until an equilibrium is reached. A numerical approach was used instead of an analytical one to calculate the salinity of the feedwater remaining after flashing because the enthalpy of the brine produced by flashing is also dependent on the salinity of the feedwater remaining after the flashing. This is calculated using a 3rd degree polynomial equation, and an analytical calculation would render being very complex.

Knowing the salinity of the feedwater remaining after the flashing and the mass flow of feedwater remaining after the flashing process, it is then possible to calculate the amount of vapor produced by evaporation, similarly to what is done in the parallel MED detailed model.

More information on the detailed MED model is available in Annex 1, where the main calculation steps are indicated in depth.

3.2.4 Model Calibration and Validation

The detailed MED model was validated using information from the following plants listed below.

1) The TVC-MED-Parallel commercial plant, Trapani, Sicily:

   This plant is operated by Siciliacque S.p.A.. and was built by the French company Sidem. It has 4 MED trains producing in total 36 000 m^3/day of fresh water and operates as a standalone plant, as it is powered by a set of boilers using natural gas. It started operations in 1995 with the purpose of producing potable water for human consumption, and it has been run on a continuous base until early 2015 [93]. Since then, Trapani has been connected to a larger regional distribution system of fresh water within the island of Sicily, and so the plant has been put on hold as a backup (being maintained only to keep its minimum operational capabilities in case of need). This plant has a very high efficiency, presenting at the time it was commissioned a GOR of 16.

2) The MED-Forward Feed low temperature experimental plant at Plataforma Solar de Almeria (PSA), Spain:

   This plant has a small production capacity and it serves only for experimental purposes. This plant has been modified several times since it was installed in 1987 [89]. Initially the plant was designed to operate with low-pressure saturated steam powering the first effect, though in 2005 this was changed and now the first effect is powered by hot water instead. During this refurbishment in 2005 a double effect absorption heat pump has been also installed by the French company Entropy in framework of the AQUASOL European project. The test field where the plant is installed can provide hot water to the first effect using several sources, including an array of CPC panels or the heat pump double effect absorption heat pump. This plant has the particularity of having a vertical configuration, unlike commercial MED plants.

3) The MED-Parallel low temperature commercial plant, Priolo-Gargallo, Sicily:

   This plant was built to provide industrial grade water [94], being located at with the Isab Energy Integrated Gasification Combined Cycle (IGCC) power plant, in the region of Siracusa, also in Sicily. This MED plant was commissioned in 1998, has 2 MED trains and produces a total of 14 400 m^3/day.

The detailed MED physical model was calibrated using data from the TVC-MED plant at Trapani, Sicily. Initially the model was built to describe the operation of that plant (TVC-MED-P with cross-flow of distillate), and later on it was adapted to describe the operation of other configurations: LT-MED-P, LT-MED-FF, and TVC-MED-FF (all of them with or without cross-flow of distillate).

Input Data Used for Validation

The main set of configurations used on the detailed MED model to simulate the three existing MED plants mentioned before are presented in Table 5, and the main inputs for nominal design conditions used to validate the model are presented in Table 6. Some of the inputs used in the model for the validation process are confidential, and although approximated values were made available during the course of this work, they cannot be disclosed. Note that pressure losses and subcooling of the condensate during the heat transfer inside the tube bundles were considered to be zero for the validation process.

Table 5 – Main set of configurations used in the detailed MED model to simulate the three existing MED plants located at Trapani, PSA and Priolo-Gargallo.

Parameter	Value		
	Trapani	**PSA**	**Priolo-Gargallo**
Plant configuration	TVC-MED-P	LT-MED-FF	LT-MED-P
TVC Strategy	Predefined saturated discharged temperature (option 2)	Not applicable	Not applicable
Steam ejector's model	Empirical model using ratios from manufacturer (option 1)	Empirical model using ratios from manufacturer (option 1)	Empirical model using ratios from manufacturer (option 1)
Crossflow of distillate	Yes	Yes	Yes
Feedwater preheaters configuration between MED effects	Preheaters between every 2 effects (with NCG ejectors) (option 3)	Preheaters beetween every effect (without NCG ejectors) (option 4)	Preheaters beetween every effect (with NCG ejectors) (option 2)
Location of preheaters powered by the NCG removal system	2nd effect	Not applicable	2nd effect
Preheaters with plate heat exchangers	Yes	No	Yes

Table 6 – Main inputs to the MED model used to simulate the real three existing MED plants located at Trapani, PSA and Priolo-Gargallo.

Parameter	Value			
	Trapani	**PSA**	**Priolo-Gargallo**	**Units**
Plant configuration	TVC-MED-P	LT-MED-FF	LT-MED-P	-
Manufacturer	Sidem	Entropy	Sidem	-
Number of effects	12	14	11	-

(n)				
Ts_sat	84.0	72.0	Confidential	ºC
$Tv_{(1)}$	62.2	68.0	Confidential	ºC
$Tv_{(n)}$	37.0	36.0	Confidential	ºC
$Tf_{(n)}$	35.0	32.5	Confidential	ºC
Tsw	22.0	25.0	Confidential	ºC
Mm	22.5	8.37E-2	Confidential	t/h
E_Mm	1.5	-	Confidential	t/h
Xf	4.0	3.5	Confidential	wt%
$Xb_{(1)}$	Confidential	3.6	Confidential	wt%
TVC_Pm	45.0	-	Confidential	barA
E_Pm	45.0	-	Confidential	barA

Validation of the Main Outputs

The results from the simulations using the current version of the physical MED model returns results within ~ +10% deviation for the main metrics when compared to real plant data at design conditions, as it is shown in Table 7.

Table 7 - Validation of the main outputs from the MED process using data from three real plants, calculated values versus design data in percentage

Plant Location	**Trapani**			**PSA**			**Priolo-Gargallo**		
Plat type	Commercial			Experimental			Commercial		
Plant configuration	TVC-MED-P			LT-MED-FF			LT-MED-P		
Manufacturer	Sidem			Entropie			Sidem		
Data type	Real	Calc.	Deviation	Real	Calc.	Deviation	Real	Calc.	Deviation
Distillate / train	375.00 t/h	377.98 t/h	**0.76 %**	3.00 t/h	3.21 t/h	**7.08 %**	300.00 t/h	326.05 t/h	**8.68 %**
Brine / train	755.00 t/h	758.11 t/h	**0.42 %**	5.00 t/h	5.60 t/h	**12.06 %**	Confidential t/h		**10.35 %**
Feedwater / train	1130.40 t/h	1137.39 t/h	**0.62 %**	8.00 t/h	8.82 t/h	**10.19 %**	Confidential t/h		**9.82 %**
Brine salinity outlet / train	5.99 wt%	5.98 wt%	**- 0.10 %**	5.6 wt%	5.51 wt%	**-1.67 %**	Confidential wt%		**- 0.76 %**

Total HTX area / effect	Confidential wt%	**5.40 %**	26.28 m^2	28.75 m^2	**9.43 %**	Confidential* m^2	**2.79 %**
References for real data	[25], [28], [94], [93] and direct contact with plant operator		[68], [69], [80], [89] and direct contact with plant operator			[94], [95] and direct contact with plant operator	

* Estimated value: ratio between Trapani's and Priolo's total mass flow rate of distillate (300 (t/h) / 375 (t/h) = 0.8), multiplied by Trapani's heat transfer area per effect).

A validation of the results from the LT-MED configuration was also performed against data from the Trapani plant, by using real data as input for: 1) the temperature and total mass flow of vapor entering the first evaporator of the MED; 2) pre-setting the temperature of the feedwater entering the first 2 effects (that is affected by the operation of the NCG steam ejector system); and 3) pre-setting the mass of motive steam used by the NCG ejection system. The results of the model output versus real plant data at design conditions for the LT-MED configuration using Trapani as reference also show a deviation of ~ +10% for the main metrics as it is presented in Table 8.

Table 8 - Main output results using inputs for design conditions for a LT-MED configuration versus info from the TVC-MED-P Trapani plant [25].

Parameter	**Real data** [28]		**Modeled** [25]		**Deviation** [25]	
Feedwater	1130	t/h	1216	t/h	7.6	%
Distillate	375	t/h	390	t/h	4.0	%
Brine	755	t/h	825	t/h	9.3	%
Salinity output	5.99	wt%	5.88	wt%	- 1.8	%

Validation of the Main Auxiliary Components

The performance of the main auxiliary components is shown in Table 9, where relevant metrics are presented for the steam ejectors and the down-condenser.

Table 9 - Validation of main auxiliary components using motive steam using data from three real plants. Calculated results versus design data in percentage.

Plant location	**Trapani**			**PSA**			**Priolo-Gargallo**		
Plant Type	Commercial			Experimental			Commercial		
Plant configuration	TVC-MED-P			LT-MED-FF			LT-MED-P		
Manufacturer	Sidem			Entropie			Sidem		
Data type	Real	Calc.	Deviation	Real	Calc.	Deviation	Real	Calc.	Deviation
Mass flow of entrained steam into the TVC	13.2 t/h	11.04 t/h	**-16.3 %**	-	-	-	-		**-**
Mass flow of motive steam powering the first NCG steam ejector	Confidential t/h		**-3.0 %**	-	-	-	Confidential t/h		**26.13 %**
Mass flow of motive	Confidential		**-1.9 %**	-	-	-	Confidential		**-23.65 %**

steam powering the second NCG steam ejector	t/h						t/h	
Total mass flow of motive steam powering both NCG ejectors	1.5 t/h	1.45 t/h	**-3.35 %**	-	-	-	Confidential t/h	**-6.23 %**
Total mass flow of motive steam powering the NCG steam ejectors versus first effect	6.67 %	6.44 %	**-3.35 %**	-	-	-	Confidential %	**6.25 %**
Mass flow of cooling water intake into the down-condenser	1280 t/h	1231.07 t/h	**-3.82 %**	16.00 t/h	17.94 t/h	**12.15 %**	Confidential t/h	**-4.85 %**
Mass flow of rejected cooling water outlet from the down-condenser	149.6 t/h	93.68 t/h	**-37.38 %**	8.00 t/h	9.13 t/h	**14.11 %**	Confidential t/h	**-16.11 %**
References for real data	[25], [28], [94], [93] and direct contact with plant operator			[68], [69], [80], [89] and direct contact with plant operator			[94] and direct contact with plant operator	

Interestingly, model predictions for the main parameters fit well the experimental data from the plant, with discrepancies laying within a ~10% margin of error when comparing with the design conditions for the main metrics. Such a small difference can be attributed to some secondary simplifying assumptions adopted within the model formulation. In fact, though the model details in a large extent the different mass flow paths through the different chambers within effects and preheaters, it does not calculate pressure losses during the vapor flow in the demisters, vapor transmission lines and vapor condensation inside the tube bundles. Moreover, no subcooling is being assumed during the heat transfer process in the tube bundle inside the several effects (as all the effects have the same heat transfer area, this subcooling process will progressively decrease along the effects chain, reaching its minimum in the last effect).

Looking at the Trapani plant in particular (as it is the plant for which more detailed data was available), the simulations show that the TVC is performing worse than in reality, entraining less ~16% of vapor from the last effect than in reality, meaning that less energy will reach the first MED effect. These simulations were done using the empirical model based on a database for steam jet ejectors performance obtained from a manufacturer. This database has only performance ratios of steam ejectors with 4” and 8” (this size refers to the inside diameter of the tubes connecting to the entrainment and discharge openings in the steam jet ejector). If the size of the ejector is calculated to be larger than 8” then it is assumed that the

ejector will have the same performance than the 8” ejector, and vice versa for sizes smaller than 4”. The size of the TVC at Trapani is much larger than 8”, though information on the exact size of the TVC was not available. It was mentioned by the company that provided the mentioned ejectors database that the bigger the ejector, the more efficient it gets, probably justifying the discrepancy shown for the calculated mass flow entrained by the TVC.

The simulations for Trapani indicate that the lower performance of the TVC (calculated by the model) is counterbalanced by the overproduction of distillate across each MED effect. Pressure losses across the effects and subcooling during the heat transfer process are not being accounted in the model (subcooling is only accounted for the heat transfer in the 1st effect), as shown by the validation results from Table 8. These two factors mean that by one side the model calculates that the TVC provides less power to the first MED effect (which lowers the total production of distillate), but on the other side the calculated performance of each MED effect is slightly higher than in reality. This justifies why the total mass flow rate of distillate, brine and feedwater are almost spot on versus real data, while considering a TVC entraining less ~16% of steam than in reality.

Having this into account, it is also possible to justify the discrepancies presented for the simulated results for the down-condenser, as simulations indicate that it should use less cooling water than it actually uses in reality: ~ -4% of cooling water intake, and ~ -37% of rejected cooling water. The model considers that the first MED effect receives less power than in reality. This means that less feedwater will be used (as the feedwater entering the plant is calculated to be directly dependent on the amount of energy powering the first effect). The discrepancies shown for the mass flow rates in the down-condenser are likely due also to slight differences between the simulated and real values of: 1) the nominal temperature at which the distillate is condensed in the down-condenser; and 2) the temperature at which the cooling water leaves the flat plate pre-heaters. This is more evident for the rejected cooling water, as it has a smaller value comparatively to the intake, and so any minor change on the intake, will lead to a larger deviation on the outlet (that is one order of magnitude smaller). The brine output was calculated to be 39.29 ºC instead of 38 ºC, and the distillate 38.73 ºC instead of 37 ºC.

Looking at the results for both the PSA and Priolo-Gargallo MED plants, the main outputs are in line with the expected results when comparing with data from Trapani using a simulation with an LT-MED configuration. Because the PSA and Priolo-Gargallo plants do not use a TVC, the heat load being dissipated in the down-condenser is higher. This explains why the intake and rejected cooling water mass flow rates for the down-condenser show similar values of deviation when comparing with real data (both variables now have the same order of magnitude, unlike the simulation for Trapani assuming the existence of a TVC).

The results obtained for the mass flow rate of steam necessary to power the NCG steam ejectors at Priolo-Gargallo indicate a deviation than can go up to ~ +/- 25%. Not all the design

information was available for this plant during the validation process of the model outputs, in particular for the NCG steam ejectors. Although an extensive list of design parameters was available, only a range of pressures used at the plant to power the steam ejectors was made available during the validation process. Data on the total heat transfer area inside each effect was also not available for Priolo- Gargallo, and so an educated guess was made considering info from the Trapani plant (as both plants were designed by the same company, and they share many similarities regarding its design, especially if one excludes the existence a TVC).

The optimization of steam ejectors is an extensive research field by itself, and it was not the aim of this work to simulate them thoroughly. The main goal was to calculate the total steam consumption to power these devices. Though simple, the model developed to simulate steam ejectors (described in detail in section 3.3), seems to provide results in line with the ~10 % margin of error that was pretended for the main variables of a MED plant. Even in the Priolo-Gargallo simulation, where less info was available, the final result provides similar deviations to the real data. It is worth mentioning that the operation of the NCG ejectors represents a small percentage of the total motive steam extracted from the Rankine cycle.

3.3 Auxiliary: Steam Jet Ejector Model

3.3.1 General Description

The steam ejector model enables a simple analysis of the performance of a steam jet ejector accounting:

1) The operational pressures, temperatures and mass flow rates of the entrained gases and motive steam used;
2) The cooling water temperatures and mass flow rates, together with the approach temperatures in the corresponding condensers receiving the discharged fluids.
3) The saturated discharge temperature for the TVC performance (if the user sets one);
4) With this information the model calculates a rough estimation of the entrainment ratio of the ejector being simulated, through an iterative process.

The steam ejector model described in this section is split in two blocks. The first block performs the mass and energy balance, while the second block calculates the entrainment ratio of the steam ejector (based on an empirical database of ejector's entrainment ratios, or based on commonly used mathematical correlations from the literature). The second block is called by the first block iteratively, and it is the first block that returns the final results.

This model does not use information regarding detailed characteristics of the ejectors, such as the velocities of the fluids crossing the different parts of the ejector, or the section area for the nozzle.

The steam ejector model describes the mass and heat flow for the inlet and outlet streams used when operating a steam jet ejector and related condensers at steady-state conditions with MED plants. This model was developed to simulate the operation of a TVC and a two-stage steam jet ejector system for the removal of NCG, being described in detail in section 3.3.2 and section 3.3.3, respectively. The steam jet ejector model uses as main inputs: one of the mass flow rates that enter the ejector plus its temperature and pressure; the temperature and pressure of the second inlet stream into the steam jet ejector; the mass flow rate, temperature and pressure of the feedwater input into the related condensers; the approach temperature used to operate these condensers; and its cooling water outlet temperature. Using this information, the first block of the steam jet ejector model obtains the remaining inputs that are required to calculate the performance of the ejectors making use of the second block of the code (that provides the entrainment ratios).

This second block requires as main inputs to simulate the entrainment ratio of a steam jet ejector: the inlet and outlet saturated pressures and inlet mass flow rates of entrained gases or motive steam. As described in the literature, section 2.4.3, there are two models available that are capable of simulating the entrainment ratio of steam jet ejectors knowing only the inputs just mentioned for the inlet and outlet saturated pressures and mass flow rates. As

these two models did not return interesting results when compared to real plant data (as explained in section 3.3.6), a new model was also developed for the calculation of these entrainment ratios using linear interpolations of values provided by a main steam jet ejector manufacturer, as explained in section 3.3.4.

The main outputs from the steam jet ejector model returns information on mass flow rate that was missing as input, together with compression ratios and a rough estimation of ejector sizes. Several boundary mechanisms were implemented into this model, in case the inputs set by the user do not allow the operation of the MED plant under the set conditions. In this cases the pressures and temperatures related to the operation of the ejectors may also be updated, as the model will try to find appropriate values that may enable the operation of the plant.

Three types of steam ejector systems are commonly used in a MED system: the TVC, the NCG ejection system, and the hogging ejector.

In this work only the TVC and the NCG ejection system were modeled. When planning the integration of the code into SAM it was assumed that the MED plant would not stop its operation for more than a couple of hours (due to its connection to a CSP plant with thermal storage). It was also considered that under these conditions no significant depressurization of the MED train would occur during the standby periods, and so no cold shut down of the MED plant would take place. With these assumptions the hogging ejector would only be used one time at the start of the simulation, and so it was not considered during model development.

The models used in this work are applicable to steam ejectors operating with a fixed nozzle, designed for constant steam pressures (the typical configuration used for steam ejectors in commercial plants [35]).

A steam ejector is comprised of three main orifices: the motive steam inlet (receiving the high pressure gas), the entrainment gas inlet (to where the low-pressure gas is drawn into), and the compressed gas outlet (discharged gases) [83]. The mass flow rate of gases discharged by the ejector is equal to the sum of mass flow rates of fluids entering it, as described in equation (14).

$$M_c = M_e + M_m \tag{14}$$

The performance of the steam ejector can be characterized by the entrainment ratio (W_r), indicating the mass flow of M_m needed to eject a determined amount of entrained gas (M_e):

$$W_r = \frac{M_e}{M_m} \tag{15}$$

During normal operation of the steam ejector, the motive steam pressure (P_m) will be higher than the pressure of the compressed gas (P_c), and the pressure of the compressed gas will be higher than the pressure of the entrained gas (P_e):

$$P_m > P_c > P_e \tag{16}$$

In order for the steam ejector to operate, the discharge pressure cannot be lower than the pressure to where the gases are discharged into (e.g. if discharging into the atmosphere, the discharge pressure assumed for the ejector cannot be lower than the atmospheric pressure).

Steam ejectors in MED plants are used to remove gases, but while doing so the discharged gases also get compressed. The compression ratio of these gases is described by the ratio between the discharge pressure and entrainment pressure of the gases passing through the ejector.

$$C_r = \frac{P_c}{P_e}, with \sim 10 \geq C_r > 1 \tag{17}$$

The compression ratio is limited at the bottom to values higher than one. If the compression ratio is below one, then equation (16) is not true, meaning that P_c is equal or lower to P_e. In this case a phenomenon commonly named “surging” or “stone wall” starts taking place, as the gases no longer follow the correct path inside the ejector. The gases would start being entrained through the discharge orifice and discharged through the entrainment inlet.

In general it is also assumed that steam ejectors will have a maximum compression ratio (C_r) possible to be achieved during their operation. Information provided by ejector manufacturers indicates that the C_r in general will not go above ~10 (depending on the exact configuration of the ejector).

3.3.2 Thermal Vapor Compressor – Energy and Mass Balance: Mathematical Model and Algorithm

A scheme with the bulk of the TVC process described in this work is presented in Figure 14. This image also indicates the unknown inputs to the model described in this section.

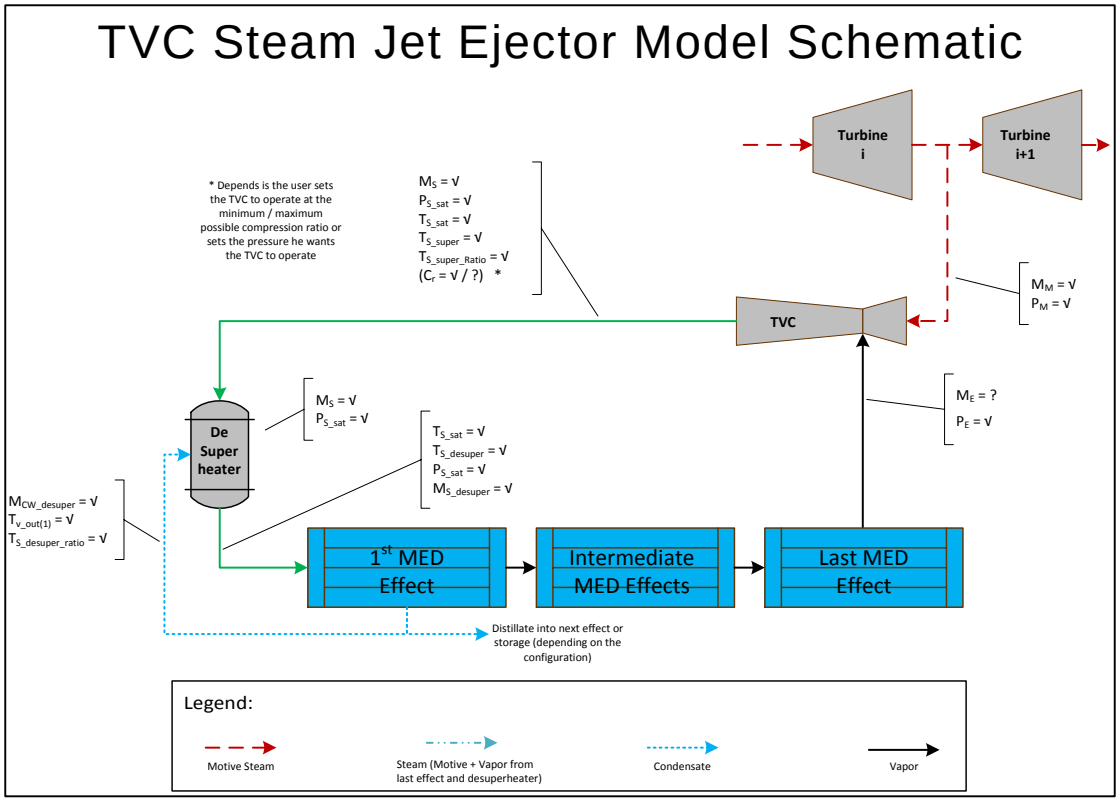

Figure 14 - TVC Steam Jet Ejector Model Schematic

A comprehensive diagram of the algorithm used for the first block of the steam jet ejectors model is presented in Annex 2, where the calculation steps are described in detail for the operation of a TVC (this diagram describes the calculations for mass and energy balance).

If a TVC is set by the user, the model assumes the existence of a desuperheater between the TVC and the first effect of the MED plant. In this case the heat load passing into the first effect is calculated by using the difference between enthalpies of the slightly superheated steam leaving the desuperheater and the subcooled distillate formed inside the heat transfer tube bundle of the first effect. The superheated steam entering the first effect and the corresponding subcooled distillate that is produced are assumed to be at the same pressure. This pressure is calculated based on the saturated temperature of the steam leaving the TVC (note that it is assumed that the steam leaving the TVC will be superheated but at a pressure defined by the saturated temperature).

A TVC is operated using high pressure motive steam. This model assumes that the TVC receives superheated steam bled from an intermediate extraction from the CSP steam turbine, and that the discharged steam will still be saturated (though steam turbines operate with superheated steam flowing through most of the stages, and depending on the type of

turbine, the steam exhausted may range between: saturated steam with quality below one, and superheated steam).

This model considers that the dimensioning of the TVC can be done in three different ways regarding its operation:

1. The TVC will be operated at its minimum possible compression ratio;
2. The TVC will be operated at a predefined discharged saturated temperature ($T_{s,\ sat}$);
3. The TVC will be operated at its maximum possible compression ratio;

The following description of the steam jet ejector model considers the usage of a database of entrainment ratios provided by the steam ejector manufacturer company to calculate this variable (although the model allows the user to use correlations available in the literature instead).

If the TVC is set to run at its lowest or its highest possible C_r, an iterative loop is used to calculate the conditions that could provide the C_r at the limit, and the $T_{s,\ sat}$ is obtained from the calculated P_c (assuming saturated conditions). In these conditions, $T_{s,\ sat}$ is calculated as a function of $P_{c,\ TVC}$ for saturated steam assuming a quality of 100%, as described in equation (18).

$$T_{s,\ sat} = f\left(P_{c,\ TVC},\ \chi\right), \qquad with\ \chi = 1\ (saturated) \tag{18}$$

If the TVC is set to run with a predefined $T_{s,\ sat}$, then the $P_{c,\ TVC}$ is calculated from the predefined $T_{s,\ sat}$ (assuming saturated steam with 100% quality), as described in equation (19).

$$P_{c,\ TVC} = f\left(T_{s,\ sat},\ \chi\right), \qquad with\ \chi = 1\ (saturated) \tag{19}$$

A TVC is added to a MED plant with the purpose of improving its efficiency, as it reuses vapor from the last effect to power the first one. If the heat transfer area cannot be decreased easily at design (in real life planning), then theoretically the plant performance could be increased by decreasing the compression ratio of the TVC, as with the same amount of steam is possible to entrain more vapor into the TVC (bounded in the first MED effect when the outlet saturated temperature of the compressed steam is equal to the brine temperature). This would increase the distillate production with the same mass flow rate and pressure of motive steam. Vice-versa in case the heat transfer area of the MED plant cannot be easily increased. Increasing the TVC compression ratio increases the TVC capacity to remove vapor from the last effect (sacrificing its efficiency though), and so more energy using the same mass flow rate of motive steam can be sent into the first effect (but in this case requiring a higher pressure and temperature of motive steam). A higher compression ratio implies a higher

temperature inlet for the steam entering the first effect. In this case a higher temperature difference is required in the first effect between the steam input and condensate outlet to keep on using the same heat transfer area, otherwise, more heat load into the first MED effect means that more heat transfer area is required per effect (as effects are considered to have the same HTX area, and this area is calculated from the heat load powering the last MED effect from what was possible to understand as "industry practice" during the execution of this work). Vice-versa is applicable when considering lower compression ratios for the TVC. In real life though, factors such as economic costs and physical site access conditions also play an important role when designing the plant (e.g. these may restrict the options available for transportation and construction of the plant). The research done during this work, lead the author to believe that these factors in particular limit the heat transfer area that can be used economically in each project, making it probably easier and less costly in some cases to optimize the plant by changing the TVC instead of the heat transfer area. For example, standards sizes may exist for several components of the MED plant, making the construction costs increase much more if using non-standard sizes, or physical conditions for site access may allow only the transportation of a specific size of MED component blocks [28] while keeping the project feasible from a financial point of view.

The compressed steam discharged by the TVC passes through a desuperheater before entering the MED plant. The usage of a desuperheater is a strategy applied when designing commercial plants using a TVC so that plant operators are able to maintain a stable steam temperature that enters the first effect, especially under different loads. There is a maximum brine temperature allowed when operating the first effect, above which, permanent $CaSO_4$ deposition is likely to take place (irreversibly damaging the plant). A direct contact type desuperheated [96] is assumed in this TVC model. Part of the distillate produced in the first effect is used as the cooling medium inside the desuperheater, entering into direct contact with the superheated steam as it mixes with it (and becoming steam again). Equation (21) is used for the calculation of the mass of cooling water required by the desuperheater ($M_{cw,\ ds}$).

$$M_{cw,\ ds} \times h'_{cw,\ out,\ Ej_2} + M_{c,\ TVC} \times h''_{c,\ TVC} = M_{cw,\ ds} \times h''_s + M_{c,\ TVC} \times h''_s \Leftrightarrow \quad (20)$$

$$\Leftrightarrow M_{cw,\ ds} = \frac{M_{c,\ TVC} \times \left(h''_{c,\ TVC} - h''_s\right)}{\left(h''_s - h'_{cw,\ out,\ Ej_2}\right)} \quad (21)$$

$$h''_{c,\ TVC} = f\left(T_{c,\ TVC},\ P_{c,\ TVC}\right) \quad (22)$$

$$h''_s = f\left(T_{s,\ ds}\right) \quad (23)$$

$$h'_{cw,\ out,\ Ej\_2} = f\left(T_{cw,\ out,\ Ej_2},\ \chi\right),\ with\ \chi = 0,\ saturated \quad (24)$$

As the superheated steam passes through the desuperheater, it is restored to a state near saturation, entering the first effect only slightly superheated. In this model it is

considered that the steam is at the same saturated pressure from the point it leaves the TVC until it enters the first effect (only the degree of superheating changes along its way to the first effect). Using the curves obtained for the ejector's entrainment ratios, it is not possible to determine in which saturation state will be the steam discharged by the ejectors. To overcome this drawback, an empirical correlation taken from the Trapani TVC-MED plant was used to estimate the temperature of the superheated steam discharged by the TVC, as described in equation (25).

$$T_{c,\ TVC} = T_{s,\ sat} \times \left(1 + T_{c,\ super\_ratio}\right) \quad (25)$$

A similar strategy is applied to calculate the temperature of the slightly superheated steam leaving the desuperheater, but in this case a fixed temperature difference is assumed between the $T_{s,\ sat}$ and the $T_{s,\ ds}$, as described in equation (26).

$$T_{s,\ ds} = T_{s,\ sat} + \Delta T_{s,\ ds} \quad (26)$$

This temperature difference can vary depending on the designer of the plant and the conditions he is challenged with, but it is assumed by the literature [96] and the manufacturers that as a rule of thumb this temperature difference will be 3 ºC above the saturated temperature (value which is used in the model).

The TVC model assumes that the P_m and M_m are inputs, and that the pressure of the entrained vapor by the TVC is set by the pressure from the last effect, as equation (27) describes.

$$P_{e,\ TVC} = P_n \quad (27)$$

The steam ejector entrainment ratio database deals with five variables: P_m, P_c, P_e, M_m and $M_{e,\ DAE}$. The ejector size and the entrainment ratio are then calculated from these values (detailed calculations for Dry Air Equivalent (DAE) temperatures and mass flow rates are provided in section 3.3.4). Knowing four of these parameters, it is possible to calculate the fifth one. When simulating the TVC, the $M_{e,\ TVC,\ DAE}$ is the incognita, and it is calculated using the known values for $P_{m,\ TVC}$, $M_{m,\ TVC}$, $P_{e,\ TVC}$, $P_{c,\ TVC}$, $M_{m,\ TVC}$, and the $W_{r,\ TVC,\ DAE}$ for the predefined points on the database, as described in equation (28).

$$W_{r,\ TVC,\ DAE} = f(P_{m,\ TVC}, M_{m,\ TVC}, P_{e,\ TVC}, P_{c,\ TVC}, M_{m,\ TVC}) \quad (28)$$

Knowing the $W_{r,\ TVC,\ DAE}$, the $M_{m,\ TVC}$ it is possible to calculate the $M_{e,\ TVC,\ DAE}$, as shown in equation (29).

$$M_{e,\ TVC,\ DAE} = W_{r,\ TVC,\ DAE} \times M_{m,\ TVC} \tag{29}$$

Using the corrections factors described for the conversion of the entrainment steam into DAE, the actual M_e is calculated using equation (30) (this equations is described in section 3.3.4).

$$T_{e,\ cf,\ steam} = \frac{\frac{(70\ ºF - 32)}{1.8\ ºC} - T_{v(n)}}{\frac{(130\ ºF - 32)}{1.8\ ºC}} + (1 - 0.958) \tag{30}$$

$$M_{e,\ TVC} = \frac{M_{e,\ TVC,\ DAE}}{T_{e,\ cf,\ s} \times M_{e,\ cf,\ s}} \tag{31}$$

The mass of steam leaving the TVC is $M_{c,\ TVC}$, and corresponds to the sum of the $M_{m,\ TVC}$ and $M_{e,\ TVC}$, as shown in equation (32).

$$M_{c,\ TVC} = M_{m,\ TVC} + M_{e,\ TVC} \tag{32}$$

The mass of steam entering the first effect corresponds to the mass of steam leaving the desuperheater, $M_{s,\ ds}$. This will be equal the sum of $M_{c,\ TVC}$ plus the mass of cooling water added to the desuperheater, $M_{cw,\ ds}$, as shown in equation (33).

$$M_{s,\ ds} = M_{c,\ TVC} + M_{cw,\ ds} \tag{33}$$

If a TVC is used, than it is assumed that the heat transfer inside the first effect of the MED plant will occur under different conditions compared to all the other MED effects. When a TVC is present, it is assumed that the energy transferred into the first effect is not only due to the latent heat released during the steam condensation, but it is also due to sensible heat released, as the steam entering the first effect is slightly superheated (as it leaves the desuperheater), and the condensate released at the end of the tube bundle is subcooled.

In all the other effects it is assumed that the energy transferred through the tube bundle is only due to latent heat released by the condensation of vapor inside the tubes. This means that the inlet and outlet temperature of the fluid inside the tube bundle is the same. Similarly in

the remaining effects, the distillate box will operate at the saturated temperature defined by the pressure at which the tube bundle operates.

The calculation of the subcooled temperature inside the first effect is obtained, as shown in equations (34) and (35), by calculating the average temperature difference in all the remaining effects between the brine temperature on the shell side, $T_{b(i)}$, and the vapor/condensate temperature on the tube side of the tube bundle $T_{v(i),\ out}$ (the latter which corresponds in practice to the T_v in the previous effect minus the average vapor temperature loss of the vapor being transferred into the tube bundle of the current effect, $T_{v,\ loss}$).

$$\Delta T_{htx(i)} = \left(T_{v(i-1)} - T_{v,\ loss}\right) - T_{b(i)} \tag{34}$$

$$MTD_{htx(1)} = \frac{\sum_{i=2}^{n} \Delta T_{htx(i)}}{n-1} \tag{35}$$

This average for the mean temperature difference within effects is then applied to calculate the subcooled temperature for the condensed steam leaving the tube bundle of the first effect, as shown in equation (36).

$$T_{d(1),\ sub} = T_{b(1)} + MTD_{htx(1)} \tag{36}$$

Using a TVC, the outlet from the first effect will be split and routed into three different directions: 1) a mass flow of condensate is equivalent to the mass of steam used to power the TVC and the NCG steam ejectors will be routed into the surface condenser (a shell-tube heat exchanger) attached to the second NCG steam ejector as cooling water before returning back to the boiler; 2) a second part will be routed into the desuperheater; 3) and a third corresponding to the remaining distillate produced in the first effect is routed into the next effect's distillate box (in case cross-flow of distillate is considered, otherwise the model assumes it is sent directly to storage).

The heat load entering the first MED effect when using a TVC is described in equation (37).

$$Q_1 = M_{s,\ ds} \times \left(H_{s,\ ds} - H_{d(1),\ sub}\right) \tag{37}$$

3.3.3 NCG Venting System – Energy and Mass Balance: Mathematical Model and Algorithm

A scheme with the bulk of the NCG two-stage steam jet ejectors process described in this work is presented in Figure 15 (for a TVC-MED configuration).

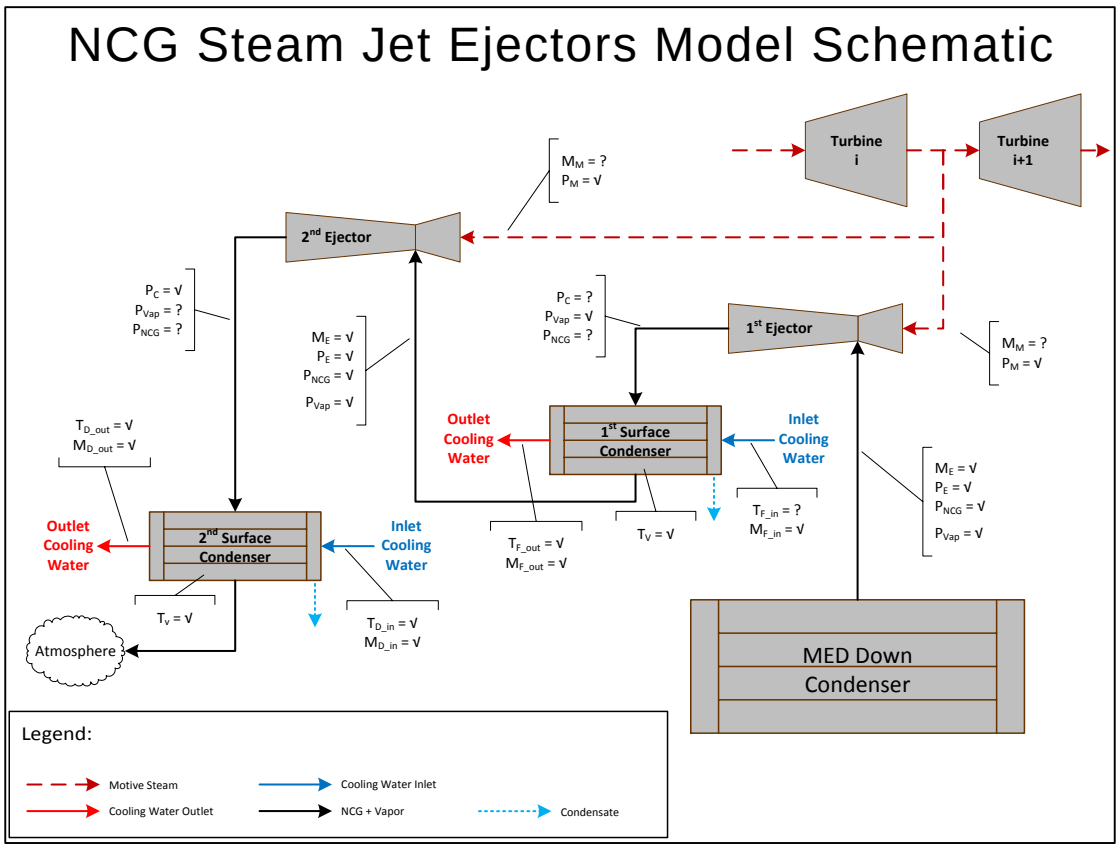

Figure 15 - NCG Steam Jet Ejectors Model Schematic (for a TVC-MED configuration).

A comprehensive diagram of the algorithm used for the steam ejectors model is presented in Annex 2, where the calculation steps are described in detail for the operation of the NCG venting system with a two-stage steam jet ejector system.

In this model the NCG venting system is assumed be ensured by a two-stage steam jet ejector. The positioning of the ejectors intercondensers can be defined by the user, but the model always considered that the effects upstream of these two intercondensers do not have more external preheaters of any kind.

Both intercondensers of the NCG ejection system are modeled to provide the maximum amount of heat possible into the MED plant, being limited by the maximum compression ratio for their size. This means that their aim is to provide the amount of energy required to preheat the cooling water into the intercondensers and not to minimize the total amount of motive steam they will use to extract the NCG from the MED system. This follows the strategy that

seemed to be implemented at the Trapani TVC-MED-P plant (taking into account that not all the info from that plant was available). This was also confirmed by the plant manager and the steam ejector manufacturers (that were contacted to obtain the ejector's database). The first ejector is dimensioned in this model to provide the maximum energy possible without over-sizing the amount of NCG assumed to be ejected. If the first NCG ejector cannot provide enough energy to the feedwater and obtain the same temperature increase that was assumed for the previous feedwater preheaters, then the model will assume a lower temperature output from the preheated feedwater of the first NCG steam ejector. On the other hand the second NCG ejector will aim at a user defined temperature output for the intercondenser cooling water output, and so the model may over-size the amount of NCG ejected by this ejector, in case the maximum energy input into it is not enough (having also into account the maximum compression ratio for the selected pressures with this ejector). This model aims to be used for feasibility studies at pre-design stage, being the main output required from it the total mass of motive steam used to operate the NCG steam ejectors. Detailed studies would imply more complex models to calculate the optimal configuration for the operation of these ejectors (and so more inputs from the user to run the model would also be required).

For a LT-MED-P configuration the model considers that the distillate from the first and second intercondensers of the NCG ejection system will enter the first effect downstream to the intercondensers position. If the condensate formed in each of the intercondensers is at the same saturated vapor temperature at which the distillate box operates no flashing will occur. Otherwise, the flashing of the condensate produced in the intercondensers will be calculated when it enters the distillate box of the effect down-stream.

For a TVC-MED configuration the first ejector's intercondenser is set to preheat the feedwater entering the first MED effects (exact position is selected by the user), and the second ejector's intercondenser is set to preheat the condensate returning to the boiler.

The calculations of the steam jet ejectors model for the ejectors removing NCG runs under the same principles than the calculations for the TVC explained in section 3.3.2. The main difference is that some of the unknown variables when applying the model to a TVC are now known when simulating the NCG ejectors and vice versa, namely: now the entrained mass flow rate is known, while the mass flow rate of motive steam is now unknown. Also the discharge pressure for the first NCG ejector is unknown.

The following paragraphs describe the strategy used to perform the mass and energy balance for the first and second NCG ejectors within the steam ejector model.

A) What is known when the steam ejector model is called by the MED detailed model:

1. The values for the mass flow rate of feedwater, its inlet and outlet temperatures and pressures at which they are being pumped;
2. Motive steam pressure;
3. Predefined temperature approach between outlet feedwater temperature and condensation temperature of steam discharged for first and second ejector, respectively;
4. Discharge pressure of second ejector (1atm + 50mbar), as the model only assumes for this purpose plants at mean sea level;
5. Inlet feedwater temperature and corresponding mass flow rate entering the condenser that is cooling the gases discharged from the second ejector;
6. Database or correlations with info relating entrainment ratio, discharge, motive and entrainment pressure;
7. Entrainment pressures and entrained mass flows are known for the first ejector (total and partial values, considering two mass flows, vapor and NCG, respectively).

The calculation of the entrained mass flows and pressures into the first NCG ejector uses the following rationale: assuming a subcooling of 3 ºC as suggested by the ejector manufacturer as rule of thumb (as it is commonly used in the industry) it is possible to calculate the partial pressure of vapor dragged with the NCG into the first ejector using Dalton's law of partial pressure and the ideal gas laws. The total pressure of entrainment into the first NCG ejector is equal to the pressure inside the last MED effect. The model then considers that the entrained partial pressure of vapor is defined by a saturated temperature equal to the vapor temperature inside the first MED effect minus 3 ºC. The pressure differential between the partial pressure of vapor and total pressure is considered to be the partial pressure corresponding to the NCG. The total mass of NCG to be ejected are known as the user defined how much would be the concentration of the NCG in the feedwater, and when the calculation of the NCG steam ejectors starts, the MED model already knows how much feedwater enters the plant. With this info it is possible to calculate the mass of entrained vapor into the first NCG ejector, and consequentially know the total mass of gases entrained. Equations (38) through (53) describe the mathematical process to obtain the main equation that enables the calculation of the mass of vapor entrained into the first NCG ejector.

$$P_T = P_T \times \gamma_{H2O} + P_T \times \gamma_{NCG} \tag{38}$$

$$P_{H2O} = P_T \times \gamma_{H2O} \Leftrightarrow P_T = \frac{P_{H2O}}{\gamma_{H2O}} \tag{39}$$

$$P_{NCG} = P_T \times \gamma_{NCG} \Leftrightarrow P_T = \frac{P_{NCG}}{\gamma_{NCG}} \tag{40}$$

$$\gamma_i = \frac{P_i}{P_T} = \frac{moles_i}{moles_T} \Rightarrow \frac{P_{H2O}}{P_{NCG}} = \frac{P_T \times \frac{moles_{H2O}}{moles_T}}{P_T \times \frac{moles_{NCG}}{moles_T}} = \frac{moles_{H2O}}{moles_{NCG}} \tag{41}$$

$$P_T = P_T \Leftrightarrow \frac{P_{H2O}}{\gamma_{H2O}} = \frac{P_{NCG}}{\gamma_{NCG}} \Leftrightarrow \frac{P_{H2O}}{P_{NCG}} = \frac{\gamma_{H2O}}{\gamma_{NCG}} \Rightarrow \frac{P_{H2O}}{P_{NCG}} = \frac{\gamma_{H2O}}{\gamma_{NCG}} = \frac{moles_{H2O}}{moles_{NCG}} \tag{42}$$

$$\frac{P_{H2O}}{P_{NCG}} = \frac{moles_{H2O}}{moles_{NCG}} \Leftrightarrow moles_{H2O} = \frac{P_{H2O}}{P_{NCG}} \times moles_{NCG} \tag{43}$$

$$M_{NCG} = moles_{NCG} \times MM_{NCG} \Leftrightarrow moles_{NCG} = \frac{M_{NCG}}{MM_{NCG}} \tag{44}$$

$$M_{H2O} = moles_{H2O} \times MM_{H2O} \Leftrightarrow M_{H2O} = \frac{P_{H2O}}{P_{NCG}} \times moles_{NCG} \times MM_{H2O} \Leftrightarrow$$
$$\Leftrightarrow M_{H2O} = \frac{P_{H2O}}{P_{NCG}} \times \frac{M_{NCG}}{MM_{NCG}} \times MM_{H2O} \Leftrightarrow M_{H2O} = M_{NCG} \times \frac{P_{H2O}}{P_{NCG}} \times \frac{MM_{H2O}}{MM_{NCG}} \tag{45}$$

B) Main iteration strategy used to calculate the entrainment ratios for the first NCG ejector:

1. Calculate the condensation temperature for vapor discharged from the NCG first ejector. Value obtained from temperature approach to the vapor being condensed inside the first intercondenser and its cooling water outlet temperature;

   Code block 26:

```
E_Tc_Vap_1_ref = E_Tcw_out_1 + E_T_approach_cond_1
water_TQ_fun (E_Tc_Vap_1_ref, 1d0, pres = E_Pc_Vap_1_ref)
```

2. Assume as guess (at the start of the iterations) a value for the discharge partial pressure of vapor equal to zero for the first ejector;

   Code block 27:

```
E_Pc_Vap_1 = 0d0
```

3. Calculate the heat flow transferred into the MED feedwater preheater that is cooling the discharged gases from the first ejector;

   Code block 28:

```
E_Qcw_1 = (E_Hcw_out_1 - Hf_Tf_eph(n_ph_NCG+1)) * E_Mcw_1
```

4. Calculate number of moles of NCG being entrained;

Code block 29:

```
E_moles_NCG = E_M_NCG_1 / MM_NCG
```

5. Mass flow rate of vapor condensed in the first intercondenser;

Code block 30:

```
E_Mcond_Vap_1 = E_Qcw_1 / ( E_LHc_Vap_1)
```

6. Calculate mass of entrained vapor;

Code block 31:

```
E_Pe_1 = Psat_VapWater_fun(Tv_out(n))
E_Te_Vap_1 = Tv_out(n) - E_subcool_deltaT_1
E_Pe_Vap_1 = Psat_VapWater_fun(E_Te_Vap_1)
E_Pe_NCG_1 = E_Pe_1 - E_Pe_Vap_1
E_Me_Vap_1 = E_M_NCG_1 * (MM_water / MM_NCG) * (E_Pe_Vap_1 / E_Pe_NCG_1)
```

7. Calculate mass flow rate of DAE gases entrained into the first ejector;

Code block 32:

```
E_Me_air_equiv_1 = (E_M_NCG_1 / E_Me_cf_NCG / E_Te_cf_DryAir_1) + (E_Me_Vap_1 / E_Te_cf_Vap_1 / E_Me_cf_Vap )
```

8. Calculate mass of vapor necessary to be condensed to provide the heat load transfer required in the first condenser (assuming latent heat transfer only at temperature of vapor discharged from the first ejector);

Code block 33:

```
E_Mcond_Vap_1 = E_Qcw_1 / (E_LHc_Vap_1)
```

9. Call the second block of the steam jet ejector model that calculates the entrainment ratios of the ejector knowing the $M_{e,\,DAE}$, P_c, P_e and P_m;
10. Calculate mass of motive steam necessary to operate the first ejector, the total mass of discharged vapor, and total mass of vapor to be entrained into the second NCG ejector;

Code block 34:

```
E_Mm_1 = E_Me_air_equiv_1 / E_Wr_1
```

```
E_Mc_Vap_1 = E_Mm_1 + E_Me_Vap_1
E_Me_Vap_2 = E_Mc_Vap_1 - E_Mcond_Vap_1
```

11. Calculate the molar fraction of NCG and vapor remaining after partial condensation;

Code block 35:

```
E_moles_e_Vap_2 = E_Me_Vap_2 / MM_water
E_moles_e_Tot_2 = E_moles_e_Vap_2 + E_moles_NCG
E_Molar_f_e_NCG_2 = E_moles_NCG / E_moles_e_Tot_2
E_Molar_f_e_Vap_2 = 1d0 - E_Molar_f_e_NCG_2
```

12. Calculate partial pressure of vapor remaining, and corresponding saturated temperature;

Code block 36:

```
E_Pc_Vap_1 = E_Pc_1 * E_Molar_f_e_Vap_2
```

13. If the mass of entrained vapor into the second NCG ejector is lower than zero (which is impossible), restart calculations for first ejector by setting a slightly higher total discharge pressure (which will imply using a higher entrainment ratio);
14. If the calculated saturated partial pressure is similar to the reference partial pressure obtained from the temperature predefined for condensation of the vapor discharged from the ejector, then set the last calculated entrainment ratio as valid, and start calculations for the second ejector.

C) Main iteration strategy used to calculate the entrainment ratios for the second NCG ejector:

1. Calculate partial pressure of the water vapor being entrained into the second ejector and total pressure of entrainment;

Code block 37:

```
E_Pe_2 = E_Pc_1 * (1d0 - E_ratio_delta_Pe_2)
E_Pe_Vap_2 = E_Pc_Vap_1 * (1d0 - E_ratio_delta_Pe_2)
```

2. Calculate mass flow rate of air equivalent gases entrained into the second ejector;

Code block 38:

```
E_Me_air_equiv_2 = (E_M_NCG_2 / E_Me_cf_NCG / E_Te_cf_DryAir_2) +
(E_Me_Vap_2 / E_Te_cf_Vap_2 / E_Me_cf_Vap )
```

3. Call the second block of the steam jet ejector model that calculates the entrainment ratios for the second ejector, knowing the entrained mass of $M_{e,\,DAE}$, P_c, P_e and P_m;
4. Calculate mass flow rate of motive steam necessary to operate the second ejector and the total mass flow rate of discharged vapor;

Code block 39:

```
E_Mm_2 = E_Me_air_equiv_2 / E_Wr_2
E_Mc_Vap_2 = E_Mm_2 + E_Me_Vap_2
```

5. Calculate the partial pressure of NCG in the compressed gases leaving the 2nd ejector;

Code block 40:

```
E_Pc_NCG_2 = E_Pc_2 - E_Pc_Vap_2_ref
```

6. Calculate the heat load transferred into the distillate cooling the gases leaving the 2nd ejector;

Code block 41:

```
E_Qcw_2 = E_Mcw_2 * (E_Hcw_out_2 - E_Hcw_in_2)
```

7. Calculate the mass flow rate of vapor necessary to be condensed to provide the heat load required in the second condenser (assuming latent heat transfer only using the temperature of vapor discharged from first ejector);

Code block 42:

```
E_Mcond_Vap_2 = E_Qcw_2 / E_LHc_Vap_2
```

8. Calculate total amount of vapor discharged into the atmosphere;

Code block 43:

```
E_Me_Vap_atm = E_Mc_Vap_2 - E_Mcond_Vap_2
```

9. Calculate molar fractions of gases entrained into the atmosphere, similarly to the calculations performed for the first ejector;
10. In case the reference partial vapor pressure discharged by the second ejector is greater than the calculated partial vapor pressure (obtained by multiplying the total discharge pressure by the molar fraction of vapor entrained into the atmosphere), then restart calculations for the second ejector assuming: 1) a slightly higher value for the partial vapor pressure entrained into the second ejector; and 2) a slightly higher mass flow rate of NCG gases (only for the second ejector). Take into account that the

mass flow rate of NCG in MED plants is normally largely overestimated, as safety factors of at least 100% are commonly used by the industry;

11. If the calculated saturated partial pressure is similar to the reference partial pressure obtained from the temperature predefined for condensation of the vapor discharged from the ejector, then set the last calculated entrainment ratio as valid, and return to the MED model.

3.3.4 Empirical Performance Curves: Database

Several models exist in the literature describing the operation of steam ejectors, but the majority requires the knowledge of very specific inputs that are only available during detailed design of the plant (e.g. velocities at each stage inside the ejector, or nozzle dimensions) [18]. The purpose of this CSP+MED model is to allow an initial analysis, without having much information available regarding the design characteristics of both the CSP and MED plants. Using a detailed model to simulate a steam ejector would be a very demanding task under these conditions, and because of this, it was decided to use a simple model, so that it would be possible to obtain results with few key inputs. At least two models were found in the literature that would fit such a requirement, presented in [18], by H.T. El-Dessouky and H.M. Ettouney. As described in the literature, section 2.4.3, at least one of these models is based on information only for low to medium compression ratios from several ejector manufacturers. Both use a spline to calculate the entrainment ratio, requiring as inputs only the P_m, P_c, P_e, T_m and T_e. Though, from the data obtained from real plants, and from contacts with ejector manufacturers, ejectors used in MED plants may be designed to operate at high a Cr , as for example it is the case of the Trapani plant, while the maximum Cr for steam ejectors is around ~10. Also, when testing the semi-empirical models described in [18], the results were very different when compared with real data from ejector manufacturers and from the Trapani TVC-MED plant, as shown in section 3.3.6.

Given the apparent lack of accuracy of the simple models available in the literature for the calculation of entrainment ratios, it was decided to create a new one for this purpose, for steady-state conditions. This new empirical model is based on a database with predefined entrainment ratios for different steam jet ejectors that are theoretically optimized to operate at different conditions. Using this information is possible to infer on the performance of ejectors that are not described in the database. After several contacts with different ejector manufacturers, it was possible to obtain data kindly provided by one of the leading companies producing some of the best performing steam ejectors used in the MED industry: the German company Körting Hannover AG. Some information was also obtained from the French company Kinetic Therm.

While contacting the different ejector manufacturers, it was possible to understand that ejectors from different companies can vary significantly in performance (as well as their prices).

Database for the New Empirical Model

From the data gathered from real MED plants, informal contacts with manufacturers, and the process of actually defining, coding and testing the detailed MED model, it was possible to establish an hypothesis for the reason why steam ejectors in MED plants may tend to be dimensioned to operate near their maximum compression ratio: plant designers aim at maximizing the amount of energy entering the plant, instead of dimensioning the ejectors to optimize and reduce their steam consumption (which would result in less heating steam powering the plant).

The obtained entrainment curves from Körting Hannover AG are described for a two-stage ejector system, and indicate the M_m necessary to eject a determined M_e of dry air at 70 ºF, for a P_m of 2.7, 8, 12, 20 and 45 bars. From this data is possible to calculate directly the W_r and the C_r at each point describing each curve using equations (15) and (17), respectively.

An example of the curves describing the first ejector is shown in Figure 16, showing entrainment ratios for with motive steam pressures using 8 and 12 bar. These curves were defined for:

- Two sizes referring to the diameter of the inlet pipe for the entrained gas: 4” and 8”;
- P_e of 42, 55, 74 and 123 mbar;
- For each of these entrainment pressures several P_c are defined, starting at 150 mbar, and increasing with intervals normally between 50 or 100 mbars. For each curve the maximum P_c described is defined by the maximum compression ratio admissible for the P_m, P_e, M_e, and ejector size defined for that same curve (that fit the nearest 50 or 100 mbar interval regarding P_c).

Following the requests for these P_m, P_c and P_e, the detail dimensioning of the ejectors used in the database was done by Körting Hannover AG. Information on the actual design of the nozzle for each configuration was not available, as it is proprietary information of the company.

The selected P_e range in the database for the first ejector was chosen having into account the typical pressures that may be used on the last effect and down-condenser of a MED plant for the zones where these plants have been typically installed (e.g. Mediterranean sea and Middle East). The pressures on the last effect and down-condenser are directly dependent of: 1) the maximum seawater temperature that the MED plant may use where it is installed, and 2) the designed temperature approach considered for the down-condenser between the vapor

being condensed and the feedwater temperature (inlet or outlet feedwater temperature, depending on the designer). The temperature approach is set higher if pumping and material costs are also higher (but more thermal energy is wasted from the MED process), and vice-versa. Again, the Trapani TVC-MED plant was used as a reference to understand the temperature ranges that MED plants may use. This plant in particular uses a feedwater outlet temperature from the down-condenser of 35ºC, and a maximum expected seawater intake temperature of 22 ºC [28] (the intake for this plant is not taken directly from the Mediterranean sea surface). In this model a range suitable for the operation of the last effect and down-condenser of MED plants in different locations, and so the requested P_e for the ejectors performance database was set for 42, 55 and 74 and 123 mbar, matching a saturation vapor temperature of 35, 40, 45 and 50 ºC, respectively (if assuming 100% vapor, without NCG, and ejectors connected to colder effects only).

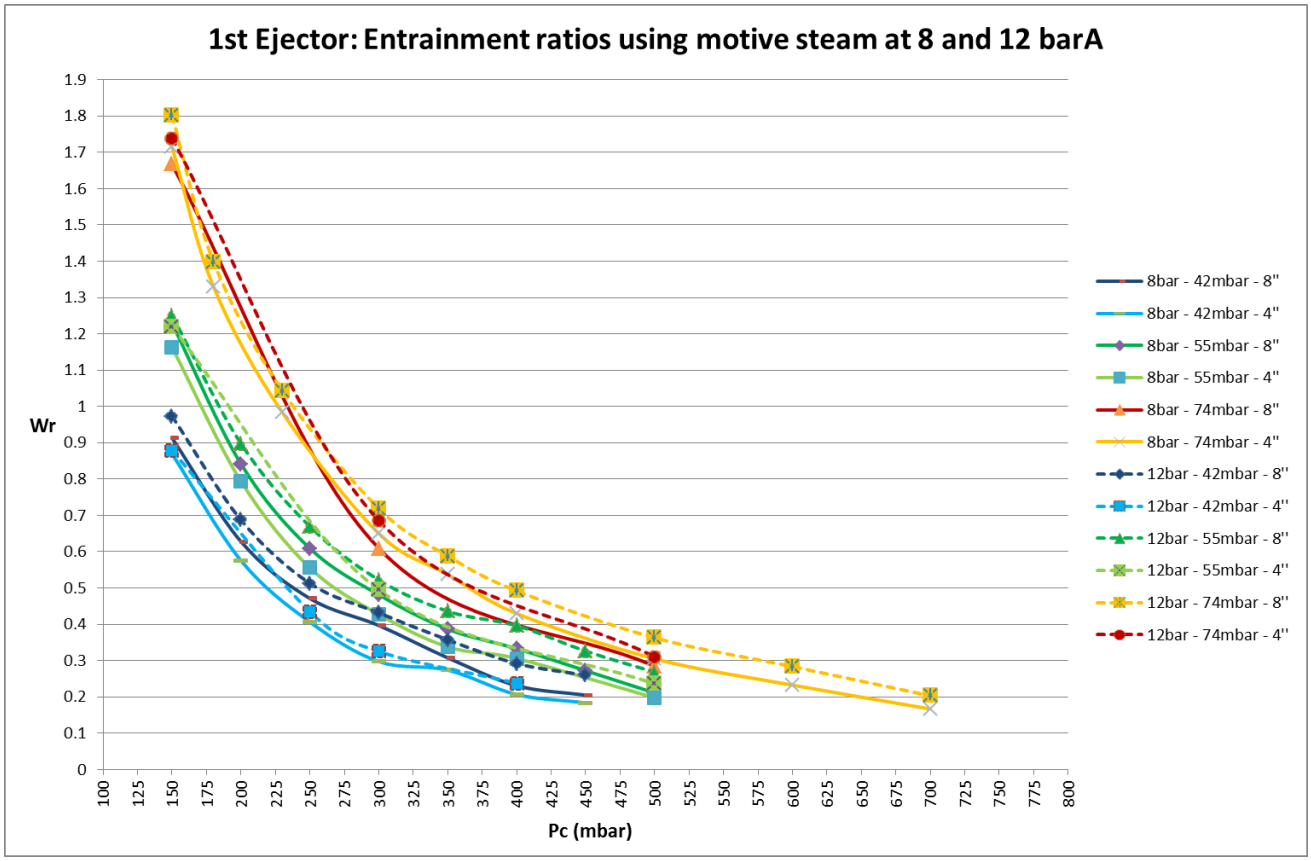

Figure 16 - Entrainment ratios using motive steam at 8 and 12 BarA for the 1st ejector of a 2 stage ejector system, provided by Korting Hannover AG.

An example of the curves describing the second ejector for 8 and 12 bars are shown in Figure 17. These curves were defined for:

- P_e of 150 mbar up to maximum allowed P_e for the first ejector in the database (with the same P_m), in intervals of 50 mbar;
- P_c is set for all points as the atmospheric pressure at sea level, plus a silencer (1063 mbar equal 1013 mbar plus 50 mbar, respectively).

The selected discharge pressure of the second steam ejector in the database was set to be the atmospheric pressure at sea level (1063 mbar), as most commercial large scale MED plants have been built in coastal zones.

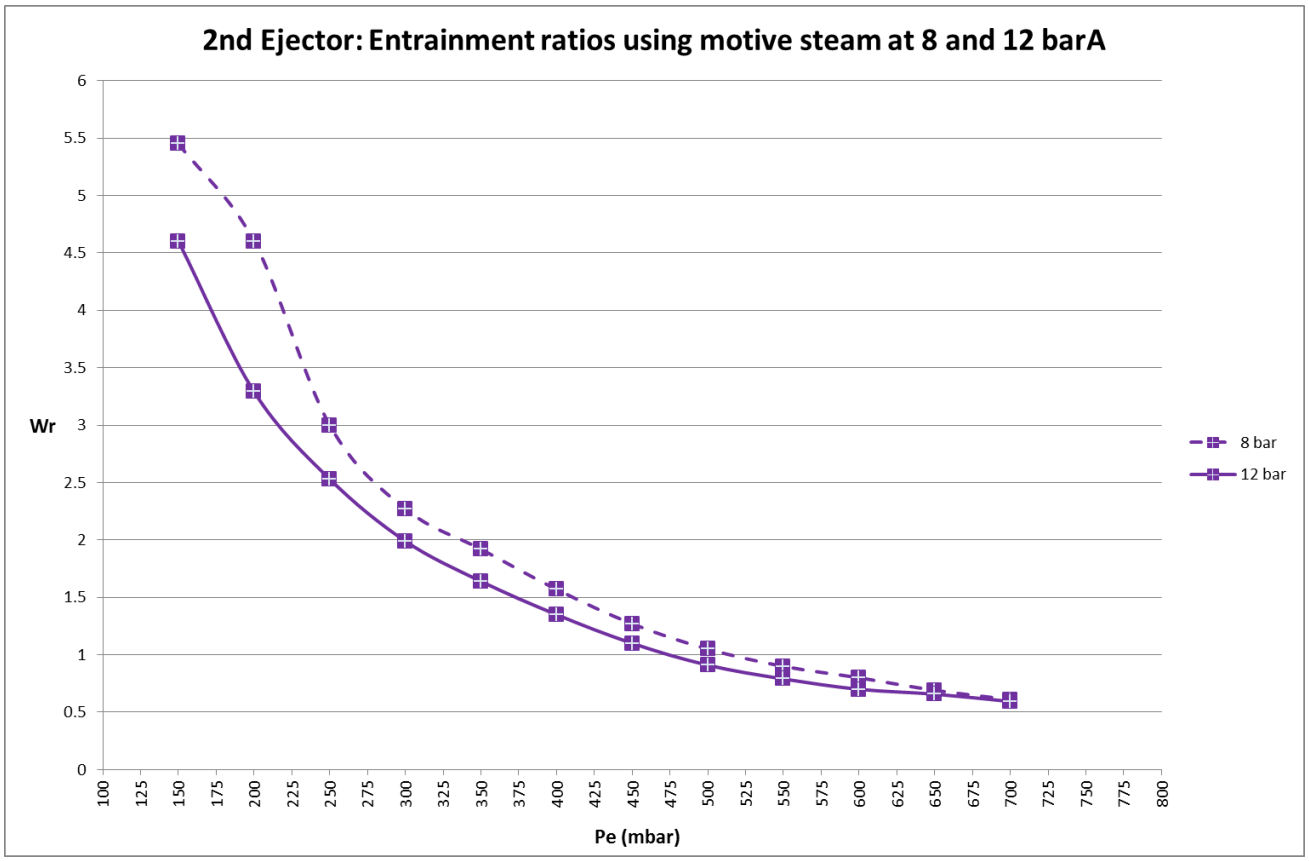

Figure 17 - Entrainment ratios using motive steam at 8 and 12 barA for the 2nd ejector of a 2 stage ejector system, provided by Korting Hannover AG

A comprehensive diagram of the algorithm used to calculate the entrainment ratios with the database provided by the steam ejector manufacturer with the steam jet ejector model and the MED detailed model is presented in Annex 3, where the calculation steps are described in detail.

This database was built in such a way that it could be easily expanded with more entrainment ratios for different P_c, P_e, P_m, and ejector sizes if necessary later on.

The ratios obtained for the performance of the steam ejectors in this database are valid when the entrained gas is dry air at 70 ºF. This is an industry practice, as it is not practical or economical for ejector manufacturers to maintain and operate testing facilities for an infinite number of gases and temperatures of those gases [97]. The Heat Exchange Institute (HEI) developed a method called “equivalent loading” that introduces the concept of dry air equivalent at 70 ºF. This method is commonly used by ejector manufacturers [98], [99] and it allows them to design the steam ejectors under standard conditions (dry air at 70 ºF entrained gas) and then apply them to actual process conditions in which the ejectors will work. With this strategy, corrections can be made for temperature and molecular weight of the entrained gas actually used, as typically it will be at a different temperature and/or have a different molecular weight. Both the correction factors for the entrainment temperature and the molecular weight (necessary to apply the DAE method) are described below, and were acquired from data obtained by the HEI [97].

Entrainment Temperature Correction Factor

Data describing the entrainment temperature correction factor for air and steam follow an inversely proportional function (almost linear) relative to the entrainment temperature, as presented in Table 10. Different temperature correction factors apply separately to steam and dry air, because condensable gases (in this case: steam) perform differently than non-condensable gases (in this case: dry air).

Table 10 - Temperature entrainment ratio [98]

Gas Temperature (ºF)		70	100	200	300	400	500	600	700	800	900	1000
$T_{e,\,cf}$	**Steam**	1	0.992	0.958	0.925	0.892	0.86	0.828	0.792	0.76	0.728	0.692
	Air	1	0.994	0.97	0.945	0.923	0.898	0.874	0.85	0.825	0.803	0.778

In this work the linear functions describing the ratio applicable for the entrainment temperature for steam and dry air, were obtained by linear interpolation using the first two points in Table 10 for each of the curves (the formulas already include the conversion between ºF and ºC, so that the metric system inputs can be used directly).

Steam: Equation for Temperature Entrainment Ratio Correction Factor

$$T_{e,\ cf,\ s\,(70^{o}F)} = 1 \tag{46}$$

$$T_{e,\ cf,\ s\,(200ºF)} = 0.958 \quad (47)$$

Temperature difference between these 2 points:

$$\Delta T_{e,\ s} = 200\ ºF - 70\ ºF = 130\ ºF\ \approx 54.4\ ºC \quad (48)$$

Conversion from ºF to ºC:

$$T\ ºC = \frac{(T\ °F\ - 32)}{1.8\ °C} \quad (49)$$

Equation (50) is used in the model to obtain the correction factor for the entrainment temperature when using steam, through a linear interpolation. Equation (50) is obtained using equations (46) to (49).

$$T_{e,\ cf,\ s} = \frac{\frac{(70\ ºF - 32)}{1.8\ ºC} - T_e}{\frac{(130\ ºF - 32)}{1.8\ ºC}} + (1 - 0.958) \quad (50)$$

Dry air: Equation for Temperature Entrainment Ratio Correction Factor

$$T_{e,\ cf,\ dry\ air\,(70ºF)} = 1 \quad (51)$$

$$T_{e,\ cf,\ dry\ air\,(200ºF)} = 0.970 \quad (52)$$

Temperature difference between these 2 points:

$$\Delta T_{e,\ dry\ air} = 200\ ºF - 70\ ºF = 130\ ºF\ \approx 54.4\ ºC \quad (53)$$

Equation (54) is used in the model to obtain the correction factor for the entrainment temperature when using dry air, through a linear interpolation. Equation (54) is obtained using equation (49), and equations (51) to (53).

$$T_{e,\ cf,\ dry\ air} = \frac{\frac{(70\ ºF - 32)}{1.8\ ºC} - T_e}{\frac{(130\ ºF - 32)}{1.8\ ºC}} + (1 - 0.970) \quad (54)$$

Theoretically these entrainment temperature correction factors for steam and dry air are only valid for temperatures above 70 ºF [97]. Yet, as they show a linear profile, and no other references were found for correction factors at lower temperatures, in this model these correction factors are also admitted to be valid when temperature of the entrained gases is below 70 ºF (though, in most MED plants the last effect and down-condenser operate at vapor temperatures higher than 70 ºF ≈ 21.1 ºC).

Entrainment Molecular Weight Correction Factor

Data describing the molecular weight entrainment ratio is presented in Table 2. This table presents average correction factors obtained by the HEI [97], which are applicable for pressures above ~1.3 kPaA. This pressure is equivalent to saturated steam temperature of ~11.2 ºC and so it is applicable for the pressure range used on the last effect and/or down-condenser of most MED plants.

Table 11 - Molecular weight entrainment ratio [98]

Molecular weight (kg/kmol)	10	20	30	40	50	60	70	80	90	100	110	120	130	140
Entrainment ratio correction factor (-)	0.58	0.85	1.02	1.14	1.23	1.32	1.38	1.43	1.46	1.49	1.52	1.55	1.57	1.6

The molecular weight of pure water is 18 kg/kmol, and from contacts with ejector manufacturers, it was possible to understand that it is standard practice (when dimensioning ejectors for MED plants) to consider the average molecular weight of NCG to be 36 kg/kmol.

$$MM_{NCG} = 36\ \text{kg/kmol} \tag{55}$$

$$MM_{s} = 18\ \text{kg/kmol} \tag{56}$$

Using the molar masses for pure water and NCG as reference with the corresponding graphic representations from [97], the entrainment molecular weight correction factors to dry air are the ones described below.

$$M_{e,\ cf,\ NCG} = 1.09 \tag{57}$$

$$M_{e,\ cf,\ s} = 0.81 \tag{58}$$

Calculation of the DAE Load

The ejectors modeled in this work entrain two types of gas flows: 100% steam (when simulating a TVC); and a mixture of NCG and steam (when simulating a NCG ejector). The HEI [97] defines a specific method to calculate the equivalent loading in each of these two cases:

1. 100% steam entrained: calculations start by first determining the correction for entrainment temperature (to obtain the 70 ºF steam equivalent), and then determine the correction for the molecular weight (to obtain the 70 ºF DAE). Equation (59) describes the equivalent entrainment loading when using only steam.

$$M_{e,DAE} = \frac{M_s}{T_{e,\ cf,\ steam} \times M_{e,\ cf,\ s}} \tag{59}$$

2. Mixture of steam and NCG entrained: The calculations to determine the 70 ºF dry air equivalent are done separately for the condensable gases and the NCG, and then added together. For NCG, calculations in practice follow the same strategy as for the calculations for 100% steam entrained gas, but with different correction factors. Calculations for steam are done as described in the previous paragraph. Equation (60) describes the equivalent entrainment loading when using a mixture of NCG and steam.

$$M_{e,DAE} = \frac{M_{NCG}}{M_{e,\ cf,\ NCG} \times T_{e,\ cf,\ dry\ air}} + \frac{M_s}{T_{e,\ cf,\ steam} \times M_{e,\ cf,\ s}} \tag{60}$$

Linear interpolations were used to calculate intermediate values from the database describing the steam ejectors entrainment ratios.

3.3.5 Empirical Performance Curves: Mathematical Model and Algorithm

The mathematical model used to calculate intermediate values that are not described directly by the entries in the database is based on linear interpolations.

Annex 3 includes a comprehensive diagram of the algorithm used to perform linear interpolations with the mentioned steam jet ejector database, together with the main calculation steps used to simulate for the operation of a TVC or a NCG venting system with a two-stage steam jet ejector arrangement.

The model first tries to find the values in the database that are near to the operational point that the user wants to simulate for the steam ejector being simulated. The model tries to find these points by first checking the nearby values sequentially in the following order: P_m, P_e, P_m and then *Size* of the ejectors described (that have matching operational pressures).

After selecting the data points to use as reference, the linear interpolations are performed initially for the values of P_e. New points are calculated, all having the same P_e (the P_e pretended by the steam ejector model). With these new points the process repeats, and linear interpolations are performed in order to obtain intermediate new datapoints now with the same P_e and P_m. The same process is repeated for P_c. After this point the model only has two points that have the required P_m, P_e and P_c, but are referent to different ejector sizes. Using the information on the database referent to the mass flows used by each ejector, a last linear interpolation is performed to estimate the size of the ejector.

If the operational point that the steam ejector model requests is between the two ejector sizes described in the database (currently there are only two sizes described), and only the curve for the largest ejector nearest to the required point describes the operation of the ejector pretended by the user (meaning that the smaller nearest ejector will not operate at the P_c required), then the model will try to check if the operation of the ejector can be done near the maximum allowed compression rate. In this situation the model will use points described by the model for the maximum P_c for the curve describing the smaller ejector, and perform a linear interpolation between this point and the point described for the largest nearest ejector datapoint. The linear interpolation between these two points will return a “line” that describes roughly the progression of the maximum compression ratio for intermediate ejectors of increasing size. In case the pretended point is beyond this line then the operation of the ejector is not possible and it will be necessary to change the operational pressures of the ejector (e.g. lower the discharge pressure).

The linear interpolations performed by the model assume a linear relationship between the variable taken as reference for each interpolation, and applies the same ratio to the calculation of the remaining parameters. For example, the model calculates the difference of P_e between two of the selected points. Then uses the point describing the smallest ejector from these two points, and calculates the difference of P_e to the point pretended by the steam ejector model. The ratio between these two pressure differences is then applied to calculate the intermediate values for the remaining variables in each linear interpolation step (in this case it applies this ratio for the calculation of the intermediate values of P_m, P_c and *Size*). It is likely that this approximation will create more discrepancies versus real values in some simulations that in others depending on the set of conditions being used. Though, the validation procedure conducted to this linear interpolation model shown in section 3.3.6 seems to indicate that this method may return better results than the existing semi-empiric models available in the literature.

3.3.6 Model Calibration and Validation

This section describes the calibration and validation implemented to simulate the steam jet ejectors with the MED detailed model. The steam jet ejector model was calibrated mainly with information from the TVC-MED-P plant at Trapani, and with some of the information available from the LT-MED-P plant at Priolo-Gargallo. The validation processed consisted on running the MED model together with the steam jet ejector model, using the three models that are able to simulate the entrainment ratio of a steam ejector knowing only information about the pressures and mass flows used in the ejector (the two semi-empirical models described in the literature and the new empirical model developed with this work).

The new empirical model was run against real plant data together with the detailed MED model presented previously on section 3.2.4. The results using this model are especially interesting for the NCG steam ejectors at Trapani showing a deviation up to ~ -3%. The database made available from the ejector's manufacturers is specifically suited to simulate smaller ejectors as the ones used for the removal of NCG in that plant. As it was explained also in the previous section 3.2.4, the TVC shows a larger deviation for Trapani, because the ejector size at Trapani is much larger than the maximum size described in the database. According to the ejector's manufacturer, for the same operating pressures, the ejectors performance at nominal capacity increase as their size also increases. This can be confirmed using the available database of entrainment ratios for this new empirical model, where per each inch of increase of the entrainment and discharge tube sections (between 4" and 8") the ejectors entrainment ratio can improve for most conditions. This can be seen in Figure 18. It is important to note that these ratios of performance increase shown in Figure 18 probably cannot be simply applied as a correction factor to calculate how much would be the improvement of the TVC entrainment ratio in the simulation of Trapani (that uses a much larger ejector), as this information is only valid for ejectors between 4" and 8", and it would be speculative to assume the same rate of increase for much larger sizes.

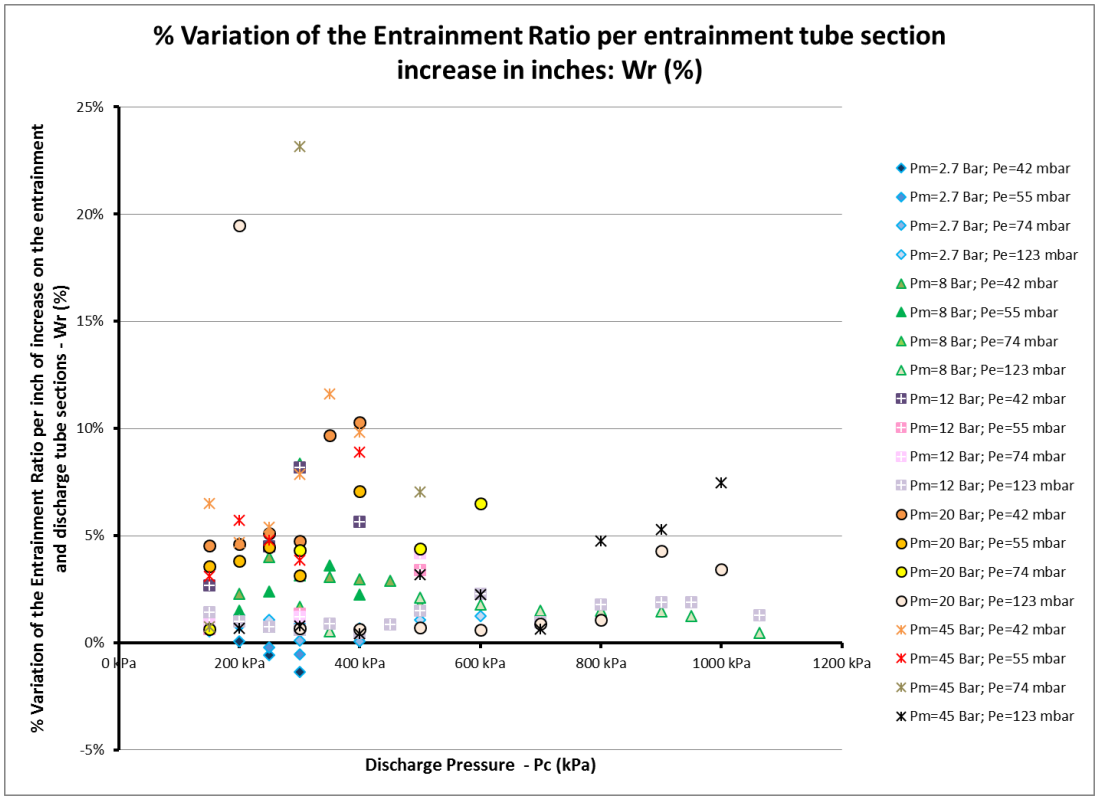

Figure 18 - % Variation of the Entrainment Ratio per entrainment tube section increase in inches using data from manufacturer.

The entrainment ratios in the mentioned database for the new empirical model developed in this work were also run against data from the two semi-empirical models described in [18], [82] and [83], and referred in the literature review, section 2.4.3 (these were the models that could potentially be applied during pre-design stage analysis using only information regarding the pressures and mass flows used, assuming optimum configuration designs under those conditions). The comparison of the results versus the model based on the curves described by Robert Power in [83] is shown in Figure 19, and the comparison of the results versus the model developed by El-Dessouky is shown in Figure 20.

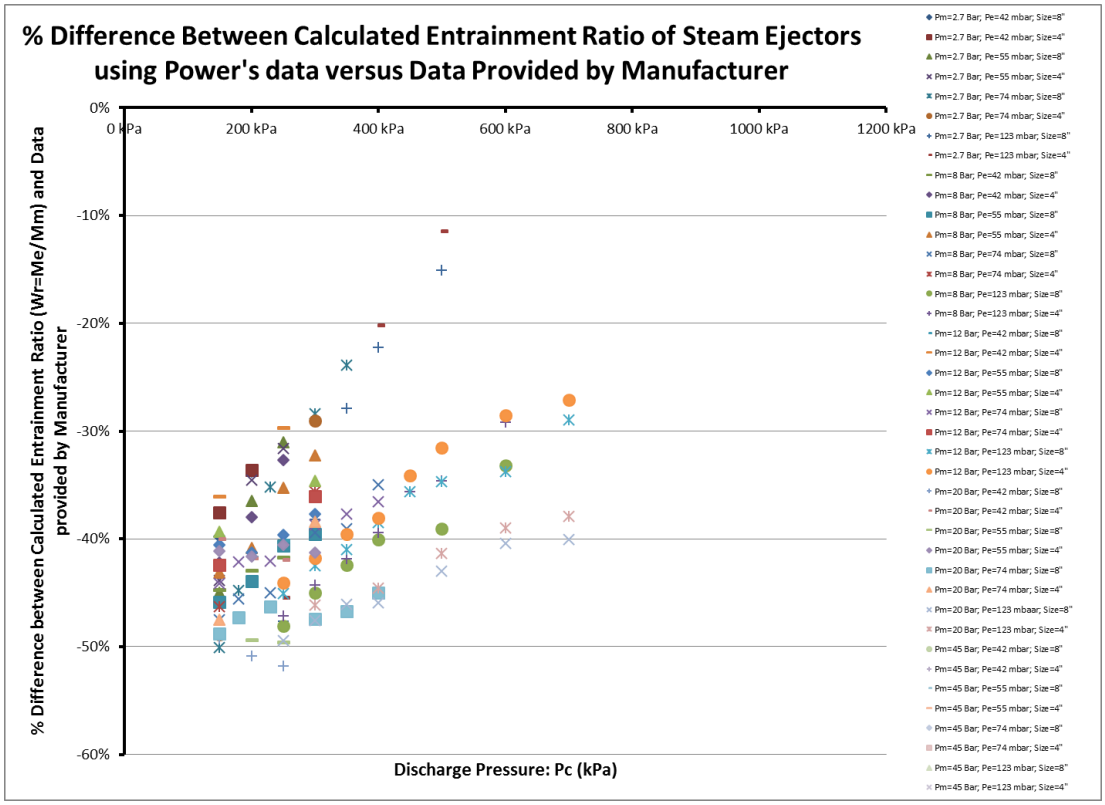

Figure 19 - % Difference between calculated entrainment ratio of steam ejectors using Power's data [83] (considering only the entrances Mm/Me equal or 4) versus data provided by manufacturer specifically ejectors applicable to MED plants.

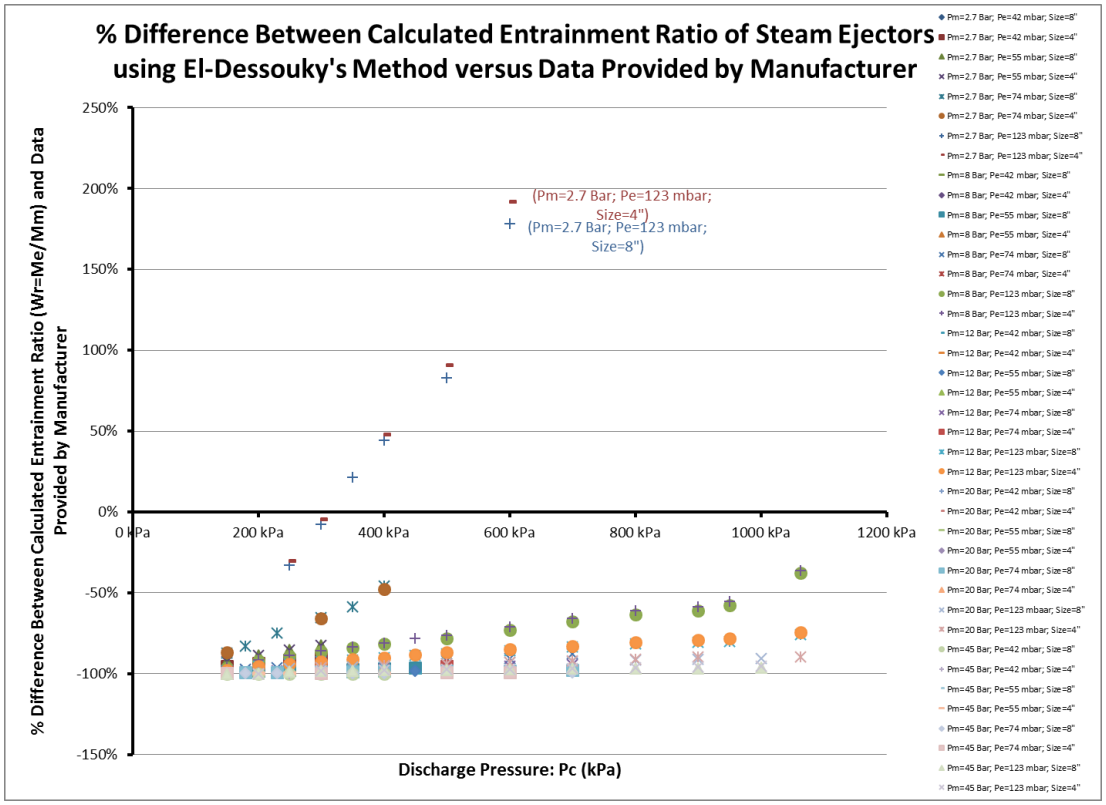

Figure 20 - % Difference between calculated entrainment ratio of steam ejectors using El-Dessouky's method in [18] and [82] versus data provided by manufacturer.

The results in Figure 19 and Figure 20 show a large gap between real data and the semi-empirical models selected. From these two semi empirical models, the one that got closer to the set of real data used in this work was the semi-empirical model based on information from Robert Power. This semi-empirical model returns results for the majority of the data points between ~25% to ~50% below the real data obtained from Koerting A.G. and Kinetic Therm. It was not possible though to analyze the sources of information used to compile the curves presented by Robert Power [83]. This author mentions in his work that the curves are most accurate for low compression ratios, and that they should agree with manufacturers' data within about 10 percent over the best-fit range. Beyond this range the uncertainty will be greater.

The semi-empirical model developed by El-Dessouky [82] shows a deviation between ~-50% to ~-100% for when compared with real data. This model is based on 51 data points acquired from major ejector manufacturers and information available on the literature. Many of these data points used by El-Dessouky do not represent operational conditions applicable to MED plants. For example: 41 of these 51 data points consider entrainment ratios below or equal to 1.7 kPa (~ 15 ºC saturated vapor temperature) and discharge pressures below or equal to 5.7 kPa (~35 ºC saturated vapor temperature) , and the remaining 10 points consider entrainment ratios between 37.01 kPa and 121.3 kPa (~74 ºC and ~105 ºC saturated vapor

temperatures, respectively) and discharge pressures between 119.9 kPa and 224.1 kPa (~104 ºC and 123 ºC saturated vapor temperature, respectively). It is also important to note that the maximum value for compression ratio in the database used by el-Dessouky in this semi-empirical model does not go above 6, being most of them referent to compression ratios between 2 and 5. At least the info from the Trapani MED plant says that these plants can use compression ratios up to ~8, though Trapani is a very special case, as it operates as a stand-alone plant, and because of that the plant designers might have chosen to use much higher steam pressures than they would if they would operate the plant in a cogeneration scheme.

The TVC is one of the most important components that can be added to a MED plant, and the correct assessment of this device is important to understand the performance of a MED plant using it. The mentioned semi-empirical models from the literature return values significantly below real data when comparing with small sized ejectors as shown in Figure 19 and Figure 20. As shown in Figure 18 the performance of steam ejectors improves in most scenarios as the size of the ejector (and load) increases. Assuming this, it is expected that the mentioned semi-empirical models from the literature will underperform in a larger scale when used to simulate larger ejectors than the ones described in the database obtained from Koerting A.G and Kinetic Therm.

In order to understand the impact of running these two semi-empirical models when simulating a MED plant versus using real ejector data from one single manufacturer, it was decided to upgrade the detailed MED model described in section 3.2, and add the option of choosing any of the three steam ejector models described when running simulations for the TVC. The results are shown in Table 12 and the deviations are shown for each model versus real plant data from Trapani. These comparative results were gathered from simulations with the same inputs as the ones described in Table 5 and Table 6 (in section 3.2.4, where results for the validation of the MED detailed model are shown). Data from the commercial MED plant at Trapani indicates that the TVC uses an entrainment ratio of ~0.587 (obtained dividing the mass of entrained vapor from the last effect, 13.2 t/h, by the mass flow rate of motive steam powering the TVC, 22.5 t/h). Using the Power's method in the ratio between the mass flow of motive steam and the mass flow of entrained vapor is above 4, then a two stage ejector system is considered for the TVC, assuming that the first ejector will have a discharge pressure that is half of the discharge pressure defined by the user.

Table 12 - Comparison of results for the Trapani TVC-MED-P plant using different ejector models for the TVC calculations

Parameter	**Real Data from Trapani**	**New empirical model using linear interpolation, with manufacturer's data**		**Semi-empirical model based on Robert Power's curves** [83]		**Semi-empirical model using El-Dessouky's method in** [18]	
		Calc.	Deviation	Calc.	Deviation	Calc.	Deviation
Entrainment Ratio	0.59 (-)	0.49 (-)	**-16.34 %**	0.04 (-)	**-92.01 %**	2.07E-3 (-)	**-99.64 %**

Distillate / train	375.00 t/h	377.98 t/h	**0.76 %**	263.71 t/h	**-29.70 %**	69.92 t/h	**-32.90 %**
Brine / train	755.00 t/h	758.11 t/h	**0.42 %**	534.98 t/h	**-29.13 %**	142.14 t/h	**-32.22 %**
Feedwater / train	1130.40 t/h	1137.39 t/h	**0.62 %**	799.78 t/h	**-29.24 %**	212.36 t/h	**-32.37 %**
Brine salinity outlet / train	5.99 wt%	5.98 wt%	**- 0.10 %**	5.96 wt%	**-0.46 %**	5.96 wt%	**-0.52 %**
Total heat transfer area per effect	Conf.	Confidential	**5.40 %**	Confidential	**-27.13 %**	Confidential	**-30.54 %**
Mass flow of entrained steam into the TVC	13.2 t/h	11.04 t/h	**-16.34 %**	1.05 t/h	**-92.01 %**	1.29E-2 t/h	**-99.64 %**
Mass flow of cooling water intake into the down-condenser	1280 t/h	1231.07 t/h	**-3.82 %**	1322.56 t/h	**3.33 %**	1329.38 t/h	**3.86 %**
Mass flow of rejected cooling water outlet from the down-condenser	149.6 t/h	93.68 t/h	**-37.38 %**	522.78 t/h	**249.45 %**	564.88 t/h	**277.59 %**
Adjusted $Tf_{(1)}$	55 ^{o}C	56.13 ^{o}C	**2.05 %**	-	**-**	-	**-**
References for real data	[25], [28], [94], [93] and direct contact with plant operator						

Any of the two simple semi-empiric models for steam jet ejectors taken from the literature return a similar impact on the total MED plant production. Distillate, brine and feedwater mass flow rates show a deviation between ~ -29 and ~ -32 % when comparing the calculated results versus real plant data. It was expected that eventually Power's method could return better results than the method presented by El-Dessouky (as it can be seen when comparing Figure 19 and Figure 20), but the Power's method also clearly mentions that it is not as accurate for motive steam pressures above 35 bars (and this simulation for Trapani considers 45 bars). Using data from Trapani as reference, the new empirical model developed in this thesis for the calculation of entrainment ratios of steam jet ejectors presents as being the best option, despite using information from only one manufacturer.

3.4 Auxiliary: Pumping Model

3.4.1 General Description

Auxiliary systems are required for pumping water to, from and inside the MED plant. A simple steady-state model was developed to simulate the electric energy necessary to pump the following mass flows:

I. Seawater intake up to both the MED and SWCC condensers;
II. Seawater inside the MED down-condenser;
III. Seawater inside the SWCC condenser;
IV. Brine between MED effects (if necessary) plus brine extraction from last effect;
V. Brine/cooling water outlet from the CSP+MED/SWCC system back to the sea;
VI. Condensate return back to the Rankine cycle;
VII. Distillate into storage reservoir.

The auxiliary pumping model as whole assumes the:

I. Piezometric head;
II. Head loss inside straight cylindrical tubes;
III. Head loss inside shell-and-tube heat exchangers (MED down-condenser and SWCC only).

The model was built so that it is adaptable when applied to a time series calculation. Part of the algorithm was built to be used when the model is dimensioning the plant, returning tube diameters and lengths, apart from the electrical consumption at nominal capacity with the pumping systems. After the first call in a time series, the model is set to return the electrical pumping costs together with the velocities of the fluids inside the tubes. As inputs the model uses the distances between the MED plant to the intakes and outlets; distances to the distillate storage and the boilers; pressure difference between MED effects (calculated by the MED model); mass flow rate, temperature, salinity and pressure of the brine, distillate and cooling water intake and rejected (calculated by the MED model); plant elevation referent to the ground and site elevation referent to the sea level; and finally the velocities of the masses flowing inside the mentioned systems using pumping equipment are also required as inputs (at nominal) for the cases where drag losses are accounted for. The user also sets the nominal efficiencies for the pumps and the net positive suction head (NPSHr) to be considered by the model as reference value.

3.4.2 Piezometric Head

The piezometric head is also called hydraulic head, which is the sum of the elevation of the water mass and the pressure head (being the pressure head the static pressure head). The calculations are based on the Bernoulli equation, which can be considered as a statement of energy conservation principles applied to fluids. Energy per unit volume before equals energy per unit volume after.

There are two typical forms of presenting the Bernoulli equation: one where the output is the total specific energy of a fluid (m^2/s^2), and a second one that presents this specific energy indexed to the pressure exerted by a determined height of a column of the fluid being analyzed (m), which is commonly adopted in technical systems. The second version was the adopted in this work [100].

$$Head = z + \frac{p}{\rho g} + \frac{u^2}{2g} \tag{61}$$

Steady-state conditions are assumed for the calculations of the piezometric head, and because of that, the last term of the equation referring to the kinetic energy ($u^2 / 2g$) is not considered when analyzing the flow of a fluid through the pipes.

When pumping water from the bottom of a reservoir (which is the case in many MED plants), the intakes can stretch a few miles underwater. The calculations for energy consumption to pump water through them are divided into two parts: above sea level and below sea level.

Below sea level, no piezometric head exists in practice as it is assumed that the sea level will not change due to the extraction of the seawater into the plant. Assuming incompressibility in a frictionless uniform steady-flow, if a fluid is moving through a tube totally submerged (vertical flow for ease of understanding), assuming the principle of the conservation of energy then no forces are acting on the fluid, and the moving fluid is neutrally buoyant relative to the surrounding fluid (Archimedes principle) [100]. Under these circumstances the moving fluid exerts always then same downward force as the surrounding fluid (same density assumed between them). In reality friction will occur with the pipe walls as the fluid flows creating drag and energy loss (which is calculated in subsequent part of the pumping model).

Above sea level the fluid is not considered to be buoyant relative to its surroundings. Applying the principle of conservation of energy, the reduction of pressure energy of the fluid as it moves upwards is compensated by an equal increase of its potential energy. It is considered that there is a minimum pressure level required from the outlet of the MED down-condenser.

Using as example the calculations made for brine and cooling water outlet from the plant, if the CSP+MED/SWCC has the MED plant in standby mode, than the pressure leaving the condensers is set to be 1 bar. Otherwise if the MED plant is operating, the pressure of leaving the down-condenser is dependent on the number of feedwater preheaters that the MED plant has installed. For each preheater it is considered a loss of 0.5 bars, and the minimum required pressure leaving the down-condenser is set to be 2 bars.

Code block 44:

```
OUT_P_Cond_outlet_MED = OUT_P_Cond_outlet + OUT_P_ph * n_ph

OUT_delta_pres_head = (OUT_P_Cond_outlet - Patm) / OUT_Gamma_Brine
```

MED plants are normally elevated a few meters above ground in part because of the pumps used to extract brine, condensate and distillate from the effects and down-condenser. A NPSH is required by the pumps for reliable operation through time (avoiding the cavitation effect). The required NPSHr is preset by the user. As a simplification, the elevation of the plant relative to the ground is set to be equal to the NPSHr.

Code block 45:

```
effect_soil_elev = NPSHr
```

This elevation of the plant relative to the ground is taken into account when calculating the total head for pumping seawater into and from the plant, as so as the distillate into storage.

Code block 46:

```
OUT_delta_piez_head = plant_elev_sea_level + OUT_delta_pres_head + effect_soil_elev
```

The piezometric head is then added to the remaining pressure losses to calculate the total electric consumption with auxiliary pumping.

3.4.3 Friction Head Losses Inside Single Straight Cylindrical Tubes

The calculation of head losses (pressure losses) due to drag inside single straight cylindrical tubes as the water masses flow through them are subdivided into two sections in this model: the first section where the tubes diameter are dimensioned, and the second section used to calculate the subsequent usage during plant operation according to the velocity of the fluid passing at each moment in time. The user sets the distance between the plants and the: intake edge, outlet edge and storage tank. The calculation of the friction head losses inside

the tube bundle of the MED down-condenser and SWCC condenser are slightly different and are addressed in the next subchapter.

Dimensioning

During the dimensioning phase, when the model is run for the first time, it calculates the size of the tubes to be used accounting design conditions set for the nominal fluid velocity of each of the mass flows mentioned before. The main output is the diameter of the tubes used and the head loss due to drag.

Using as example the calculations made for brine and cooling water outlet from the plant, the pipe section is calculated using the formula that relates it to the cross section area and the velocity of the flow [100].

Code block 47:

```
OUT_pipe_section = (OUT_B)* 1D-3 / OUT_velocity_sw
```

Knowing this, it is possible to calculate the pressure losses with drag along the tubes. In order to do so, it is necessary to calculate the Reynolds number (which gives the ratio of inertial forces to viscous forces).

Code block 48:

```
OUT_Re = (OUT_velocity_sw * OUT_pipe_diameter) / OUT_Kin_Visc_B
```

Using the dimensionless Reynolds number, a friction coefficient is calculated depending on the type of flow: laminar or turbulent. The threshold used in this model to distinguish between laminar and turbulent flow was a flow with a Reynolds number equal to 2000. Depending on the type of fluid and tubes used the type of flow can change significantly, and because of this, a simplification of the model is assumed by neglecting the transitional flow regimes. If the calculated Reynolds number is below or equal to 2000, a laminar flow is assumed.

Code block 49:

```
OUT_Friction_c = DBLE(16)/OUT_Re
```

If the Reynolds coefficient is above 2000 the flow is considered to be turbulent, and the Haaland formula is used [100].

Code block 50:

```
OUT_Friction_c = (-3.6D0 * LOG10 ((6.9D0/OUT_Re) +
+(OUT_Pipe_roughness/(3.71D0*OUT_pipe_diameter))**(1.11D0)))**(-2)
```

The friction factor is very dependent on the shape and material of tubes considered, and there are various formulas applicable to calculate it. Amongst these, the Haaland formula was one of the best performing, while still remaining relatively simple to use and accurate (within 1.5%) according to the literature [100].

Using this data, the friction losses as water flows through the pipes are calculated using the Fanning equation [72]. In the example being followed here, these refer to the pressure loss while pumping water from the plant back into the sea (outlet).

Code block 51:

```
OUT_Head_friction = (4D0 * OUT_Friction_c * OUT_Plant_distance /  OUT_pipe_diameter) *
(OUT_velocity_sw**2) / (2*grav)
```

Head losses are described in meters, and pressure in Pascals. The head to be surpassed in order to be able to pump water back into the sea is the difference between the total plant height relative to the sea level minus the head loss with friction through the pipe.

Code block 52:

```
OUT_Delta_head = OUT_Head_friction - OUT_delta_piez_head
```

In this case as the brine flows to the sea, because the plant stands above sea level, the potential energy is converted to kinetic energy favoring the flow. Depending on the type of tubes and velocities selected, the height of the plant may not be enough to overcome the drag losses with the selected pipe diameter and nominal velocity. In such a case the model calculates if a pump will actually be necessary to return the brine back to the sea.

If the total head loss is lower than zero, it means that the pretended pipe section is too large, and not enough drag is produced, leading to fluid velocities above the initially set. In such case a small iterative blocks is used, and the diameter of the outlet pipes are progressively reduced until the total head loss is equal to zero, while it is considered that the total electric consumption to pump this brine is zero.

Calculations after dimensioning

At this point the tube diameter for each tube section has been calculated, so that in nominal conditions the flow in each tube section is able to keep the preset velocity. After the dimensioning phase, the model calculates the velocity of the flow at each moment, which will vary according to the mass flow (as the tube diameter is now fixed). The friction head loss will also change accordingly to the fluid velocity.

Code block 53:

```
OUT_velocity_sw = (OUT_B)* 1D-3 / OUT_pipe_section
```

3.4.4 Head Losses Inside Shell-and-Tube Heat Exchangers

The main head losses due to friction inside a standard shell-and-tube heat exchanger [72] refer to the flow through: the channel inlet and outlet nozzles, headers and shell-side nozzles (Figure 21 details the mention shell-and-tube exchanger sections).

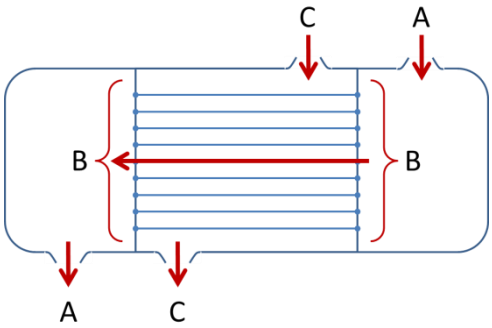

Figure 21 - General schematic of the sections of a shell-and-tube heat exchanger considered for the calculation of pressure losses (as described in [72]): A – channel inlet and outlet nozzles, B- headers, C – shell-side nozzles.

Currently this model accounts for the pressure losses of the seawater flowing inside the MED down-condenser and SWCC only, and because of that the pressure losses at the shell side nozzles are not considered.

Friction head losses inside straight cylindrical tubes

The calculation of pressure losses due to drag inside the tube bundle is very similar to the calculations described in the previous section, though in this case the length of the tubes is unknown at the start, while the tube's diameter is preset (the opposite when compared to the previous section). This subchapter describes the methodology used to calculate the tube length only inside the condensers, as the rest follows the same mathematical model.

To obtain the length of the tubes in the down-condenser the key is to find the heat load entering the condenser. An average temperature is calculated for the seawater inside the tube bundle that is used to calculate intermediate variables (e.g. seawater density inside the tube bundle).

Code block 54:

```
C_Tbulk = (med_Tf + Tsw) / 2D0
```

The tube wall temperature is set to be equal to the vapor temperature on the shell side. The volumetric flow rate of the cooling water passing through the MED down-condenser is calculated, and from there the total cross section area of the heat transfer tubes (sum of the individual cross section of each tube, not accounting pitch space in between), through the relationship between volumetric flow, section area and fluid velocity.

Code block 55:

```
C_HTX_area_tot_section = C_Vol_dot_sw / C_veloc_sw_pipes
```

The tube diameter is preset, using standard sizes for MED plant down-condensers, and using this value the total number of tubes in the tube bundle is calculated.

Code block 56:

```
C_number_of_pipes = C_HTX_area_tot_section / C_pipe_Section_in
```

The overall heat transfer coefficient is calculated using a spline developed by H.T. El-Dessouky and H.M. Ettouney for specifically for MED down-condensers [18].

Code block 57:

```
C_U = 1D-3 * (1617.5D0 + 0.1537D0*Tv(n) + 0.1825D0*Tv(n)**2 - 0.00008026D0*Tv(n)**3 )
```

Using the logarithmic mean temperature difference describing the heat transfer, the total heat transfer area can be calculated.

Code block 58:

```
C_LMTD = (med_Tf - Tsw) / DLOG ( (Tv(n) - Tsw ) / (Tv(n) - med_Tf) )

C_A_pipes_out = C_Q / (C_U * C_LMTD)
```

Knowing the number of tubes, their shape, and the total area required transfer the heat load, it is possible to know the length of the tube bundle.

Code block 59:

```
C_tot_pipe_lenght = (C_A_pipes_out) / (2D0*pi*C_pipe_radius_out)
```

From this point onwards the pressure loss calculations follow the same structure as described for single straight cylindrical tubes in the previous section.

Channel inlet and outlet nozzles

The pressure loss as the seawater flows through the channel inlet and outlet nozzels are calculated based on fluid velocity, density and a correction factor.

Code block 60:

```
C_Delta_P_nozzle_in = C_Knt_in * ( C_dens_sw * C_vel_nozzle_pipe**2 ) / 2D0
C_Delta_P_nozzle_out = C_Knt_out * ( C_dens_sw * C_vel_nozzle_pipe**2 ) / 2D0
```

The correction factors are dimensionless and refer to the velocity head (dynamic pressure component measured in meters of a water column), with values of 1.1 and 0.7, for the inlet and outlet nozzles, respectively [72].

Headers

The calculation of the pressure loss within the headers is performed similarly as with the channel inlet and outlet nozzles, but accounts for the number of passes that the tube bundle may have. In the case of the MED down-condenser and SWCC condenser it is assumed only one pass. For a one tube pass the pressure loss is due to a contraction loss at entry, expansion and exit.

Code block 61:

```
C_Delta_P_Headers =  C_Kh * (C_dens_sw * C_veloc_sw_pipes**2 * C_tube_side_passes )
/ 2D0
```

In this section of the HTX, the correction factor used for the velocity head equals to 0.9, which is applicable when the number of tube passes is one [72].

3.4.5 Pumping Power Required

The necessary power required by the pumps is calculated using the isentropic and mechanic predefined efficiencies for the pumps. These are the last calculations performed in the pumping model. At this stage the pressure input into the pumps, and fluid densities are

known. The required pressure increase at the pumps output is calculated adding the piezometric head and the friction head losses.

Code block 62:

```
OUT_Delta_head = OUT_Head_friction - OUT_delta_piez_head
```

The isentropic outlet enthalpy of the fluid leaving the pump is calculated using the required pressure increase and the inlet enthalpy.

Code block 63:

```
OUT_h_pbrine_out_s = (OUT_Delta_P_pump / OUT_Dens) + OUT_h_pbrine_in
```

This enthalpy reflects the specific energy if the pumping process would be totally reversible [70]. As there are losses in the compression of the fluid, these are accounted using the predefined isentropic efficiency, and the real enthalpy outlet is calculated.

Code block 64:

```
OUT_h_pbrine_out = OUT_h_pbrine_in + (OUT_h_pbrine_out_s -
OUT_h_pbrine_in)/eta_pcw_s
```

Finally the pumps are assumed to be powered by an electric motor, and because of that, extra inefficiencies need to be accounted to calculate the final electric consumption.

Code block 65:

```
OUT_W_dot_pump = (OUT_h_pbrine_out - OUT_h_pbrine_in) * (OUT_B) /eta_pump
```

3.4.6 Model Calibration and Validation

A MED plant implies the transfer of large amounts of water between the different components of the plant. Only a few metrics were available regarding the pumping requirements and related equipment for the Trapani MED plant, which is used as the main reference in the validation of the models presented in this work. No detailed information was available regarding pumping requirements of both the PSA and Priolo-Gargallo MED plants. It is mentioned on the literature [28] (and confirmed by the plant manager) that the Trapani MED plant uses in average 3 kWh/m^3 of distillate produced. This plant is equipped with 5 vertical centrifugal pumps, each capable of moving 2100 m^3/h using 600 kW, being located at a pumping station on the shoreline near the plant, providing seawater to the MED process. The plant has also 3 horizontal centrifugal pumps for the extraction of process fluids: distillate, brine and condensate returning to the boiler. Excluding boilers and seawater pumping this

plant uses 1 kWh/m^3. A multitude of other pumping equipment is used across the plant for which no detailed data is available. Examples of such equipment's that also require pumps are the boiler and the remineralization equipment, which this model does not account regarding pumping energy costs.

Nonetheless it was possible to verify some of the data from the pumping model. At Trapani the feedwater pumps use 600 kW, capable of pumping 2100 m^3/h, and at nominal capacity the plant requires 1280 t/h of feedwater per MED train. As the plant has four MED trains in total, the plant requires 5120 t/h (~m^3/h) of seawater input at nominal capacity. Considering a linear relationship between these values and pump performance at part load operation, the plant requires 0.975 kWh/m^3 to pump water from the sea all the way into the outlet of the MED down-condenser (there are no intermediate pumps between the pumping station and the MED down-condenser). The inputs used to simulate the pumping system of the Trapani MED plant are shown in Table 13.

Table 13 – List of inputs used to validate the auxiliary pumping costs in the MED detailed model to validate results versus real data from the TVC-MED-P plant in Trapani.

Parameter	Value	Unit	Reference
Vap_Veloc_1st	Confidential *	m/s	Estimated for average velocity calculated considering the mass flow of steam entering the HTX tubes of the first MED effect in slightly superheated conditions (coming from the desuperheater) and the steam velocity inside the HTX tubes at saturated conditions. Data provided from technical plant visit.
ratio_Shell_vs_HTX_tubes	Confidential	-	Calculated value from data provided through technical plant visit.
eta_pcw_s	80% †	-	Estimated value for standard water pump efficiencies used in SAM [20], [101].
eta_pump	75% †	-	Estimated value for standard water pump efficiencies also used in SAM [20], [101].
NPSHr	4.5 *	m	Estimated value from technical plant visit.
plant_elev_sea_level	5 *	m	Estimated value retrieved from satellite information (37° 59' 34.8108"N, 12° 32' 21.498"E) [102].
IN_Pipe_roughness	5.00E-05	m	Trapani uses fiber glass for intake mains. Fiber glass roughness factor value for a typical fiber glass pipe [103].
IN_Plant_distance	2100	m	Distance of the shortest intake pipe providing seawater to Trapani [28].
IN_velocity_sw	0.3 *	m/s	Estimated value from data provided through technical plant visit and literature information on Trapani MED plant [28].
OUT_P_Cond_outlet	Confidential	bara	Value from data provided through technical plant visit.
OUT_Pipe_roughness	5.00E-05	m	Trapani uses fiber glass for the main outfall. Fiber glass roughness factor value for a typical fiber glass pipe [103]
OUT_Plant_distance	2778	m	Distance of the outlet from the shore line [28].
OUT_velocity_sw	0.3 *	m/s	Assumed value estimated from the main intake velocity.
C_pipe_diameter_in	Confidential	m	Value from data provided through technical plant visit.
C_pipe_diameter_out	Confidential	m	Value from data provided through technical plant visit.
C_Pipe_roughness	5.00E-05	m	Material information provided through plant visit. Roughness

			factor taken from literature [104].
C_vel_nozzle_pipe	0.3 *	m/s	Assumed value estimated from the main intake velocity.
C_veloc_sw_pipes	Confidential *	m/s	Calculated value from data provided through technical plant visit.
C_tube_side_passes	1 *	-	Value assumed from plant visit conducted to Carregado fuel oil power plant using a once-through brackish condenser.
Patm	1	bara	Value from literature [71].
STOR_tank_height	5 *	m	Estimated value from data provided through technical plant visit.
STOR_distance	100 *	m	Estimated value from data provided through technical plant visit.
STOR_velocity	0.3 *	m/s	Assumed value estimated from the main intake velocity.
STOR_Pipe_roughness	5.00E-05 *	m	Pipes assumed to be from stainless steel. Average roughness factor used from literature. [104]
STOR_T_Subcooling	2.5 *	ºC	Value from data provided through technical plant visit.
RC_velocity	0.3 *	m/s	Assumed value estimated from the main intake velocity.
RC_Pipe_roughness	5.00E-05 *	m	Pipes assumed to be from stainless steel. Average roughness factor used from literature [104].
RC_distance	100 *	m	Estimated value from data provided through technical plant visit.

* Value estimated through calculations using other inputs available for the MED Trapani plant.
† Value estimated with the aid of information available on the literature for these types of systems.

These inputs are also used on the simulation run to validate the MED detailed model shown previously in section 3.2.4 were real data from the Trapani MED plant is used as reference. The simulation results in Table 14 present the electrical needs by pumps at Trapani versus real plant data, when considering: 1) only the seawater/brine pumping to and from the plant, respectively; and 2) total pumping consumption. The presented values are indexed to each m^3 of distillate produced.

Table 14 - Comparison of results from the pumping model with real data from the Trapani TVC-MED-Parallel plant

Parameter	**Real value** [28]	**Calculated value**	**Deviation**
Seawater/brine pumping to and from the MED plant	0.98 kWh/m^3	1.03 kWh/m^3	6.06 %
Total pumping consumption	3.00 kWh/m^3	1.31 kWh/m^3	-56.23 %

The values referent only to the consumption of seawater to and from the plant (inlet and outlet mains), return very good results below the ~10 % margin of error pretended from the model. The value referent to total plant consumption return a larger deviation as it was expected (~ -56%) as not all the pumps for this specific plant are described in the model (in particular the pumps necessary to operate the boiler system, and the remineralization, though the latter probably with a much smaller impact on overall results). This pumping model was built aiming MED plants in cogeneration with power plants, and the boiler pumping

consumption will be included in the model that simulates the Rankine cycle, theoretically reducing the error shown for total plant consumption with pumps.

4. CSP+MED Model Development: SAM Add-On

4.1 General Description

This chapter presents the main steps that were necessary to merge the newly developed MED and auxiliary models into SAM. The new CSP+MED add-on to SAM is capable of simulating thermodynamically the performance of a CSP plant in cogeneration with a MED unit. The presented model allows SAM to simulate the cogeneration of water and electricity using the technologies presented in Table 15, and the cogeneration schemes mentioned in Table 16.

Table 15 - Cogeneration technologies possible to be simulated by the new CSP+MED add-on in SAM.

	Technology Type
CSP Technologies	Trough (physical model) Molten Salt Power Tower (physical model) Linear Fresnel
MED technologies	Parallel Feed Forward Feed MED plants with TVC or LT

Table 16 - Cogeneration schemes possible to be simulated by the new CSP+MED add-on in SAM

CSP + MED Cogeneration Schemes	**Details**
1. CSP with TVC-MED (using an oversized CSP)	The steam powering the MED comes from an intermediate extraction from the turbine, and not from its exhaust
2. CSP with LT-MED (using a 1:1 configuration)	The MED receives 100 % of the steam exhaust from the CSP plant
3. CSP with LT-MED (using an oversized CSP plant)	the MED receives only part of the steam exhausted by the steam turbine, while the remaining part is condensed by a SWCC at the same pressure)

The Rankine cycles described in this work assume condensing steam turbines(not backpressure turbines). Using the current Rankine cycle performance curves to simulate an oversized CSP plant powering a LT-MED does not optimize the electrical production, as the model assumes that the SWCC condenses the steam at the same pressure that it enters the first MED effect. It is important to note that this only occurs with the last configuration shown in Table 16. Using this configuration with the current version of this SAM add-on there is a waste of energy, as the steam condensed by the SWCC could theoretically still produce work with a smaller low-pressure turbine. Future upgrades to the code built now can produce Rankine cycle performance curves that simulate steam extractions at lower pressures than the 3 bars assumed by the current curves, or assume back pressure turbines followed by a

secondary smaller steam turbine just for the steam that is not used by the MED plant (when the CSP is oversized when using an LT-MED).

The CSP code in SAM is split into several TRNSYS types, which are individual files that act as blocks when the TRNSYS solver tries to reach a convergence within the entire mathematical problem it addresses in each simulation. Figure 22 shows a diagram with the new pieces of code introduced into SAM to accomplish the add-on of the MED related models explained in section 3.

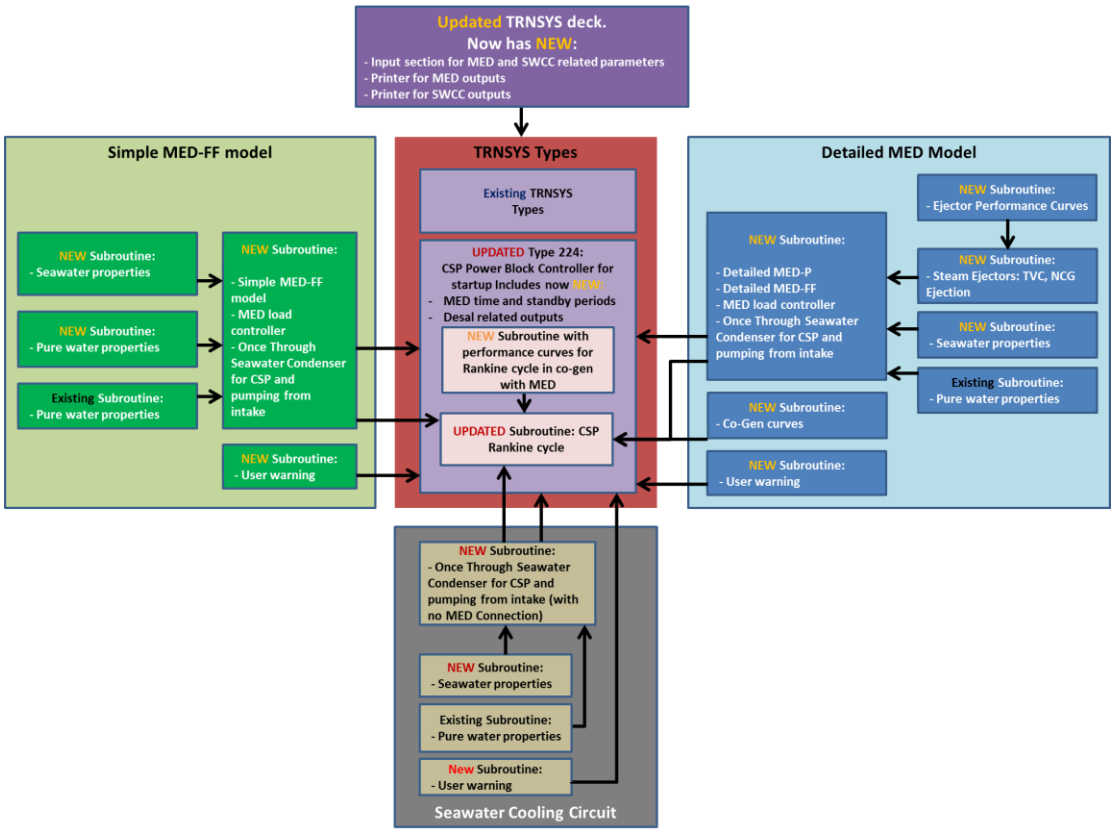

Figure 22 - Diagram with new code blocks introduced into SAM as part of the CSP+MED add-on.

Originally type 224 in SAM included the time controller for the operation of the Rankine cycle. The file containing type 224 also includes the Rankine cycle subroutine that simulates the physical performance of this cycle on a CSP plant. Each box in Figure 22 represents a Fortan computer file with the exception of the TRNSYS deck file. All the desal related code added to SAM was written in the form of subroutines that are called by type 224 and/or the Rankine cycle subroutine.

To simulate a MED process in cogeneration with a CSP plant, a new controller for the startup of the desalination process was added to type 224. New inputs and outputs were also added to this type so that it is possible to input and retrieve data related to the desalination process at the end of the simulations. The code related to the heat rejection calculation inside

type 224 was also slightly modified to add the option of wet cooling using salt water. The Rankine cycle subroutine was updated to account for the operation of the MED plant. This subroutine calls a new subroutine that includes the performance curves of a Rankine cycle similar to the one described in the original version of SAM, but that is capable of operating in cogeneration with a MED plant.

New subroutines were created for the simulation of pure and salt water properties (some pure water properties necessary to simulate the MED process were not described in the existing subroutine used by SAM). This two subroutines were used on both the detailed and simple MED models, and on the SWCC model (that simulates the once-through seawater condenser). The MED detailed model was also fitted with two subroutines: one that performs the mass and energy balance regarding the operation of the steam jet ejectors used on a MED plant, and a second with the database describing the operation of the ejectors together with the code to perform the linear interpolations retrieving data for intermediate operational points. A new subroutine was also made to show warnings messages during the simulation process, informing the user of any events originating from the new desalination related blocks. Both the simple and detailed MED models were fitted with an energy and mass load controller so that part load operations can be accounted for. Finally the TRNSYS deck originally used by SAM to simulate the operation of CSP plants was also modified, including now the new desal related inputs that need to be transfer to the updated type 224. The TRNSYS deck also includes now two printing sections: one for the MED/SWCC combination, and a second one for the operation of a CSP plant with a SWCC only. Figure 23 shows a simplified diagram describing the algorithm used for the operation of the CSP+MED add-on in SAM.

The inputs for the CSP plant necessary to run the new add-on for solar desalination are split into various categories referent to: location, solar field, collectors, receivers, power cycle, thermal storage, parasitics, performance adjustment, costs, financing, incentives, depreciation, utility rate and electric load [20]. The inputs necessary to simulate the MED plant in this add-on refer to several categories as: MED main configuration, energy input, temperature profile, salinity profile, TVC, NCG venting system, auxiliary pumping and SWCC. A list of the main inputs and outputs used by the add-on is described in Annex 5.

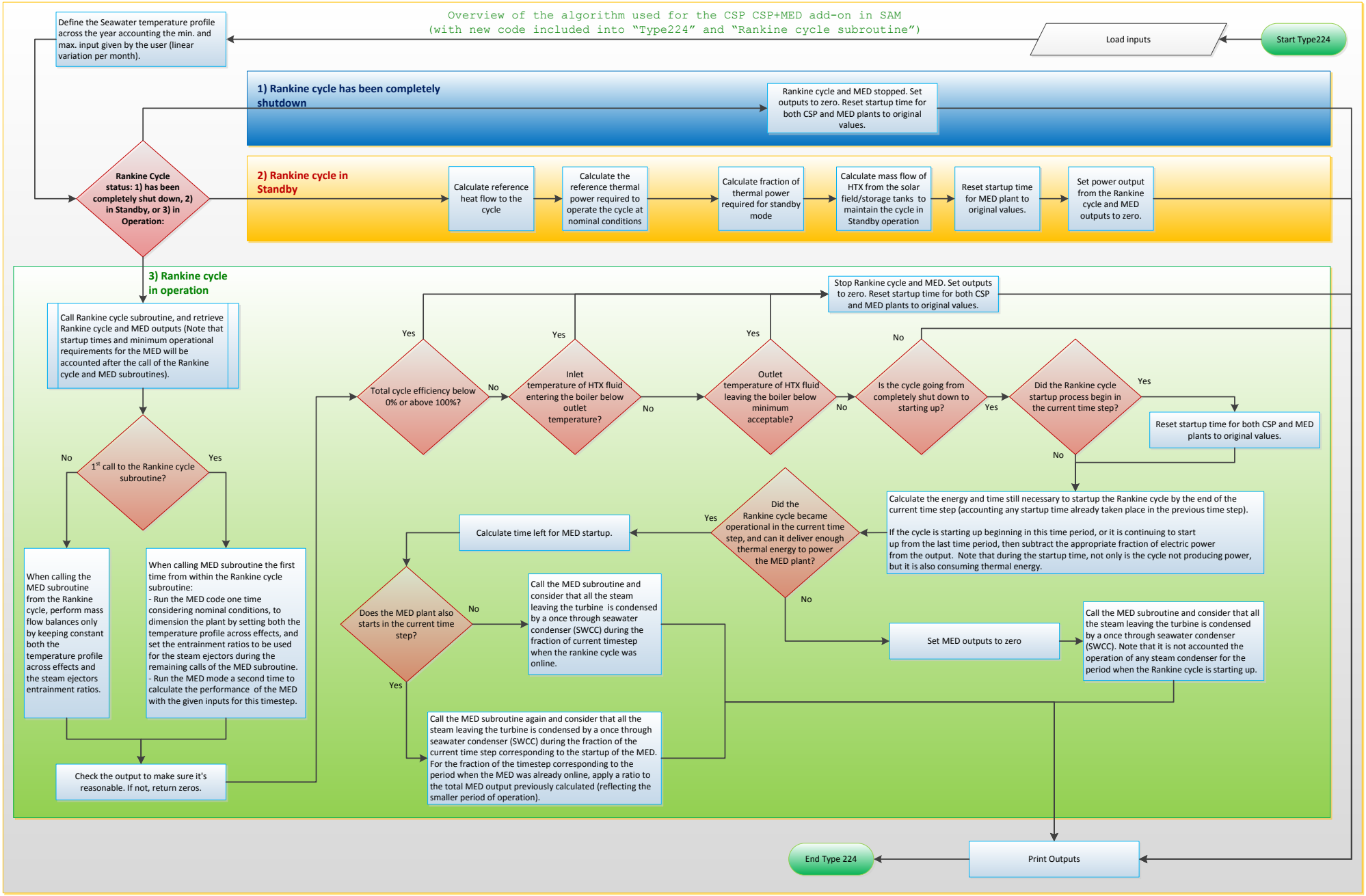

Figure 23 - Overview of the algorithm used for the CSP+MED add-on in SAM (with new code included into "Type224" and "Rankine cycle subroutine".

4.2 MED Plant Dimensioning Strategy

It was assumed that the MED plant capacity is sized according to the required CSP installed power. The MED plant will operate at nominal conditions for a determined percentage of the steam output from the CSP Rankine cycle. For a LT-MED configuration the code currently allows the user to set a fraction of the rejected heat by the steam turbine from which the MED plant should be dimensioned.

Code block 66:

```
MED_Qs_design = MED_Qdes_frac * q_pb_reject_design
```

For a TVC-MED configuration, the code allows the user to input either the total amount of steam extracted from the turbine (and the corresponding saturated temperature), or the ratio of steam extracted from an intermediate point in the turbines, relative to the total mass of steam that enters the high pressure turbine at design conditions.

The remaining steam is assumed to be condensed by the SWCC. With this strategy the user running the simulations can influence the amount of time that the MED plant will operate under nominal conditions even with variable heat load output from the steam turbine, at a cost of limiting the maximum distillate production during peaks in the day. The SWCC was dimensioned assuming that the whole output from the turbine could be condensed solely by it.

4.3 CSP-MED Controller

4.3.1 MED/SWCC Controlling Strategy

The MED plant is set to have a minimum startup time, and it was assumed that it will preserve temperature and vacuum conditions during the periods when it does not operate. During this period the plant is in standby mode. No allowance was made for the MED plant to stop production throughout the year due to maintenance, failures, or a prolonged halt of the CSP plant. Because of that no cold startup was considered, as it would only occur once during a one year simulation (in average these cold startups take 2h30m in commercial MED plants). No minimum stopping time was considered, as this type of plants can take less than 10 minutes to come to a full standby condition.

The MED plant is only assumed to operate during the periods when the Rankine cycle is operating above the minimum cutoff fraction, and providing energy to the MED system above the MED minimum cutoff load. During these periods the extra steam load from the turbine not condensed by the MED plant is directed to the SWCC. In this way the fluctuations during operation are assumed to be mostly compensated by the SWCC, which is a much more resilient component and easier to operate than the whole MED plant.
There is a minimum startup period for the MED plant to become operational after every stop in production. The MED plant will only pass from a standby to an operational mode after the turbine in the Rankine cycle has already gone through its own startup period and is working above its own minimum cutoff fraction. The steam consumption of the MED plant during the startup period is not accounted, and all the steam from the turbine is considered to be condensed by the SWCC in this period.

There is a minimum cutoff fraction for the MED plant relative to its own design conditions, under which it will not operate. There is also a maximum over design fraction for the MED plant, above which it will continue to operate at his maximum capacity, but the system will divert the excess steam coming from the CSP plant into the SWCC, as in these conditions it has reached its maximum heat load input (percentage above design conditions).

The MED plant will not operate without the Rankine cycle. The SWCC will work as needed without restrictions, and will be stopped if no heat load needs to be rejected. The SWCC model can also be used in simulations together with the CSP plant without assuming the existence of the MED system. The current version of the code implies that when a LT-MED configuration is selected and the user sets the MED plant to be undersized versus the CSP installed capacity, the steam will be extracted at the same temperature and pressure from the turbine into the MED and the SWCC, even during periods when only the SWCC is working and the MED is in standby.

With that design, when the CSP exhaust steam heat load goes above the maximum heat absorption capacity set for the MED plant (e.g. the MED might be set to receive 40% of the nominal heat load output from the CSP), the remaining exhaust steam is routed into the SWCC (the once-through condenser using seawater). The SWCC is set to operate at the same vapor pressure than the steam entering the MED plant. In these conditions, only part of the exhaust steam is being used to power the MED and produce fresh water. This produces an excessive cutback on electric production due to the forced condensation at high pressure of the entire mass steam flow, and not only of the steam flowing into the MED. On the other hand this strategy ensures that the MED plant will operate more times during the year at nominal capacity. It is important to mention that if the LT-MED plant is not oversized versus the CSP, this excessive cutback will not occur during the simulations. With the a TVC-MED configuration this issue does not happen, as no company producing MED plants publicizes that they use a TVC with motive steam using pressures below 1.5 bars (the minimum pressure allowed by the performance curves in SAM for an intermediate steam extraction to power a MED plant).

The parasitic consumptions are calculated whenever the MED or SWCC are considered to be starting-up or operating. The current model also accounts for the impact on the turbine of the extra steam withdrawn to eject the NCG.

4.3.2 MED/SWCC Operating Modes

Different operating modes are assumed possible with the MED + SWCC:

1. CSP Turbine: below cutoff fraction and/or during startup period
    - MED (standby) + SWCC (off);

2. CSP Turbine: above cutoff fraction
    - MED (standby) + SWCC (on) : below MED cutoff load, all steam goes to SWCC;
    - MED (startup) + SWCC (on): starting-up MED, and all steam goes to SWCC;
    - MED (on) + SWCC (off): above MED cutoff load and below MED maximum load, steam only goes to MED;
    - MED (on) + SWCC(on): MED above maximum over design fraction, and steam goes to MED and SWCC;

The MED and SWCC are defined to work in conjunction, but the SWCC is designed to be able to work without the aid of MED plant to condense all the steam from turbine. Even if the MED plant is designed to condense the full load of the CSP plant in nominal conditions, the SWCC is assumed to be also present as it is programed to be used whenever the MED plant is starting up.

4.4 Rankine Cycle Performance Curves

The CSP power block is simulated in SAM, using performance curves described inside a dedicated subroutine used by the TRNSYS type 224, both developed by NREL. These performance curves describe the power output and heat input to the cycle. These group of curves were developed by NREL for the operation of CSP plants using a Rankine cycle, and organic Rankine cycle [20] (the user can also choose an option to predefine the performance of the plant indirectly by setting the hourly capacity factors of the CSP plant for each month of the year, adjust the conversion efficiencies and the parasitic consumption).

This work focused on the operation of Rankine cycles using steam as working fluid. This cycle is a proven technology for more than a century, most commercial CSP plants (and fossil-fuel power stations) use it, and commercial cogeneration of electricity and water with MED plants has been implemented using fossil-fueled power stations with Rankine cycles. The description of the work originally done by NREL is important to understand the structure of the work performed to obtain new performance curves for thesis.

4.4.1 Original Model

The Rankine cycle model originally developed by NREL, considers three turbine stages and two intermediate steam extractions used to preheat the condensate as it returns to the boiler (using two feedwater preheaters and three feedwater pumps). The original model also considered a pre-heater, boiler, super-heater, and a condenser at the end of the low-pressure turbine. No reheater is considered in this model. The model can simulate cycles with constant or sliding pressure turbines [20], [101].

The solar concentration factor of the different CSP technologies varies significantly, and because of that, CSP plants using central receivers are able to achieve much higher temperatures in the solar field than CSP plants using parabolic and Fresnel mirrors. To properly simulate the operation of the Rankine cycle of plants using higher solar field HTF outlet temperatures than others, NREL developed initially two groups of performance curves: one group for Rankine cycles operating at “high temperature” (~510ºC) for central receiver towers; and a second group for “low” temperature (~372ºC) used for parabolic and linear Fresnel. In practice central receiver plants can reach much higher temperatures than 510ºC, but due to operational limits imposed by the materials and costs in steam turbines at least, the maximum temperature of the fluid (in this case steam), cannot be much higher than ~600 ºC.

These groups of performance curves were obtained by NREL through several steps. The first step was to develop two models on EES [101] for the high temperature and low temperature cycles. One of the models was developed to obtain the design parameters, and a second to run parametric simulations under different conditions. Information obtained from proprietary software was used as input into the EES design models, namely referring to the

isentropic performance of the steam turbines, and feedwater pumps. Secondly, using the design EES models, it was possible to optimize the mass flow from each intermediate steam extraction, and obtain the reference thermal conductance (UA) for the boiler, condenser pre-heater and super-heater. Thirdly, information from several runs at different loads was obtained with the parametric EES models, and used by NREL as inputs to a regression model to capture the off-design performance behavior of the power cycle described in EES. The calculated performance curves use as input: the temperature and mass flow of the heat transfer fluid from the solar field, and the condensation pressure at the condenser. The Rankine cycle described, simulates a 10MW power block. The outputs and some of the inputs necessary to apply the performance curves in SAM are set in normalized form, so that they are not dependent on the power block size, namely: the power output, heat input, HTF mass flow rate and temperature. The normalization is set by dividing their value by the design-point values. Condenser pressure is the exception as it does not vary with the power block size. Upper and lower boundaries were selected based on practical operational limits of the power cycle.

Using this strategy, a power cycle with a different efficiency and size than the one described specifically on EES, can be assessed regarding its off-design performance.

The cogeneration of water and electricity using CSP plants and MED units, imply the transfer of steam from the CSP plant into the desalination process. The Rankine cycle model developed by NREL only assumes two intermediate steam extractions, which are only used to preheat the condensate as it returns to the boiler. Performance curves describing the power output and heat input to the cycle were calculated using data from this particular cycle. Because of this, it would not be possible to use these performance curves to properly simulate a Rankine cycle operating in cogeneration with a MED plant through the usage of intermediate steam extractions. There are several possible configurations for a MED plant regarding its connection with the power plant. The easiest case to simulate using the existing performance curves in SAM, would be a low temperature MED unit. Though, in most MED plants the ejection of NCG is performed using steam ejectors, and their operation cannot be accounted for on the electric production from the CSP plant using SAM's original curves. The NCG removal with steam ejectors can reach values of up to 6% of the total steam consumption of a MED plant [28]. If these would be accounted, not only the total electric production of the CSP plant would be lower, but the total amount of steam powering the first MED effect would also be lower, reducing the total water production (although, the impact on water production would be smaller than in the electric production, as most of the steam powering the NCG steam ejectors would be transferred into the MED effects downstream, depending on the exact plant configuration).

4.4.2 Upgraded Model

To allow the simulation in SAM of a CSP plant using a Rankine cycle in a cogeneration with a MED plant, new performance curves were calculated and integrated into SAM. This upgrade was performed in collaboration with two other researchers. The work was subdivided in four main parts, namely:

1. Upgrade the original EES to assume intermediate steam extractions;
2. Obtain data from the modified EES models;
3. Calculate new performance curves;
4. Integrate the new performance curves into SAM.

Upgrade the original EES to assume intermediate steam extractions

The first part of this upgrade was done by Eng. João P. Cardoso, a researcher from LNEG. The original EES models used by NREL for sizing and perform parametric evaluation of Rankine cycles using constant pressure were extensively modified to account two intermediate steam extractions to be used as steam source of a MED process [21]. In total the model now assumes five steam extractions, three at a fixed pressure. The fixed ones provide steam for the feedwater preheaters at 35.8, 9.3, and 1.5 bara. The remaining two provide steam for the MED process, and the model assumes that their position can be user defined within the range of]1.5, 35.8[bara. The high pressure intermediate steam extraction is named “k”, and the low-pressure intermediate steam extraction is named “j”. The EES design model was used to obtain the cycle’s configuration to be used as input in the parametric EES model. When designing the cycle in EES, the intermediate steam extractions were assumed to be turned “off” so that it would be possible to use the previous cycle as reference when comparing efficiencies during the optimization design process. This was also useful to make straight comparisons when running the upgraded SAM model with the original version (e.g. CSP vs. CSP+MED/SWCC). With this configuration the main difference between the original and the upgraded EES design codes is the number of fixed intermediate steam extractions (as the non-fixed steam extractions were set to be off).

On the parametric EES model, in case the “k” and “j” extractions are set to be extracted at the same pressure, a slight adjustment is assumed and the pressure from the “j” extraction is assumed to be slightly lower. Because one of the fixed extractions is amongst this]1.5, 35.8[bara range (the 9.3 bara extraction), three submodels were developed for the parametric EES model, to account for all three possible combinations regarding the positioning of intermediate steam extractions, namely:

A. $P_{ext\_k} \in]9.3, 35.8[\cap P_{ext\_j} \in]9.3, 1.5[$, shown in Figure 24;
B. $P_{ext\_k} \cap P_{ext\_j} \in]1.5, 9.3[$, shown in Figure 25;
C. $P_{ext\_k} \cap P_{ext\_j} \in]9.3, 35.8[$, shown in Figure 26.

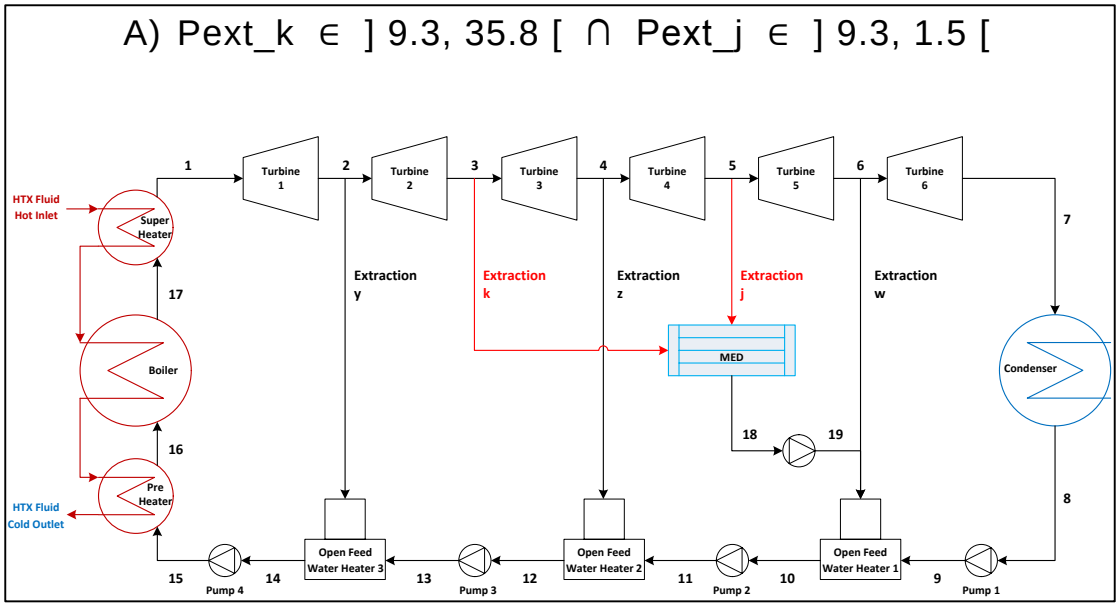

Figure 24 – Representation of the Rankine cycle described in EES, using a high and a low-pressure intermediate steam extraction to power the MED plant.

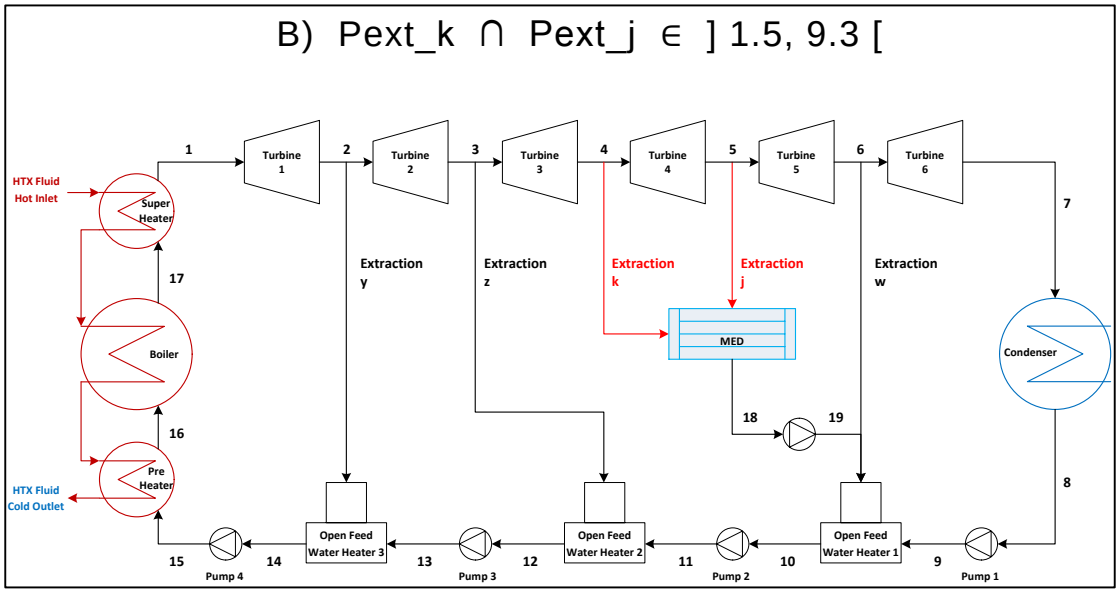

Figure 25 - Representation of the Rankine cycle described in EES, using two intermediate steam extractions at low-pressure to power the MED plant.

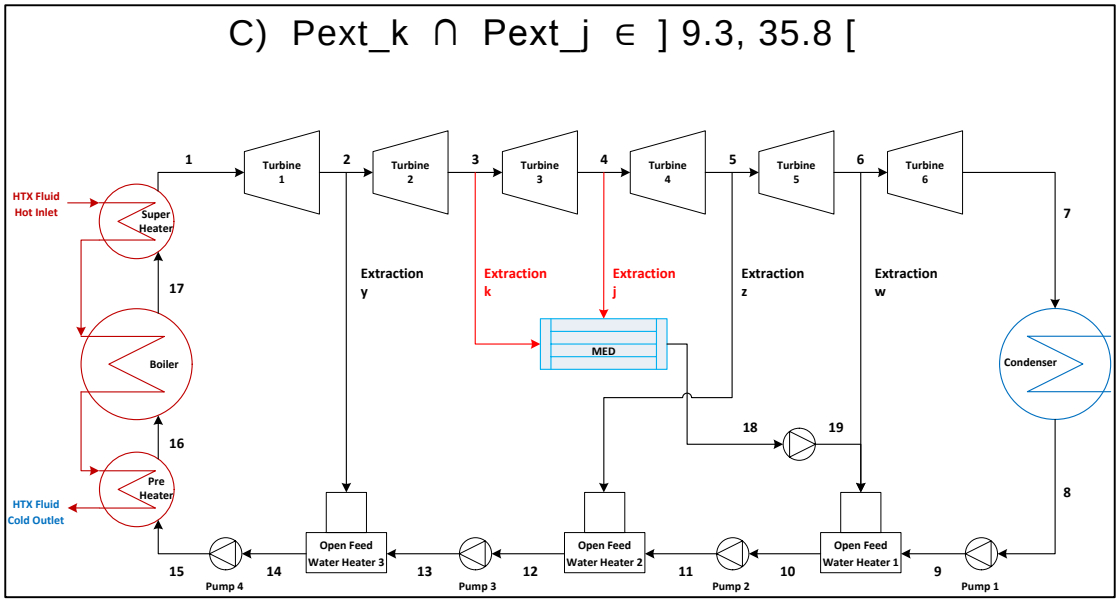

Figure 26 - Representation of the Rankine cycle described in EES, using two intermediate steam extractions at high pressure to power the MED plant.

The model considers that the condensed steam from the intermediate extractions fed into the MED plant returns to the Rankine cycle through the first feedwater preheater, where it mixes with the condensate from the condenser and the steam from the low-pressure fixed steam extraction at 1.5 bar.

The inputs necessary to run the design EES models are described in Table 17 (discriminating the original and newly added inputs):

Table 17 – Inputs necessary to run the Design EES model.

Inputs into the Design model	Code version
HTF inlet temperature	Original
HTF outlet temperature	
Turbine mechanical power	
Condenser pressure	
Turbine efficiency	
Pumps efficiency	
Inlet turbine steam temperature	
Inlet turbine steam pressure	
Difference between sat. temp and inlet temp	
Difference between sat. temp and outlet temp	
Fixed steam quality at boiler inlet	
Fixed steam quality at boiler outlet	
First fixed steam extraction	New
Second fixed steam extraction	
Third fixed steam extraction	

The inputs necessary to run the parametric EES models are described in Table 18 (discriminating the original and newly added):

Table 18 – Inputs necessary to run the Parametric EES model.

Input	Code version
Temperature of the inlet heat transfer fluid from the solar field Mass flow of the inlet heat transfer fluid from the solar field Condenser pressure.	Original
Pressure of extraction “k” Pressure of extraction “j” Condensate return temperature from the MED plant Percentage mass flow of steam retrieved with extraction “k” Percentage mass flow of steam retrieved with extraction “j”	New

The percentage mass flow of extraction “k” and “j” represent the ratio between the actual mass extracted in each extraction relative to the total amount of steam entering the high pressure turbine in nominal conditions.

The SAM version used as the basis for this work (version 2014.1.14, revision 1) uses TRNSYS to simulate the physical output of the plants, and the main blocks of computer code in which SAM was written were built as TRNSYS “types” (Fortran language). It would theoretically be possible to connect SAM and EES through a dedicated type that exists in TRNSYS for that purpose, though the aim of this work was also to create an add-on to SAM that can be released to the public, and the usage of EES would probably imply extra licensing. Due to this reason, it was decided to use the same strategy used by NREL for the model upgrade, and obtain performance curves that simulate the Rankine cycle’s model built in EES.

The list of outputs necessary to simulate the operation of the cycle in cogeneration is presented in Table 19:

Table 19 – List of performance outputs describing the Rankine cycle in cogeneration with the upgraded model

Output description	Output variable name	Units
Normalized cycle efficiency	Eta_ND	-
Normalized heat input to the cycle	Q_ND	-
Normalized mass flow from extraction “k”	M_dot_k_ND	-
Normalized mass flow from extraction “j”	M_dot_j_ND	-
Temperature of steam outlet from low-pressure turbine	Ts_out	ºC
Quality of steam outlet from low-pressure turbine	Qual_s	%

Several of these outputs are normalized, similarly to the strategy used previously by NREL. This normalization allows the usage of size dependent variables with cycles of different sizes.

Gathering data from the modified EES models

The effort in which consisted this second part to obtain data from the modified EES models was performed in equal shares between the author of this work and Eng. João P. Cardoso, from LNEG.

In order to obtain sufficient data to calculate performance curves for the different Rankine cycles, the performance of the Rankine cycle was calculated for different operational conditions. The design inputs necessary to run the parametric model were gathered from the design model. A simple code was used to generate randomly 50 000 points of operation. For each input variable a valid range was set from where the 50 000 points were extracted for each Rankine cycle ("high" and "low" temperature). The parametric EES model was then used to run 50 000 lines of inputs and obtain the corresponding outputs.

Calculation of the performance curves

The calculation of the performance curves was done using a model previously developed in Matlab that made use of genetic algorithms [21]. This model was developed and made available to this work by engineer Filipe Marques, from IST. Most of the effort to accomplish this third part to obtain the performance curves was mainly executed by the author of this work, with the helpful guidance of engineer Filipe Marques regarding the usage of the genetic algorithm he developed.

The database of ~50 000 points for each of the Rankine cycles, was used in the genetic algorithm so that different splines could be obtained for the necessary outputs needed to describe the cogeneration operation with a MED plant.

To simulate in SAM the operation of the cycle in cogeneration it was necessary to calculate with the parametric model splines for the outputs mentioned in Table 19. This process required several runs using the genetic algorithm built in Matlab, using a mini cluster of 12 computers for roughly a month, while trying multiple configurations within the genetic algorithm model and the database used in each simulation. The curves obtained are described in Annex 7 and their validation is presented in below in Table 20.

Table 20 – Standard deviation and Chi Square for the high (HT) and low (LT) temperature Rankine cycles performance curves obtained

Output	Units	Rank. Cycle type	Standard Deviation Σ	Chi Square
Eta_ND	(-)	HT	2.19E-02	7.21E-04
		LT	2.37E-02	8.45E-04
Q_ND	(-)	HT	7.78E-02	1.16E-02
		LT	7.11E-02	1.08E-02
m_dot_k_ND	(-)	HT (A)	3.81E-02	1.14E-01
		HT (B)	3.46E-02	1.15E-01
		HT (C)	3.84E-02	1.30E-01
		LT (A)	3.89E-02	1.26E-01
		LT (B)	3.47E-02	1.44E-01
		LT (C)	3.91E-02	1.38E-01
m_dot_j_ND	(-)	HT (A)	2.97E-02	9.18E-02
		HT (B)	3.00E-02	1.23E-01
		HT (C)	3.34E-02	1.07E-01
		LT (A)	2.95E-02	9.86E-02
		LT (B)	2.99E-02	9.67E-02
		LT (C)	3.38E-02	1.16E-01
Ts_out	K	HT	1.31E+00	4.64E-03
		LT	2.89E-02	2.39E-06
Qual_s	%	HT (A)	2.94E-03	9.26E-06
		HT (B)	2.86E-03	8.78E-06
		HT (C)	2.72E-03	7.89E-06
		LT (A)	1.99E-03	4.62E-06
		LT (B)	1.97E-03	4.54E-06
		LT (C)	2.01E-03	4.71E-06

The Eta_ND and Q_ND were calculated using as input all the eight variables described for the upgraded model. The outputs referring to the mass flow of the “k” and “j” extractions and quality of the steam outlet from the low-pressure turbine are subdivided in 3 blocks each, as it was not possible to obtain good correlations using all the eight inputs with the genetic algorithm. They were separated into 3 blocks according to the three possible combinations regarding pressure for the non-fixed steam extractions (A, B and C). For these particular curves, the pressure input for the non-fixed extractions, and the return temperature of the

condensate from the MED were removed from the database used with the genetic algorithm model. These curves calculate a mass extracted within turbine stages, so the pressure at which they are removed does not impact the total mass of steam extracted between the fixed steam extractions (as the extracted mass flow rate is set as a percentage of the total mass flow entering the high pressure turbine). Similarly, the curve describing the quality of the steam outlet from the low-pressure steam turbine was calculated without assuming the condensate return temperature from the MED plant into the Rankine cycle, as it was verified that it did not return a significant impact (~0.1% difference at extremes).

Integrate the curves into SAM

The effort in which consisted this fourth part to integrate the performance curves into SAM was performed by the author of this work.

The Eta_ND and Q_ND are used to calculate the work produced by the cycle. The Ts_out and Qual_s are used to calculate the quality of the steam leaving the low-pressure turbine, in case it is assumed that the exhaust steam powers directly the MED plant. The variables m_dot_k and m_dot_j are used to calculate the total mass of steam extracted at each point in time during the simulation.

It is preset the percentage of steam extracted from each of the two non-fixed intermediate steam extractions relative to the nominal mass flow of steam entering the steam turbine. The variation within a same cycle described on EES (using the parametric model), maintaining the nominal conditions and changing only the condenser pressure between 8481 and 84810 Pa, gave a variation for the mass flow of steam entering the high pressure turbine of 12.4 kg/s to 12.48 kg/s, respectively. It is considered irrelevant the mass variation when changing only the condenser pressure (variation of ~0.64%). This means that, the mass flow of steam entering the high pressure steam turbine for the same cycle operating at different condenser pressures is practically always the same, and there is a very strong linear dependence with the size of the cycle.

Considering two standard Rankine cycles, polynomial regressions were calculated for the high and low temperature cycles, respectively, and describe the amount of steam entering the high pressure turbine as a function of the cycle's efficiency at different loads.

Code block 67:

```
HT_m_dot_steam_10MWe = (147.1d0  * eta_ref**2) - (141.4d0  * eta_ref) + 43.7d0

LT_m_dot_steam_10MWe = (163.68d0 * eta_ref**2) - (153.59d0 * eta_ref) + 47.038d0
```

These two cycles consider no intermediate steam extractions, and were used as reference for the calculation of the mass flow of steam taken as reference when calculating the non-fixed intermediate steam extractions, to simulate the cogeneration of water and electricity with CSP and MED plants.

If no TVC is assumed to be present, than the “j” extraction is set to be at 5 bars, but with a mass flow very near to zero (to avoid eventual errors). The amount of mass flow of motive steam necessary to power the NCG extraction is unknown at the beginning of each time step, as it is dependent on the amount of feedwater entering the plant. This value is obtained through a convergence of the outputs following a damped harmonic oscillation effect, when a LT-MED plant is assumed to be used. The iteration starts by setting to zero the mass flow of motive steam necessary to eject the NCG. This will lead to more steam available to make work in the turbine and enter the MED plant, requiring more feedwater. More feedwater implies a higher amount of NCG released. The result from the first run will be the maximum calculated value of steam needed to power the NCG ejection during this iteration process. This value is then used as input in the second run, and as a consequence now less steam is available to power the MED, producing the lowest calculated cycle efficiency. Progressively both the output values for: 1) the percentage of steam required to power the NCG ejection system on the MED plant, and 2) the Rankine cycle’s efficiency will converge. This loop goes on until the efficiency of the plant is kept stable at the end of each iterative cycle for each time step. For a TVC-MED configuration these calculations only run once, as it is known from the beginning of the iterative process the amount of steam powering the turbines (the user sets as input either mass flow rate of motive steam for the TVC, or the percentage it uses versus the total mass flow rate of steam produced by the boiler.

It was not possible to validate with real data the new Rankince cycles performance curves because no data was available from a real plant in a cogeneration scheme that made use of a Rankine cycle.

4.5 Rankine Cycle Subroutine

In order to simulate the operation of the Rankine cycle in cogeneration with the MED system, the original code written in SAM for this cycle had to be upgraded. To understand better the upgrade to the Rankine subroutine, a small description of the rational used to perform calculations in the original version of this subroutine is made before describing the updated code.

4.5.1 Original Model

The original Rankine cycle subroutine is able to simulate the operation of this cycle in a CSP plant producing exclusively electricity. This subroutine is embedded into TRNSYS type 224 in SAM.

The Rankine cycle subroutine uses as main inputs several inputs set by the user related to the characteristics and type of CSP plant being simulated, e.g. the installed capacity, the reference operational temperatures coming from the solar field/molten storage tanks, information related to the temperatures and pressures used in the cooling system at design. Other inputs are also required at each time step of the yearly simulations, and refer to the actual temperature and mass of HTX coming from the solar field/molten storage tanks, air temperature (dry and bulb depending on the cooling system used).

The main outputs from the Rankine cycle subroutine at each time step of the simulations are the power output, the cycle's efficiency the cold temperature of the HTX flowing back into the solar field/molten storage tanks, the Wet cooling makeup water flow rate, heat transfer fluid demand flow rate, cooling parasitic load, and condenser pressure [20].

The rational used to simulate the Rankine cycle in the original SAM code, was to use performance curves that describe the operation of a typical Rankine cycle from a known CSP plant, with 10 MW_e (as described in sections 4.4.1 and 4.4.2), and extrapolate the operation of different cycles using information from this one [20], [101]. The original subroutine calculates how much should be the performance of the cycle described in SAM to match the output of the cycle described by the user at nominal conditions referent to 1) condenser pressure, and to the HTX fluid from the solar field/storage tank system 2) input temperature and 3) mass flow rate.

Code block 68:

```
eta_adj = eta_ref/(Interpolate(TT,12,2,Psat_ref)/Interpolate(TT,22,2,Psat_ref))
```

The latter two are normalized, opposite to the first that is left in dimensional form, as the condenser pressure does not generally scale up or down with changing sizes of the power block [20]. With this info the original code calculates the reference heat flux into the cycle and corresponding mass flow of HTX fluid. Knowing the reference mass flow of HTX, it is possible

to normalize its value. The nominal HTX temperature inlet is set by the user. The temperature inlet of the HTX is normalized with respect to the inlet temperature provided at each hour by other types in the SAM TRNSYS deck (though the boiler temperature is the temperature used as reference for the normalization).

Code block 69:

```
q_dot_ref = P_ref/eta_adj

m_dot_htf_ref = q_dot_ref/(c_htf_ref*(T_htf_hot_ref - T_htf_cold_ref))

T_htf_hot_ND = (T_htf_hot - T_ref)/(T_htf_hot_ref - T_ref)

m_dot_htf_ND = m_dot_htf/m_dot_htf_ref
```

With these values, the Rankine cycle subroutine can now calculate the normalized power output and heat rejected by the cycle using the three inputs provided for the actual time step, making use of its database of performance curves for these two outputs. The normalized output values are then multiplied by the reference values to calculate the actual power output and rejected heat load from the cycle. The cycle's efficiency and the boiler's HTX fluid outlet are calculated with the previous outputs.

Code block 70:

```
P_cycle = P_ND_tot*P_ref

T_htf_cold = T_htf_hot-Q_ND_tot*q_dot_ref/(m_dot_htf*c_htf)

eta = P_cycle/(Q_ND_tot*q_dot_ref)

q_reject = (1.-eta)*q_dot_ref*Q_ND_tot*1000.
```

4.5.2 Upgraded Model

The upgraded Rankine cycle subroutine in SAM is able to simulate the operation of this cycle for a CSP plant cogenerating fresh water and electricity with an MED plant. This subroutine is embedded into TRNSYS type 224 in SAM.

Adding to the inputs described previously for the original Rankine cycle subroutine, the upgraded version requires also the mass of steam powering the MED plant or its percentage relative to the total mass flow of steam produced by the boiler, the temperature, the pressures at which steam is extracted to power the MED plant (namely the NCG steam jet ejectors, and TVC or first the MED effect depending on the configuration selected for the MED plant), the reference temperature at which the cycle should operate its condenser, and the condenser temperature related to the "Rated cycle conversion efficiency" set by the user. Apart from

these inputs the subroutine also requires the call of all the inputs necessary to run the MED model, the steam jet ejector model and the pumping model.

Adding to the main outputs described previously for the original Rankine cycle subroutine, the upgraded version returns the values of both gross electrical generation, together with the total water output. Values for the electrical consumption required for pumping water to the CSP+MED/SWCC system are also outputs from this subroutine, together with the total amount of motive steam required to run the NCG venting system using steam jet ejectors. Outputs from the MED model, the steam jet ejector model and the pumping model, are routed into type 224 through the Rankine cycle subroutine as they are called within it.

A comprehensive diagram of the algorithm used in the upgraded Rankine cycle subroutine is presented in Annex 4, where the calculation steps are described in depth.

In summary: the subroutine now calculates the performance of the cycle described in SAM at nominal conditions so that it matches the performance of the cycle described by the user (so that it is possible to calculate the reference mass of HTF from the solar field). Then checks the performance of the cycle described by the user under the conditions that he specified for cogeneration with the MED plant. Then the subroutine recalculates the performance required by the cycle in SAM to deliver the same performance as the cycle described by the user in cogeneration. And with this information then the simulations run for each hour of the year every time the subroutine is called.

The model applied to upgrade the Rankine cycle subroutine uses the following rationale, described below more in detail:

1. The user sets an efficiency for the cycle without intermediate steam extractions, and the user also indicates at which temperature the condenser needs to operate to get this reference efficiency (the reason behind this is the assumption that the user will only know the efficiency of the cycle from catalogs, where no intermediate steam extractions are considered, and only reference condenser pressures are defined). The user will also input the condenser temperature at which he actually wants the cycle to operate (which may be different from the temperature that he indicated for the nominal cycle's efficiency). In case the user knows the efficiency of the cycle operating at the condenser temperature he actually wants to operate, then he only needs to set equal both of these temperatures.

2. The model calculates the required efficiency from the 10MW Rankine cycle described in SAM (for the specific CSP technology) that would be required in order for this cycle to deliver the same performance than the cycle defined by the user at nominal conditions from the solar field and at the user defined steam exhaust pressure

(assuming no intermediate steam extractions yet). This is made using the new performance curves (with the option of high or low temperature cycles, applicable to CSP plants using towers or troughs/Fresnel, respectively).

Code block 71:

```
Eta_ND = (T_htf_hot_ND, P_cond  , m_dot_htf_ND, P_ext_k, P_ext_j, T_med_ret    ,
pct_ext_k, pct_ext_j)  ← This describes the inputs to run this function

IF (TT .EQ. 1) Eta_ND = HT_Eta_ND_fun (1d0, Psat_ref, 1d0, P_ext_k, P_ext_j,
Rank_Td_return, 1d-6, 1d-6), for Rankine cycles using High Temperature

IF (TT .EQ. 2) Eta_ND = LT_Eta_ND_fun (1d0, Psat_ref, 1d0, P_ext_k, P_ext_j,
Rank_Td_return, 1d-6, 1d-6), for Rankine cycles using Low Temperature

eta_adj = eta_ref / Eta_ND
```

3. Calculate the reference heat flux into the cycle and corresponding mass flow of HTX fluid in the same way described for the original version of the subroutine.

Code block 72:

```
q_dot_ref = P_ref/eta_adj
m_dot_htf_ref = q_dot_ref/(c_htf_ref*(T_htf_hot_ref - T_htf_cold_ref))
```

4. Set the normalized values for the mass flow rate and temperature inlet of HTX fluid from the solar field/storage tanks to nominal (equal to one) if it is the first call, or to the actual conditions for the time step being calculated if it is not the first call.

Code block 73:

```
For first call:
T_htf_hot_ND = 1
m_dot_htf_ND = 1
```

Code block 74:

```
Not the first call:
T_htf_hot_ND = (T_htf_hot - T_ref)/(T_htf_hot_ref - T_ref)
m_dot_htf_ND = m_dot_htf/m_dot_htf_ref
```

5. Calculate the mass flow rate of steam produced by the boiler, as a function of the reference power input by the user, the adjusted efficiency required by the cycle defined in SAM, and the technology type. These correlations are detailed in section 4.4.2.

Code block 75:

```
HT_m_dot_steam_10MWe = (147.1d0  * eta_ref**2) - (141.4d0  * eta_ref) + 43.7d0
LT_m_dot_steam_10MWe  =  (163.68d0  *  eta_ref**2)  -  (153.59d0  *  eta_ref)  +
47.038d0
m_dot_steam_User = (P_ref * m_dot_steam_10MWe_User ) / 10d3
```

6. If a TVC configuration is set, calculate the mass flow of steam powering the TVC, or the percentage of steam that it uses versus the total amount of steam produced by the boiler.

Code block 76:

```
IF (TVC_ext_flag .EQ. 1) pct_ext_j = TVC_Mm_des / m_dot_steam_User,
if using the "TVC_Mm_des" as an input and the "pct_ext_j" as output



IF (TVC_ext_flag .EQ. 2) TVC_Mm_des = m_dot_steam_User * pct_ext_j,
if using the "pct_ext_j" as an input, and the "TVC_Mm_des" as output
```

7. Set the mass flow rate and percentage of steam extracted that is necessary to power the NCG venting system to near zero.

Code block 77:

```
m_dot_j = 1d-6, if using the j extraction to power the NCG venting system
pct_ext_j = 1d-6
```

8. Calculate the normalized performance of the cycle described by the user considering the necessary intermediate steam extractions to power the MED, using the harmonic oscillation process described in section 4.4.2. Assume nominal conditions for the condenser pressure, the heat flux into the cycle and the corresponding mass flow of HTX fluid. The normalized outputs are: Eta_ND, Q_ND_tot, m_dot_k_ND, m_dot_j_ND and Ts_out.

9. Calculate the cycle's performance when operating with the MED plant, with the inputs set in the previous point. Outputs are: efficiency, heat load, electric power output, cold temperature of the HTX outlet, rejected heat load by the cycle, mass flow of steam exhaust and corresponding quality.

Code block 78:

```
eta = eta_ref * Eta_ND
Q_cycle = q_dot_ref * Q_ND_tot
```

```
P_cycle = eta * Q_cycle
T_htf_cold = T_htf_hot - Q_ND_tot * q_dot_ref / (m_dot_htf * c_htf)
q_reject = (1. - eta) * q_dot_ref * Q_ND_tot * 1000.
Mm_out = (q_reject/1D3) /(Hs_dry_out-Hw_out), when exhaust steam is superheated
Mm_out = (q_reject/1D3) / (Hs_wet_out - Hw_out), when exhaust steam is wet
```

10. Call the MED subroutine to calculate the performance of the MED system, and retrieve the amount of steam required to power the NCG venting system (in a case a LT-MED configuration is selected. If so go back to point 8. until a convergence is reached (according to the harmonic oscillation process described in section 4.4.2).
11. If it is the first call: recalculate the required efficiency from the 10MW Rankine cycle described in SAM (for the specific CSP technology) in cogeneration at nominal conditions.

Code block 79:

```
eta_adj = eta_ref / Eta_ND
```

12. If it is the first call: go back to point 3. and recalculate the reference load and mass flow rate of HTX from the solar field/storage tanks, now having into account the actual performance that is required to operate the cycle in cogeneration with the MED plant at the nominal conditions set by the user.
13. Run the calculations for each hour of the year, assuming this new efficiency of the cycle.

5. CSP+RO Models: SAM and ROSA Integration

The physical simulation of a cogeneration scheme is possible to be conducted using available simulation tools, without the need to integrate them as it is necessary in the case of CSP+MED. To accomplish this task, the selected tools were SAM and ROSA, developed by NREL and Dow Chemical Company, respectively. The outputs of both this computer programs were combined in Microsoft Excel environment, and a simple algorithm was developed for it.

This work was conducted through the joint work and supervision of a Master's student (Mahran Abdelkarim Ahmed) in the context of his internship at LNEG between July and December 2014.

The simulation of a CSP+RO plant in cogeneration was performed using SAM to simulate the CSP plant and ROSA to simulate the outputs from the RO plant. As mentioned in the literature, sections 2.4.4 and 2.5, both of these models are validated. A simple connection and controlling scheme was implemented between SAM and ROSA through Microsoft Excel environment, although it is not a straight forward simulation process, as it requires the usage of two distinct models that are not directly connected. Parametric simulations are not as easy to perform as with the new CSP+MED model developed for SAM.

The CSP+RO model can use inputs for different temperatures of seawater across the year, and considers that each RO each train is operated either at 100% capacity or it is shut down, depending on availability of power under different water temperatures across the simulation period (one year). The feed water pressure is adjusted during the simulation, to conserve a constant permeate flow rate into the membranes, maintaining the same ratio of permeate flow against feed flow during operation. This adjustment is dependent of the seawater temperature: the warmer the seawater, the less pressure is required to produce the same mass flow rate of permeate as the membranes pores size increase slightly (though the quality of permeate also decreases slightly, as more salt passes through). Vice versa for lower seawater temperatures.

In order to run the CSP+RO simulations with the strategy described, it is required to run several simulations with ROSA for the same plant configuration, but using different seawater input temperatures, so that it is possible create a database to simulate a yearly operation with seasonal fluctuations.

The main inputs into the SAM has been described in section 4.1. The main inputs required by ROSA comprise of the number of membranes, seawater quality and temperature, and membrane's type. ROSA assumes steady-state operation and can only simulate single point operation, which is then adapted to hourly values in the CSP-RO simulation in Microsoft Excel environment.

The operational strategy is shown in Figure 27, for an example using six RO trains.

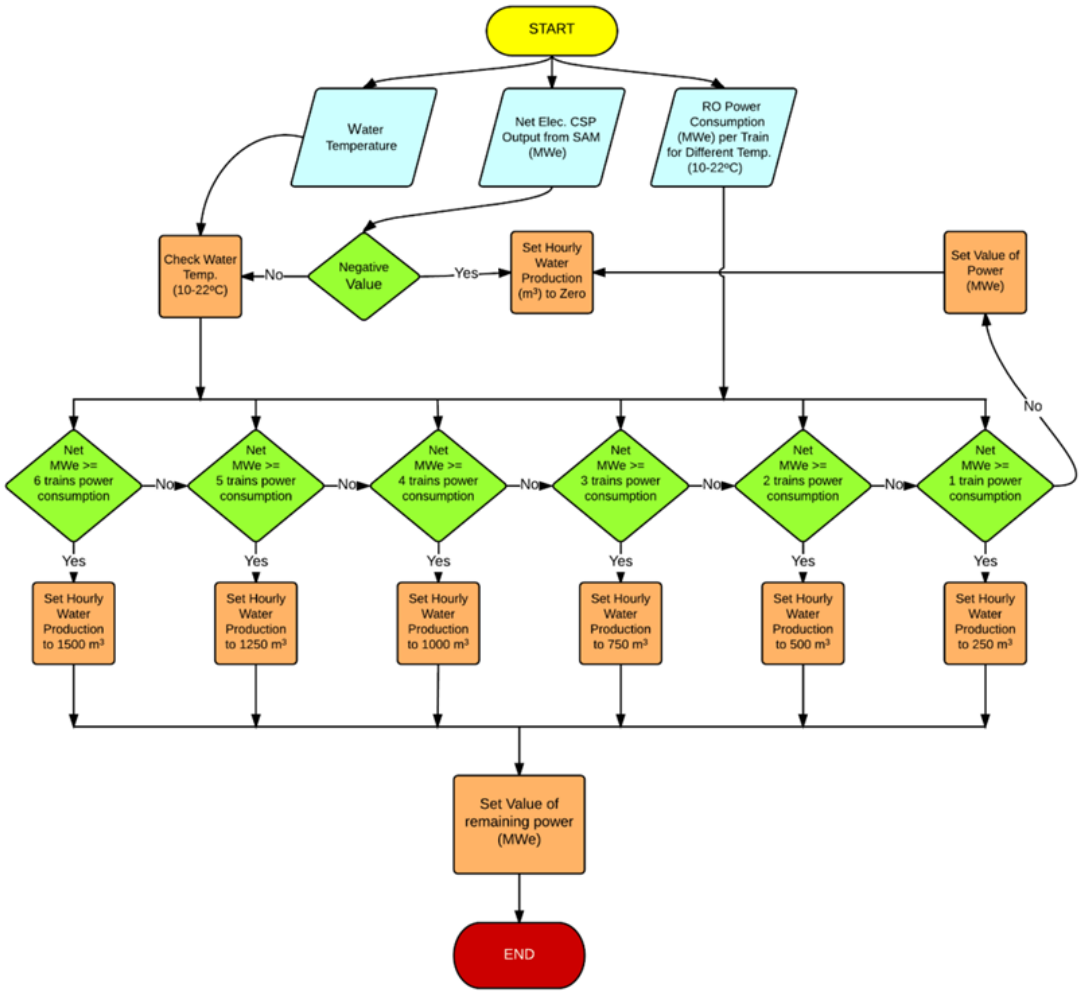

Figure 27 - Operational Strategy of CSP-RO model for an example using a plant with 6 RO trains.

The algorithm used considered that whenever the CSP plant produces electricity, the present water temperature is read (water temperature affects the viscosity and subsequently the quality and flow rate of water through the membrane, therefore affecting RO system power consumption). Afterwards the algorithm checks whether the available power from the CSP system is sufficient to run the number of RO trains defined by the user and registers the corresponding water production. Otherwise, it runs the same test for less one RO train and so on in a descending manner until it reaches one trains. If the power available is not enough to operate even one train, the CSP-RO system considers that it will only produce electricity (if the CSP is actually producing energy). If there is power to operate more than one train, then the system considers the water output from the operating trains while the remaining power from the CSP is set as net electrical output. All the remaining net electricity produced by the CSP that is not used by the RO system is considered to be available to be injected into the electrical grid or used by some other process that may be connected directly to the CSP

plant. No electrical energy storage is considered though in this model to balance the RO production with the irregular output from the CSP plant.

It is important to note that this CSP+RO model neglects:

1. Minimum startup and shut down time;
2. The feedwater pretreatment process;
3. The post treatment processes;
4. Pumping costs of seawater from the intake into the high pressure pump;
5. Pumping costs of brine and permeate into outlet and storage, respectively.

Minimum startup and shut down procedures vary significantly between plants, being especially dependent on the plant size and water quality used (ranging somewhere between 5 to 30 minutes). This is not accounted in the model, but it can be easily added for a second version of the model as a input set by the user.

During this work it was also possible to validate the ROSA model with data from an existing RO plant in Alvor [27], located in the Southern region of Portugal, Algarve. The plant is used to provide fresh water for nearby gulf courses. This plant has a pre-treatment system, one RO train with 9 pressure vessels, each having six RO membranes. The plant has an energy recovery device, a post treatment system and a reservoir tank. The wells are located near the coast and the changing tide levels can have an impact on the operation of the plant by causing a mixture of underground fresh water streams with the seawater underground intake, which can lead to a decrease in the salinity of the feed water throughout the year (depending on the rainfall precipitation levels). The data provided during the technical field visit to this plant was relative to nominal conditions. The main inputs used to simulate this RO plant are described in Table 21, and the main outputs of the simulation with ROSA are presented in Table 22.

Table 21 - Inputs used for the validation of ROSA versus real data from Alvor RO plant in the South of Portugal [27].

Parameter	***Value***	***Units***
Pre-stage ΔP	0.345	Bar
Feed Water salinity (TDS)	33800	mg/l
No. of passes	1	-
No. of stages	1	-
Flow factor	1	-
Recovery rate	40	%
Feed Flow rate	87	m^3/h
Membrane type	SW30XHR-400i	-
No. of membranes in pressure vessel	6	-
No. of pressure vessels	9	-
pH	5.7	-
Water Temperature	18	^oC
Pump efficiency	80	%

Table 22 - ROSA validation outputs using real data from Alvor RO plant in the South of Portugal [27].

Parameter	Real data	Modelled data	Difference (%)
Permeate flow rate	34.0 m^3/h	34.8 m^3/h	+2.4 %
Concentrate flow rate	54.0 m^3/h	52.5 m^3/h	-2.7 %
Permeate salinity	165 mg/l	149.6 mg/l	-9.3 %
Concentrate salinity	52 988 mg/l	55 431 mg/l	+4.6 %
Feed pump pressure	60.0 bar	55.5 bar	-7.5 %

The results show that the main performance outputs fell within a 10% margin of error compared to the full-scale data used [27]. These discrepancies can be attributed to the assumptions used in ROSA and the data gathered at the site. At the time of the readings the plant was shut down, and the membrane system had been flushed with freshwater as part of the maintenance procedures. The salinity of the permeate was measured from the fresh water reservoir, to where part of this flushed water was sent.

6. Case Study: Trapani, Sicily

The city of Trapani in the southwest of Sicily, Italy was used as a case study for the analysis of the operation of a CSP plant powering MED and RO units for the cogeneration of water and electricity. Two scenarios were analyzed: CSP+MED and CSP+RO. Both scenarios were compared to the real output of the existing commercial TVC-MED plant operating at Trapani.

6.1 CSP+MED System

6.1.1 System Description

The studied CSP+D system consists of a parabolic trough CSP plant with a Rankine cycle coupled with a low temperature MED parallel-feed plant.

The commercial TVC-MED-P plant, installed in Trapani, is used as reference for the analysis of simulation results. Several metrics are available for this plant making it the ideal location for this study, as shown in previous sections 3.2.4, 3.3.6 and 3.4.6. Therefore, a TVC-MED-P unit coupled with a CSP plant was considered in these simulations.

The existing plant at Trapani does not operate under a cogeneration scheme. It works with a stand-alone configuration, using boilers powered by natural gas that provide steam at a very high pressure to the TVC of the MED plant (45 bars). Using such a high-pressure steam to power the MED unit is not the optimum in a cogeneration scheme for water and electricity that uses a CSP plant. The electrical cutback will be progressively higher as steam is bled at higher pressures from the steam turbines in the Rankine cycle of the CSP plant, though it has the advantage of producing more distillate with the MED plant, as more energy will be available to power it. Using very high steam pressures with an MED plant also implies the usage of a TVC, as the first MED effect cannot cope with such high temperatures with a stable operation.

When using a TVC the lowest pressure that is currently used by plant manufacturers is roughly ~3 bars, while the lowest steam pressure used without a TVC configuration to power an MED plant can go as low as 0.3 to 0.12 bars (depending on the top brine temperature selected).

A low-pressure steam was used in these simulations in order to minimize losses on the electrical output, following the practice used in the real world for most power plants cogenerating water and electricity. Figure 28 presents a general scheme of the CSP+TVC-MED/SWCC cogeneration system assumed for the case study.

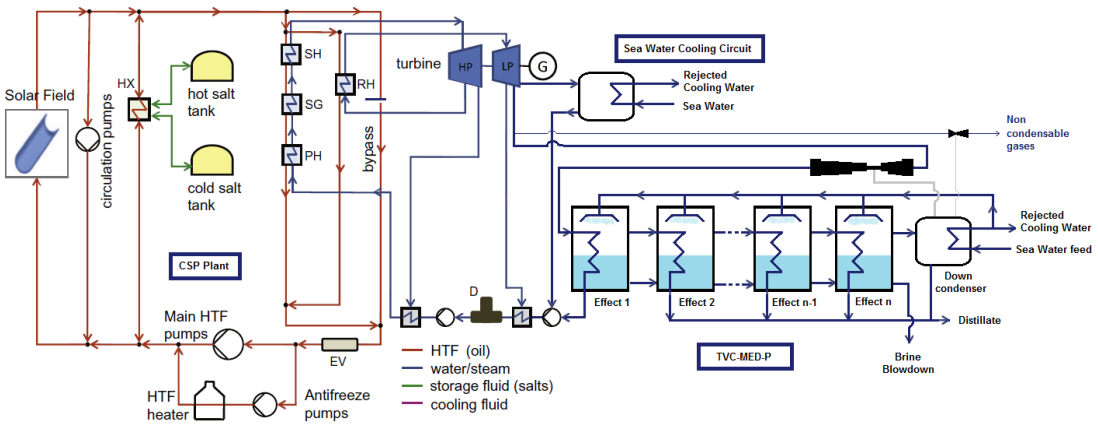

Figure 28 - General schematic of the simulated CSP+MED/SWCC system

The thermodynamic simulation for the CSP plant was done using the SAM's physical trough system developed in TRNSYS environment [20], making use of the new desalination add-on developed with this work (described in section 4), using the MED-detailed models (described in section 3.2). In summary, the model assumes the existence of a SWCC connected to the CSP-MED plants, which is dimensioned to absorb the entire amount of the rejected heat by the CSP plant at nominal design conditions. The MED plant can be undersized regarding the reference value of 100 % for the nominal heat load output from the CSP plant (this is a user defined input), with the aim of improving the MED plant performance during part load operation of the CSP plant. During the startup of the MED plant in the simulation, the SWCC is assumed to take over the cooling process. If both a MED and a SWCC are considered to exist, then the SWCC will operate at the same condenser pressure than the MED. The MED plant will only start operating above a user-determined percentage of heat load output from the CSP plant (compared to its nominal value). Below that determined percentage, the SWCC takes over the cooling process. The user can also define the startup period for the MED plant. During the simulations, the MED is not assumed to shut down completely, and only hot standbys are considered. The CSP plant, on the other hand, is assumed to be able to shut down completely or be maintained in hot standby during a user defined amount of time. The model can calculate the amount of motive steam used to eject NCG. All scenarios assumed no electrical grid connection to the CSP plant.

6.1.2 Inputs

The weather data used for the simulations in Trapani was gathered from 2 sources: Meteonorm 5.1 database available with TRNSYS 16, and [105] using satellite data from the year of 1997. The main inputs used for the Trapani simulation in SAM with the MED-P add-on are described in Table 23. Inputs for the CSP plant were set to be the same as the standard case study available in SAM (2014.1.14, revision 1) for plants using troughs, excluding: location, installed power, solar multiple and number of storage hours with molten salt tanks.

Table 23 - CSP+MED: Main inputs used for the Trapani simulation using the new solar desalination add-on in SAM.

CSP plant	**Value**	**Units**
Installed CSP Power (trough using oil as HTF):	99 net (110 gross)	MW_e
Thermal Storage with Molten Salts	6	Hours
Rated cycle conversion efficiency:	37.74	%
Condenser temperature for Rated Cycle conversion efficiency	35	ºC
Solar multiple *	3	-
Irradiation at design (reaching the solar field)	950	W/m^2
Solar collector loop conversion efficiency (Solargenix SGX-1)	71.69	%
Inlet temp (outlet boiler)	391	ºC
Outlet temp (inlet boiler)	293	ºC
Boiler pressure	100	Bar
Hot Standby period	2	Hours
Fraction of thermal power for standby	20	%
Turbine overdesign	105	%
Turbine Minimum	25	%
Direct Normal Irradiation (DNI)	2004 [105], [106]	$kWh/m^2/yr$
Saturated temperature Turbine Outlet	64.5	ºC
Fossil fill fraction †	0	%

MED	**Value**	**Units**
Total number of effects (n)	n = 12	-
Total distillate production capacity at design	36 000	m^3/day
Number of MED trains	1	-
Mass flow rate of steam powering the MED	22.5	t/h
Intake distance	2.1	km
Intake velocity	0.3	m/s
Seawater temperature	10 (Jan); 22 (Jul)	ºC
Hot Restart time ‡	100	minutes
Maximum MED load	100	%
Minimum MED load	20	%
Ts_sat	68.0	ºC
$Tv_{(1)}$	62.2	ºC
$Tv_{(n)}$	37.0	ºC
$Tf_{(n)}$	35.0	ºC
Xf	3.5	wt%
$Xb_{(1)}$	3.6	wt%
Motive steam pressure (powering TVC and NCG venting system)	3	Bar
Average temperature loss per effect	0.5	ºC

SWCC	**Value**	**Units**
Pressure required at the condenser outlet	Confidential	Pa
Temperature approach	5	ºC

Condensation temperature (CSP+SWCC only)	33	ºC

Dry Cooling	**Value**	**Units**
Minimum condenser pressure	2	inHg
Initial Temperature difference at design	16	ºC

Wet Cooling		
Minimum condenser pressure	1.25	inHg
Approach temperature	5	ºC

* Solar multiple is the solar field aperture area expressed as a multiple of the aperture area required to operate the power cycle at nominal capacity. The aperture area is the total solar energy collection area of the solar field in square meters, and it is less than the total mirror surface area (as the mirrors are curved, with a parabolic shape). The aperture area is calculated by dividing the solar field thermal output at design by both the irradiation at design (W/m^2) and the conversion efficiency specifications for the chosen solar collector loop. The calculation of the solar field thermal output at design (MW_t) is made by dividing the gross electric installed capacity (MW_e) by the nominal cycle rated efficiency [20].

† fraction of the power, at nominal capacity, that can be generated by the aid of a backup boiler fed with conventional fossil fuel.

‡ 100 minutes is a conservative estimate for a hot startup of an MED plant. An optimistic approach would be just above ~30 minutes.

The MED plant was simulated assuming one train instead of four as the real plant, as the model used does not make a distinction on the performance of using one train or four trains as long as the total capacity is the same.

The detailed MED model used in these simulations was run with the following configurations (similarly to the configurations set in Table 5, section 3.2.4, for the validation results of this model versus the real data from the Trapani MED plant):

- TVC Strategy: Predefined saturated discharged temperature,
- Steam ejector's model: Empirical model using ratios from the manufacturer
- Crossflow of distillate: Yes
- Feedwater preheaters configuration between MED effects: Preheaters between every 2 effects (with NCG ejectors)
- Location of preheaters powered by the NCG removal system: second effect
- Preheaters with plate heat exchangers: Yes

6.1.3 Results

Several simulations were run for the location of Trapani to dimension the CSP+MED-P plant operating in cogeneration to reach the configuration used in this exercise.

Independently of the installed capacity for thermal storage and solar multiples assumed (within reasonable ranges) while using only the solar resource it would not be possible to run the CSP and/or the MED plants continuously during winter time because the solar resource would simply not be enough. This simulation set the CSP trough solar collectors with a North-South alignment so that the collectors are oriented 90 degrees east of the azimuth angle in the morning and track the daily movement of the sun from east to west [20]. This configuration improves production during the morning and afternoon, although some radiation is lost during the peak of the day (the cosine losses) [49]. This is the configuration used in most CSP plants installed in Spain for example. Though even with a North-South alignment of the CSP solar collectors it was not possible to achieve stable production during winter time in any of the simulations performed for Trapani.

The CSP+MED plant configuration was set for the simulation so that at least between May and August the CSP capacity factor would be between 70% and 80%, and the MED near 80% as shown in Figure 29 (thus increasing the number of days where both the CSP and MED plants would operate continuously for 24 hours). Using the selected configuration of 13 hours of storage and solar multiple of 3, the CSP and the MED yearly capacity factors are 45.5% and 42.2%, respectively (considering the gross electric output as reference).

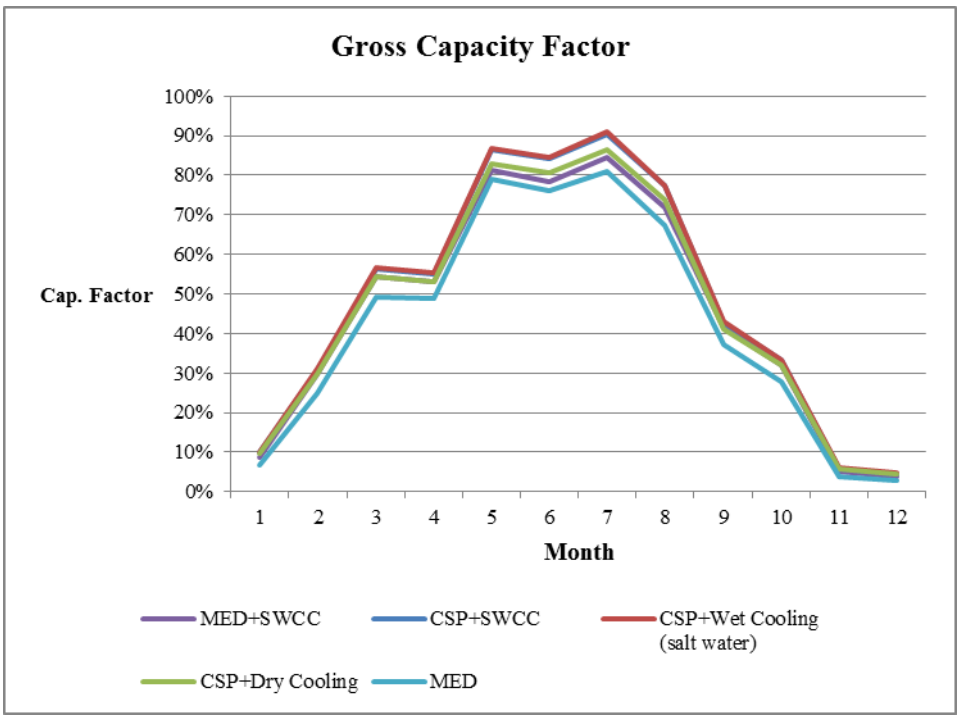

Figure 29 - CSP+MED: Capacity Factor for MED and CSP simulations (using gross electrical output for CSP as reference).

The installed power for the CSP plant was determined for this simulation so that the capacity factor of the plant would not go below the mentioned ~70% between May and

August. At nominal capacity the steam extracted to power the TVC represents 16.8% of the total mass flow rate entering the high-pressure steam turbine. For example, if the cycle is assumed to have 50 MW of installed power using the same installed capacity for the MED plant then the extracted steam to power the TVC would represent ~37% of the steam released by the boiler, and the capacity factor of the CSP plant between the months of May and August would result in values between 20% and 25% for the same period of time.

The levelized cost of electricity (LCOE) could not be used as a metric to optimize the size of the solar field, as economic costs and selling prices were not accounted in this work. Table 24 shows the general performance characteristics of the CSP and MED plants (when working in cogeneration), and the maximum and minimum main operating values when compared with nominal conditions. The Gained Output Ratio (GOR) reaches ~16, similarly to the value for the real Trapani MED plant when new, despite the lower saturated temperature of steam discharged by the TVC compared with the real plant. In this simulation the configuration used for the saturated steam input was optimized to match the same total production as in Trapani, and to have a similar ratio between the energy provided by the last effect to the down-condenser versus the energy required to preheat the feedwater to the set feedwater temperature. A conservative approach was used for the MED hot startup time of 100 minutes.

Table 24 - CSP+MED: General performance characteristics of the CSP+MED/SWCC plants for the Trapani simulation.

Metric	Value	Units
Time Step used	1	Hours
Nominal MED production capacity	36 074	m^3/day
Total MED production	5 555 331	m^3/year
Potential MED production	13 166 874	m^3/year
Nominal Heat load MED	59.1	MW_t
Minimum MED load	11.8	MW_t
Maximum MED load	59.1	MW_t
MED Capacity Factor	42.2	%
Gained Output Ratio (GOR)	16.6	-
CSP+MED/SWCC specific electric consumption at design	6.1	kWh_e/m^3
CSP NET output at design	99	MW_e
CSP design gross output	110	MW_e
CSP Capacity factor (net electric)	34.2	%
CSP total electric Gross production	336 130	MWh_e /year
CSP total electric NET production	297 017	MWh_e /year
Potential CSP GROSS elect.	963 600	MWh_e /year

Four cooling options were considered when simulating the operation of a CSP plant at Trapani, namely: MED-P/SWCC, dry cooling, evaporative wet cooling (using saltwater), and SWCC without MED.

When analyzing the option of running a CSP+TVC-MED-P at Trapani, from Figure 30 it is possible to see that the production profile is in line with the typical Mediterranean climate (as the power comes from solar irradiation). Production peaks during summer and decreases sharply during winter time, despite the usage of a CSP plant with a large thermal storage capacity (13 hours) and solar multiple of 3. During summer time, capacity factors are higher (normally above 50%), and in winter time they are low (below 10%). In line with this profile is also the rate for CSP plant parasitic consumption. The CSP parasitic consumptions accounted are shown in Figure 31, These are described in [20] and include: auxiliary boiler parasitic load, fixed parasitic load, balance of plant parasitic load, total parasitic power for tank freeze protection, solar collector assemblies drives and electronics parasitic power, thermal energy storage and power block heat transfer fluid pumping power, collector field required pumping power, power block cooling parasitic power, and collector field required freeze protection. In relation to the gross electrical production, the CSP plant parasitic consumption is especially high between November and January. During these winter months, the anti-freezing protection system for the CSP thermal storage tanks operates more often, as the CSP plant almost does not run (and in a smaller scale, thermal losses in the molten storage tanks are also higher than in summer time, as air temperatures are lower).

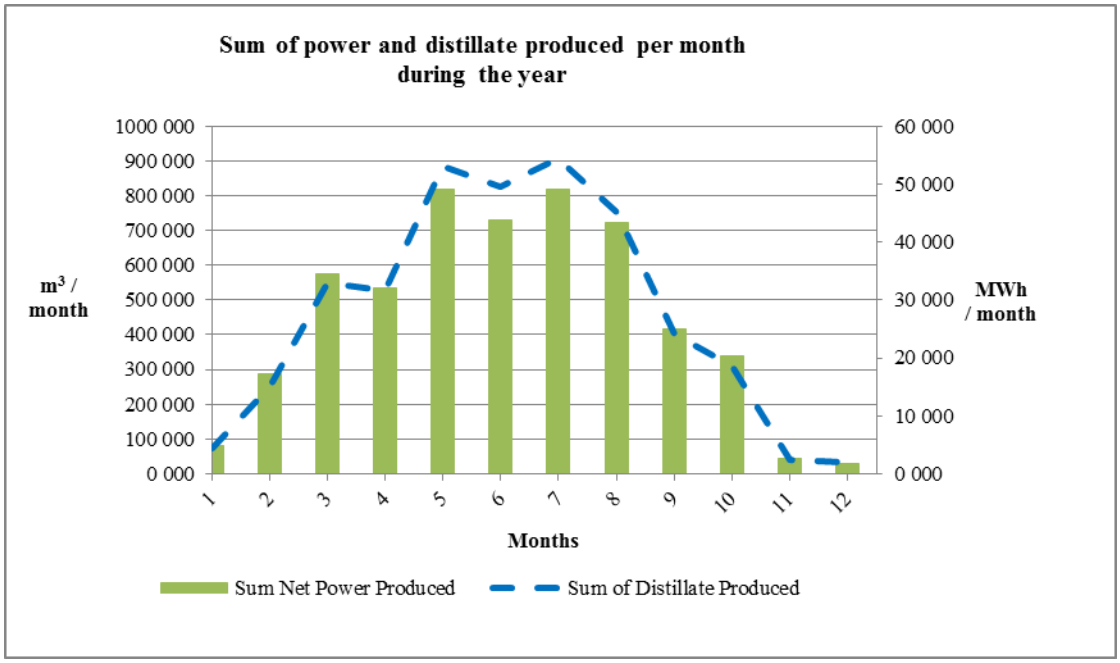

Figure 30 - CSP+MED: Sum of Power and Distillate produced per month during one year.

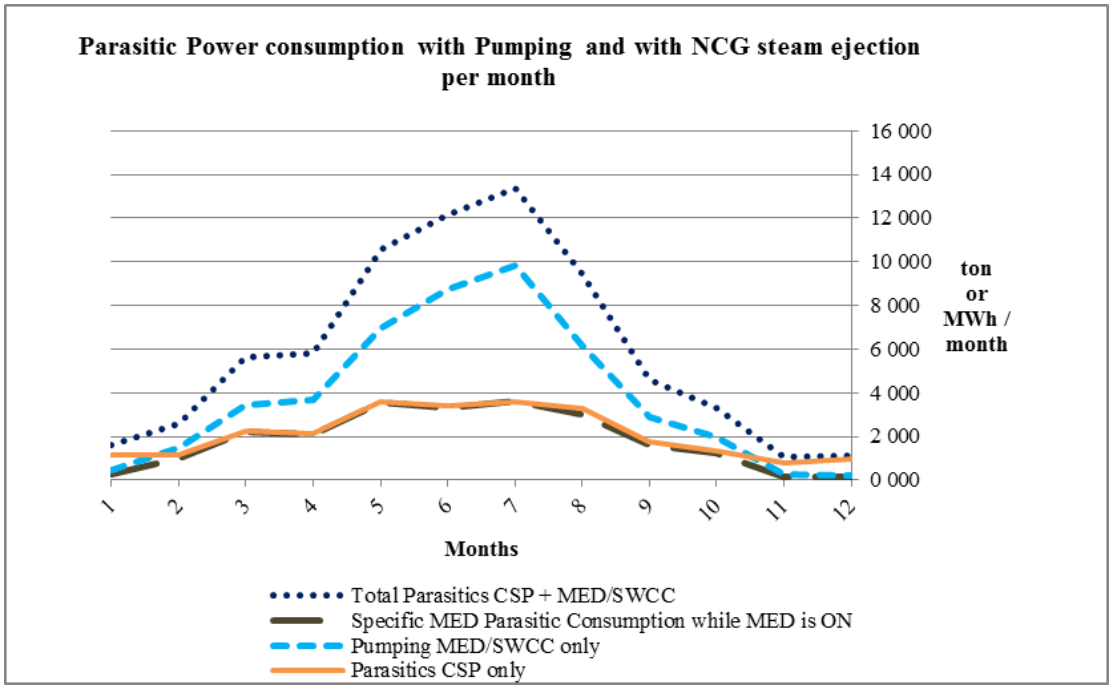

Figure 31 - CSP+MED: Parasitic consumption with pumping and with NCG steam ejection per month during one year.

In Figure 32 and Figure 33 it is possible to see the detailed outputs of the CSP+MED/SWCC operation for a typical day during winter (3rd of January) and summer (1st of July).

During this winter day the operation of both plants is only possible during a few hours because the solar resource is scarce. It is possible to see also that during this day the SWCC system absorbs the variability of the CSP output, enabling the MED to operate during those few hours near nominal conditions. The slight increase in production of the MED plant between 13:00 and 15:00 is due to the MED startup time getting completed only during the latter time step, and so the nominal production will occur just for a percentage of this time step (time steps in this simulation represent 1 hour).

On the first day of July the panorama is totally different, as the solar resource is higher and the CSP plant can operate continuously using the thermal storage tanks to provide heat to power the Rankine cycle during the hours with insufficient solar irradiation. A 24 hour operation is possible during this summer day as the CSP plant was fit with a large thermal storage capability and an adequate solar multiple for the solar field. As consequence result, the MED plant can also operate uninterruptedly during this period. Again, it is possible to notice that the SWCC absorbs the variability of the rejected heat load coming from the CSP plant allowing the MED plant to operate at a constant load.

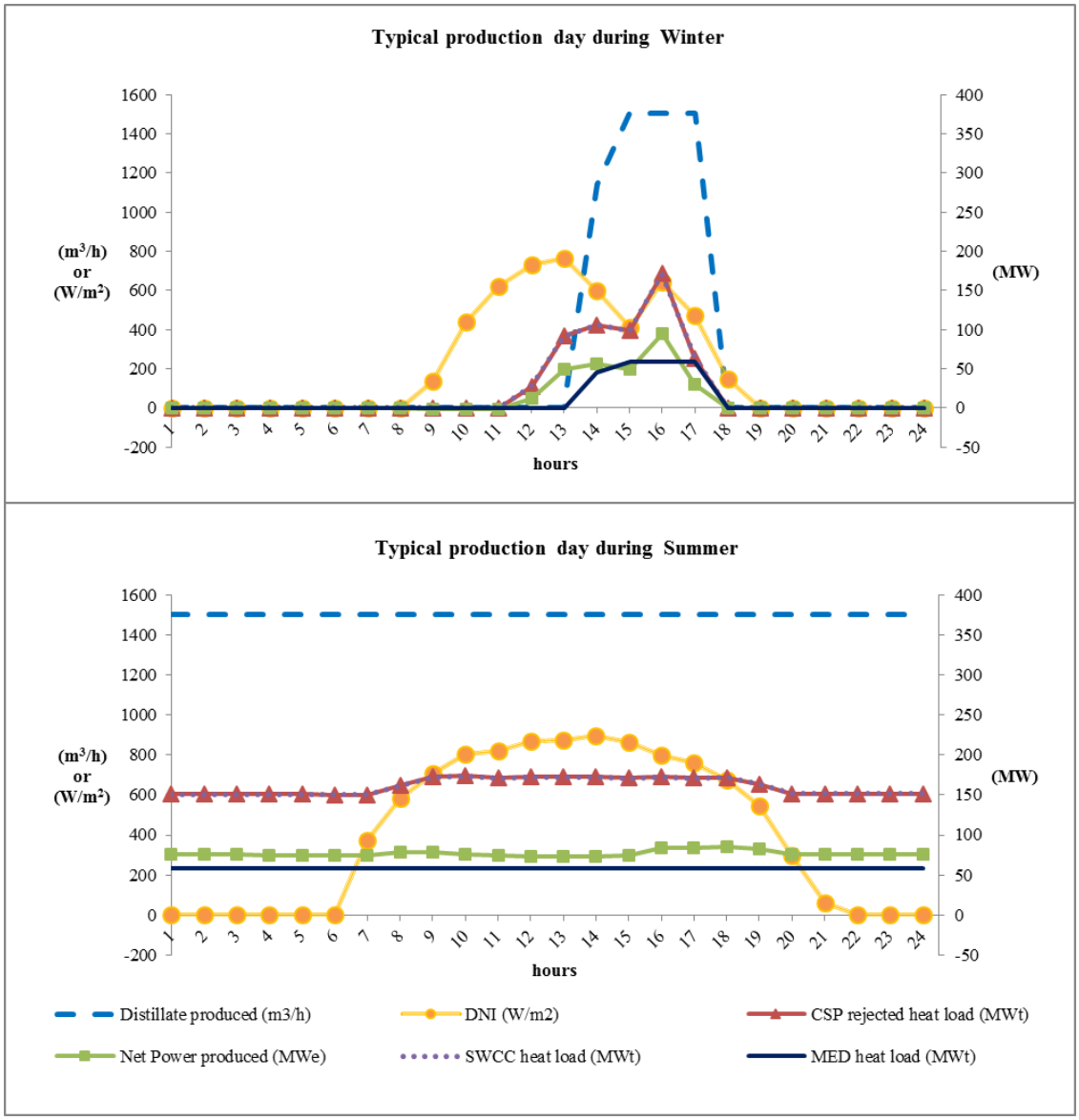

Figure 32 - CSP+MED: Typical operation days for a CSP plant with MED/SWCC during winter (3rd of January) and summer time (1st of July): main outputs.

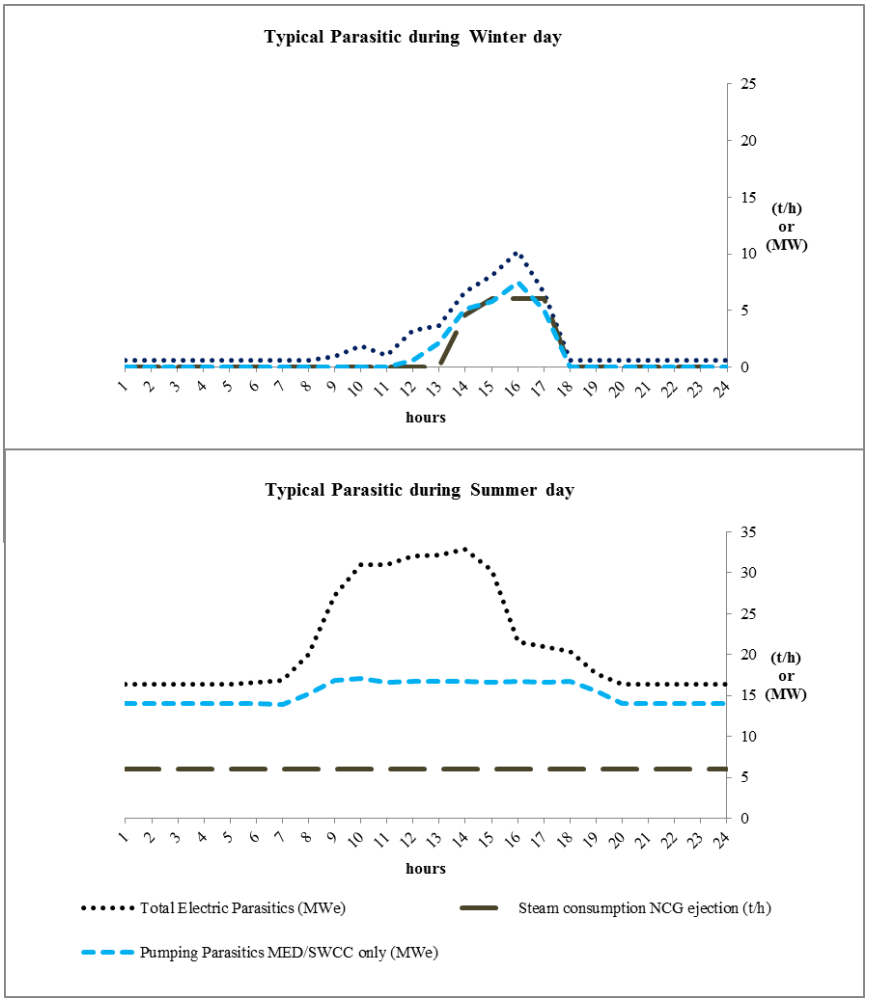

Figure 33 - CSP+MED: Typical operation days for a CSP plant with MED/SWCC during winter (3rd of January) and summer time (1st of July): Main parasitic.

Figure 34 and Figure 35 show a comparison of electrical generation for all scenarios taking as a reference the power output of the CSP+MED/SWCC system. The scenario with the highest electrical production is obtained when using the CSP plant with wet cooling, followed by the CSP with SWCC. In average the CSP plant using wet cooling or the SWCC configurations produces ~21% more electricity than the CSP+MED/SWCC configuration, and dry cooling produces more ~13% (considering net electrical outputs). On the other hand, the CSP+MED/SWCC allows the production of ~5.5 million m^3/year of fresh water.

Wet cooling using “saltwater” versus “fresh water” has a negligible difference in performance, although the operation in the long run with saltwater will be more costly due to a faster degradation of the plant components [107]. In this simulation the performance of a CSP+SWCC is slightly below CSP+Wet Cooling because of the condensation temperature forced to the SWCC being slightly higher than the one with wet cooling for the most profitable months, and the distances and depth from which the seawater is assumed to be pumped from the sea in this simulation (the SWCC would have a better performance if a lower

condensation temperature would be considered and the intakes would be nearer the plant). Dry cooling is dependent on the dry bulb temperature, implying higher temperatures in the down-condenser of the Rankine cycle (yearly average of 42.6ºC with dry cooling versus 40ºC with SWCC, and 33.0ºC with wet cooling).

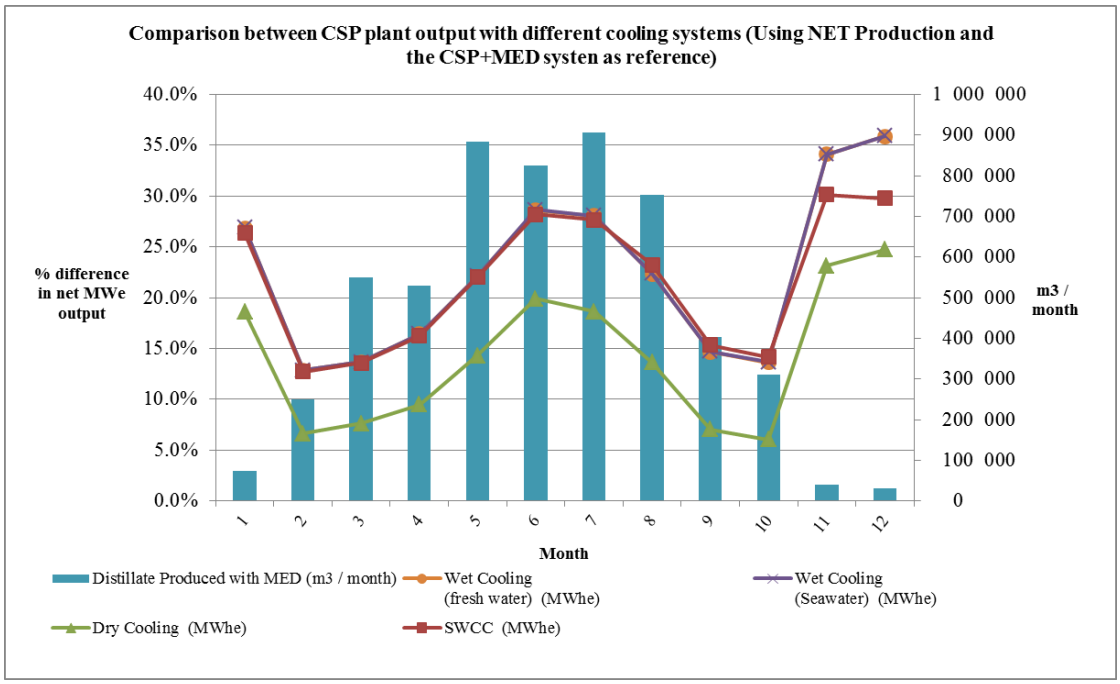

Figure 34 - CSP+MED: Comparative power output for the CSP plant with different cooling systems (and distillate production when MED is used) considering net electrical output and the CSP+MED system as reference.

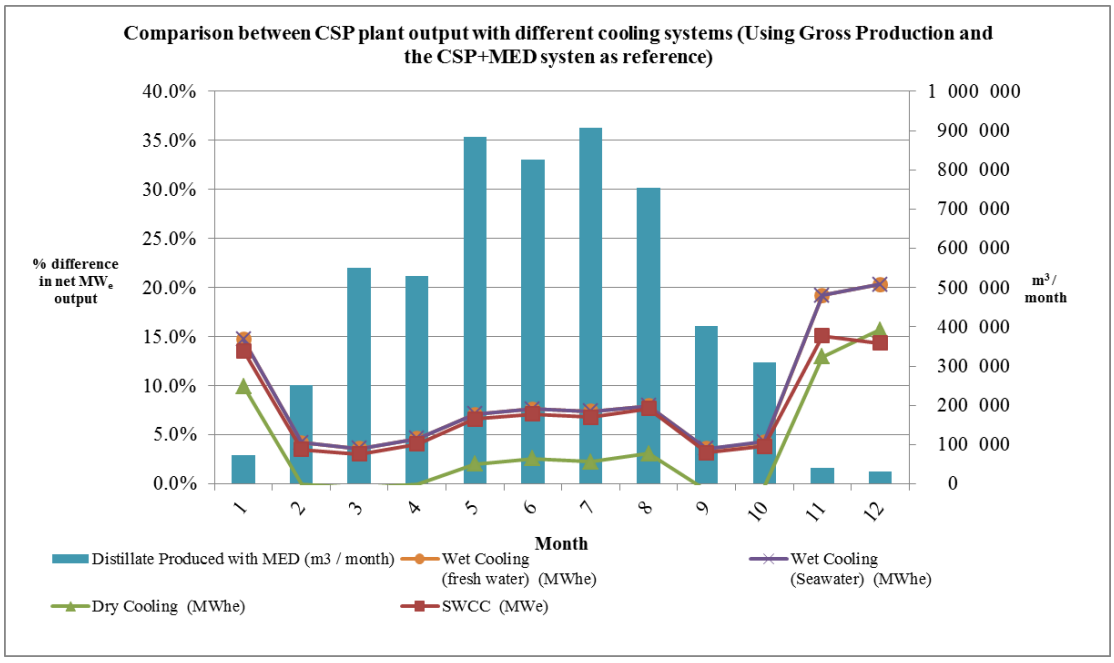

Figure 35 - CSP+MED: Comparative power output for the CSP plant with different cooling systems (and distillate production when MED is used), considering gross electrical output and the CSP+MED system as reference.

CSP and MED production during winter months is much lower than in summer time. There are several days during this period in which the CSP plant will not start at all or it will only operate at a very low capacity below the minimum for the MED operation. As the CSP plant in these conditions will operate near its minimum load, in some cases the CSP+MED/SWCC system may not start at all while the CSP with other cooling options (with higher performance) would still operate. The total yearly electrical output will not suffer much with these performance differences during winter time, but when analyzing graphics showing outputs in relative percentages, large differences during winter months may appear between performance curves.

In theory the CSP+SWCC configuration will have less parasitic consumption with water pumping than CSP+MED/SWCC, as the MED plant will use more seawater to reject the same amount of heat load from the CSP plant. The CSP+SWCC configuration increases its performance relative to the CSP+MED/SWCC through the warmer season of the year (April up to September, regarding the net electrical production only) as during these months the CSP plant will operate more hours above the minimum load for the MED plant to start. For these situations below minimum loads, in both configurations the CSP plant will operate in practice only with the SWCC (as the MED will not be turned on). In the summer time, as the heat load provided by the CSP plant increases in power and time span, the MED plant will operate more often, and the parasitic consumptions will increase compared to the SWCC usage only. Table 25 shows the detailed results of the simulations for the Trapani case study.

Table 25 – CSP+MED: Annual and monthly sum of net electrical output, parasitic consumption, and distillate produced when the MED is used.

	MED+SWCC (ref. scenario)			Dry Cooling		Wet Cooling (Seawater)		SWCC	
	MWh_e		m^3	MWh_e		MWh_e		MWh_e	
	Net Elect.	**Parasit.**	**Distillate**	**Net Elect.**	**Parasit.**	**Net Elect.**	**Parasit.**	**Net Elect.**	**Parasit.**
Jan	4 843	1 587	73 924	5 743	1 325	6 145	1 232	6 119	1 182
Feb	17 181	2 604	250 433	18 321	1 454	19 392	1 226	19 364	1 114
Mar	34 515	5 657	550 123	37 143	2 859	39 239	2 381	39 196	2 197
Apr	31 983	5 813	528 378	35 015	2 767	37 237	2 310	37 176	2 149
May	49 159	10 593	882 955	56 177	4 771	60 019	3 978	59 971	3 727
Jun	43 765	12 171	825 169	52 478	4 911	56 301	3 903	56 104	3 825
Jul	48 980	13 368	906 889	58 112	5 639	62 731	4 231	62 532	4 055
Aug	43 398	9 468	753 274	49 303	5 189	53 101	3 972	53 470	3 456
Sep	24 981	4 615	402 339	26 743	2 639	28 653	2 013	28 808	1 730
Oct	20 289	3 302	309 692	21 514	2 014	23 059	1 544	23 158	1 341
Nov	2 568	1 075	40 670	3 162	953	3 444	900	3 341	853
Dec	1 688	1 150	31 485	2 106	1 177	2 295	1 121	2 191	1 055
Total	323 351	71 403	5 555 331	365 817	35 697	391 616	28 809	391 430	26 684

The electrical cutback on the electrical output was calculated comparing the performance of the CSP+MED/SWCC system with a stand-alone CSP plant with different cooling processes, as shown Table 26 and Figure 36. Using the gross output as reference, the cogeneration scheme returned an average annual cutback on electrical production of 1.22 kWh/m^3 produced when comparing with CSP using dry cooling, and 4.62 kWh/m^3 if compared with CSP using wet cooling. These values increase if the net electrical output is used as reference, namely to 12.27 kWh/m^3 and 7.64 kWh/m^3 respectively.

Table 26 – CSP+MED: Annual average for the cutback on the potential electric production per amount of fresh water produced, considering both gross and net electrical production.

	CSP+MED vs. Wet Cooling (fresh water)	**CSP+MED vs. Dry Cooling**	**CSP+MED vs. Wet Cooling (salt water)**	**CSP+MED vs. SWCC**
Cutback considering gross elect. production	4.60 kWh/m^3	1.22 kWh/m^3	4.62 kWh/m^3	4.20 kWh/m^3
Cutback considering net elect. production	12.29 kWh/m^3	7.64 kWh/m^3	12.29 kWh/m^3	12.25 kWh/m^3
Cutback considering net elect. Production (excluding pumping costs up to the plant)	5.02 kWh/m^3	1.61 kWh/m^3	5.04 kWh/m^3	4.64 kWh/m^3

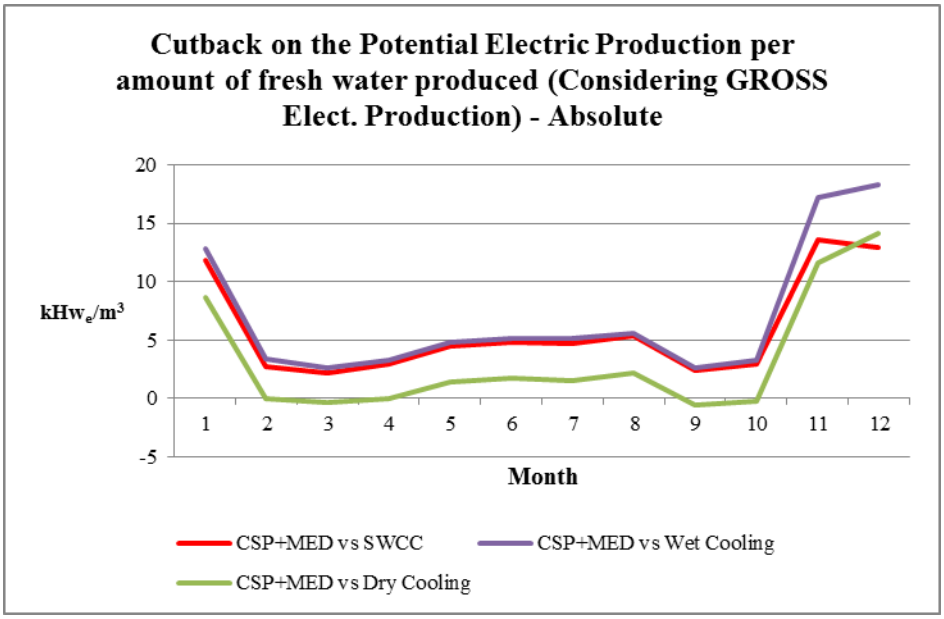

Figure 36 – CSP+MED: Cutback on the potential electric production per amount of fresh water produced considering gross electrical production vs. CSP with other cooling systems, average monthly values.

More information regarding the simulations described in this section is presented in Annex 7 in the form of tables and graphs for other parameters not described in detail in the text above.

6.2 CSP+RO System

6.2.1 System Description

The aim of this section is to simulate the performance of a parabolic trough plant coupled with a seawater desalination RO unit. The sizing of both the CSP and RO plants were defined so that these simulation results can be compared to the existing Trapani commercial TVC-MED-P desalination plant, and to allow for the subsequent comparison with the results obtained from CSP+MED. Because of this, the simulated RO plant is capable of producing 36 000 m^3/d and the CSP plant 110 MW_e, using parabolic trough system with a conventional Rankine cycle, assuming the same size for the molten salt storage tanks and solar field. The weather data used for the simulation of the solar plant in the location of Trapani was also the same as the one used for the simulations described in section 6.1 for the CSP+MED.

The simulations were carried out considering four different cooling options for the power plant: wet cooling (using fresh and salt water), dry cooling, and a once-through seawater condenser (SWCC). All the simulations consider no electrical grid connection between to the CSP+RO system. The CSP physical model from SAM (version 2014.1.14 that uses TRNSYS solver) was used to run the calculations, and the simulation of the CSP+SWCC was done using the new solar desalination add-on to SAM, described in section 4. The simulation of the RO system was done using ROSA (version 9.1). The algorithm developed in Microsoft Excel environment (described in section 5) was then used to match the simulations for the CSP and RO plants. The RO plant was assumed to have 6 identical trains. ROSA was used to simulate the operation of one train, and the total plant performance was extrapolated from this information assuming a linear relationship between installed capacity and mass flow rates required/produced.

A general description of the cogeneration scheme simulate in this section is presented in Figure 37.

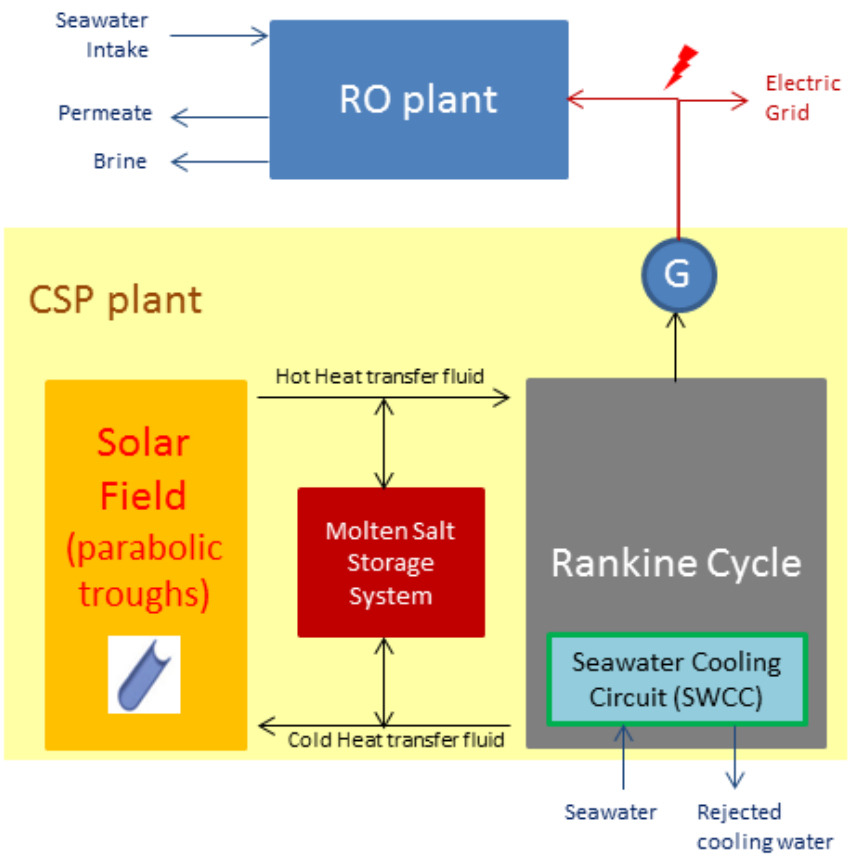

Figure 37 - Generic schematic diagram of the simulated CSP-RO system.

The Trapani MED plant was chosen as reference for this case study because it is one of the few plants with detailed design information available in the literature, and detailed data was available from direct contact with the plant manager and site technical visits.

The coupling of the CSP-RO system will assume that the CSP plant powers the RO high pressure pump (both pre and post-treatment systems are currently neglected by the model used in this simulation, described in section 5). The main inputs set to size the RO plant were the recovery and feed pressure. These are established by considering membrane control and operation limits. The RO plant is simulated to have several RO trains in parallel, allowing flexible partial operation.

6.2.2 Inputs

Several simulations were carried out to determine the optimum configuration for the RO system, according the recommendations from the literature [39] , [108]. The simulated RO plant is comprised of 6 trains, each with 2 stages, using an energy recovery device (from the high pressure brine leaving RO stages). The number of trains was set so that it would allow a

relevant degree of operation at part load of the entire RO plant, increasing the number of hours of continuous operation. The first stage assumed to have 49 pressure vessels, and second stage 36 pressure vessels, each pressure vessel with 6 elements. A two-stage configuration for an RO plant means that there are two sets of pressure vessels in a row for each RO train (each RO plant is made of several RO trains). The first stage receives seawater (after it has passed through a pretreatment process with filters), and produces both permeate (fresh water) and brine. Then, the brine produced by the first stage is routed into the inlet of the second stage, and more fresh water is produced from this brine, meaning that the brine concentration increases as it crosses the stages. This RO configuration is applicable where the salinity of the feedwater is not excessively high, as it happens to be the case in the Mediterranean. Otherwise, if the seawater salinity were higher (as for example in the Arabian Sea) a two or more pass system would be applied (instead of brine it would be the permeate produced in the first set of pressure vessels that would be sent as feed to the second set of pressure vessels). In total, the RO plant is assumed to have 3060 membranes for high salt rejection and low energy consumption, with 40.9m^2 each.

The total recovery ratio for the RO plant is set to 45% (as recommended by [39]). The first stage recovers 37.6 % and the second stage 11.8 % (the second stage receives as feed the brine produced on the first stage). Each simulated RO train produces 6000 m^3/day of fresh water, with a total of 36000 m^3/day at nominal capacity.

The power consumption of the RO plant at nominal is ~6.7 MW_e, but the size selected for the CSP plant was set to be much larger than necessary (~110 MW_e instead of ~6.7 MW_e gross) in order to compare the performance of the modelled CSP-RO system to the outputs obtained in section 6.1.1 for the CSP+TVC-MED system.

The results of the CSP plant running with wet cooling, dry cooling and a SWCC were taken from the simulations shown in section 6.1.1. The CSP plant in both sections were meant to be identical when using these cooling processes, so that a direct comparison of results would be possible. Inputs for the CSP plant were set to be the same as the standard case study available in SAM (2014.1.14, revision 1) for plants using troughs, excluding: location, installed power, solar multiple and number of storage hours with molten salt tanks, as shown in Table 27, where the main list of inputs used for the CSP+RO simulations is described.

Table 27 – CSP+RO: Main simulations inputs for the CSP+RO simulations with SAM and ROSA.

Input Value	Value	Units
CSP Plant		
Installed CSP Power (PT using oil as HTF)	99 net (110 gross)	MW_e
Thermal Storage	13	h
Rated cycle conversion efficiency	37.74	%
Condenser temperature for rated cycle conversion efficiency	35	^oC

Solar Multiple*	3	-
Irradiation at design (reaching the solar field)	950	W/m^2
Total collector loop conversion efficiency (Solargenix SGX-1)	71.69	%
Design inlet temperature	391	^oC
Design outlet temperature	291	^oC
Operating boiler pressure	100	bar
Hot standby period	2	h
Thermal power fraction for standby	20	%
Max. turbine overdesign operation	105	%
Min. turbine operation	25	%
Direct normal irradiation (DNI)	2004	$kWh/m^2/yr$
Fossil fill fraction†	0	%

RO

Total number of pressure vessels	n=85	-
Pressure vessels staging Ratio	49:36	-
Total number of membranes	n=3060	-
Feed water flow rate	13333	m^3/day
System recovery rate	45	%
Flow factor	1	-
Water Temperatures	10(min)/22(max)	^oC
Feed water salinity (TDS)	40000	mg/l
pH	7.6	-
Pre-stage ΔP	0.345	Bar
Membrane Type	SW30HRLE-400i	-
Pump Efficiency	90	%
Energy Recovery Device Efficiency	90	%

Once-through seawater cooling

Distance between plant and water intake tube	2000	m
Intake tube water velocity	0.3	m/s
Temperature approach	5	^oC
Distance between plant and end of brine discharge tube	2000	m
Brine tube water velocity	0.3	m/s
Plant site elevation above sea level	10	m
Water storage tank distance from plant	100	m
Water storage tank height	5	m
Condensation temperature	33	^oC

Dry cooling

Minimum condenser pressure	2	inHg
Initial temperature difference at design	16	^oC

Wet cooling

Minimum condenser pressure	1.25	inHg
Approach temperature	5	^oC

6.2.3 Results

Results show that both the net electricity produced by the CSP+RO systems (already excluding the RO consumption) and the total fresh water production were very similar in pattern as it can be seen in Figure 38. This production profile is also very similar to the production profile shown for the CSP+MED simulations.

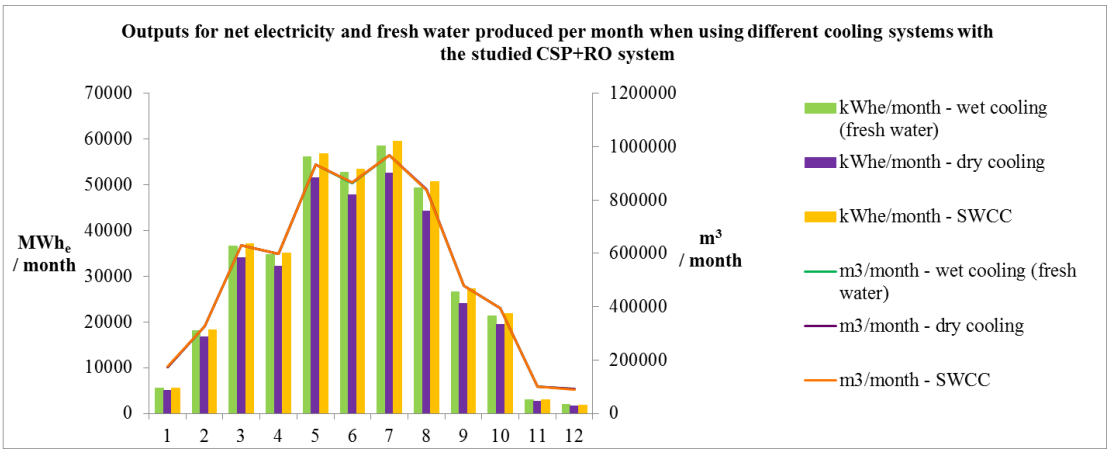

Figure 38 - CSP+RO: Outputs for net electricity and fresh water produced per month when using different cooling systems with the studied CSP+RO system.

The total annual production is the same for the cases using the SWCC or wet cooling (using either fresh or salt water). Table 28 shows that only the dry cooling returned slightly lower production of electricity and water, in the order of - 0.1 % and -7%.

Table 28 - CSP+RO: Total outputs summary for m^3 of fresh water produced and net electrical production with the different configurations assumed (already accounting for the RO electrical consumption).

	CSP+RO (Dry cooling)		CSP+RO (Wet cooling)		CSP-RO (SWCC)	
	m^3/yr	MWh_e/yr	m^3/yr	MWh_e/yr	m^3/yr	MWh_e/yr
Total production (elect production accounting RO consumption)	6 401 250	344 566	6 401 500	370 305	6 402 250	370 204
Comparative result versus Dry cooling	-	-	0.1 %	7.5 %	0.1	7.4 %

Results show that as expected the water quality of permeate produced decreases with the increase in seawater temperature across the year and vice versa. In January and December (the coldest months for water temperature) the permeate is produced with 100 mg/l of total dissolved solids, while in June and July (the warmest months for water temperature) this value rises to 215 mg/l (the maximum value for this parameter recommended by the World Health Organization is 250 mg/l for drinking water [109]).

Capacity factors for the CSP plant are the same as shown in section 6.1.3 (for the simulations that do not consider cogeneration), as the inputs are the same.

The cutback on electrical production per m^3 produced is presented in Table 29. This value is very similar independently of the cooling system used: 3.32 kWh/m^3 of fresh water produced.

Table 29 – CSP+RO: Annual average for the cutback on the potential electric production per amount of fresh water produced, considering net electrical production.

	CSP+RO with Wet Cooling (fresh water)	**CSP+RO with Dry Cooling**	**CSP+RO with Wet Cooling (salt water)**	**CSP+RO with SWCC**
Electrical cutback considering net elect. production	3.32 kWh/m^3	3.32 kWh/m^3	3.32 kWh/m^3	3.32 kWh/m^3

6.3 CSP+MED vs. CSP+RO

This section compares the yearly performance of comparable systems using the two leading desalination technologies available in the market, MED and RO, powered by a CSP plant for the location of Trapani, Sicily. The simulated systems have similar installed capacities: in both cases the CSP plant is designed to produce 110 MWh_e at design and the desalination units 36 000 m^3/day. The desalination plants have been sized to match at design the total production of the commercial TVC-MED-P stand-alone plant at Trapani.

The simulations for both CSP+MED and CSP+RO systems are presented in sections 6.1 and 6.2, respectively. Both systems show a very similar production profile for water and electricity across the year, in line with the typical Mediterranean climate, as seen in Figure 39. The solar resource is simply not available to power the CSP plant during the winter; therefore productions plunge during this period. Figure 39 also shows that the total production of water and electricity is lower across the entire year when using a CSP+TVC-MED-P system than when using a CSP/SWCC+RO system.

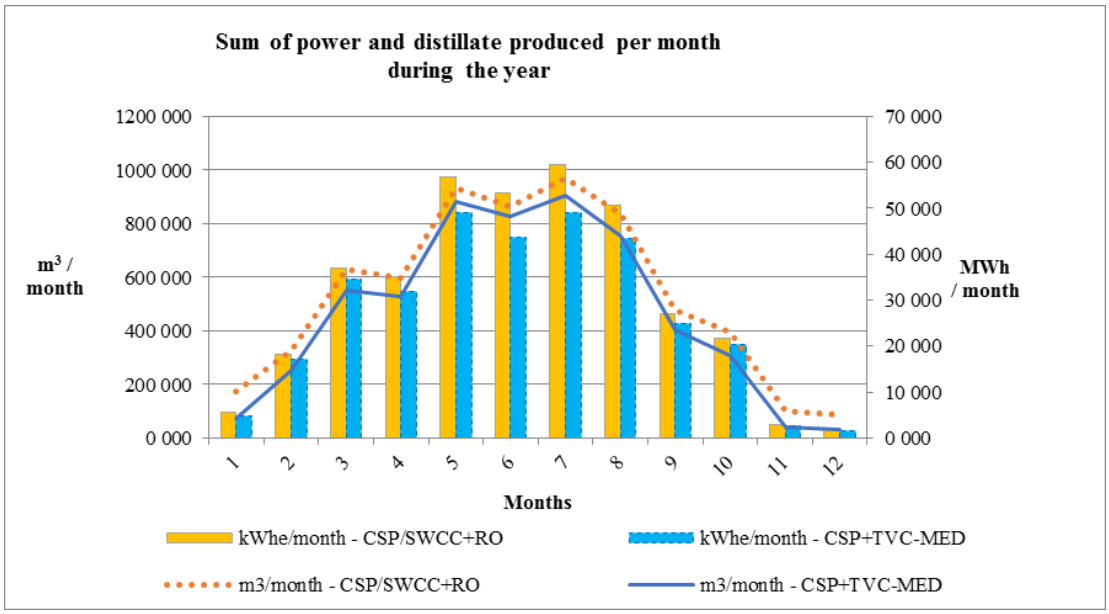

Figure 39 - CSP+MED vs. CSP+RO: Comparison of net electrical and fresh water production, for the location of Trapani, Sicily

For both configurations capacity factors for the CSP and the desalination plants are very low during the winter months (below 10%), while peaking during the summer (ranging between 75 and 90%, considering gross electrical outputs for the CSP plants), despite the use of a large thermal storage capacity and solar multiples.

It is likely that with a CSP+RO system, both plants would be located close to sea, therefore a SWCC would be used. This configuration also allows a more straightforward comparison with the CSP+MED/SWCC system as it also uses a once-through seawater

condenser. The simulation run for the CSP+RO system indicates that a wet cooling system would return a slightly better performance, but it would not probably be the first choice because: 1) lack of fresh water; 2) using salt water deteriorates the plant faster due to the spray of salt on cooling towers [107]; and 3) the performance of the CSP plant using the SWCC in practical terms returns the same results as using a wet cooling system.

The simulated CSP+RO system produces in average more than 15% of water and has a net electrical output of 14% higher than the CSP+MED system. These comparative results are presented in Figure 40. The numbers presented for the net electrical output of the CSP+RO system deduct the electrical consumption of the RO system from its gross output, together with the other parasitic consumptions mentioned for the CSP plant (auxiliary boiler parasitic load, fixed parasitic load, balance of plant parasitic load, total parasitic power for tank freeze protection, solar collector assemblies drives and electronics parasitic power, thermal energy storage and power block heat transfer fluid pumping power, collector field required pumping power, power block cooling parasitic power, and collector field required freeze protection parasitics [20], and pumping required for the SWCC).

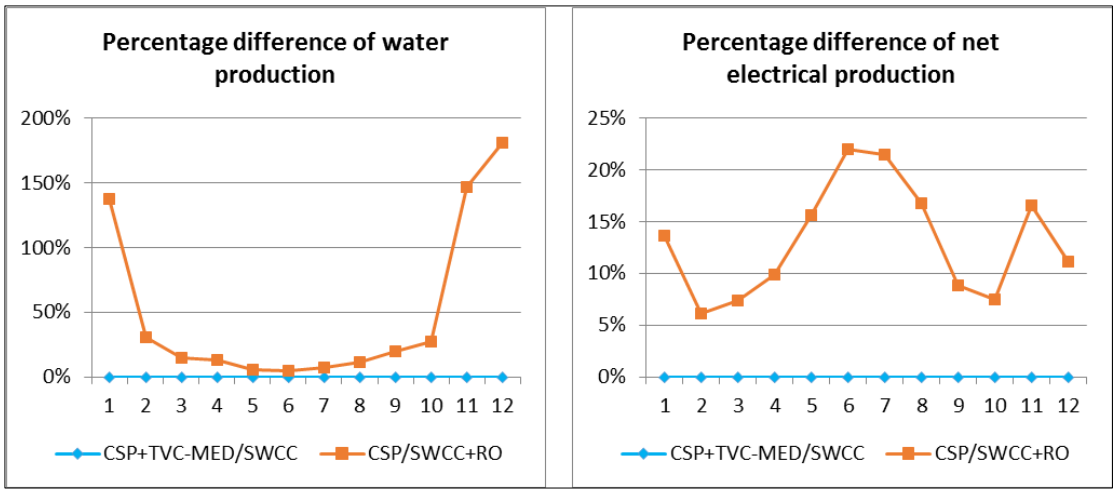

Figure 40 – CSP+MED vs. CSP+RO: percentage difference of water and net electrical production (net electrical consumption for the CSP+RO system accounts the RO electrical consumption).

The bulk of water and electrical production occurs between February and October. Water outputs tend to be very similar during the peak of summer, as both the MED and the RO plants operate near design point more often, as enough power is available. Results from Figure 40 show that the biggest discrepancy during this period is the net electrical output. The CSP+RO configuration produces more electricity even if the RO electrical consumption is accounted for in the net electrical output (as it is shown in the previous figures).

For the location of Trapani, excluding pumping costs up to the plants (specially up to the down condenser for the MED plants, or up to the high pressure pumps for the RO plants), the average electrical cutback per m^3 of fresh water produced is 4.64 kWh/m^3 using the

CSP+TVC-MED system, and 3.32 kWh/m^3 using the CSP+RO system, as shown in Table 30. This represents a ~28% difference between these two values. The RO model does not account for the energy consumption to pump feedwater through the pre-treatment processes before reaching the high pressure pumps. This is likely to be the main reason why the simulated electrical cutback of the CSP production is below the expected ranges mentioned in the literature (3.32 kWh/m^3 versus 4-7 kWh/m^3, respectively), as referred in section 2.1.3.

Table 30 – CSP+MED vs CSP+RO: Annual average for the cutback on the potential electric production per amount of fresh water produced, considering net electrical production (excluding pumping costs up to the plant).

	CSP+MED vs. CSP+SWCC	**CSP/SWCC+RO vs. CSP/SWCC**
Cutback considering net elect. Production (excluding pumping costs to and from the plant)	4.64 kWh/m^3	3.32 kWh/m^3 (does not include costs with feedwater pretreatment)

Between February and October it is also noticeable that the RO production increases faster than the MED as the seawater temperature gets warmer. This increase is a direct effect of the increase in water temperature, as membrane pores increase in size, and so less pressure is required to produce the same amount of permeate. Less pressure means less energy used by the high-pressure pumps, resulting in a higher value for the net electrical production (the permeate quality decreases though in warmest months as described before in section 6.2.3). On the MED system, on the other hand, the fluctuation in seawater temperature has a lower impact, as an increase of this parameter implies only a relatively smaller increase in the total cooling water required by the down-condenser. This cooling water is pumped at a much lower pressure compared to the RO system, having a lower impact on the total net electrical output of the CSP+TVC-MED system. Figure 41 shows the evolution of the monthly average values of the Direct Solar Irradiation (DNI), air and seawater temperatures used in the simulations.

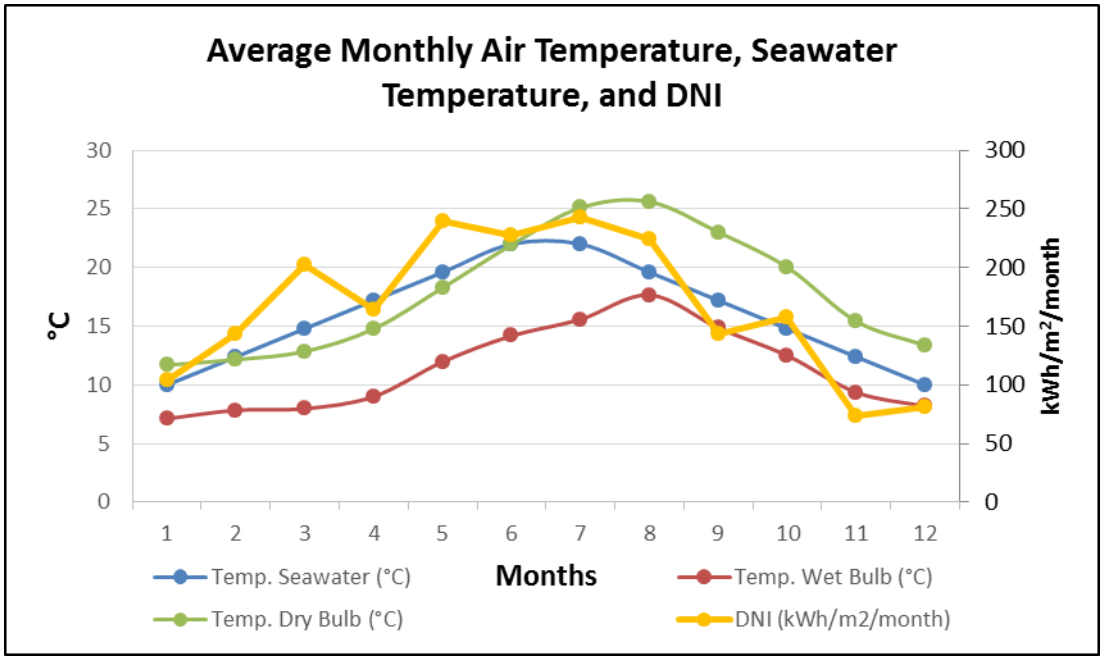

Figure 41 - Average monthly air temperature, seawater temperature, and DNI used in the simulations for Trapani.

Results from Figure 40 regarding percentage of net electrical production show peaks during winter time in favor of the CSP+RO. This is due to the values being shown in percentage, as both cogeneration systems produce very low amounts of electricity and water. As the CSP plant in the CSP+RO configuration is more efficient than in the CSP+MED, in some days of the year the latter one will not start at all, while with the CSP+RO configuration it might be turned on, but working near the minimum acceptable load.

It is important to have in mind that the CSP+MED model accounts for minimum startup times and pumping consumption of seawater into the plant, and that the CSP+RO model does not have these into account. Taking these into account for the CSP+RO system would likely return more convergent results.

Other cogeneration configurations for CSP powered desalination units might achieve better results than the one studied in this work in other locations, implying that the present conclusions might not be generally valid for all CSP+MED and CSP+RO integration schemes but only for the configurations and site described in this case study. Also, site conditions influence the physical performance of the plants, so do the financial aspects of these investments, which are not within the scope of in this work.

6.4 Comparison with Real MED Plant

From the above analysis it is clear how during winter time there is not enough solar resource to power a CSP system at full load, independently of the thermal storage and solar multiple used (within reasonable ranges). Because of this, the CSP plant could not be simulated to run with the same operational base-load profile of the existing TVC-MED plant at Trapani. Otherwise natural gas boilers would need to be used as backup to provide steam whenever solar thermal energy is not available (either to the CSP plant or to the MED plant directly, in case of a CSP+MED configuration).

However, it is worth noting that water and electricity consumption in Trapani, and in Sicily in general show a seasonal profile, with high demand in the summer time and low demand in the winter. Moreover, in this region, large scale water storage is possible as rain water is typically collected in winter time and stored in artificial lakes, acting as large open reservoirs.

Having these factors into account, for the location of Trapani producing water with a desalination plant does not strictly require a constant output throughout the year. In summer time the peak demand could be met by a CSP+MED/SWCC or a CSP+RO system, while in winter time lakes and reservoirs could provide the fresh water (gathered from rain fall or storage of excess production from the MED plant during summer time). Such an electrical and water production profile is actually something that current utility electrical and water operators would favor for this Italian region in order to face the large seasonal variability of water availability/demand.

Finally, in order to obtain the same water production as the real TVC-MED plant installed at Trapani (and assuming a capacity factor of 90%), the above-mentioned CSP+MED/SWCC system would need to be oversized, requiring an installed capacity of 234 MW_e gross and an MED plant capable of producing ~77 000 m^3/day at design (instead of 110 MW_e gross and 36 000 m^3/day). With this oversized CSP+MED/SWCC system (roughly 2.2 times larger), the water production curve would have the same profile as in Figure 30 and **Error! Reference ource not found.**, sections 6.1.3 and 6.2.3, respectively (with water and electricity production peaking during summer time), but the production curve would be oversized. Similarly, the above-mentioned CSP/SWCC+RO system would be required to be ~1.8 times larger, with a 203 MWh_e CSP plant and a 66 500 m^3/day MED plant at design.

These results show that both the CSP+MED and CSP+RO systems may have the potential to be economically attractive in regions such as Sicily, as in this specific case this would probably be a good match with the local needs as both water and electricity demand peak during summer time.

7. Conclusions

The work described in this document was focused on the detailed analysis of the physical performance of Concentrating Solar Power (CSP) with Multi-Effect Distillation (MED) or Reverse Osmosis for the cogeneration of fresh water and electricity. Two main conclusions can be taken from this work:

1. There is no straight answer to which is the best combination of technologies within the several possible CSP+D configurations. The answer to this question will probably always be case specific, which is why the simulation models developed in this thesis are important.
2. The operation of CSP+D plants can be an interesting option for the cogeneration of fresh water and electricity, using as reference the case study of Trapani, Sicily.

Many zones around the globe suffer from water scarcity, because the resource is simply not there or due to water pollution or excessive consumption. Fresh water production is a necessity that will likely keep on growing during the coming decades. In many places the only reliable water source is the salt water from oceans and seas, as it happens in particular through the Middle East and other regions with high solar irradiation levels. The current desalination technologies are very energy intensive and although they are commercially proven, they are normally connected to fossil fueled power stations, and a heavy toll is paid in carbon emissions into the atmosphere for each cubic meter of fresh water produced. The pairing of CSP and desalination technologies has the potential to be technically feasible, as shown in this thesis. No tools were available to make a preliminary assessment on such kind of investments that would integrate the entire solar desalination cogeneration process in one platform. This thesis addresses this issue by adapting existing tools and specially developing new ones that can be used exactly for this purpose. In particular, a new detailed model was developed for the simulation of multi effect distillation plants and integrated into existing software that simulates the operation of CSP plants (SAM from NREL). This same program for CSP plants was also combined with freely available software that enables the simulation of RO plants (ROSA from Dow Chemical Company). Using these two blocks of tools, it is now possible to make the evaluation on the physical performance of CSP plants powering MED and RO plants, the two dominant desalination technologies available in the market. Both the new MED and the existing RO models were validated against real data from existing desalination plants, and the results match within a +/-10% deviation range.

A case study was selected for the evaluation of the performance of all these technologies working in cogeneration to produce fresh water and electricity. The city of Trapani, in the South West of Sicily, Italy was chosen, as detailed data from an existing commercial TVC-MED parallel plant was available for comparison. With the selected dimensioning strategies

used for this case study, the CSP+RO configuration got a clear advantage over the CSP+MED with ~15% more production capacity throughout a simulation for one year regarding both water and electricity. Using RO also has the advantage of being able to use other power sources if the plant is assumed to be connected to the electric grid. This is a clear advantage for RO, though, it does not represent a clear victory, as RO is heavily penalized by the increase of feedwater salinity contrary to MED. Also, the work conducted in this thesis is only focused on the physical performance of CSP and desalination plants, while the economic side of the equation was not addressed. Although the physical performance is paramount to understanding the soundness of such investments in a determined place, the economic aspects still need to be delved and added to the models used in this work, especially regarding desalination.

This case study of Trapani also showed that although CSP+RO had potential advantage using the design characteristics chosen for the simulation, the CSP+MED configuration could also perform well for the needs in the region matching the solar irradiance profile throughout the year.

Answering the research questions defined earlier in this work:

RQ1: Is it thermodynamically feasible to cogenerate water and electricity with CSP using MED and RO desalination plants?

The simulations described in section 6 indicate that solar desalination is thermodynamically feasible in locations with similar conditions as Trapani, Sicily. It is likely that many locations in the Mediterranean region would allow the same type of performances from solar desalination cogeneration systems. Although the simulations show that the plants would practically be offline between November through January, during the rest of the year they would be productive. In particular, between May and September the capacity factor would be roughly between 50% and 85%.

RQ2: Can physical, semi-empirical, or empirical models be used to support findings on this matter?

The work presented in sections 2.5, 3.1.3, 3.2.4, 3.3.6, 3.4.6 and Annex 1 shows that the outputs from these models are valid for a preliminary assessment of solar desalination investments when using CSP with MED and RO plants for the cogeneration of fresh water and electricity. The validation results for the desalination models developed and used in this work return an average deviation versus real data in the range of +/- 10%, which is in line with what is expected from models suitable for a feasibility analysis at a pre-design stage.

RQ3: Which desalination technology is better suited to work in a system powered by a specific type of CSP plant?

From the knowledge gathered through the elaboration of this work, there is no clear winner. Each combination type of solar desalination technologies has its own group of advantages and disadvantages, which are balanced. However, it is likely that in locations with lower salinities as the ones in the Pacific or Atlantic Ocean CSP+RO may have a higher advantage, especially if the option to connect the plants to a stable and robust electric grid is available. The CSP+MED combination, on the other hand, is likely to be more suitable for locations with higher salinity and worse water quality, as the ones in the Middle East, for instance. In zones like these there is ample experience operating thermal desalination systems, and plant reliability may be more valued than in other locations due to the severe impacts of having any of these desalination plants offline.

RQ4: What is the optimum configuration for a CSP+D plant scheme for a particular case-study and can that configuration be possibly used in other case studies also?

The results of the detailed simulations performed in this work for the Trapani case study in Sicily show that there is potentially an advantage of using the CSP+RO configuration as opposed to the CSP+MED option. The results indicate a performance ~15% higher with CSP+RO considering the total amount of fresh water and net electricity produced over a period of one year. However, the CSP+RO model did not take into account the power consumptions with seawater intake and minimum startup and shutdown times for the RO plant that the CSP+MED model accounted for. These would penalize the CSP+RO performance. In that case, it is likely that the results would fall into the +/- 10% deviation measured when validating the models.

8. Future Perspectives and Lines of Investigation

The work developed in this thesis was conducted in a way that it could be used as a platform from where new upgrades could be added, either by the author of this thesis or other researchers.

The next logical step will be to develop the economic model for both the MED and RO systems by adapting the CSP economic models already available in SAM and integrating them with the newly developed physical desalination models. This will allow for a comprehensive evaluation of these investments, which will also help determine the installed capacities to be used in each of the plants using the Levelized Cost Of Energy (LCOE) and the Levelized Cost Of Water (LCOW) as reference metrics. The economic structure of both types of plants can be very complex, as they normally require large investments, several stakeholders are involved, and the plants are built to operate for decades. It is common that governmental bodies are also involved in the decision making process, as these plants provide vital goods: fresh water and electricity. Long term subsidies can be involved, many times connected with the national energy and water security interests, which tend to be defined by these entities meaning that more than the straight physical and financial outputs of these projects are taken into account in the decision process.

The second next logical step regarding future work would be to perform an in-depth analysis on the usage of CSP+D with the software developed in this thesis for other locations than the one studied in this work. This will allow for a better understanding of the difference in performance for different site conditions and CSP+D configurations. This analysis would be especially interesting if applied to the Middle East or California, where these technologies currently have the highest chances of being deployed to operate in cogeneration. Gathering real data from more commercial plants is important to validate results from these models (especially from desalination plants working in a cogeneration scheme with conventional fossil fuel power plants).

Thirdly, this work was introduced into the last version of SAM using the TRNSYS solver, written in Fortran. The new versions use a new solver developed by NREL written in C language instead. In order to constantly keep the desalination models developed in this thesis up to date and allow a potential release to the public within SAM, it will be necessary to adapt the computer code written for the new add-ons to C.

Another interesting line of work would be the development of a framework for the life cycle assessment of solar desalination plants, and its coupling to the models developed in this work.

Finally, future efforts could be directed towards the development of the code in different areas such as: the optimization of the CSP and desalination plants sizing and configuration; the usage of hot water to power a MED plant instead of steam, and a hot water storage system for the MED system; the simulation of back pressure turbines for the CSP+MED system; or the simulation of the main pretreatment processes for RO systems.

References

[1] WHO/UNICEF Joint Monitoring Programme for Water Supply and Sanitation (JMP), "2014 Update: Progress on Drinking Water and Sanitation," Geneva, 2014.

[2] International Desalination Association, "IDA Desalination Yearbook 2014-2015," Media Analytics, Ltd., Oxford, 2014.

[3] Global Water Intelligence, "GWI Desalination.com," Global Water Intelligence, [Online]. Available: http://www.desalination.com/. [Acedido em 04 December 2014].

[4] Global Water Intelligence (GWI), "Desalination," *Water Desalination Report,* vol. 50, n.º 38, 13 October 2014.

[5] T. Pankratz, "Multi-State Salinity Coalition," 27 January 2012. [Online]. Available: http://multi-statesalinitycoalition.com/storage/summit/2012/presPankratz.ppt. [Acedido em 04 December 2014].

[6] German Aerospace Center (DLR), "Aqua-CSP Study Report, Concentrating Solar Power for Seawater Desalination, Final Report," German Aerospace Center (DLR), Stuttgart, 2007.

[7] B. Dunn, "Electrical Energy Storage for the Grid: A Battery of Choices," *Science,* vol. 334, pp. 928-935, 2011.

[8] European Solar Thermal Electricity Association (ESTELA), Solar Thermal Electricity Strategic Research Agenda 2020-2025, ESTELA, 2012.

[9] Intergovernamental Panel on Climate Change (IPCC), "Synthesis Report of the Fifth Assessment Report of the Intergovernmental Panel on Climate Change, Summary for Policymakers," United Nations Environment Programme (UNEP), Geneva, 2014.

[10] International Energy Agency (IEA), "World Energy Outlook 2014, Executive Summary," International Energy Agency (IEA), PAris, 2014.

[11] International Energy Agency (IEA), "Technology Roadmap, Solar Thermal Electricity, 2014 Edition," International Energy Agency (IEA), Paris, 2014.

[12] C. Sommariva, Desalination and Advanced Water Treatment - Economics and Financing, Hopkinton: Desalinations Publications, 2010.

[13] SolarPaces, "Concentrating Solar Power: Outlook 2009," SolarPaces, Tabernas, 2009.

[14] F. Trieb, “Global Potential of Concentrating Solar Power,” em *SolarPACES 2009*, Berlin, 2009.

[15] C. Vörösmarty, “Global Water Resources: Vulnerability from Climate Change and Population Growth,” *Science,* Vols. %1 de %2284-288, pp. 289-24, 2000.

[16] P. Gilman, “System Advisor Model (SAM),” National Renewable Energy Laboratory, 2 November 2013. [Online]. Available: https://sam.nrel.gov/content/sam-against-csp-plants-operation. [Acedido em 06 December 2014].

[17] C. K. Ho, “Software and Codes for Analysis of Concentrating Solar Power Technologies,” Sandia National Laboratories, Albuquerque, 2008.

[18] H. T. El-Dessouky e H. M. Ettouney, Fundamentals of Salt Water Desalination, Amesterdam: ELSEVIER SCIENCE B.V., 2002.

[19] GSE Systems, “Modeling Tools for Water Desalination,” 2014. [Online]. Available: http://www.gses.com/products/desalination. [Acedido em 09 December 2014].

[20] M. Wagner e P. Gilman, “Technical Manual for the SAM Physical Trough Model,” National Renewable Energy Laboratory, Golden, 2011.

[21] J. P. Cardoso, F. Marques e S. Casimiro, “Performance curves of Rankine cycles for solar co-generation of water and electricity (in-preparation),” *(in-preparation),* 2016.

[22] E. Mancha, “Part II. Performance Evaluation of Reverse Osmosis Membrane Computer Models,” Texas Water Development Board, Austin, 2014.

[23] D. H. Paul, How to Correct the Biggest BWRO and SWRO Problems, Version 20140115, Farmington, NM: David H. Paul, Inc., 2014.

[24] S. Casimiro, “Experimental validation of MED forward feed steady-state model,” em *2013 ISES Solar World Congress*, Cancun, 2014.

[25] S. Casimiro, “MED parallel system powered by concentrating solar power (CSP). Model and case study: Trapani, Sicily,” *Desalination and Water Treatment,* 2014.

[26] S. Casimiro, “Modeling multi effect distillation powered by CSP in TRNSYS,” em *SolarPaces2013*, Las Vegas, 2014.

[27] M. Ahmed e S. Casimiro, “Reverse Osmosis powered by Concentrating Solar Power (CSP): A case study for Trapani, Sicily,” *Desalination and Water Treatment Journal,* 2015.

[28] C. Temstet, G. Canton, J. Laborie e A. Durante, “A large high-performance MED plant in Sicily,” vol. 105, pp. 109-114, 1996.

[29] World Health Organization, “Desalination for Safe Water Supply, Guidance for the Health and Environmental Aspects Applicable to Desalination,” World Health Organization, Geneva, 2007.

[30] C. Sommariva, “Thermal Desalination Processes and Economics,” THERMAL DESALINATION PROCESSES Spring 2009. [Online]. Available: http://ocw.mit.edu/. [Acedido em 21 December 2014].

[31] A. Ophir e F. Lokiec, “Review of MED Fundamentals and Costing,” em *International Conference on Desalination Costing*, Limassol, 2004.

[32] N. Lior, “Formulas for Calculating the Approach to Equilibrium in Open Channel Flash Evaporators for Saline Water,” *Desalination,* vol. 60, pp. 223-249, 1986.

[33] U.S. Department of Energy, “Use Steam Jet Ejectors or Thermocompressors to Reduce Venting of Low-Pressure Steam,” January 2012. [Online]. Available: https://www1.eere.energy.gov/manufacturing/. [Acedido em 24 December 2014].

[34] Northeast Control Inc., “Using Jacoby Tarbox Eductors for Pumping Gases,” Northeast Control Inc., New Jersey, 2010.

[35] H. Shemer, “Sliding pressure turbine integrated with seawater desalination facility (multi-effect distillation - MED),” em *IDA World Congress*, Perth, 2011.

[36] A. Amer, “Development and optimization of ME-TVC desalination system,” *Desalination,* pp. 1315-1331, 2009.

[37] C. Mineo, “A General Overview of the Trapani's Desalination Plant,” Trapani, 2013.

[38] German Aerospace Center (DLR), “Concentrating Solar Power for Seawater Desalination, Final Report,” German Aerospace Center (DLR), Stuttgart , 2007.

[39] Dow Chemical Campany, “FILMTEC Reverse Osmosis Membranes,” Dow Chemical Campany, 2014.

[40] United Nations Environment Programme (UNEP), “Resource and Guidnace Manual for Environmental Impact Assessments,” United Nations Environment Programme (UNEP), Nairobi, 2008.

[41] SolarPaces, “SolarPaces,” 2014. [Online]. Available: www.solarpaces.org. [Acedido em 2014].

[42] H. Rahman, “Historical development of concentrating solar power technologies to generate clean electricity efficiently – A review,” *Renewableand Sustainable Energy Reviews,* vol. 41, pp. 996-1027, 2015.

[43] C. Villada, “Thermal evaluation of molten salts for solar thermal energy storage,” *Renewable Energy and Power Quality Journal,* 2104.

[44] N. Siegel e R. Bradshaw, “Molten Nitrate Salt Development for Thermal Energy Storage in Parabolic Trough Solar Power Systems,” em *Proceeding of ES2008, Energy Sustainability 2008*, Jacksonville, 2008.

[45] C. Kutscher e C. Turchi, “Water Use in Parabolic Trough Power Plants: Summary Results from WorleyParsons' Analyses,” National Renewable Energy Laboratory, Golden, 2010.

[46] D. Consoli, “Impianto Solare Termodinamico Archimede,” ENEL Ingegneria e Innovazione Spa - A.T. Ricerca, Priolo, 2010.

[47] National Renewable Energy Laboratory, “Concentrating Solar Power Projects by Technology,” National Renewable Energy Laboratory, 2014. [Online]. Available: www.nrel.gov/csp/solarpaces/by_technology.cfm. [Acedido em 13 December 2014].

[48] C. Turchi, “Estimating the Performance and Economic Value of Multiple Concentrating Solar Power Technologies in a Production Cost Model,” National Renewable Energy Laboratory, Golden, 2013.

[49] J. Duffie e W. Beckman, Solar Engineering of Thermal Processes, 4h Edition, New York: Wiley , 2013.

[50] K. Lovegrove e W. Stein, Concentrating Solar Power Technology: Principles, Developments and Applications, Oxford: Woodhead Publishing, 2012.

[51] International Renewable Energy Agency, “Concentrating Solar Power - Technology Brief,” IRENA, Abu Dhabi, 2013.

[52] S. Kuravi e Y. Goswami, “Thermal energy storage technologies and systems for concentrating solar power plants,” *Progress in Energy and Combustion Science,* n.º 39, pp. 285-319, 2013.

[53] D. Canavarro e M. Collares-Pereira, “Increasing the eficiency of conventional LFR technologies: a new CLFR “Etendue Matched” CSP collector,” em *17th International SolarPaces Symposium*, Granada, 2011.

[54] “Novatec Solar,” [Online]. Available: http://www.novatecsolar.com/. [Acedido em November 2015].

[55] D. Canavarro e M. Collares-Pereira, “Simultaneous Multiple Surface method for Linear Fresnel concentrators with tubular receiver.,” *Solar Energy,* vol.

110, pp. 105-116, 2014.

[56] L. Guerreiro e M. Collares-Pereira, "Efficiency improvement and potential LCOE reduction with an LFR-XX SMS plant with storage," em *International Conference on Concentrating Solar Power and Chemical Energy Systems, SolarPACES 2014*, Cape Town, 2015.

[57] R. Wilde, "Case study of a Concentrating Solar Power Plant for the Cogeneration of Water and Electricity," RWTH Aachen, Aachen, 2005.

[58] C. Burgess e K. Lovegrove , "Solar thermal powered desalination: membrane versus distillation," em *43rd Annual Conference of the Australian and New Zealand Solar Energy Society*, Dunedin, 2005.

[59] J. Blanco, "Advanced Solar Desalination: A Feasible Technology to the Mediterranean Area," em *EuroSun 2002*, Bologna, 2002.

[60] L. Roca, "Control and Modeling of Seawater Desalination Using Solar Technology," em *SolarPaces*, Seville, 2006.

[61] International Atomic Energy Agency (IAEA), Desalination Economic Evaluation Program (DEEP-3.0), Vienna: International Atomic Energy Agency (IAEA), 2006.

[62] A. Nafey e L. Garcia-Rodriguez, "A new visual library for design and simulation of solar desalination systems (SDS)," *Desalination,* vol. 259, n.º 1-3, pp. 197-207, 2010.

[63] U. B. o. R. (USBR), "2008 WT Cost II Modeling the Capital and Operating Costs of Thermal Desalination Processes (USBR)," US Bureau of Reclamation (USBR), Denver, 2008.

[64] SimTech, "SimTech," 2014. [Online]. Available: http://www.simtechnology.com. [Acedido em 21 December 2014].

[65] GSE Systems, "GSE Systems," 2014. [Online]. Available: http://www.gses.com. [Acedido em 21 December 2014].

[66] N. Aly e M. Marwan, "Dynamic response of multi-effect evaporators," *Desalination,* vol. 114, pp. 189-196, 1997.

[67] K. Mistry e J. Lienhard V, "An improved model for multiple effect distillation," *Desalination and Water Treatment,* pp. 807-821, 2013.

[68] A. Calle e P. Palenzuela, "Dynamic modeling and simulation of a solar-assisted multi-effect distillation plant," *Desalination,* vol. 357, pp. 65-76, 2015.

[69] A. Calle e P. Palenzuela, "Dynamic modeling and performance of the first cell of a multi-effect distillation plant," *Applied Thermal Engineering,* vol.

70, pp. 410-420, 2014.

[70] M. Shapiro, Fundamentals of Engineering Thermodynamics, 5th Edition, Danvers: John Willey and Sons, 2004.

[71] F. Incropera, Introduction to Heat Transfer, 5th Edition, John Wiley and Sons, 2004.

[72] E. Saunders, Heat Exchangers, Selection, Design and Construction, Harlow: Longman Group, 1988.

[73] H. Ettouney e H. El-Dessouky, "Steady-State Analysis of the Multiple Effect Evaporation Desalination Process," *Chemical Engineering and Technology,* vol. 21, n.º 5, 1998.

[74] S. Bingulac e H. El-Dessouky, "Solving equations simulating the steady-state behavior of the multi-stage flash desalination process," *Desalination,* vol. 107, pp. 171-193, 1996.

[75] S. Vanini e R. Kamali, "A simulation model and parametric study of MED–TVC process," *Desalination,* vol. 235, pp. 340-351, 2009.

[76] A. Mitsos e T. Dahdah, "Structural optimization of seawater desalination - A Flexible superstructure and novel MED configurations," *Desalination,* vol. 344, pp. 252-265, 2014.

[77] A. Nashar e A. Qamhiyeh, "Simulation of the steady-state operation of a multi-effect stack seawater distillation plant," *Desalination,* vol. 101, pp. 2231-243, 1995.

[78] L. Bromley e S. Read, "Multiple Effect Flash (MEF) Evaporator," *Desalination,* vol. 7, pp. 343-391, 1970.

[79] "Steady state model for multi-effect distillation case study: Plataforma Solar de Almeria MED pilot plant," *Desalination,* vol. 337, pp. 31-42, 2014.

[80] P. Palenzuela e D. Padilla, "Parametric equations for the variables of a steady-State model of a multi-effect desalination plant," *Desalination,* pp. 1-13, 2012.

[81] N. Aly e M. Shamloul, "Modelling and simulation of steam jet ejectors," *Desalination,* vol. 123, pp. 1-8, 1999.

[82] H. El-Dessouky, H. Ettouney e G. Al-Nuwaibit, "Evaluation of steam jet ejectors," *Chemical Engineering and Processing,* vol. 41, pp. 551-561, 2002.

[83] R. B. Power, Steam jet ejectors for the process industries, New York: McGraw-Hill, 1994.

[84] WRA, “WRA,” 2014. [Online]. Available: http://www.wraengineering.com/. [Acedido em 21 December 2014].

[85] S. Mason, “World Wide Overview of Concentrating Solar Thermal Simulation Tools,” em *Solar2011, the 49th AuSES Annual Conference*, Sidney, 2011.

[86] N. Blair, “Sensitivity of Concentrating Solar Power Trough Performance Cost and Financing with the Solar Advisor Model,” National Renewable Energy Laboratory, Golden, 2008.

[87] Thermal Energy Systems Specialists, “Getting Started,” em *TRNSYS 16, a TRaNsient SYstem Simulation program - User Manual*, vol. 1, Madison, Thermal Energy Systems Specialists, 2007, pp. 1-87.

[88] P. Schwarzbozl, “A TRNSYS Model Library for Solar Thermal Electric Components (STEC) - Reference Manual, Release 3.0,” SolarPaces, Cologne, 2006.

[89] P. Palenzuela, “Modeling of the heat transfer of a solar multi-effect distillation plant at the Plataforma Solar de Almería,” *Desalination and Water Treatment,* 2011.

[90] H. El-Dessouky, “Modeling and simulation of thermal vapor compression desalination plant,” em *Symposium on Desalination of Seawater with Nuclear Energy*, Taejon, 1997.

[91] H. El-Dessouky e H. Ettouney, “Steam jet ejectors: Modeling and analysis,” *Chemical Engineering and Processing,* 2001.

[92] L. Rizzuti e A. Cipollina, “Investigation of flashing phenomena in MSF chambers,” *Desalination,* vol. 216, pp. 183-195, 2005.

[93] C. Mineo, “A brief description of the Trapani desalination plant,” Siciliacque, Trapani, 2015.

[94] C. Mineo, “A practical experience on a large seawater multi-effect distillation plant in southern Italy,” *Desalination and water treatment,* 2015.

[95] A. Cipollina e L. Rizzuti, “A critical assessment for desalination operations in Siciliy,” *Desalination,* vol. 182, pp. 1-12, 2005.

[96] Spirax-Sarco, “Basic Desuperheating Theory,” Spirax-Sarco, [Online]. Available: http://www.spiraxsarco.com/resources/steam-engineering-tutorials/desuperheating/basic-desuperheating-theory.asp. [Acedido em 2014 07 2014].

[97] Heat Exchange Institute, Inc., Standards for Steam Jet Vacuum Systems,

Fith Edition, Cleaveland, Ohio: Heat Exchange Institute, Inc., 2000.

[98] Northeast Controls, Inc., "Using jerguson®jacoby-tarbox® eductors for pumping gases," Northeast Controls Inc., STRONGSVILLE, 1993.

[99] Tyco Valves & Controls / Penberthy, "Jet pump technical data, pumping gases," Pentair Valves & Control, Prophetstown, 1987.

[100] B. Massey, Mechanics of Fluids, 8th Edition, London: Taylor & Francis, 1998.

[101] M. Wagner, Simulation and Predictive Performance Modeling of Utility-Scale Central Receiver System Power Plants, Master Thesis, Madison, Wisconsin: University of Wisconsin, 2008.

[102] "Elevation finder," [Online]. Available: http://www.freemaptools.com/elevation-finder.htm. [Acedido em 2015].

[103] American Water Works Association (AWWA), "Addendum to AWWA Manual M45, Fiberglass Pipe Design," *Journal - American Water Works Association,* p. 30, 2007.

[104] Norsok, "Standard P-001 - Process design," Norsok, Lysaker, 2006.

[105] Satel-light, "The European Database of Daylight and Solar Radiation," 2014. [Online]. Available: http://www.satel-light.com/core.htm. [Acedido em 11 April 2014].

[106] Meteonorm, "TMY2 weather file for the location of Trapani, Sicily, Meteonorm Database 5.1".

[107] J. Maulbetsch e M. DiFilippo, "Performance, cost, and environmental effects of saltwater cooling towers," 2008.

[108] A. Delgado-Torres, "Preliminary design of a solar-thermal powered reverse osmosis system," *Desalination,* pp. 292-205, 2007.

[109] World Health Organization, "Guidelines for Drinking-Water Quality - 4th ed.," WHO, Geneva, 2011.

[110] M. Romero, "Advances in CSP technology: towards the next generation," Institute IMDEA Energy, Tunis, 2012.

[111] R. Pitz-Paal, "Parabolic Trough, Linear Fresnel, Power Tower: A Technology Comparison," 2012. [Online]. Available: http://www.iass-potsdam.de/sites/default/files/files/12.5-iass_pitz-paal.pdf. [Acedido em 14 December 2014].

[112] Y. Zhu e Y. Li, "Fuel ejector design and simulation model for anodic recirculation SOFC system," *Journal of Power Sources,* vol. 173, pp. 437-

449, 2007.

[113] A. Massardo e F. Marsano, “Ejector performance influence on a solid oxide fuel cell anodic recirculation system,” *Journal of Power Sources,* vol. 129, pp. 216-228, 2004.

[114] A. Altaee, “Computational model for estimating reverse osmosis system design and performance - Part one binary feed solution,” *Desalination,* vol. 291, pp. 101-105, 2012.

[115] M. Wilf, The Guidebook to Membrane Desalination Technology : Reverse Osmosis, Nanofiltration and Hybrid Systems Process, Design, Applications and Economics, Balaban Desalination Publications, 2007.

[116] A. Gambier, “Dynamic Modeling of a Simple Reverse Osmosis Desalination Plant for Advanced Control Purposes,” em *2007 American Control Conference*, New York, 2007.

Annex 1 – Diagram: MED Detailed Model

Table 31 - List of main inputs into the MED Detailed model

Parameter/Variable	Units	Description
n	-	Number of Effects
CT	-	Flag indicating the Cooling technology used with the Rankine cycle: 7) MED-Parallel Low temp ; 8) MED-Parallel TVC; 9) MED-FF Low temp; 10) MED-FF TVC
TVC_Strategy	-	Flag indicating how the TVC is to be dimensioned considering the compression ratio or a fixed Ts_sat input (it will force a specific Pc and a compression ratio)). Values: 1 - TVC uses the lowest possible commpression ratio; 2 - Ts_sat is a user defined (defines the saturated pressure leaving the TVC and compression ratio); 3 - TVC uses the highest possible compression ratio.
d_Cross_flow_flag	-	Flag indicating the existance of CROSS-FLOW for the distillate routing. If the configuration is set to have the distillate: 1) flowing between effects (and so flashing when entering the distillate boxes, representing CROSS-FLOW configuration); 0) if it is routed directly into a collecting pipe, and sent for storage (this in practice represents a Parallel configuration without a CROSS-FLOW).
eph_flag	-	Flag indicating if the plant has feedwater preheaters, and if so, if they are placed between every effect or between every 2 effects. 0) there are NO preheaters; 1) preheaters beetween every effect (with NCG ejectors); 2) preheaters between every 2 effects (with NCG ejectors); 3) preheaters beetween every effect (>> without << NCG ejectors); 4) preheaters between every 2 effects (>> without << NCG ejectors). It is always assumed in both configurations 1) and 2) that: A) there are no preheaters beetween effects that receive feedwater preheated by the NCG ejectors system intercondensers, and B) that the effect just after the 1st NCG intercondenser will have no preheater also.
n_ph_NCG	-	Number of >> the effect << from where it is assumed that the external preheating of the feedwater will be suported by NCG steam extraction. The rest of the code will adapt automatically.
pre_PlateHTX_flag	-	Flag indicating if the plate heat exchanger preheaters of the feedwater entering the down condenser are present or not. 0 - The Plate Heat Exchangers are NOT present; 1 - The Plate Heat Exchangers ARE present.
Mm	kg/s	Mass flow of steam powering the MED plant, >> Except << steam used for NCG steam ejectors (entering the TVC if one exists, or entering directly the 1st effect if not TVC is present).
Q_Loss	-	Fraction of the thermal losses incurred in average in each effect (compared to the calculated heat load that each effect would receive)
Ts_sat	ºC	Temperature of Saturated Steam from the turbine (if no TVC) or from the TVC discharge.
Tv1	ºC	Vapor temperature in the first effect (input cannot be an array)
Tvn	ºC	Temperature of Vapor in the last effect (input cannot be an array)
Tf_dc_out	ºC	Temperature of Feedwater leaving the down condenser.
pre_Tsw_out	ºC	Temperature of the seawater leaving the plate heat exchangers
Tsw	ºC	Temperature of Seawater
Tv_Loss	ºC	Average temperature Loss with pressure losses assumed to occur when the vapour formed inside each effects flows into the HTX tubes of the next effect until it reaches the distillate box of the next effect (heat transfer inside each effect assumed to be at Tv - Tv_Loss).
Xsw	wt%	Salinity concentration of the seawater entering the MED plant
Xb1	wt%	Salinity concentration predefined to be assumed when starting iterations to calculate mass flow rate of feedwater needed for the 1st effect (input cannot be an array)
Xbn_max	wt%	Maximum allowed Salinity concentration of the brine produced in the last effect

Table 32 - List of main outputs from the MED Detailed model

Parameter/Variable	Units	Description
B	kg/s	Total Mass flow of Brine inside EACH effect (sum of the produced brine + the brine entering from the previous effects - the mass of brine that originated vapor by flashing when the brine enters each effect)
B(n)	kg/s	Total Mass flow of Brine inside EACH effect (sum of the produced brine + the brine entering from the previous effects - the mass of brine that originated vapor by flashing when the brine enters each effect)
B_b_flash_remain	kg/s	Mass flow of Brine flowing into the NEXT effect that REMAINS after part of it flashed due to the pressure difference.
B_evap	kg/s	Mass flow of Brine produced inside each effect as a result of the evaporation process (not the flashing)
D	kg/s	Total Mass flow of Distillate produced PER effect
D_Total	kg/s	Total Mass flow of Distillate produced in the System (sum of D produced in all effects)
Delta_H_iph	kJ/kg	Difference between the Specific enthalpy of the Brine and Feedwater in each effect.
Delta_H_iph	kJ/kg	Difference between the Specific enthalpy of the Brine and Feedwater in each effect.
Delta_T_b_NEA	ºC	Non Equilibrium Allowance between the hotter brine (and not the feedwater) entering each effect and the colder brine after flashing.
F	kg/s	Mass flow of Feedwater entering each effect
F_flash_remain	kg/s	Mass flow of feedwater that remains after it flashed when it entered each effect (this variable is actually only used when MED-FF, as feedwater is actually the brine from the last effect; and when MED-P this variable has a value of zero).
F_Total	kg/s	Total mass flow of feedwater used at the MED plant
Hb_b_flash_remain	kJ/kg	Specific Enthalpy of the brine entering each effect AFTER part of it has flashed
Hb_Tb	kJ/kg	Specific Enthalpy of the Brine formed by evaporation inside each effect
Hb_Tb	kJ/kg	Specific Enthalpy of the Brine formed by evaporation inside each effect
Hb_Tb_out	kJ/kg	Specific Enthalpy of the brine leaving each effect (it is a mixture of the brine from the previous effect plus the brine formed in the current effect)
Hf_Tf	kJ/kg	Specific Enthalpy of the Feedwater entering each effect
LHv_b_flash	kJ/kg	Latent Heat of the vapor formed by the brine flashing when entering each effect
n	-	Number of Effects (-)
PR	-	Performance Ratio of the MED plant
Q	kW	Thermal Load in each effect
Q	kW	Thermal Load in each effect
Q_iph	kW	Thermal Load used in each effect o preheat the feedwater entering each effect
Q_iph_total	kW	Sum of all Thermal Load used in each effect o preheat the feedwater entering each effect
Qv	kW	Total sum of the heat load of vapor formed inside each effect
Qv_b_flash	kW	Thermal Load released from the flashing occuring when brine moves from effect to effect (temperature before and after flash are due to the NEA).
Qv_b_flash	kW	Thermal Load released from the flashing occuring when brine moves from effect to effect (temperature before and after flash are due to the NEA).
Qv_evap	kW	Heat load of vapor formed inside each effect by evaporation process alone
Qv_evap_remain	kW	Heat load of vapor formed inside each effect by evaporation process only, that actually is used to power the next effect. It is the remain of the Qv_evap after Q_eph is deducted.

Qv_f_flash	kW	Heat load of vapor formed when the feedwater enters each effect (when MED-P) this variable will be equal to zero, as only preheated seawater enters the effect, but when MED-FF Qv_f_flash will be higher than zero because what is sprayed on the top of the tube bundle is brine from the last effect.
Qv_remain_out	kW	Total sum of the heat load of vapor transfered into the next effect condensed at "Tv_out" (it assumed therefore the temperature of vapor after energy losses have occured).
Rank_Md_return	kg/s	Mass of distillate returning from the MED plant into the Rankine cycle (that compensate the input of motive steam)
S	grams	Mass of salt contained in the brine produced by evaporation in each effect
S_out	grams	Mass of Salt in the brine output leaving each effect (sum of the salt in the brine formed in the current effect by evaporation + salt of the brine from the previous effects that enters the current effect)
Tb_b_flash	ºC	Final temperature of the brine (and not the feedwater) after flashing inside the effect when passing from effect i-1 to effect i. Temperature difference between Tb(i) and Tb_b_flash(i) is due to the Non Equilibrium Allowance.
Tb_out	ºC	Temperature of the brine leaving each effect (it will be a balance between accounting the Temperature and mass of the brine formed by evaporation and the brine remaining after flashing (that came from the previous effect).
Td_out	ºC	Final temperature of the Distillate leaving each distillate box from each effect.
Td_out	ºC	Final temperature of the Distillate leaving each distillate box from each effect.
Tf	ºC	Temperature of Feedwater entering each effect
Tf_eph	ºC	Temperature of Feedwater leavig each feedwater preheater
Ts_sat	ºC	Temperature of Saturated Steam from the turbine (if no TVC) or from the TVC discharge.
Tv	ºC	Temperature of vapor formed inside each effect
Tv_b_flash	ºC	Temperature of vapor produced with the flashing of brine at each effect
V	kg/s	Total Mass of Vapour produced inside the effect. Evaporation + flashing of distillate and brine from previous effect + flashing of condensate from preheater from previous effect
V_b_flash	kg/s	Mass flow of Vapour produced inside the effect from the flashing process ocurring when the brine enters it.
V_evap	kg/s	Mass flow of Vapor produced by evaporation (not flashing) inside the effect.
V_f_flash	kg/s	Mass flow of Vapor produced by flash when the feedwater enters each effect (this variable is actually only used when MED-FF as feedwater is actually the brine from the last effect; and when MED-P this variable has a value of zero).
Xb	wt%	Salinity concentration of the brine produced in each effect by evaporation
Xb_out	wt%	Salinity concentration of the brine leaving each effect (balance between salinity of brine formed by evaporation in the current effect and brine from the previous effects)
Xf	wt%	Salinity concentration of the feedwater entering each effect
Xf_f_flash_remain	wt%	Salinity concentration of the feedwater that remains after it flashes when entering the effect (this variable is actually only used when MED-FF as feedwater is actually the brine from the last effect; and when MED-P this variable has a value of zero).

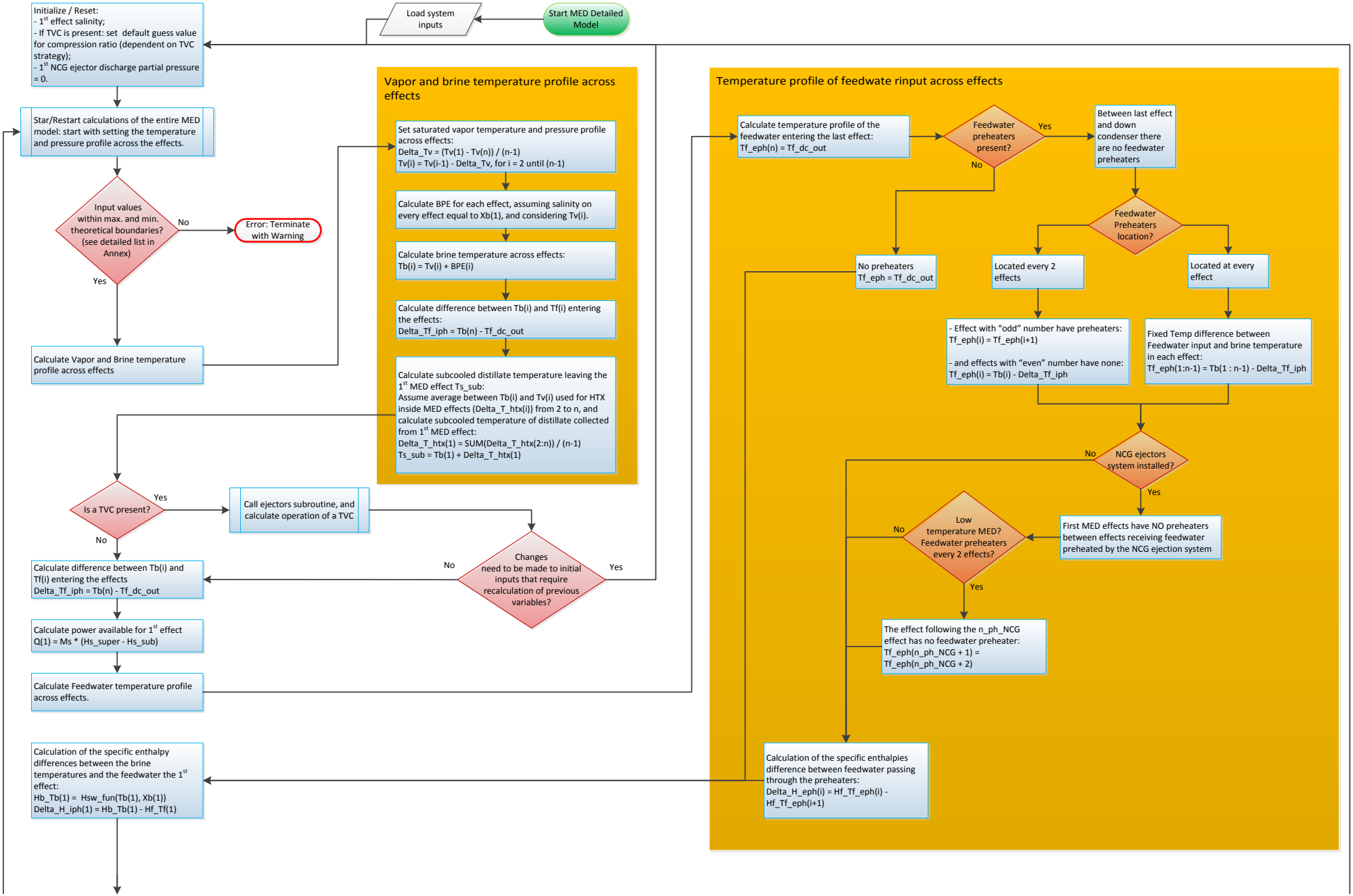
Start MED Detailed Model
Load system inputs
Initialize / Reset:
- 1st effect salinity;
- If TVC is present: set default guess value for compression ratio (dependent on TVC strategy);
- 1st NCG ejector discharge partial pressure = 0.
Star/Restart calculations of the entire MED model: start with setting the temperature and pressure profile across the effects.
Input values within max. and min. theoretical boundaries? (see detailed list in Annex)
No
Error: Terminate with Warning
Yes
Calculate Vapor and Brine temperature profile across effects
Vapor and brine temperature profile across effects
Set saturated vapor temperature and pressure profile across effects:
Delta_Tv = (Tv(1) - Tv(n)) / (n-1)
Tv(i) = Tv(i-1) - Delta_Tv, for i = 2 until (n-1)
Calculate BPE for each effect, assuming salinity on every effect equal to Xb(1), and considering Tv(i).
Calculate brine temperature across effects:
Tb(i) = Tv(i) + BPE(i)
Calculate difference between Tb(i) and Tf(i) entering the effects:
Delta_Tf_iph = Tb(n) - Tf_dc_out
Calculate subcooled distillate temperature leaving the 1st MED effect Ts_sub:
Assume average between Tb(i) and Tv(i) used for HTX inside MED effects (Delta_T_htx(i)) from 2 to n, and calculate subcooled temperature of distillate collected from 1st MED effect:
Delta_T_htx(1) = SUM(Delta_T_htx(2:n)) / (n-1)
Ts_sub = Tb(1) + Delta_T_htx(1)
Is a TVC present?
Yes
No
Call ejectors subroutine, and calculate operation of a TVC
Calculate difference between Tb(i) and Tf(i) entering the effects
Delta_Tf_iph = Tb(n) - Tf_dc_out
Changes need to be made to initial inputs that require recalculation of previous variables?
No
Yes
Calculate power available for 1st effect
Q(1) = Ms * (Hs_super - Hs_sub)
Calculate Feedwater temperature profile across effects.
Temperature profile of feedwate rinput across effects
Calculate temperature profile of the feedwater entering the last effect:
Tf_eph(n) = Tf_dc_out
Feedwater preheaters present?
Yes
No
Between last effect and down condenser there are no feedwater preheaters
Feedwater Preheaters location?
No preheaters
Tf_eph = Tf_dc_out
Located every 2 effects
Located at every effect
- Effect with “odd” number have preheaters:
Tf_eph(i) = Tf_eph(i+1)
- and effects with “even” number have none:
Tf_eph(i) = Tb(i) - Delta_Tf_iph
Fixed Temp difference between Feedwater input and brine temperature in each effect:
Tf_eph(1:n-1) = Tb(1 : n-1) - Delta_Tf_iph
NCG ejectors system installed?
No
Yes
Low temperature MED? Feedwater preheaters every 2 effects?
No
Yes
First MED effects have NO preheaters between effects receiving feedwater preheated by the NCG ejection system
The effect following the n_ph_NCG effect has no feedwater preheater:
Tf_eph(n_ph_NCG + 1) =
Tf_eph(n_ph_NCG + 2)
Calculation of the specific enthalpies difference between feedwater passing through the preheaters:
Delta_H_eph(i) = Hf_Tf_eph(i) - Hf_Tf_eph(i+1)
Calculation of the specific enthalpy differences between the brine temperatures and the feedwater the 1st effect:
Hb_Tb(1) = Hsw_fun(Tb(1), Xb(1))
Delta_H_iph(1) = Hb_Tb(1) - Hf_Tf(1)

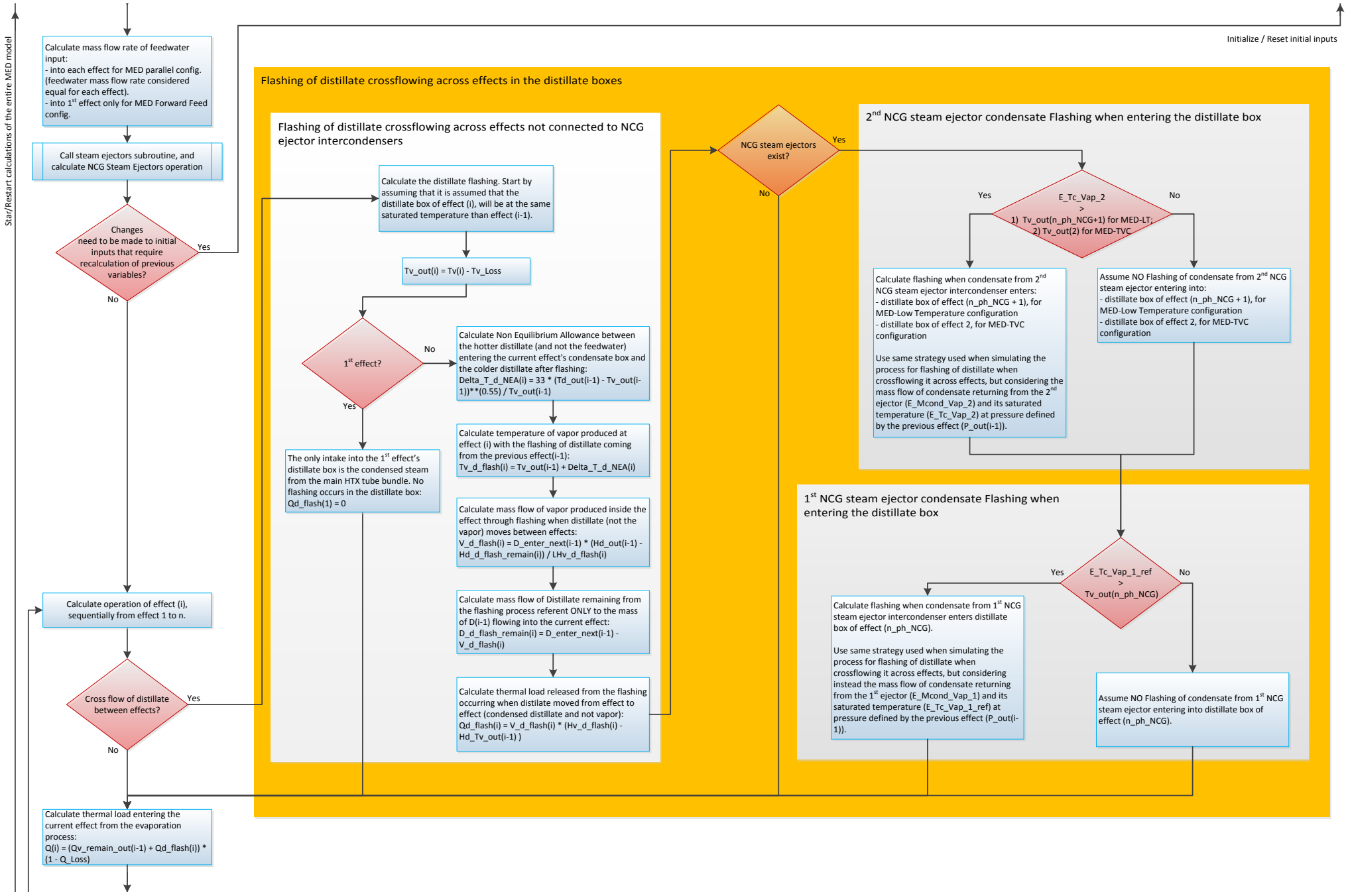
Star/Restart calculations of the entire MED model
Calculate mass flow rate of feedwater input:
- into each effect for MED parallel config. (feedwater mass flow rate considered equal for each effect).
- into 1st effect only for MED Forward Feed config.
Call steam ejectors subroutine, and calculate NCG Steam Ejectors operation
Changes need to be made to initial inputs that require recalculation of previous variables?
Yes
No
Initialize / Reset initial inputs
Calculate operation of effect (i), sequentially from effect 1 to n.
Cross flow of distillate between effects?
Yes
No
Calculate thermal load entering the current effect from the evaporation process:
Q(i) = (Qv_remain_out(i-1) + Qd_flash(i)) * (1 - Q_Loss)
Flashing of distillate crossflowing across effects in the distillate boxes
Flashing of distillate crossflowing across effects not connected to NCG ejector intercondensers
Calculate the distillate flashing. Start by assuming that it is assumed that the distillate box of effect (i), will be at the same saturated temperature than effect (i-1).
Tv_out(i) = Tv(i) - Tv_Loss
1st effect?
No
Yes
Calculate Non Equilibrium Allowance between the hotter distillate (and not the feedwater) entering the current effect's condensate box and the colder distillate after flashing:
Delta_T_d_NEA(i) = 33 * (Td_out(i-1) - Tv_out(i-1))**(0.55) / Tv_out(i-1)
The only intake into the 1st effect's distillate box is the condensed steam from the main HTX tube bundle. No flashing occurs in the distillate box:
Qd_flash(1) = 0
Calculate temperature of vapor produced at effect (i) with the flashing of distillate coming from the previous effect(i-1):
Tv_d_flash(i) = Tv_out(i-1) + Delta_T_d_NEA(i)
Calculate mass flow of vapor produced inside the effect through flashing when distillate (not the vapor) moves between effects:
V_d_flash(i) = D_enter_next(i-1) * (Hd_out(i-1) - Hd_d_flash_remain(i)) / LHv_d_flash(i)
Calculate mass flow of Distillate remaining from the flashing process referent ONLY to the mass of D(i-1) flowing into the current effect:
D_d_flash_remain(i) = D_enter_next(i-1) - V_d_flash(i)
Calculate thermal load released from the flashing occurring when distilate moved from effect to effect (condensed distillate and not vapor):
Qd_flash(i) = V_d_flash(i) * (Hv_d_flash(i) - Hd_Tv_out(i-1))
NCG steam ejectors exist?
Yes
No
2nd NCG steam ejector condensate Flashing when entering the distillate box
E_Tc_Vap_2 > 1) Tv_out(n_ph_NCG+1) for MED-LT; 2) Tv_out(2) for MED-TVC
Yes
No
Calculate flashing when condensate from 2nd NCG steam ejector intercondenser enters:
- distillate box of effect (n_ph_NCG + 1), for MED-Low Temperature configuration
- distillate box of effect 2, for MED-TVC configuration
Use same strategy used when simulating the process for flashing of distillate when crossflowing it across effects, but considering the mass flow of condensate returning from the 2nd ejector (E_Mcond_Vap_2) and its saturated temperature (E_Tc_Vap_2) at pressure defined by the previous effect (P_out(i-1)).
Assume NO Flashing of condensate from 2nd NCG steam ejector entering into:
- distillate box of effect (n_ph_NCG + 1), for MED-Low Temperature configuration
- distillate box of effect 2, for MED-TVC configuration
1st NCG steam ejector condensate Flashing when entering the distillate box
E_Tc_Vap_1_ref > Tv_out(n_ph_NCG)
Yes
No
Calculate flashing when condensate from 1st NCG steam ejector intercondenser enters distillate box of effect (n_ph_NCG).
Use same strategy used when simulating the process for flashing of distillate when crossflowing it across effects, but considering instead the mass flow of condensate returning from the 1st ejector (E_Mcond_Vap_1) and its saturated temperature (E_Tc_Vap_1_ref) at pressure defined by the previous effect (P_out(i-1)).
Assume NO Flashing of condensate from 1st NCG steam ejector entering into distillate box of effect (n_ph_NCG).

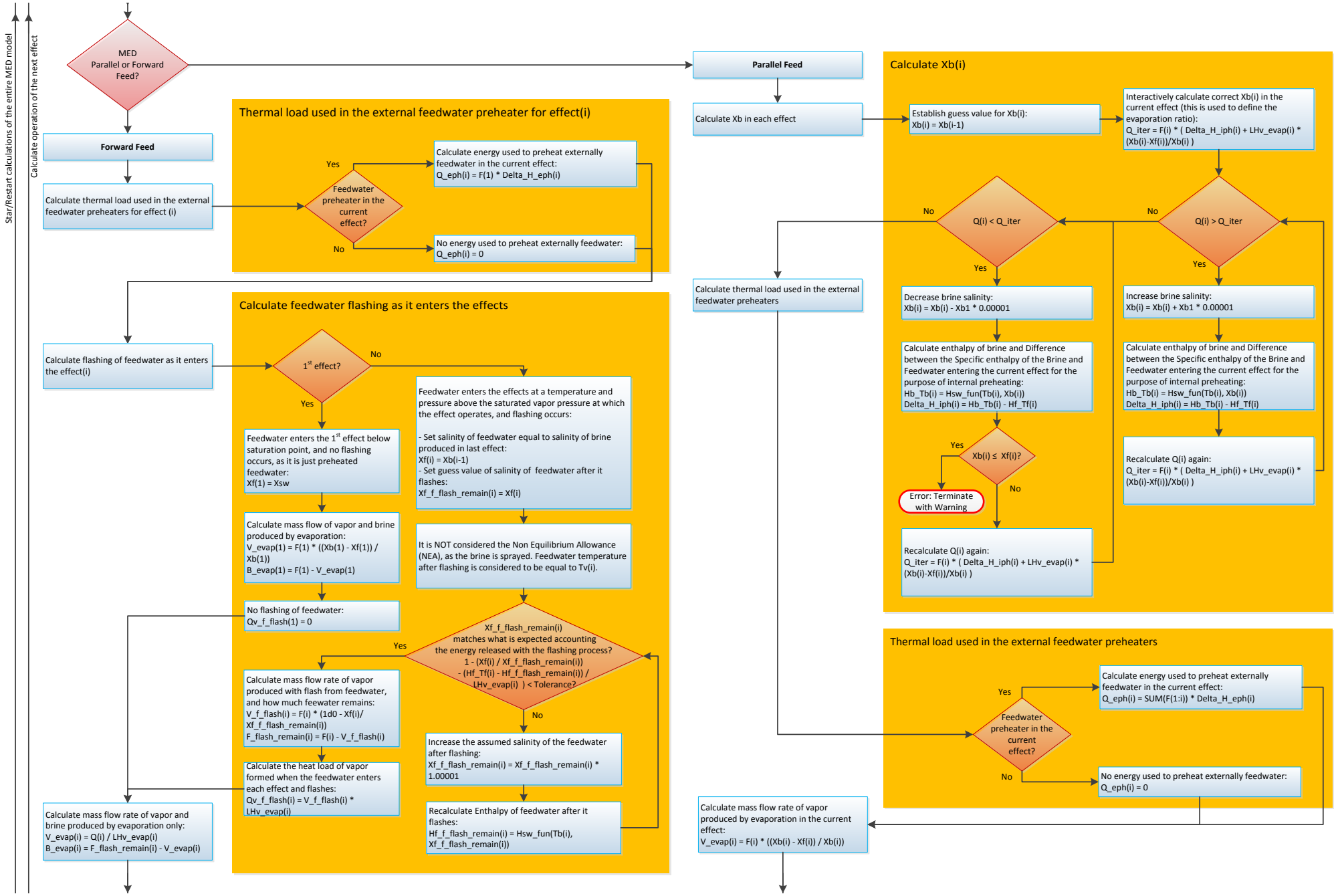
Star/Restart calculations of the entire MED model
Calculate operation of the next effect
MED Parallel or Forward Feed?
Forward Feed
Calculate thermal load used in the external feedwater preheaters for effect (i)
Thermal load used in the external feedwater preheater for effect(i)
Feedwater preheater in the current effect?
Yes
No
Calculate energy used to preheat externally feedwater in the current effect:
Q_eph(i) = F(1) * Delta_H_eph(i)
No energy used to preheat externally feedwater:
Q_eph(i) = 0
Calculate flashing of feedwater as it enters the effect(i)
Calculate feedwater flashing as it enters the effects
1st effect?
Feedwater enters the 1st effect below saturation point, and no flashing occurs, as it is just preheated feedwater:
Xf(1) = Xsw
Feedwater enters the effects at a temperature and pressure above the saturated vapor pressure at which the effect operates, and flashing occurs:
- Set salinity of feedwater equal to salinity of brine produced in last effect:
Xf(i) = Xb(i-1)
- Set guess value of salinity of feedwater after it flashes:
Xf_f_flash_remain(i) = Xf(i)
Calculate mass flow of vapor and brine produced by evaporation:
V_evap(1) = F(1) * ((Xb(1) - Xf(1)) / Xb(1))
B_evap(1) = F(1) - V_evap(1)
It is NOT considered the Non Equilibrium Allowance (NEA), as the brine is sprayed. Feedwater temperature after flashing is considered to be equal to Tv(i).
No flashing of feedwater:
Qv_f_flash(1) = 0
Xf_f_flash_remain(i) matches what is expected accounting the energy released with the flashing process?
1 - (Xf(i) / Xf_f_flash_remain(i)) - (Hf_Tf(i) - Hf_f_flash_remain(i)) / LHv_evap(i)) < Tolerance?
Calculate mass flow rate of vapor produced with flash from feedwater, and how much feewater remains:
V_f_flash(i) = F(i) * (1d0 - Xf(i)/Xf_f_flash_remain(i))
F_flash_remain(i) = F(i) - V_f_flash(i)
Increase the assumed salinity of the feedwater after flashing:
Xf_f_flash_remain(i) = Xf_f_flash_remain(i) * 1.00001
Calculate the heat load of vapor formed when the feedwater enters each effect and flashes:
Qv_f_flash(i) = V_f_flash(i) * LHv_evap(i)
Recalculate Enthalpy of feedwater after it flashes:
Hf_f_flash_remain(i) = Hsw_fun(Tb(i), Xf_f_flash_remain(i))
Calculate mass flow rate of vapor and brine produced by evaporation only:
V_evap(i) = Q(i) / LHv_evap(i)
B_evap(i) = F_flash_remain(i) - V_evap(i)
Parallel Feed
Calculate Xb in each effect
Calculate thermal load used in the external feedwater preheaters
Calculate Xb(i)
Establish guess value for Xb(i):
Xb(i) = Xb(i-1)
Interactively calculate correct Xb(i) in the current effect (this is used to define the evaporation ratio):
Q_iter = F(i) * (Delta_H_iph(i) + LHv_evap(i) * (Xb(i)-Xf(i))/Xb(i))
Q(i) < Q_iter
Q(i) > Q_iter
No
Yes
Decrease brine salinity:
Xb(i) = Xb(i) - Xb1 * 0.00001
Increase brine salinity:
Xb(i) = Xb(i) + Xb1 * 0.00001
Calculate enthalpy of brine and Difference between the Specific enthalpy of the Brine and Feedwater entering the current effect for the purpose of internal preheating:
Hb_Tb(i) = Hsw_fun(Tb(i), Xb(i))
Delta_H_iph(i) = Hb_Tb(i) - Hf_Tf(i)
Xb(i) ≤ Xf(i)?
Error: Terminate with Warning
Recalculate Q(i) again:
Q_iter = F(i) * (Delta_H_iph(i) + LHv_evap(i) * (Xb(i)-Xf(i))/Xb(i))
Thermal load used in the external feedwater preheaters
Feedwater preheater in the current effect?
Calculate energy used to preheat externally feedwater in the current effect:
Q_eph(i) = SUM(F(1:i)) * Delta_H_eph(i)
No energy used to preheat externally feedwater:
Q_eph(i) = 0
Calculate mass flow rate of vapor produced by evaporation in the current effect:
V_evap(i) = F(i) * ((Xb(i) - Xf(i)) / Xb(i))

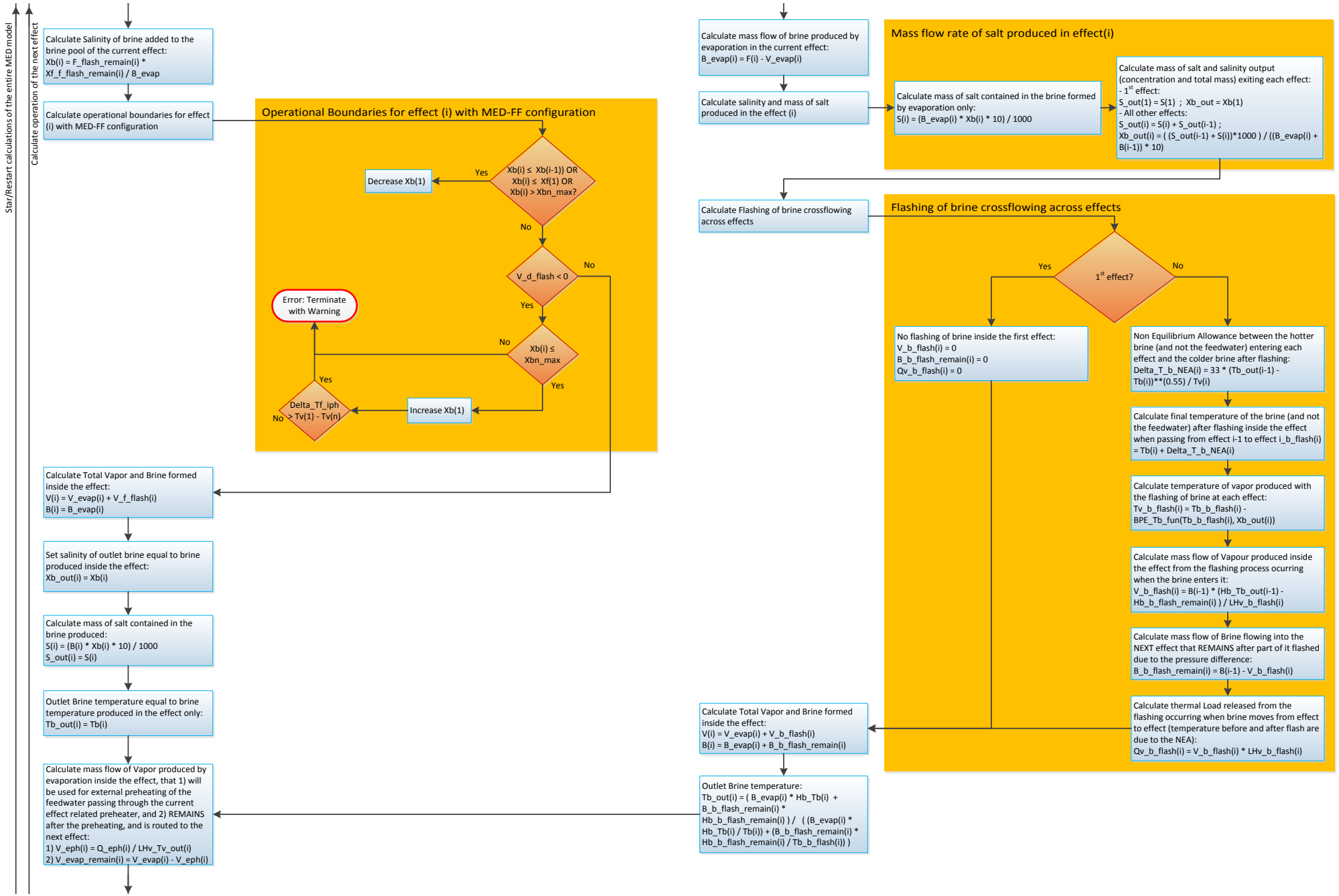
Star/Restart calculations of the entire MED model
Calculate operation of the next effect
Calculate Salinity of brine added to the brine pool of the current effect:
Xb(i) = F_flash_remain(i) * Xf_f_flash_remain(i) / B_evap
Calculate operational boundaries for effect (i) with MED-FF configuration
Operational Boundaries for effect (i) with MED-FF configuration
Xb(i) ≤ Xb(i-1)) OR Xb(i) ≤ Xf(1) OR Xb(i) > Xbn_max?
Yes
Decrease Xb(1)
No
V_d_flash < 0
No
Yes
Error: Terminate with Warning
Xb(i) ≤ Xbn_max
No
Yes
Yes
Delta_Tf_iph > Tv(1) - Tv(n)
No
Increase Xb(1)
Calculate Total Vapor and Brine formed inside the effect:
V(i) = V_evap(i) + V_f_flash(i)
B(i) = B_evap(i)
Set salinity of outlet brine equal to brine produced inside the effect:
Xb_out(i) = Xb(i)
Calculate mass of salt contained in the brine produced:
S(i) = (B(i) * Xb(i) * 10) / 1000
S_out(i) = S(i)
Outlet Brine temperature equal to brine temperature produced in the effect only:
Tb_out(i) = Tb(i)
Calculate mass flow of Vapor produced by evaporation inside the effect, that 1) will be used for external preheating of the feedwater passing through the current effect related preheater, and 2) REMAINS after the preheating, and is routed to the next effect:
1) V_eph(i) = Q_eph(i) / LHv_Tv_out(i)
2) V_evap_remain(i) = V_evap(i) - V_eph(i)
Calculate mass flow of brine produced by evaporation in the current effect:
B_evap(i) = F(i) - V_evap(i)
Calculate salinity and mass of salt produced in the effect (i)
Mass flow rate of salt produced in effect(i)
Calculate mass of salt contained in the brine formed by evaporation only:
S(i) = (B_evap(i) * Xb(i) * 10) / 1000
Calculate mass of salt and salinity output (concentration and total mass) exiting each effect:
- 1st effect:
S_out(1) = S(1) ; Xb_out = Xb(1)
- All other effects:
S_out(i) = S(i) + S_out(i-1) ;
Xb_out(i) = ((S_out(i-1) + S(i))*1000) / ((B_evap(i) + B(i-1)) * 10)
Calculate Flashing of brine crossflowing across effects
Flashing of brine crossflowing across effects
1st effect?
Yes
No
No flashing of brine inside the first effect:
V_b_flash(i) = 0
B_b_flash_remain(i) = 0
Qv_b_flash(i) = 0
Non Equilibrium Allowance between the hotter brine (and not the feedwater) entering each effect and the colder brine after flashing:
Delta_T_b_NEA(i) = 33 * (Tb_out(i-1) - Tb(i))**(0.55) / Tv(i)
Calculate final temperature of the brine (and not the feedwater) after flashing inside the effect when passing from effect i-1 to effect i_b_flash(i) = Tb(i) + Delta_T_b_NEA(i)
Calculate temperature of vapor produced with the flashing of brine at each effect:
Tv_b_flash(i) = Tb_b_flash(i) - BPE_Tb_fun(Tb_b_flash(i), Xb_out(i))
Calculate mass flow of Vapour produced inside the effect from the flashing process ocurring when the brine enters it:
V_b_flash(i) = B(i-1) * (Hb_Tb_out(i-1) - Hb_b_flash_remain(i)) / LHv_b_flash(i)
Calculate mass flow of Brine flowing into the NEXT effect that REMAINS after part of it flashed due to the pressure difference:
B_b_flash_remain(i) = B(i-1) - V_b_flash(i)
Calculate thermal Load released from the flashing occurring when brine moves from effect to effect (temperature before and after flash are due to the NEA):
Qv_b_flash(i) = V_b_flash(i) * LHv_b_flash(i)
Calculate Total Vapor and Brine formed inside the effect:
V(i) = V_evap(i) + V_b_flash(i)
B(i) = B_evap(i) + B_b_flash_remain(i)
Outlet Brine temperature:
Tb_out(i) = (B_evap(i) * Hb_Tb(i) + B_b_flash_remain(i) * Hb_b_flash_remain(i)) / ((B_evap(i) * Hb_Tb(i) / Tb(i)) + (B_b_flash_remain(i) * Hb_b_flash_remain(i) / Tb_b_flash(i)))

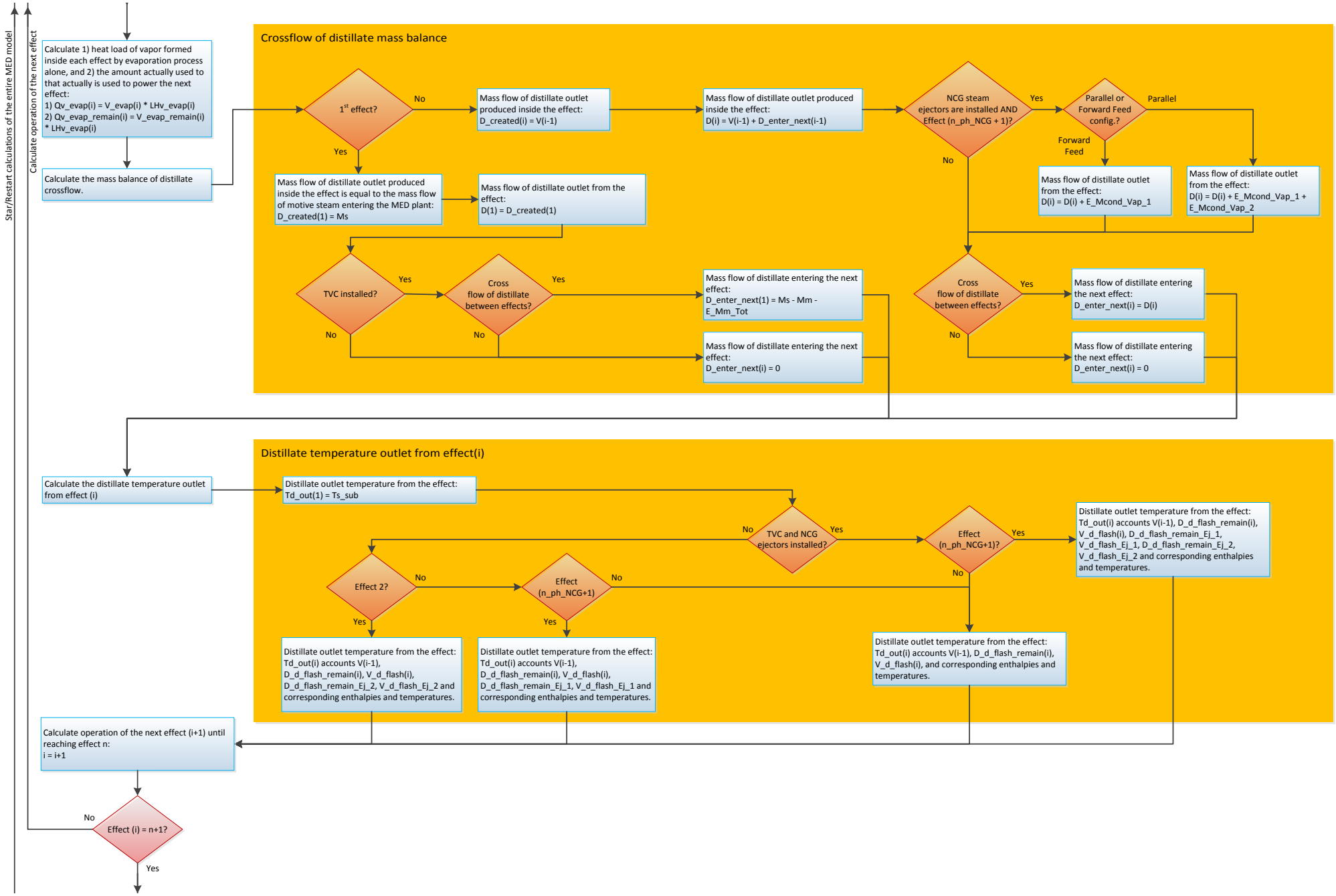
Star/Restart calculations of the entire MED model
Calculate operation of the next effect
Calculate 1) heat load of vapor formed inside each effect by evaporation process alone, and 2) the amount actually used to that actually is used to power the next effect:
1) Qv_evap(i) = V_evap(i) * LHv_evap(i)
2) Qv_evap_remain(i) = V_evap_remain(i) * LHv_evap(i)
Calculate the mass balance of distillate crossflow.
Crossflow of distillate mass balance
1st effect?
No
Yes
Mass flow of distillate outlet produced inside the effect:
D_created(i) = V(i-1)
Mass flow of distillate outlet produced inside the effect is equal to the mass flow of motive steam entering the MED plant:
D_created(1) = Ms
Mass flow of distillate outlet from the effect:
D(1) = D_created(1)
Mass flow of distillate outlet produced inside the effect:
D(i) = V(i-1) + D_enter_next(i-1)
NCG steam ejectors are installed AND Effect (n_ph_NCG + 1)?
Yes
No
Parallel or Forward Feed config.?
Parallel
Forward Feed
Mass flow of distillate outlet from the effect:
D(i) = D(i) + E_Mcond_Vap_1
Mass flow of distillate outlet from the effect:
D(i) = D(i) + E_Mcond_Vap_1 + E_Mcond_Vap_2
TVC installed?
Yes
No
Cross flow of distillate between effects?
Yes
No
Mass flow of distillate entering the next effect:
D_enter_next(1) = Ms - Mm - E_Mm_Tot
Mass flow of distillate entering the next effect:
D_enter_next(i) = 0
Cross flow of distillate between effects?
Yes
No
Mass flow of distillate entering the next effect:
D_enter_next(i) = D(i)
Mass flow of distillate entering the next effect:
D_enter_next(i) = 0
Calculate the distillate temperature outlet from effect (i)
Distillate temperature outlet from effect(i)
Distillate outlet temperature from the effect:
Td_out(1) = Ts_sub
TVC and NCG ejectors installed?
No
Yes
Effect (n_ph_NCG+1)?
Yes
No
Distillate outlet temperature from the effect:
Td_out(i) accounts V(i-1), D_d_flash_remain(i), V_d_flash(i), D_d_flash_remain_Ej_1, V_d_flash_Ej_1, D_d_flash_remain_Ej_2, V_d_flash_Ej_2 and corresponding enthalpies and temperatures.
Effect 2?
No
Yes
Effect (n_ph_NCG+1)
No
Yes
Distillate outlet temperature from the effect:
Td_out(i) accounts V(i-1), D_d_flash_remain(i), V_d_flash(i), D_d_flash_remain_Ej_2, V_d_flash_Ej_2 and corresponding enthalpies and temperatures.
Distillate outlet temperature from the effect:
Td_out(i) accounts V(i-1), D_d_flash_remain(i), V_d_flash(i), D_d_flash_remain_Ej_1, V_d_flash_Ej_1 and corresponding enthalpies and temperatures.
Distillate outlet temperature from the effect:
Td_out(i) accounts V(i-1), D_d_flash_remain(i), V_d_flash(i), and corresponding enthalpies and temperatures.
Calculate operation of the next effect (i+1) until reaching effect n:
i = i+1
Effect (i) = n+1?
No
Yes

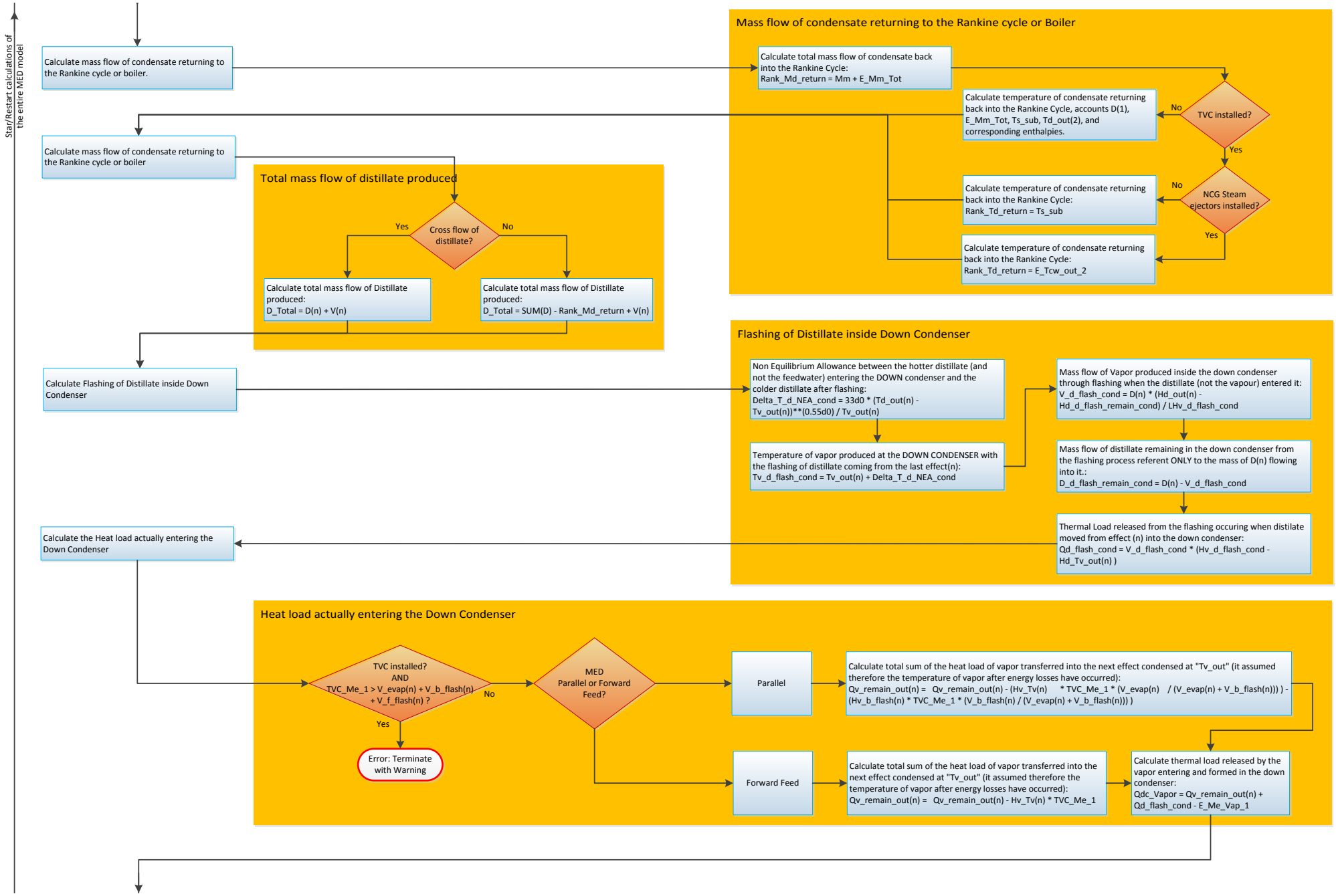
Star/Restart calculations of the entire MED model
Calculate mass flow of condensate returning to the Rankine cycle or boiler.
Calculate mass flow of condensate returning to the Rankine cycle or boiler
Mass flow of condensate returning to the Rankine cycle or Boiler
Calculate total mass flow of condensate back into the Rankine Cycle:
Rank_Md_return = Mm + E_Mm_Tot
Calculate temperature of condensate returning back into the Rankine Cycle, accounts D(1), E_Mm_Tot, Ts_sub, Td_out(2), and corresponding enthalpies.
TVC installed?
No
Yes
Calculate temperature of condensate returning back into the Rankine Cycle:
Rank_Td_return = Ts_sub
NCG Steam ejectors installed?
No
Yes
Calculate temperature of condensate returning back into the Rankine Cycle:
Rank_Td_return = E_Tcw_out_2
Total mass flow of distillate produced
Cross flow of distillate?
Yes
No
Calculate total mass flow of Distillate produced:
D_Total = D(n) + V(n)
Calculate total mass flow of Distillate produced:
D_Total = SUM(D) - Rank_Md_return + V(n)
Calculate Flashing of Distillate inside Down Condenser
Flashing of Distillate inside Down Condenser
Non Equilibrium Allowance between the hotter distillate (and not the feedwater) entering the DOWN condenser and the colder distillate after flashing:
Delta_T_d_NEA_cond = 33d0 * (Td_out(n) - Tv_out(n))**(0.55d0) / Tv_out(n)
Temperature of vapor produced at the DOWN CONDENSER with the flashing of distillate coming from the last effect(n):
Tv_d_flash_cond = Tv_out(n) + Delta_T_d_NEA_cond
Mass flow of Vapor produced inside the down condenser through flashing when the distillate (not the vapour) entered it:
V_d_flash_cond = D(n) * (Hd_out(n) - Hd_d_flash_remain_cond) / LHv_d_flash_cond
Mass flow of distillate remaining in the down condenser from the flashing process referent ONLY to the mass of D(n) flowing into it.:
D_d_flash_remain_cond = D(n) - V_d_flash_cond
Thermal Load released from the flashing occuring when distilate moved from effect (n) into the down condenser:
Qd_flash_cond = V_d_flash_cond * (Hv_d_flash_cond - Hd_Tv_out(n))
Calculate the Heat load actually entering the Down Condenser
Heat load actually entering the Down Condenser
TVC installed? AND TVC_Me_1 > V_evap(n) + V_b_flash(n) + V_f_flash(n) ?
No
Yes
Error: Terminate with Warning
MED Parallel or Forward Feed?
Parallel
Calculate total sum of the heat load of vapor transferred into the next effect condensed at "Tv_out" (it assumed therefore the temperature of vapor after energy losses have occurred):
Qv_remain_out(n) = Qv_remain_out(n) - (Hv_Tv(n) * TVC_Me_1 * (V_evap(n) / (V_evap(n) + V_b_flash(n)))) - (Hv_b_flash(n) * TVC_Me_1 * (V_b_flash(n) / (V_evap(n) + V_b_flash(n))))
Forward Feed
Calculate total sum of the heat load of vapor transferred into the next effect condensed at "Tv_out" (it assumed therefore the temperature of vapor after energy losses have occurred):
Qv_remain_out(n) = Qv_remain_out(n) - Hv_Tv(n) * TVC_Me_1
Calculate thermal load released by the vapor entering and formed in the down condenser:
Qdc_Vapor = Qv_remain_out(n) + Qd_flash_cond - E_Me_Vap_1

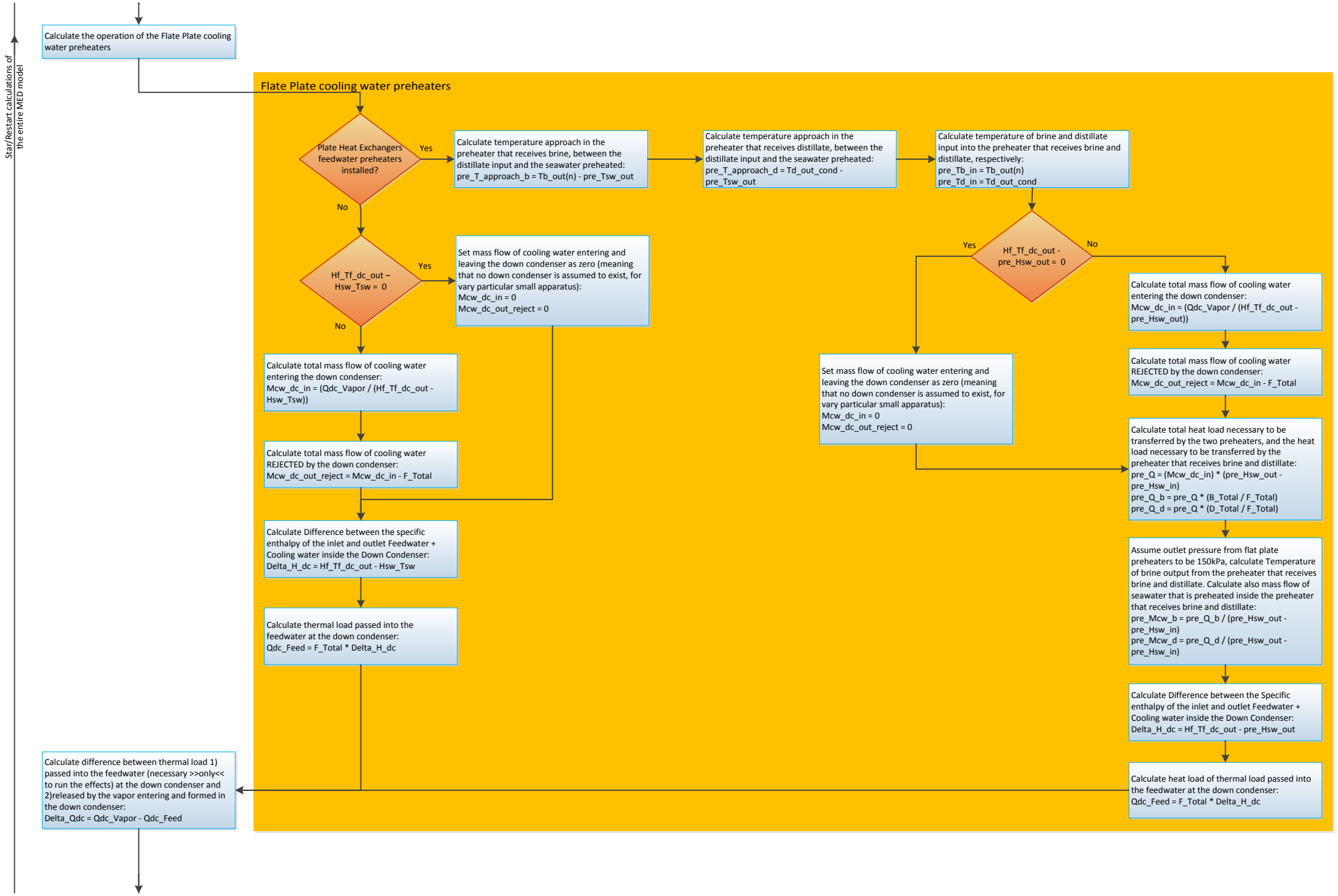
Star/Restart calculations of the entire MED model
Calculate the operation of the Flate Plate cooling water preheaters
Flate Plate cooling water preheaters
Plate Heat Exchangers feedwater preheaters installed?
Yes
No
Calculate temperature approach in the preheater that receives brine, between the distillate input and the seawater preheated:
pre_T_approach_b = Tb_out(n) - pre_Tsw_out
Calculate temperature approach in the preheater that receives distillate, between the distillate input and the seawater preheated:
pre_T_approach_d = Td_out_cond - pre_Tsw_out
Calculate temperature of brine and distillate input into the preheater that receives brine and distillate, respectively:
pre_Tb_in = Tb_out(n)
pre_Td_in = Td_out_cond
Hf_Tf_dc_out – Hsw_Tsw = 0
Yes
No
Set mass flow of cooling water entering and leaving the down condenser as zero (meaning that no down condenser is assumed to exist, for vary particular small apparatus):
Mcw_dc_in = 0
Mcw_dc_out_reject = 0
Calculate total mass flow of cooling water entering the down condenser:
Mcw_dc_in = (Qdc_Vapor / (Hf_Tf_dc_out - Hsw_Tsw))
Calculate total mass flow of cooling water REJECTED by the down condenser:
Mcw_dc_out_reject = Mcw_dc_in - F_Total
Calculate Difference between the specific enthalpy of the inlet and outlet Feedwater + Cooling water inside the Down Condenser:
Delta_H_dc = Hf_Tf_dc_out - Hsw_Tsw
Calculate thermal load passed into the feedwater at the down condenser:
Qdc_Feed = F_Total * Delta_H_dc
Hf_Tf_dc_out - pre_Hsw_out = 0
Yes
No
Set mass flow of cooling water entering and leaving the down condenser as zero (meaning that no down condenser is assumed to exist, for vary particular small apparatus):
Mcw_dc_in = 0
Mcw_dc_out_reject = 0
Calculate total mass flow of cooling water entering the down condenser:
Mcw_dc_in = (Qdc_Vapor / (Hf_Tf_dc_out - pre_Hsw_out))
Calculate total mass flow of cooling water REJECTED by the down condenser:
Mcw_dc_out_reject = Mcw_dc_in - F_Total
Calculate total heat load necessary to be transferred by the two preheaters, and the heat load necessary to be transferred by the preheater that receives brine and distillate:
pre_Q = (Mcw_dc_in) * (pre_Hsw_out - pre_Hsw_in)
pre_Q_b = pre_Q * (B_Total / F_Total)
pre_Q_d = pre_Q * (D_Total / F_Total)
Assume outlet pressure from flat plate preheaters to be 150kPa, calculate Temperature of brine output from the preheater that receives brine and distillate. Calculate also mass flow of seawater that is preheated inside the preheater that receives brine and distillate:
pre_Mcw_b = pre_Q_b / (pre_Hsw_out - pre_Hsw_in)
pre_Mcw_d = pre_Q_d / (pre_Hsw_out - pre_Hsw_in)
Calculate Difference between the Specific enthalpy of the inlet and outlet Feedwater + Cooling water inside the Down Condenser:
Delta_H_dc = Hf_Tf_dc_out - pre_Hsw_out
Calculate heat load of thermal load passed into the feedwater at the down condenser:
Qdc_Feed = F_Total * Delta_H_dc
Calculate difference between thermal load 1) passed into the feedwater (necessary >>only<< to run the effects) at the down condenser and 2)released by the vapor entering and formed in the down condenser:
Delta_Qdc = Qdc_Vapor - Qdc_Feed

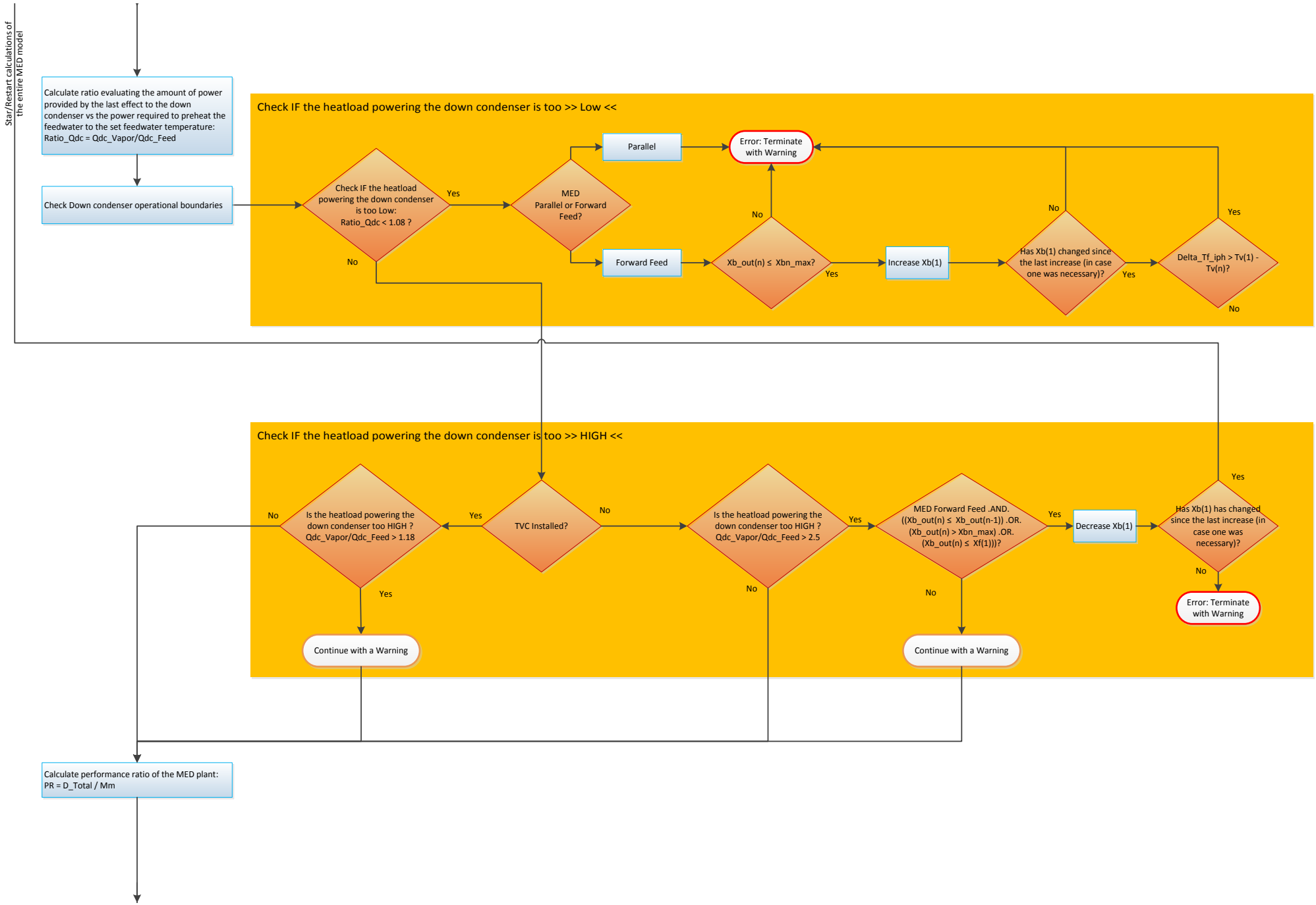
Star/Restart calculations of the entire MED model
Calculate ratio evaluating the amount of power provided by the last effect to the down condenser vs the power required to preheat the feedwater to the set feedwater temperature: Ratio_Qdc = Qdc_Vapor/Qdc_Feed
Check Down condenser operational boundaries
Check IF the heatload powering the down condenser is too >> Low <<
Check IF the heatload powering the down condenser is too Low: Ratio_Qdc < 1.08 ?
Yes
No
MED Parallel or Forward Feed?
Parallel
Forward Feed
Error: Terminate with Warning
Xb_out(n) ≤ Xbn_max?
No
Yes
Increase Xb(1)
Has Xb(1) changed since the last increase (in case one was necessary)?
No
Yes
Delta_Tf_iph > Tv(1) - Tv(n)?
Yes
No
Check IF the heatload powering the down condenser is too >> HIGH <<
Is the heatload powering the down condenser too HIGH ? Qdc_Vapor/Qdc_Feed > 1.18
No
Yes
Continue with a Warning
TVC Installed?
Yes
No
Is the heatload powering the down condenser too HIGH ? Qdc_Vapor/Qdc_Feed > 2.5
Yes
No
MED Forward Feed .AND. ((Xb_out(n) ≤ Xb_out(n-1)) .OR. (Xb_out(n) > Xbn_max) .OR. (Xb_out(n) ≤ Xf(1)))?
Yes
No
Continue with a Warning
Decrease Xb(1)
Has Xb(1) has changed since the last increase (in case one was necessary)?
Yes
No
Error: Terminate with Warning
Calculate performance ratio of the MED plant: PR = D_Total / Mm

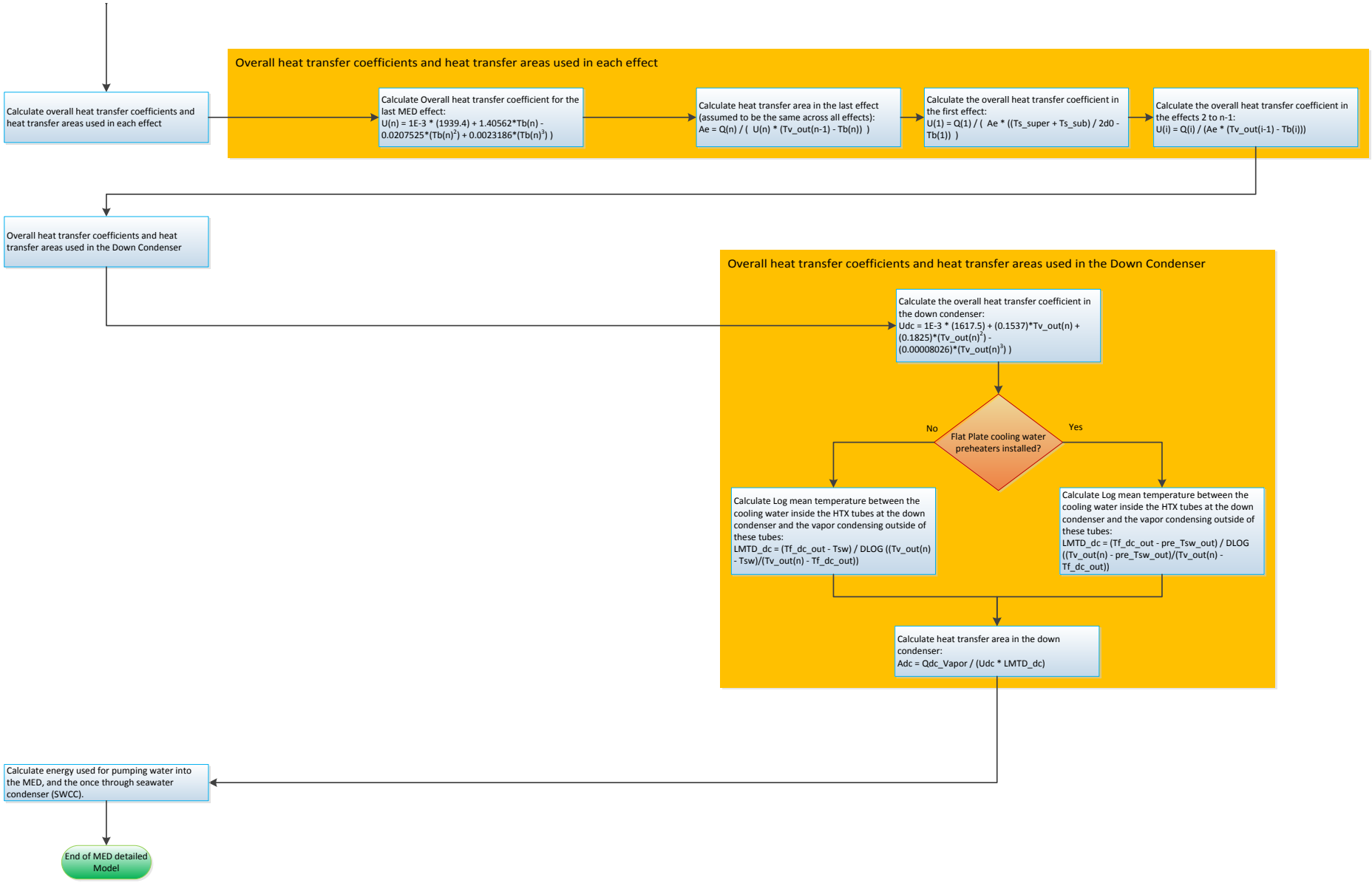
Calculate overall heat transfer coefficients and heat transfer areas used in each effect
Overall heat transfer coefficients and heat transfer areas used in each effect
Calculate Overall heat transfer coefficient for the last MED effect:
U(n) = 1E-3 * (1939.4) + 1.40562*Tb(n) - 0.0207525*(Tb(n)^2) + 0.0023186*(Tb(n)^3))
Calculate heat transfer area in the last effect (assumed to be the same across all effects):
Ae = Q(n) / (U(n) * (Tv_out(n-1) - Tb(n)))
Calculate the overall heat transfer coefficient in the first effect:
U(1) = Q(1) / (Ae * ((Ts_super + Ts_sub) / 2d0 - Tb(1)))
Calculate the overall heat transfer coefficient in the effects 2 to n-1:
U(i) = Q(i) / (Ae * (Tv_out(i-1) - Tb(i)))
Overall heat transfer coefficients and heat transfer areas used in the Down Condenser
Overall heat transfer coefficients and heat transfer areas used in the Down Condenser
Calculate the overall heat transfer coefficient in the down condenser:
Udc = 1E-3 * (1617.5) + (0.1537)*Tv_out(n) + (0.1825)*(Tv_out(n)^2) - (0.00008026)*(Tv_out(n)^3))
Flat Plate cooling water preheaters installed?
No
Yes
Calculate Log mean temperature between the cooling water inside the HTX tubes at the down condenser and the vapor condensing outside of these tubes:
LMTD_dc = (Tf_dc_out - Tsw) / DLOG ((Tv_out(n) - Tsw)/(Tv_out(n) - Tf_dc_out))
Calculate Log mean temperature between the cooling water inside the HTX tubes at the down condenser and the vapor condensing outside of these tubes:
LMTD_dc = (Tf_dc_out - pre_Tsw_out) / DLOG ((Tv_out(n) - pre_Tsw_out)/(Tv_out(n) - Tf_dc_out))
Calculate heat transfer area in the down condenser:
Adc = Qdc_Vapor / (Udc * LMTD_dc)
Calculate energy used for pumping water into the MED, and the once through seawater condenser (SWCC).
End of MED detailed Model

Annex 2 – Diagram: Steam Jet Ejector Model

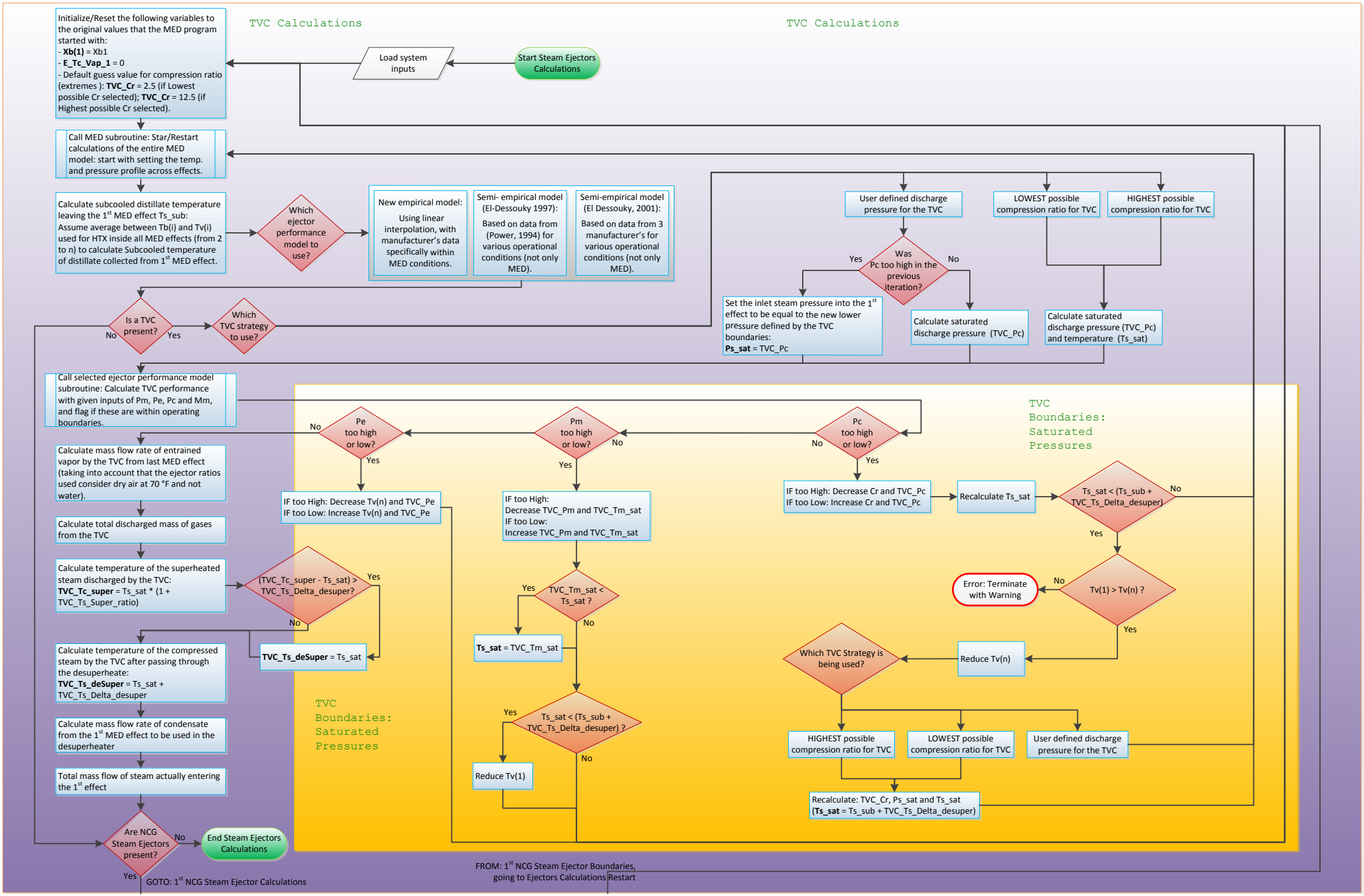
TVC Calculations
TVC Calculations
Initialize/Reset the following variables to the original values that the MED program started with:
- Xb(1) = Xb1
- E_Tc_Vap_1 = 0
- Default guess value for compression ratio (extremes): TVC_Cr = 2.5 (if Lowest possible Cr selected); TVC_Cr = 12.5 (if Highest possible Cr selected).
Load system inputs
Start Steam Ejectors Calculations
Call MED subroutine: Star/Restart calculations of the entire MED model: start with setting the temp. and pressure profile across effects.
Calculate subcooled distillate temperature leaving the 1st MED effect Ts_sub: Assume average between Tb(i) and Tv(i) used for HTX inside all MED effects (from 2 to n) to calculate Subcooled temperature of distillate collected from 1st MED effect.
Which ejector performance model to use?
New empirical model: Using linear interpolation, with manufacturer's data specifically within MED conditions.
Semi- empirical model (El-Dessouky 1997): Based on data from (Power, 1994) for various operational conditions (not only MED).
Semi-empirical model (El Dessouky, 2001): Based on data from 3 manufacturer's for various operational conditions (not only MED).
Is a TVC present?
No
Yes
Which TVC strategy to use?
User defined discharge pressure for the TVC
LOWEST possible compression ratio for TVC
HIGHEST possible compression ratio for TVC
Was Pc too high in the previous iteration?
Yes
No
Set the inlet steam pressure into the 1st effect to be equal to the new lower pressure defined by the TVC boundaries: Ps_sat = TVC_Pc
Calculate saturated discharge pressure (TVC_Pc)
Calculate saturated discharge pressure (TVC_Pc) and temperature (Ts_sat)
Call selected ejector performance model subroutine: Calculate TVC performance with given inputs of Pm, Pe, Pc and Mm, and flag if these are within operating boundaries.
Pe too high or low?
Pm too high or low?
Pc too high or low?
TVC Boundaries: Saturated Pressures
IF too High: Decrease Tv(n) and TVC_Pe
IF too Low: Increase Tv(n) and TVC_Pe
IF too High: Decrease TVC_Pm and TVC_Tm_sat
IF too Low: Increase TVC_Pm and TVC_Tm_sat
IF too High: Decrease Cr and TVC_Pc
IF too Low: Increase Cr and TVC_Pc
Recalculate Ts_sat
Ts_sat < (Ts_sub + TVC_Ts_Delta_desuper)
Calculate mass flow rate of entrained vapor by the TVC from last MED effect (taking into account that the ejector ratios used consider dry air at 70 °F and not water).
Calculate total discharged mass of gases from the TVC
Calculate temperature of the superheated steam discharged by the TVC: TVC_Tc_super = Ts_sat * (1 + TVC_Ts_Super_ratio)
(TVC_Tc_super - Ts_sat) > TVC_Ts_Delta_desuper?
TVC_Ts_deSuper = Ts_sat
TVC_Tm_sat < Ts_sat ?
Ts_sat = TVC_Tm_sat
Ts_sat < (Ts_sub + TVC_Ts_Delta_desuper) ?
Reduce Tv(1)
Tv(1) > Tv(n) ?
Error: Terminate with Warning
Reduce Tv(n)
Which TVC Strategy is being used?
HIGHEST possible compression ratio for TVC
LOWEST possible compression ratio for TVC
User defined discharge pressure for the TVC
Recalculate: TVC_Cr, Ps_sat and Ts_sat (Ts_sat = Ts_sub + TVC_Ts_Delta_desuper)
Calculate temperature of the compressed steam by the TVC after passing through the desuperheate: TVC_Ts_deSuper = Ts_sat + TVC_Ts_Delta_desuper
Calculate mass flow rate of condensate from the 1st MED effect to be used in the desuperheater
Total mass flow of steam actually entering the 1st effect
Are NCG Steam Ejectors present?
End Steam Ejectors Calculations
GOTO: 1st NCG Steam Ejector Calculations
FROM: 1st NCG Steam Ejector Boundaries, going to Ejectors Calculations Restart

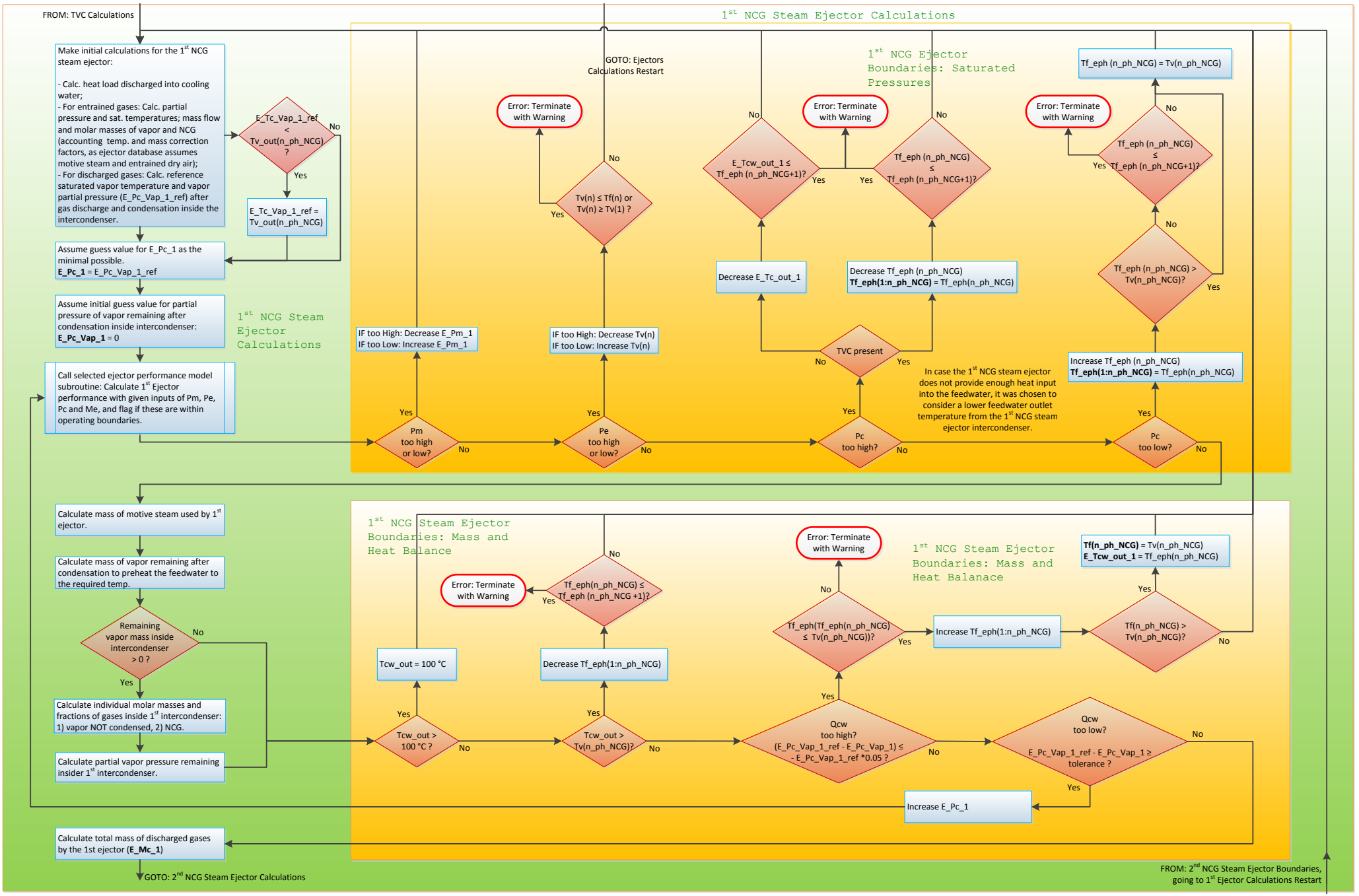
FROM: TVC Calculations
1st NCG Steam Ejector Calculations
Make initial calculations for the 1st NCG steam ejector:
- Calc. heat load discharged into cooling water;
- For entrained gases: Calc. partial pressure and sat. temperatures; mass flow and molar masses of vapor and NCG (accounting temp. and mass correction factors, as ejector database assumes motive steam and entrained dry air);
- For discharged gases: Calc. reference saturated vapor temperature and vapor partial pressure (E_Pc_Vap_1_ref) after gas discharge and condensation inside the intercondenser.
E_Tc_Vap_1_ref < Tv_out(n_ph_NCG) ?
No
Yes
E_Tc_Vap_1_ref = Tv_out(n_ph_NCG)
Assume guess value for E_Pc_1 as the minimal possible.
E_Pc_1 = E_Pc_Vap_1_ref
Assume initial guess value for partial pressure of vapor remaining after condensation inside intercondenser:
E_Pc_Vap_1 = 0
1st NCG Steam Ejector Calculations
Call selected ejector performance model subroutine: Calculate 1st Ejector performance with given inputs of Pm, Pe, Pc and Me, and flag if these are within operating boundaries.
GOTO: Ejectors Calculations Restart
Error: Terminate with Warning
Tv(n) ≤ Tf(n) or Tv(n) ≥ Tv(1) ?
IF too High: Decrease E_Pm_1
IF too Low: Increase E_Pm_1
IF too High: Decrease Tv(n)
IF too Low: Increase Tv(n)
Pm too high or low?
Pe too high or low?
1st NCG Ejector Boundaries: Saturated Pressures
E_Tcw_out_1 ≤ Tf_eph (n_ph_NCG+1)?
Tf_eph (n_ph_NCG) ≤ Tf_eph (n_ph_NCG+1)?
Decrease E_Tc_out_1
Decrease Tf_eph (n_ph_NCG)
Tf_eph(1:n_ph_NCG) = Tf_eph(n_ph_NCG)
TVC present
Pc too high?
In case the 1st NCG steam ejector does not provide enough heat input into the feedwater, it was chosen to consider a lower feedwater outlet temperature from the 1st NCG steam ejector intercondenser.
Tf_eph (n_ph_NCG) = Tv(n_ph_NCG)
Tf_eph (n_ph_NCG) > Tv(n_ph_NCG)?
Increase Tf_eph (n_ph_NCG)
Tf_eph(1:n_ph_NCG) = Tf_eph(n_ph_NCG)
Pc too low?
Calculate mass of motive steam used by 1st ejector.
Calculate mass of vapor remaining after condensation to preheat the feedwater to the required temp.
Remaining vapor mass inside intercondenser > 0 ?
Calculate individual molar masses and fractions of gases inside 1st intercondenser: 1) vapor NOT condensed, 2) NCG.
Calculate partial vapor pressure remaining insider 1st intercondenser.
1st NCG Steam Ejector Boundaries: Mass and Heat Balance
Tf_eph(n_ph_NCG) ≤ Tf_eph (n_ph_NCG +1)?
Tcw_out = 100 °C
Decrease Tf_eph(1:n_ph_NCG)
Tcw_out > 100 °C ?
Tcw_out > Tv(n_ph_NCG)?
1st NCG Steam Ejector Boundaries: Mass and Heat Balanace
Tf_eph(Tf_eph(n_ph_NCG) ≤ Tv(n_ph_NCG))?
Increase Tf_eph(1:n_ph_NCG)
Tf(n_ph_NCG) > Tv(n_ph_NCG)?
Tf(n_ph_NCG) = Tv(n_ph_NCG)
E_Tcw_out_1 = Tf_eph(n_ph_NCG)
Qcw too high? (E_Pc_Vap_1_ref - E_Pc_Vap_1) ≤ - E_Pc_Vap_1_ref *0.05 ?
Qcw too low? E_Pc_Vap_1_ref - E_Pc_Vap_1 ≥ tolerance ?
Increase E_Pc_1
Calculate total mass of discharged gases by the 1st ejector (E_Mc_1)
GOTO: 2nd NCG Steam Ejector Calculations
FROM: 2nd NCG Steam Ejector Boundaries, going to 1st Ejector Calculations Restart

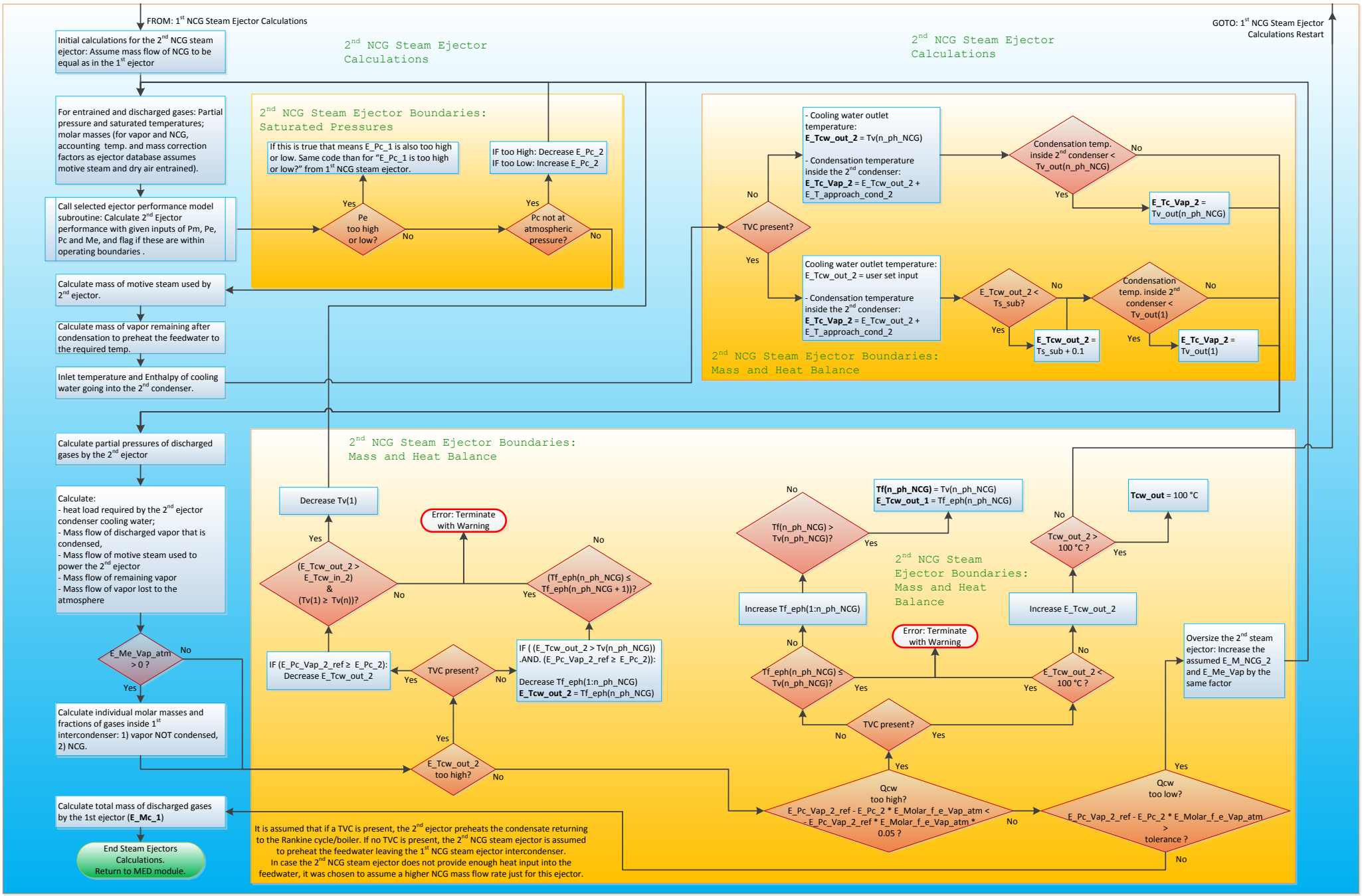
FROM: 1st NCG Steam Ejector Calculations
Initial calculations for the 2nd NCG steam ejector: Assume mass flow of NCG to be equal as in the 1st ejector
2nd NCG Steam Ejector Calculations
2nd NCG Steam Ejector Calculations
GOTO: 1st NCG Steam Ejector Calculations Restart
For entrained and discharged gases: Partial pressure and saturated temperatures; molar masses (for vapor and NCG, accounting temp. and mass correction factors as ejector database assumes motive steam and dry air entrained).
2nd NCG Steam Ejector Boundaries: Saturated Pressures
If this is true that means E_Pc_1 is also too high or low. Same code than for "E_Pc_1 is too high or low?" from 1st NCG steam ejector.
IF too High: Decrease E_Pc_2
IF too Low: Increase E_Pc_2
Yes
Pe too high or low?
No
Yes
Pc not at atmospheric pressure?
No
Call selected ejector performance model subroutine: Calculate 2nd Ejector performance with given inputs of Pm, Pe, Pc and Me, and flag if these are within operating boundaries .
Calculate mass of motive steam used by 2nd ejector.
Calculate mass of vapor remaining after condensation to preheat the feedwater to the required temp.
Inlet temperature and Enthalpy of cooling water going into the 2nd condenser.
2nd NCG Steam Ejector Boundaries: Mass and Heat Balance
No
TVC present?
Yes
- Cooling water outlet temperature:
E_Tcw_out_2 = Tv(n_ph_NCG)
- Condensation temperature inside the 2nd condenser:
E_Tc_Vap_2 = E_Tcw_out_2 + E_T_approach_cond_2
Condensation temp. inside 2nd condenser < Tv_out(n_ph_NCG)
No
Yes
E_Tc_Vap_2 = Tv_out(n_ph_NCG)
Cooling water outlet temperature:
E_Tcw_out_2 = user set input
- Condensation temperature inside the 2nd condenser:
E_Tc_Vap_2 = E_Tcw_out_2 + E_T_approach_cond_2
E_Tcw_out_2 < Ts_sub?
No
Yes
E_Tcw_out_2 = Ts_sub + 0.1
Condensation temp. inside 2nd condenser < Tv_out(1)
No
Yes
E_Tc_Vap_2 = Tv_out(1)
2nd NCG Steam Ejector Boundaries: Mass and Heat Balance
Calculate partial pressures of discharged gases by the 2nd ejector
Calculate:
- heat load required by the 2nd ejector condenser cooling water;
- Mass flow of discharged vapor that is condensed,
- Mass flow of motive steam used to power the 2nd ejector
- Mass flow of remaining vapor
- Mass flow of vapor lost to the atmosphere
Decrease Tv(1)
Yes
(E_Tcw_out_2 > E_Tcw_in_2) & (Tv(1) ≥ Tv(n))?
No
Error: Terminate with Warning
No
(Tf_eph(n_ph_NCG) ≤ Tf_eph(n_ph_NCG + 1))?
Yes
IF (E_Pc_Vap_2_ref ≥ E_Pc_2): Decrease E_Tcw_out_2
TVC present?
Yes
No
IF ((E_Tcw_out_2 > Tv(n_ph_NCG)) .AND. (E_Pc_Vap_2_ref ≥ E_Pc_2)):
Decrease Tf_eph(1:n_ph_NCG)
E_Tcw_out_2 = Tf_eph(n_ph_NCG)
Yes
E_Tcw_out_2 too high?
No
No
Tf(n_ph_NCG) > Tv(n_ph_NCG)?
Yes
Tf(n_ph_NCG) = Tv(n_ph_NCG)
E_Tcw_out_1 = Tf_eph(n_ph_NCG)
2nd NCG Steam Ejector Boundaries: Mass and Heat Balance
Increase Tf_eph(1:n_ph_NCG)
No
Tf_eph(n_ph_NCG) ≤ Tv(n_ph_NCG)?
Yes
Error: Terminate with Warning
No
Tcw_out_2 > 100 °C ?
Yes
Tcw_out = 100 °C
Increase E_Tcw_out_2
No
E_Tcw_out_2 < 100 °C ?
Yes
TVC present?
No
Yes
Oversize the 2nd steam ejector: Increase the assumed E_M_NCG_2 and E_Me_Vap by the same factor
Qcw too high?
E_Pc_Vap_2_ref - E_Pc_2 * E_Molar_f_e_Vap_atm < - E_Pc_Vap_2_ref * E_Molar_f_e_Vap_atm * 0.05 ?
No
Qcw too low?
E_Pc_Vap_2_ref - E_Pc_2 * E_Molar_f_e_Vap_atm > tolerance ?
Yes
No
E_Me_Vap_atm > 0 ?
No
Yes
Calculate individual molar masses and fractions of gases inside 1st intercondenser: 1) vapor NOT condensed, 2) NCG.
Calculate total mass of discharged gases by the 1st ejector (E_Mc_1)
End Steam Ejectors Calculations. Return to MED module.
It is assumed that if a TVC is present, the 2nd ejector preheats the condensate returning to the Rankine cycle/boiler. If no TVC is present, the 2nd NCG steam ejector is assumed to preheat the feedwater leaving the 1st NCG steam ejector intercondenser. In case the 2nd NCG steam ejector does not provide enough heat input into the feedwater, it was chosen to assume a higher NCG mass flow rate just for this ejector.

Annex 3 – Diagram: Linear Interpolation Model for the Calculation of Entrainment Ratios Using Database with Steam Jet Ejectors Performance

Table 33 - List of main inputs for the linear interpolation model for the calculation of entrainment ratios for steam jet ejectors.

Parameter/Variable	Units	Description
E_Me_air_equiv_1	kg/s	Mass flow of air equivalent entrained gases into the 1st ejector
E_Me_air_equiv_2	kg/s	Mass flow of air equivalent entrained gases into the 2nd ejector
E_Mm_1	kg/s	Mass flow of motive steam powering the 1st ejector
E_Mm_2	kg/s	Mass flow of motive steam powering the 2nd ejector
E_Pc_1	Pa	Pressure of compressed gas from 1st ejector
E_Pc_2	Pa	Pressure of compressed gas from 2nd ejector
E_Pe_1	Pa	Pressure of Entrained gases into the 1st ejector
E_Pe_2	Pa	Pressure of Entrained gases into the 2nd ejector
E_Pm	Pa	Motive steam pressure used to power both steam ejectors
TVC_Me_air_equiv	kg/s	Mass flow of air equivalent entrained gases into the TVC
TVC_Mm	kg/s	Motive steam mass flow rate used in the TVC
TVC_Pc	Pa	Compression pressure of the steam leaving the TVC
TVC_Pe	Pa	Entrainement pressure used in the TVC
TVC_Pm	Pa	Motive steam pressure used in the TVC

Table 34 - List of main oututs for the linear interpolation model for the calculation of enrainment ratios for steam ject ejectors.

Parameter/Variable	Units	Description
E_Me_air_equiv_1	kg/s	Mass flow of air equivalent entrained gases into the 1st ejector
E_Me_air_equiv_2	kg/s	Mass flow of air equivalent entrained gases into the 2nd ejector
E_Mm_1	kg/s	Mass flow of motive steam powering the 1st ejector
E_Mm_2	kg/s	Mass flow of motive steam powering the 2nd ejector
E_Pc_1	Pa	Pressure of compressed gas from 1st ejector
E_Pc_2	Pa	Pressure of compressed gas from 2nd ejector
E_Pe_1	Pa	Pressure of Entrained gases into the 1st ejector
E_Pe_2	Pa	Pressure of Entrained gases into the 2nd ejector
E_Pm	Pa	Motive steam pressure used to power both steam ejectors
TVC_Me_air_equiv	kg/s	Mass flow of air equivalent entrained gases into the TVC
TVC_Mm	kg/s	Motive steam mass flow rate used in the TVC
TVC_Pc	Pa	Compression pressure of the steam leaving the TVC
TVC_Pe	Pa	Entrainement pressure used in the TVC
TVC_Pm	Pa	Motive steam pressure used in the TVC

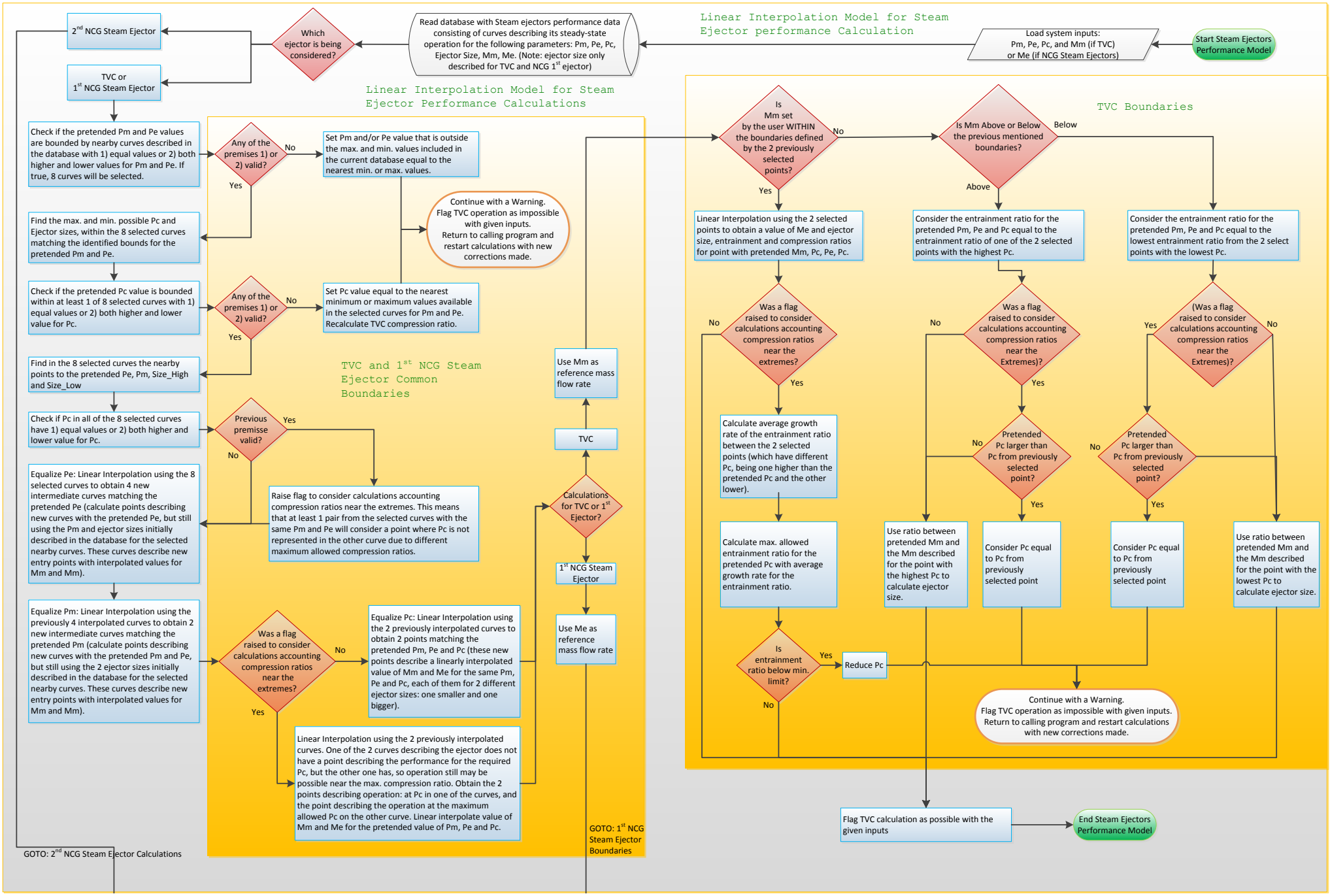
Linear Interpolation Model for Steam Ejector performance Calculation
Start Steam Ejectors Performance Model
Load system inputs: Pm, Pe, Pc, and Mm (if TVC) or Me (if NCG Steam Ejectors)
Read database with Steam ejectors performance data consisting of curves describing its steady-state operation for the following parameters: Pm, Pe, Pc, Ejector Size, Mm, Me. (Note: ejector size only described for TVC and NCG 1st ejector)
Which ejector is being considered?
2nd NCG Steam Ejector
TVC or 1st NCG Steam Ejector
Linear Interpolation Model for Steam Ejector Performance Calculations
Check if the pretended Pm and Pe values are bounded by nearby curves described in the database with 1) equal values or 2) both higher and lower values for Pm and Pe. If true, 8 curves will be selected.
Any of the premises 1) or 2) valid?
No
Yes
Set Pm and/or Pe value that is outside the max. and min. values included in the current database equal to the nearest min. or max. values.
Continue with a Warning. Flag TVC operation as impossible with given inputs. Return to calling program and restart calculations with new corrections made.
Find the max. and min. possible Pc and Ejector sizes, within the 8 selected curves matching the identified bounds for the pretended Pm and Pe.
Check if the pretended Pc value is bounded within at least 1 of 8 selected curves with 1) equal values or 2) both higher and lower value for Pc.
Any of the premises 1) or 2) valid?
No
Yes
Set Pc value equal to the nearest minimum or maximum values available in the selected curves for Pm and Pe. Recalculate TVC compression ratio.
Find in the 8 selected curves the nearby points to the pretended Pe, Pm, Size_High and Size_Low
TVC and 1st NCG Steam Ejector Common Boundaries
Check if Pc in all of the 8 selected curves have 1) equal values or 2) both higher and lower value for Pc.
Previous premisse valid?
Yes
No
Raise flag to consider calculations accounting compression ratios near the extremes. This means that at least 1 pair from the selected curves with the same Pm and Pe will consider a point where Pc is not represented in the other curve due to different maximum allowed compression ratios.
Equalize Pe: Linear Interpolation using the 8 selected curves to obtain 4 new intermediate curves matching the pretended Pe (calculate points describing new curves with the pretended Pe, but still using the Pm and ejector sizes initially described in the database for the selected nearby curves. These curves describe new entry points with interpolated values for Mm and Mm).
Equalize Pm: Linear Interpolation using the previously 4 interpolated curves to obtain 2 new intermediate curves matching the pretended Pm (calculate points describing new curves with the pretended Pm and Pe, but still using the 2 ejector sizes initially described in the database for the selected nearby curves. These curves describe new entry points with interpolated values for Mm and Mm).
Was a flag raised to consider calculations accounting compression ratios near the extremes?
No
Yes
Equalize Pc: Linear Interpolation using the 2 previously interpolated curves to obtain 2 points matching the pretended Pm, Pe and Pc (these new points describe a linearly interpolated value of Mm and Me for the same Pm, Pe and Pc, each of them for 2 different ejector sizes: one smaller and one bigger).
Linear Interpolation using the 2 previously interpolated curves. One of the 2 curves describing the ejector does not have a point describing the performance for the required Pc, but the other one has, so operation still may be possible near the max. compression ratio. Obtain the 2 points describing operation: at Pc in one of the curves, and the point describing the operation at the maximum allowed Pc on the other curve. Linear interpolate value of Mm and Me for the pretended value of Pm, Pe and Pc.
Calculations for TVC or 1st Ejector?
TVC
1st NCG Steam Ejector
Use Mm as reference mass flow rate
Use Me as reference mass flow rate
GOTO: 1st NCG Steam Ejector Boundaries
GOTO: 2nd NCG Steam Ejector Calculations
TVC Boundaries
Is Mm set by the user WITHIN the boundaries defined by the 2 previously selected points?
No
Yes
Is Mm Above or Below the previous mentioned boundaries?
Above
Below
Linear Interpolation using the 2 selected points to obtain a value of Me and ejector size, entrainment and compression ratios for point with pretended Mm, Pc, Pe, Pc.
Consider the entrainment ratio for the pretended Pm, Pe and Pc equal to the entrainment ratio of one of the 2 selected points with the highest Pc.
Consider the entrainment ratio for the pretended Pm, Pe and Pc equal to the lowest entrainment ratio from the 2 select points with the lowest Pc.
Was a flag raised to consider calculations accounting compression ratios near the extremes?
No
Yes
Was a flag raised to consider calculations accounting compression ratios near the Extremes)?
No
Yes
(Was a flag raised to consider calculations accounting compression ratios near the Extremes)?
Yes
No
Calculate average growth rate of the entrainment ratio between the 2 selected points (which have different Pc, being one higher than the pretended Pc and the other lower).
Pretended Pc larger than Pc from previously selected point?
No
Yes
Pretended Pc larger than Pc from previously selected point?
No
Yes
Calculate max. allowed entrainment ratio for the pretended Pc with average growth rate for the entrainment ratio.
Use ratio between pretended Mm and the Mm described for the point with the highest Pc to calculate ejector size.
Consider Pc equal to Pc from previously selected point
Consider Pc equal to Pc from previously selected point
Use ratio between pretended Mm and the Mm described for the point with the lowest Pc to calculate ejector size.
Is entrainment ratio below min. limit?
Yes
No
Reduce Pc
Continue with a Warning. Flag TVC operation as impossible with given inputs. Return to calling program and restart calculations with new corrections made.
Flag TVC calculation as possible with the given inputs
End Steam Ejectors Performance Model

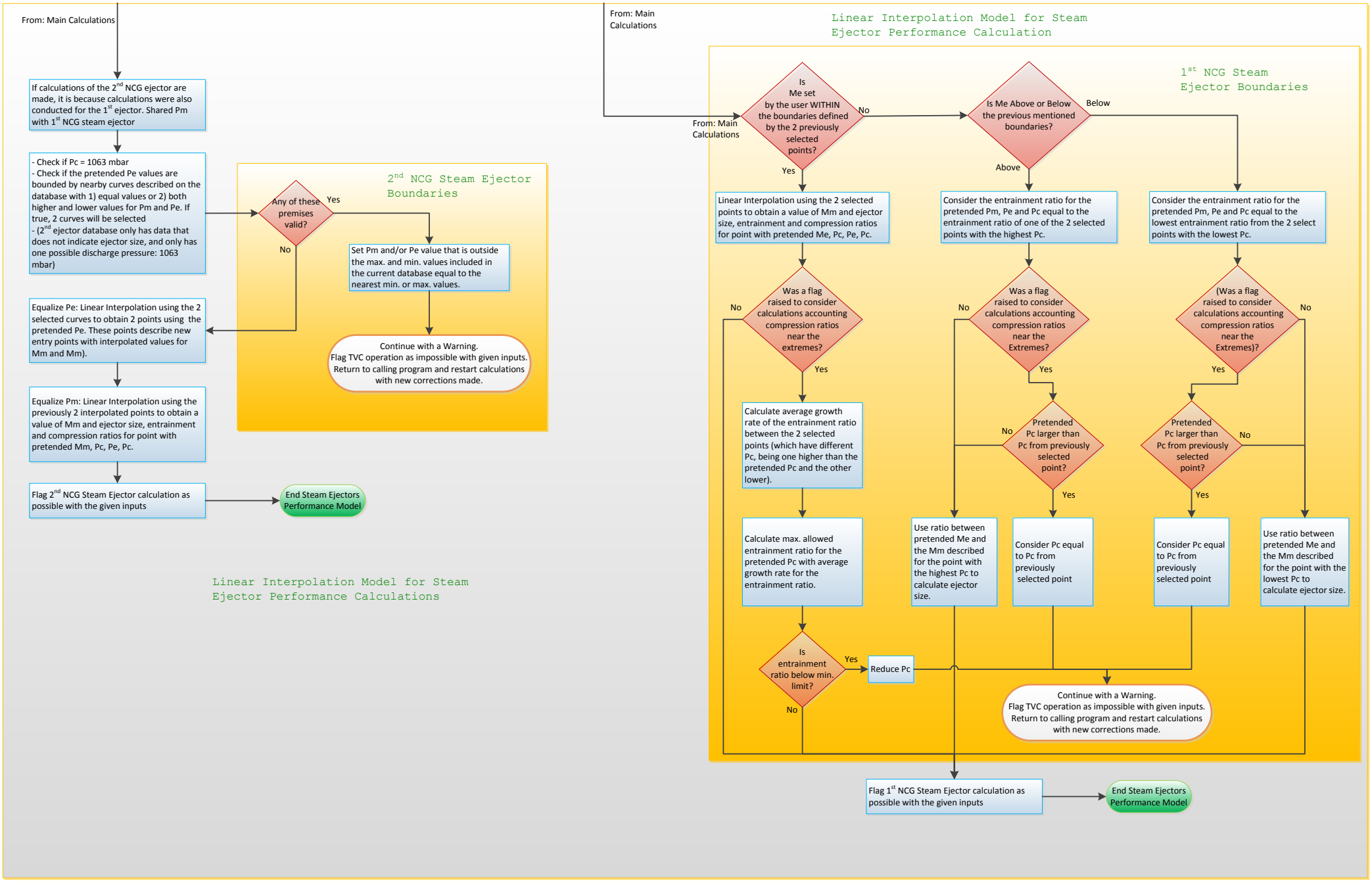
From: Main Calculations
If calculations of the 2nd NCG ejector are made, it is because calculations were also conducted for the 1st ejector. Shared Pm with 1st NCG steam ejector
- Check if Pc = 1063 mbar
- Check if the pretended Pe values are bounded by nearby curves described on the database with 1) equal values or 2) both higher and lower values for Pm and Pe. If true, 2 curves will be selected
- (2nd ejector database only has data that does not indicate ejector size, and only has one possible discharge pressure: 1063 mbar)
2nd NCG Steam Ejector Boundaries
Any of these premises valid?
Yes
No
Set Pm and/or Pe value that is outside the max. and min. values included in the current database equal to the nearest min. or max. values.
Continue with a Warning.
Flag TVC operation as impossible with given inputs.
Return to calling program and restart calculations with new corrections made.
Equalize Pe: Linear Interpolation using the 2 selected curves to obtain 2 points using the pretended Pe. These points describe new entry points with interpolated values for Mm and Mm).
Equalize Pm: Linear Interpolation using the previously 2 interpolated points to obtain a value of Mm and ejector size, entrainment and compression ratios for point with pretended Mm, Pc, Pe, Pc.
Flag 2nd NCG Steam Ejector calculation as possible with the given inputs
End Steam Ejectors Performance Model
Linear Interpolation Model for Steam Ejector Performance Calculations
From: Main Calculations
Linear Interpolation Model for Steam Ejector Performance Calculation
1st NCG Steam Ejector Boundaries
From: Main Calculations
Is Me set by the user WITHIN the boundaries defined by the 2 previously selected points?
No
Yes
Is Me Above or Below the previous mentioned boundaries?
Below
Above
Linear Interpolation using the 2 selected points to obtain a value of Mm and ejector size, entrainment and compression ratios for point with pretended Me, Pc, Pe, Pc.
Consider the entrainment ratio for the pretended Pm, Pe and Pc equal to the entrainment ratio of one of the 2 selected points with the highest Pc.
Consider the entrainment ratio for the pretended Pm, Pe and Pc equal to the lowest entrainment ratio from the 2 select points with the lowest Pc.
Was a flag raised to consider calculations accounting compression ratios near the extremes?
Was a flag raised to consider calculations accounting compression ratios near the Extremes?
(Was a flag raised to consider calculations accounting compression ratios near the Extremes)?
No
Yes
Calculate average growth rate of the entrainment ratio between the 2 selected points (which have different Pc, being one higher than the pretended Pc and the other lower).
Pretended Pc larger than Pc from previously selected point?
Calculate max. allowed entrainment ratio for the pretended Pc with average growth rate for the entrainment ratio.
Use ratio between pretended Me and the Mm described for the point with the highest Pc to calculate ejector size.
Consider Pc equal to Pc from previously selected point
Use ratio between pretended Me and the Mm described for the point with the lowest Pc to calculate ejector size.
Is entrainment ratio below min. limit?
Reduce Pc
Continue with a Warning.
Flag TVC operation as impossible with given inputs.
Return to calling program and restart calculations with new corrections made.
Flag 1st NCG Steam Ejector calculation as possible with the given inputs
End Steam Ejectors Performance Model

Annex 4 – Diagram: Rankine Cycle Subroutine in Cogeneration with a MED plant

Table 35 - List of main inputs for Rankine cycle subroutine

Parameter/Variable	Units	Description
d_Cross_flow_flag	-	Flag indicating the existance of CROSS-FLOW for the distillate routing
E_mass_concentr_NCG	g/m3	Concentration of NCG in the seawater
E_mass_safe_NCG	-	Safety Factor of total mass of NCG to be ejected
E_Pcw_2	Pa	Pressure at which the cooling water is pumpued through the 2nd intercondenser of the NCG ejection system
E_Pm	Pa	Motive steam pressure used to power both steam ejectors
E_T_approach_cond	ºC	Temperature approach between Feedwater outlet temperature and saturated vapor pressure inside condenser receiving gases from the 1st NCG steam ejector (Assuming a 2 stage NCG steam ejection system
E_Tcw_out_2	ºC	Temperature outlet of the cooling water used in the 2nd intercondenser
eph_flag	-	Flag indicating if the plant has feedwater preheaters, and if so, if they are they placed
IN_Plant_distance	m	Plant Distance to the Intake
IN_velocity_sw	m/s	Velocity of Seawater inside intake pipe
Mb	kg/s	Brine Total Mass flow rate flowing out of the MED plant
MC_T_approach	ºC	Temperature approach between Steam temperature and cooling water outlet in the SWCC Main Condenser
MED_max_Qdes_frac	-	Maximum fraction of the design rejected steam produced by the steam turbine allowed to power the MED plant
MED_min_Qdes_frac	-	Minimum fraction of the design rejected steam produced by the steam turbine allowed to power the MED plant
MED_Mm	kg/s	Mass flow of motive steam powering the MED plant, except steam used for NCG steam ejectors
MED_Qdes_frac	-	Fraction of the rejected heat by the steam turbine from which the MED plant should be dimentioned
MED_Qs_design	-	Heat load used to dimention the MED plant for nominal conditions
MED_Tf	ºC	Temperature of feedwater leaving the down condenser of the MED plant (outlet temp of cooling water)
MED_Ts_sat	ºC	Temperature of Saturated Steam from the turbine (if no TVC) or from the TVC discharge.
n	-	Total number of effects on the MED plant
n_ph_NCG	-	Number of the effect from where it is assumed that the external preheating of the feedwater will be suported by NCG steam extraction
OUT_Plant_distance	m	Plant Distance to the Outlet
OUT_velocity_sw	m/s	Velocity of Seawater/brine inside outlet pipe
plant_elev_sea_level	m	Site elevation (where MED plant is installed) compared with sea level
pre_PlateHTX_flag	-	Flag indicating if the plate heat exchanger preheaters of the feedwater entering the down condenser are present or not
pre_Tsw_out	ºC	Temperature of the seawater leaving the plate heat exchangers
Q_Loss	%	Ratio of the total heat load loss in average per effect with extra thermodynamic losses compared with heat load from first effect
STOR_distance	m	Distance between MED down condenser and distillate Storage tank
STOR_tank_height	m	Heigh of storage tank (taking as reference the MED plant elevation and not the sea level)
T_cond_ref	ºC	Condenser temperature related to the "Rated cycle conversion efficiency" set as input
Tbn	ºC	Temperature of brine inside the last effect of the MED plant
Tf1	ºC	Feedwater temperature entering the first effect
tolerance	-	Tolerance used to reach an equilibrium with the MED model from El-Dessouky
Ts _sat	ºC	Saturated Temperature of steam assumed to run the simulations
Tsw	ºC	Temperature of Seawater used in MED plant at each iteration
Tsw_Jan	ºC	Temperature of Seawater during begining of January
Tsw_Jul	ºC	Temperature of Seawater during middle of July
Tv_Loss	ºC	Average temperature Loss with pressure losses assumed to occur when the vapour formed inside each effects flows into the HTX tubes of the next effect until it reaches the distillate box of the next effect

Tv1	ºC	Vapor temperature in the first effect
TVC_Mm_des	kg/s	Mass flow of motive steam extracted from the turbine to power the TVC at design point
TVC_pct_steam_ext	%	Ratio of steam extracted from an intermediate point from the turbines of the rankine cycle, relative to the total mass of steam that enters the high pressure turbine at design conditions
TVC_Pm	Pa	ressure at which steam powering the MED-TVC plant is extracted from the Turbine
TVC_Strategy	-	Flag indicating how the TVC is to be dimensioned
Tvn	ºC	Temperature of Vapor in the last effect
Xb1	wt%	Salinity concentration predefined to be assumed when starting iterations to calculate mass flow rate of feedwater needed for the 1st effect
Xbn_max	wt%	Maximum allowed Salinity concentration of the brine produced in the last effect
Xsw	wt%	Salinity concentration of the seawater entering the MED plant

Table 36 - List of main outputs for Rankine cycle subroutine

Parameter/Variable	Units	Description
Am	m2	Average heat transfer area per effect
E_Mm_tot	t/h	Total Mass flow rate of motive steam powering all the ejectors
eta_adj_des	-	Rankine cycle efficiency at design point adjusted to the curves available to SAM's database
eta_adj_ref	-	Rankine cycle efficiency at reference point adjusted to the curves available to SAM's database
eta_des	-	Rankine cycle efficiency at design point for the actual rankine cycle described by the user at Ts temperature
MC_Mcw	kg/s	Total mass flow of cooling water used in the SWCC Main Condenser
MC_Mm	kg/s	Total mass flow of motive steam leaving the low pressure turbine entering the SWCC.
MC_Qs	kW	Heat Load transfered into the SWCC Main Condenser
MC_Total_pump_e	W	Total electrical consumptiomn with pumping just with the SWCC Main Condenser
MC_W_dot_pump	W	Total electrical consumption necessary to pump water inside the SWCC main condenser ONLY
Md	kg/s	Distillate Total Mass flow rate flowing out of the MED plant
MED_Mcw	kg/s	Mass flow rate of cooling water REJECTED directly into the sea after passing through the MED down condenser
MED_Qs	kW	Heat load delivered by the motive steam powering the MED plant
MED_SWCC_Total_pump_e	W	Total electrical consumption with water pumping using both MED and SWCC systems combined (Includes also pumping from and to the sea)
MED_Total_pump_e	W	Total pumping wihin the MED plant (excluding pumping from and back to the sea)
Mf	kg/s	Total Mass flow of feedwater entering the 1st effect of the MED plant
Mm_out	kg/s	Total mass flow of steam leaving the low pressure steam turbine
q_pb_reject_design	kW	Total amount of heat rejected by the rankine cycle for nominal conditions
q_reject	kW	Total amount of heat rejected by the rankine cycle at each time step
sA	-	Specific heat transfer area of the MED plant
sMcw	-	Specific cooling water flow rate of the MED plant
Tsw_avg	ºC	Average temperature of the seawater during the year, used to dimention the MED plant
TVC_Mm	kg/s	Mass flow of motive steam extracted from the turbine to power the TVC at each time step

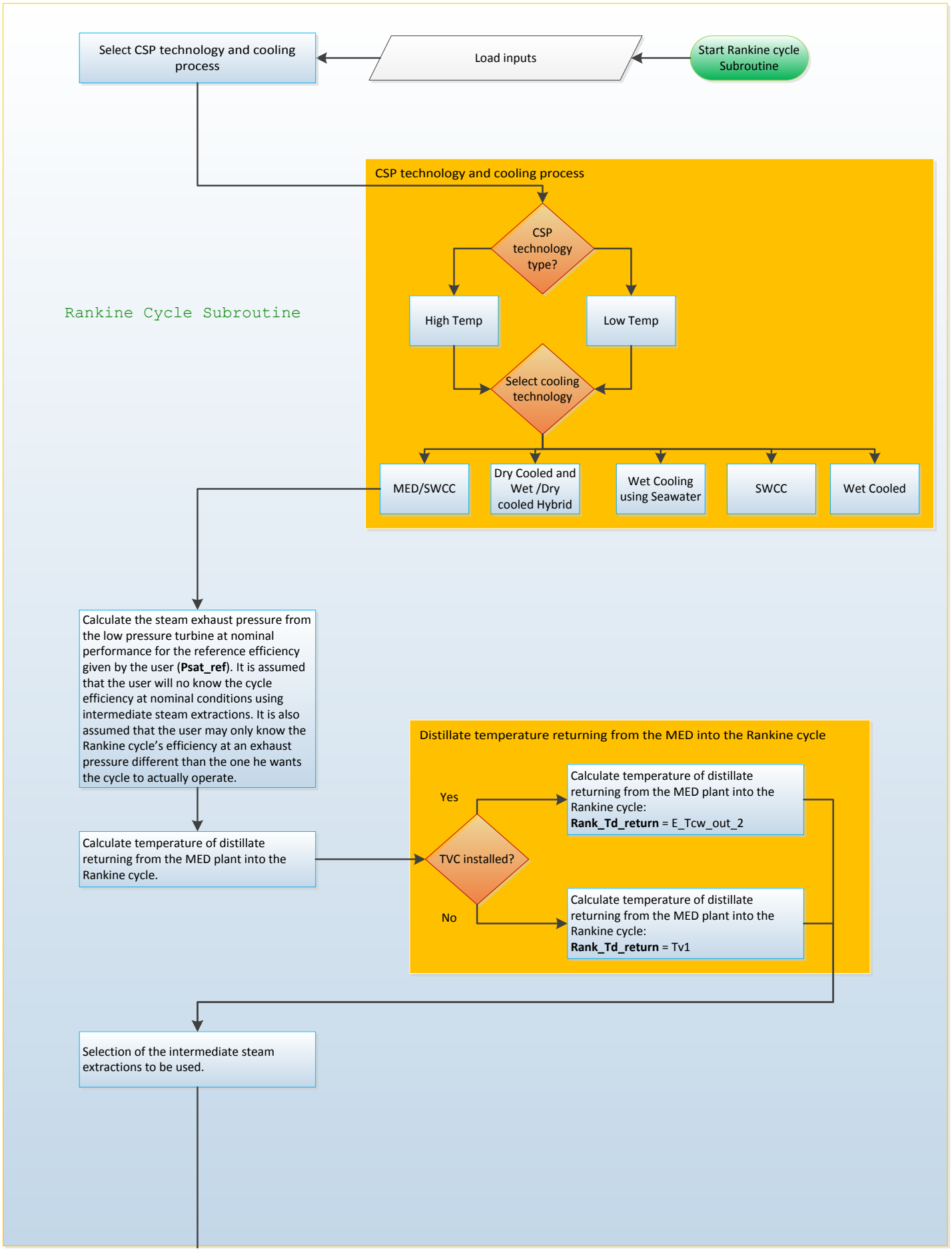
Select CSP technology and cooling process
Load inputs
Start Rankine cycle Subroutine
Rankine Cycle Subroutine
CSP technology and cooling process
CSP technology type?
High Temp
Low Temp
Select cooling technology
MED/SWCC
Dry Cooled and Wet /Dry cooled Hybrid
Wet Cooling using Seawater
SWCC
Wet Cooled
Calculate the steam exhaust pressure from the low pressure turbine at nominal performance for the reference efficiency given by the user (Psat_ref). It is assumed that the user will no know the cycle efficiency at nominal conditions using intermediate steam extractions. It is also assumed that the user may only know the Rankine cycle's efficiency at an exhaust pressure different than the one he wants the cycle to actually operate.
Calculate temperature of distillate returning from the MED plant into the Rankine cycle.
Distillate temperature returning from the MED into the Rankine cycle
Yes
TVC installed?
No
Calculate temperature of distillate returning from the MED plant into the Rankine cycle:
Rank_Td_return = E_Tcw_out_2
Calculate temperature of distillate returning from the MED plant into the Rankine cycle:
Rank_Td_return = Tv1
Selection of the intermediate steam extractions to be used.

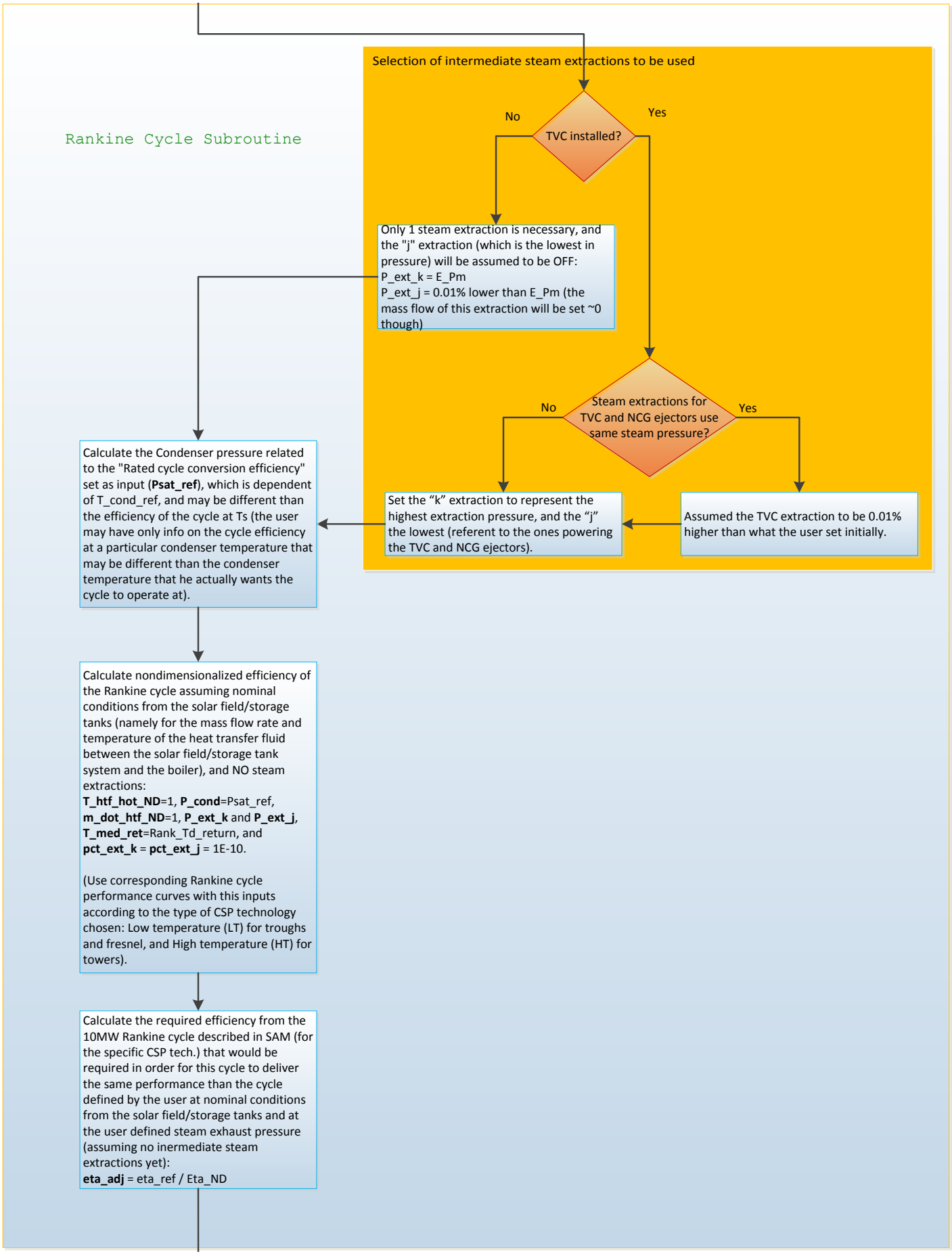
Rankine Cycle Subroutine
Selection of intermediate steam extractions to be used
TVC installed?
No
Yes
Only 1 steam extraction is necessary, and the "j" extraction (which is the lowest in pressure) will be assumed to be OFF:
P_ext_k = E_Pm
P_ext_j = 0.01% lower than E_Pm (the mass flow of this extraction will be set ~0 though)
Steam extractions for TVC and NCG ejectors use same steam pressure?
No
Yes
Set the “k” extraction to represent the highest extraction pressure, and the “j” the lowest (referent to the ones powering the TVC and NCG ejectors).
Assumed the TVC extraction to be 0.01% higher than what the user set initially.
Calculate the Condenser pressure related to the "Rated cycle conversion efficiency" set as input (Psat_ref), which is dependent of T_cond_ref, and may be different than the efficiency of the cycle at Ts (the user may have only info on the cycle efficiency at a particular condenser temperature that may be different than the condenser temperature that he actually wants the cycle to operate at).
Calculate nondimensionalized efficiency of the Rankine cycle assuming nominal conditions from the solar field/storage tanks (namely for the mass flow rate and temperature of the heat transfer fluid between the solar field/storage tank system and the boiler), and NO steam extractions:
T_htf_hot_ND=1, P_cond=Psat_ref, m_dot_htf_ND=1, P_ext_k and P_ext_j, T_med_ret=Rank_Td_return, and pct_ext_k = pct_ext_j = 1E-10.
(Use corresponding Rankine cycle performance curves with this inputs according to the type of CSP technology chosen: Low temperature (LT) for troughs and fresnel, and High temperature (HT) for towers).
Calculate the required efficiency from the 10MW Rankine cycle described in SAM (for the specific CSP tech.) that would be required in order for this cycle to deliver the same performance than the cycle defined by the user at nominal conditions from the solar field/storage tanks and at the user defined steam exhaust pressure (assuming no inermediate steam extractions yet):
eta_adj = eta_ref / Eta_ND

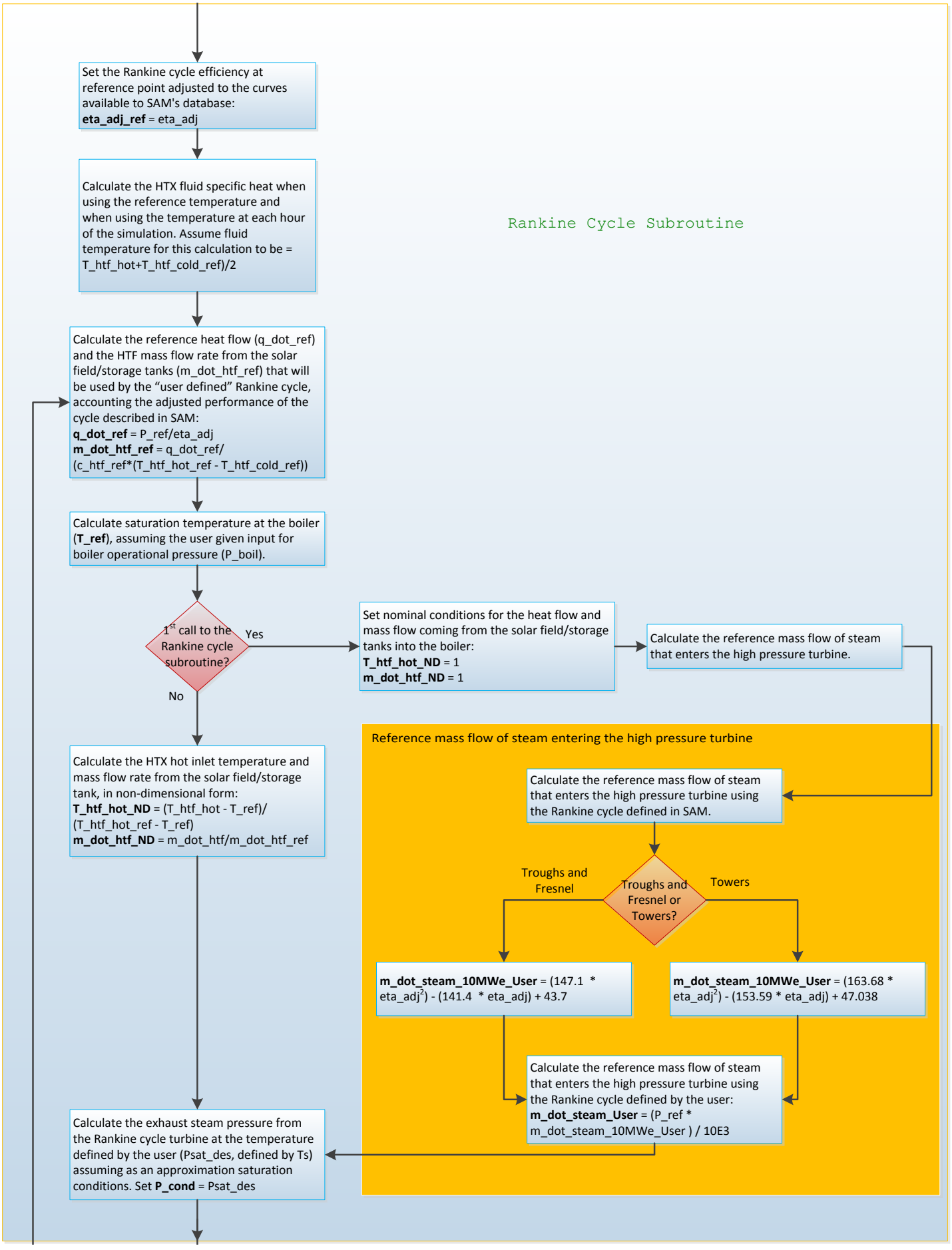
Rankine Cycle Subroutine
Set the Rankine cycle efficiency at reference point adjusted to the curves available to SAM's database:
eta_adj_ref = eta_adj
Calculate the HTX fluid specific heat when using the reference temperature and when using the temperature at each hour of the simulation. Assume fluid temperature for this calculation to be = T_htf_hot+T_htf_cold_ref)/2
Calculate the reference heat flow (q_dot_ref) and the HTF mass flow rate from the solar field/storage tanks (m_dot_htf_ref) that will be used by the "user defined" Rankine cycle, accounting the adjusted performance of the cycle described in SAM:
q_dot_ref = P_ref/eta_adj
m_dot_htf_ref = q_dot_ref/ (c_htf_ref*(T_htf_hot_ref - T_htf_cold_ref))
Calculate saturation temperature at the boiler (**T_ref**), assuming the user given input for boiler operational pressure (P_boil).
1st call to the Rankine cycle subroutine?
Yes
No
Set nominal conditions for the heat flow and mass flow coming from the solar field/storage tanks into the boiler:
T_htf_hot_ND = 1
m_dot_htf_ND = 1
Calculate the reference mass flow of steam that enters the high pressure turbine.
Calculate the HTX hot inlet temperature and mass flow rate from the solar field/storage tank, in non-dimensional form:
T_htf_hot_ND = (T_htf_hot - T_ref)/ (T_htf_hot_ref - T_ref)
m_dot_htf_ND = m_dot_htf/m_dot_htf_ref
Reference mass flow of steam entering the high pressure turbine
Calculate the reference mass flow of steam that enters the high pressure turbine using the Rankine cycle defined in SAM.
Troughs and Fresnel or Towers?
Troughs and Fresnel
Towers
m_dot_steam_10MWe_User = (147.1 * eta_adj^2) - (141.4 * eta_adj) + 43.7
m_dot_steam_10MWe_User = (163.68 * eta_adj^2) - (153.59 * eta_adj) + 47.038
Calculate the reference mass flow of steam that enters the high pressure turbine using the Rankine cycle defined by the user:
m_dot_steam_User = (P_ref * m_dot_steam_10MWe_User) / 10E3
Calculate the exhaust steam pressure from the Rankine cycle turbine at the temperature defined by the user (Psat_des, defined by Ts) assuming as an approximation saturation conditions. Set **P_cond** = Psat_des

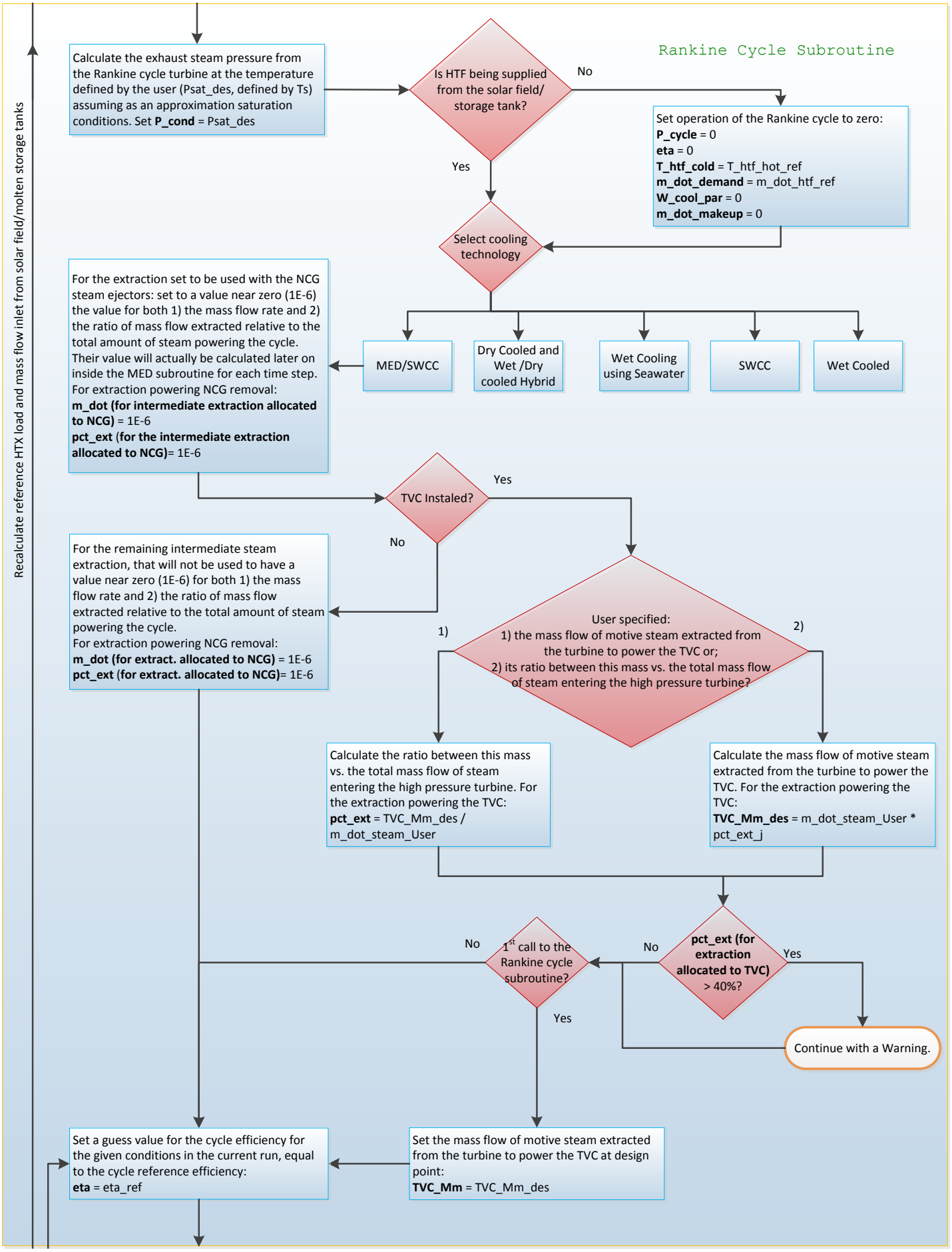
Rankine Cycle Subroutine
Recalculate reference HTX load and mass flow inlet from solar field/molten storage tanks
Calculate the exhaust steam pressure from the Rankine cycle turbine at the temperature defined by the user (Psat_des, defined by Ts) assuming as an approximation saturation conditions. Set **P_cond** = Psat_des
Is HTF being supplied from the solar field/ storage tank?
No
Yes
Set operation of the Rankine cycle to zero:
P_cycle = 0
eta = 0
T_htf_cold = T_htf_hot_ref
m_dot_demand = m_dot_htf_ref
W_cool_par = 0
m_dot_makeup = 0
Select cooling technology
MED/SWCC
Dry Cooled and Wet /Dry cooled Hybrid
Wet Cooling using Seawater
SWCC
Wet Cooled
For the extraction set to be used with the NCG steam ejectors: set to a value near zero (1E-6) the value for both 1) the mass flow rate and 2) the ratio of mass flow extracted relative to the total amount of steam powering the cycle. Their value will actually be calculated later on inside the MED subroutine for each time step.
For extraction powering NCG removal:
m_dot (for intermediate extraction allocated to NCG) = 1E-6
pct_ext (for the intermediate extraction allocated to NCG)= 1E-6
TVC Instaled?
Yes
No
For the remaining intermediate steam extraction, that will not be used to have a value near zero (1E-6) for both 1) the mass flow rate and 2) the ratio of mass flow extracted relative to the total amount of steam powering the cycle.
For extraction powering NCG removal:
m_dot (for extract. allocated to NCG) = 1E-6
pct_ext (for extract. allocated to NCG)= 1E-6
User specified:
1) the mass flow of motive steam extracted from the turbine to power the TVC or;
2) its ratio between this mass vs. the total mass flow of steam entering the high pressure turbine?
1)
2)
Calculate the ratio between this mass vs. the total mass flow of steam entering the high pressure turbine. For the extraction powering the TVC:
pct_ext = TVC_Mm_des / m_dot_steam_User
Calculate the mass flow of motive steam extracted from the turbine to power the TVC. For the extraction powering the TVC:
TVC_Mm_des = m_dot_steam_User * pct_ext_j
pct_ext (for extraction allocated to TVC) > 40%?
No
Yes
1st call to the Rankine cycle subroutine?
No
Yes
Continue with a Warning.
Set a guess value for the cycle efficiency for the given conditions in the current run, equal to the cycle reference efficiency:
eta = eta_ref
Set the mass flow of motive steam extracted from the turbine to power the TVC at design point:
TVC_Mm = TVC_Mm_des

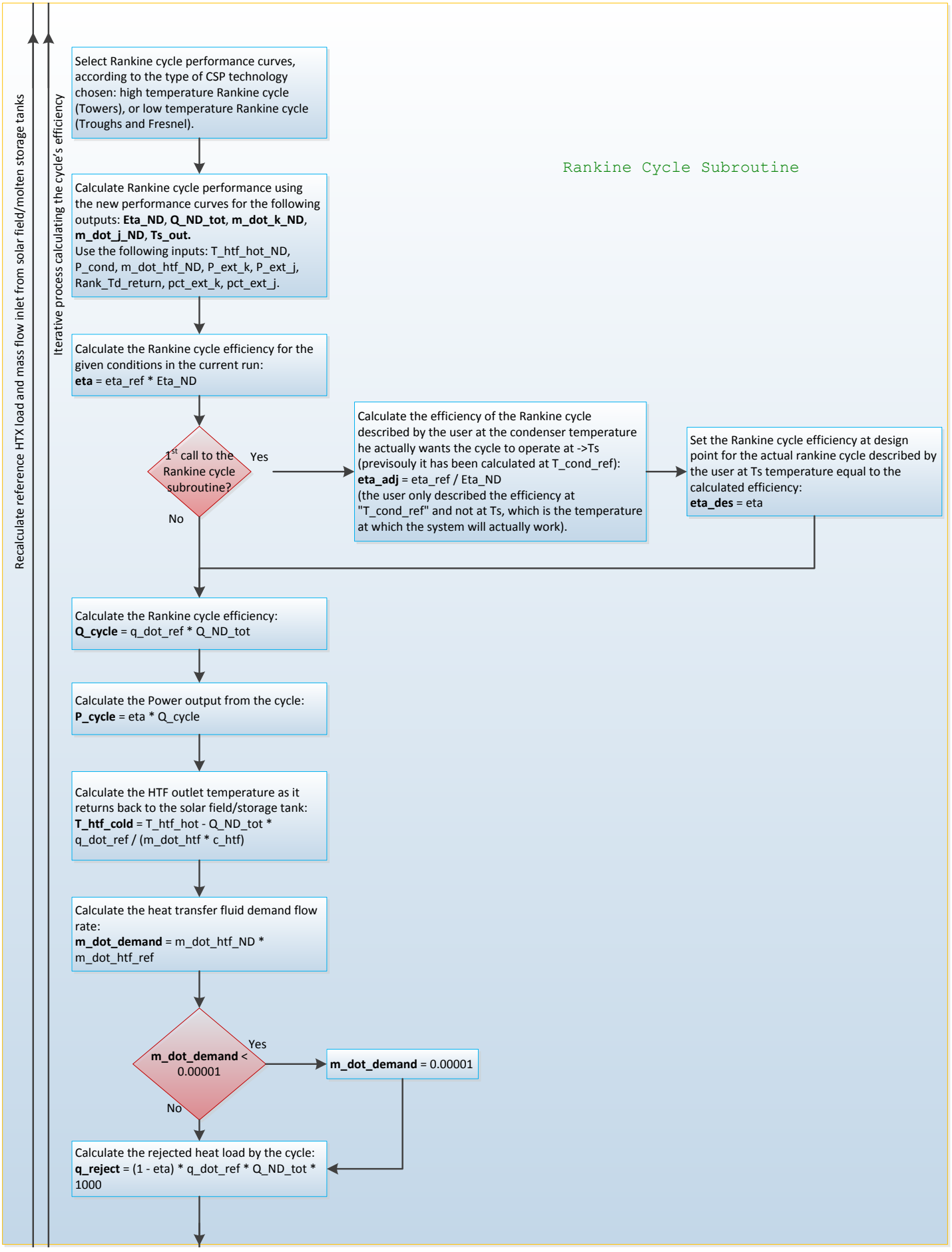
Rankine Cycle Subroutine
Recalculate reference HTX load and mass flow inlet from solar field/molten storage tanks
Iterative process calculating the cycle's efficiency
Select Rankine cycle performance curves, according to the type of CSP technology chosen: high temperature Rankine cycle (Towers), or low temperature Rankine cycle (Troughs and Fresnel).
Calculate Rankine cycle performance using the new performance curves for the following outputs: Eta_ND, Q_ND_tot, m_dot_k_ND, m_dot_j_ND, Ts_out.
Use the following inputs: T_htf_hot_ND, P_cond, m_dot_htf_ND, P_ext_k, P_ext_j, Rank_Td_return, pct_ext_k, pct_ext_j.
Calculate the Rankine cycle efficiency for the given conditions in the current run:
eta = eta_ref * Eta_ND
1st call to the Rankine cycle subroutine?
Yes
No
Calculate the efficiency of the Rankine cycle described by the user at the condenser temperature he actually wants the cycle to operate at ->Ts (previsouly it has been calculated at T_cond_ref):
eta_adj = eta_ref / Eta_ND
(the user only described the efficiency at "T_cond_ref" and not at Ts, which is the temperature at which the system will actually work).
Set the Rankine cycle efficiency at design point for the actual rankine cycle described by the user at Ts temperature equal to the calculated efficiency:
eta_des = eta
Calculate the Rankine cycle efficiency:
Q_cycle = q_dot_ref * Q_ND_tot
Calculate the Power output from the cycle:
P_cycle = eta * Q_cycle
Calculate the HTF outlet temperature as it returns back to the solar field/storage tank:
T_htf_cold = T_htf_hot - Q_ND_tot * q_dot_ref / (m_dot_htf * c_htf)
Calculate the heat transfer fluid demand flow rate:
m_dot_demand = m_dot_htf_ND * m_dot_htf_ref
m_dot_demand < 0.00001
Yes
No
m_dot_demand = 0.00001
Calculate the rejected heat load by the cycle:
q_reject = (1 - eta) * q_dot_ref * Q_ND_tot * 1000

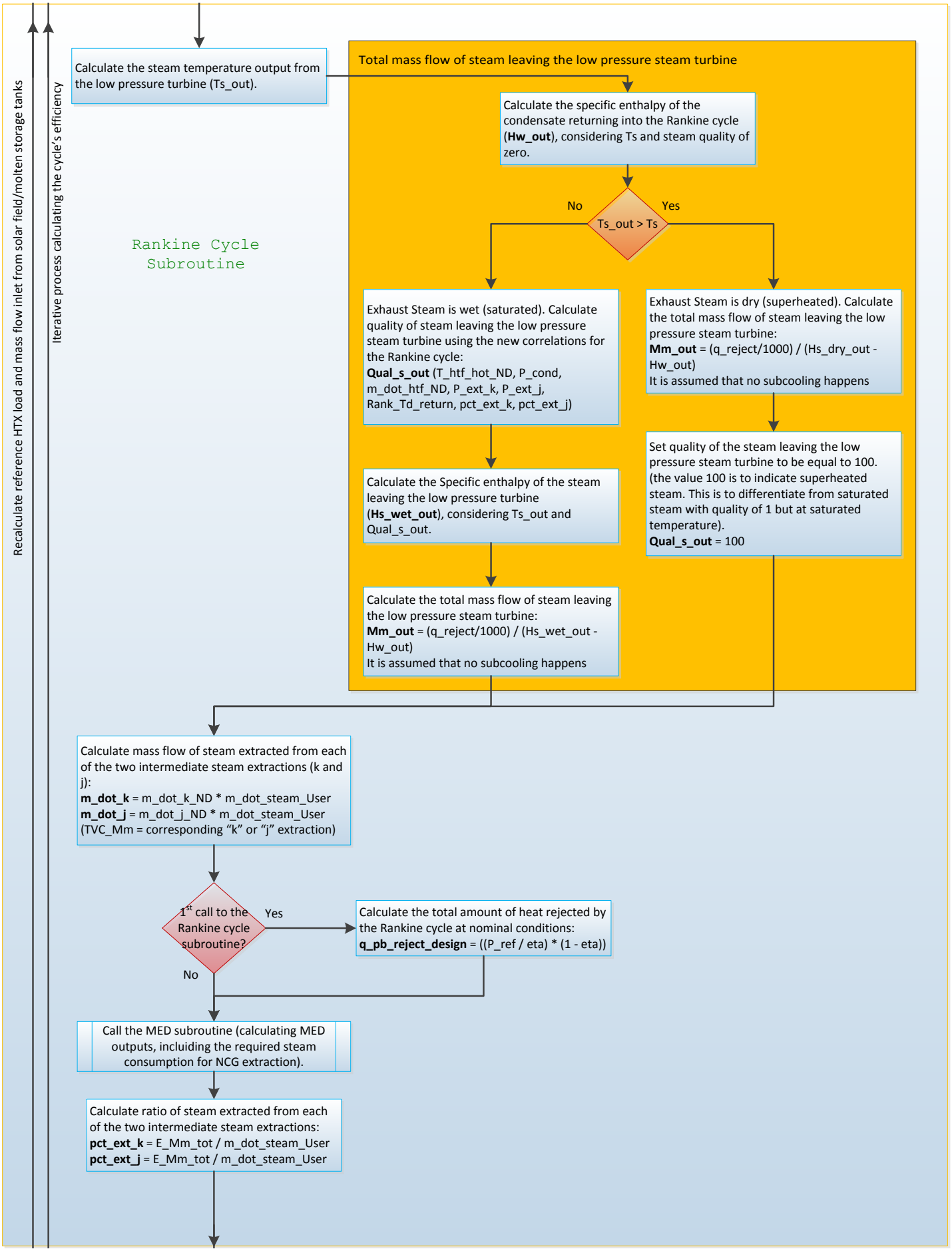
Recalculate reference HTX load and mass flow inlet from solar field/molten storage tanks
Iterative process calculating the cycle's efficiency
Rankine Cycle Subroutine
Calculate the steam temperature output from the low pressure turbine (Ts_out).
Total mass flow of steam leaving the low pressure steam turbine
Calculate the specific enthalpy of the condensate returning into the Rankine cycle (Hw_out), considering Ts and steam quality of zero.
No
Yes
Ts_out > Ts
Exhaust Steam is wet (saturated). Calculate quality of steam leaving the low pressure steam turbine using the new correlations for the Rankine cycle:
Qual_s_out (T_htf_hot_ND, P_cond, m_dot_htf_ND, P_ext_k, P_ext_j, Rank_Td_return, pct_ext_k, pct_ext_j)
Exhaust Steam is dry (superheated). Calculate the total mass flow of steam leaving the low pressure steam turbine:
Mm_out = (q_reject/1000) / (Hs_dry_out - Hw_out)
It is assumed that no subcooling happens
Calculate the Specific enthalpy of the steam leaving the low pressure turbine (Hs_wet_out), considering Ts_out and Qual_s_out.
Set quality of the steam leaving the low pressure steam turbine to be equal to 100. (the value 100 is to indicate superheated steam. This is to differentiate from saturated steam with quality of 1 but at saturated temperature).
Qual_s_out = 100
Calculate the total mass flow of steam leaving the low pressure steam turbine:
Mm_out = (q_reject/1000) / (Hs_wet_out - Hw_out)
It is assumed that no subcooling happens
Calculate mass flow of steam extracted from each of the two intermediate steam extractions (k and j):
m_dot_k = m_dot_k_ND * m_dot_steam_User
m_dot_j = m_dot_j_ND * m_dot_steam_User
(TVC_Mm = corresponding "k" or "j" extraction)
1st call to the Rankine cycle subroutine?
Yes
No
Calculate the total amount of heat rejected by the Rankine cycle at nominal conditions:
q_pb_reject_design = ((P_ref / eta) * (1 - eta))
Call the MED subroutine (calculating MED outputs, incluiding the required steam consumption for NCG extraction).
Calculate ratio of steam extracted from each of the two intermediate steam extractions:
pct_ext_k = E_Mm_tot / m_dot_steam_User
pct_ext_j = E_Mm_tot / m_dot_steam_User

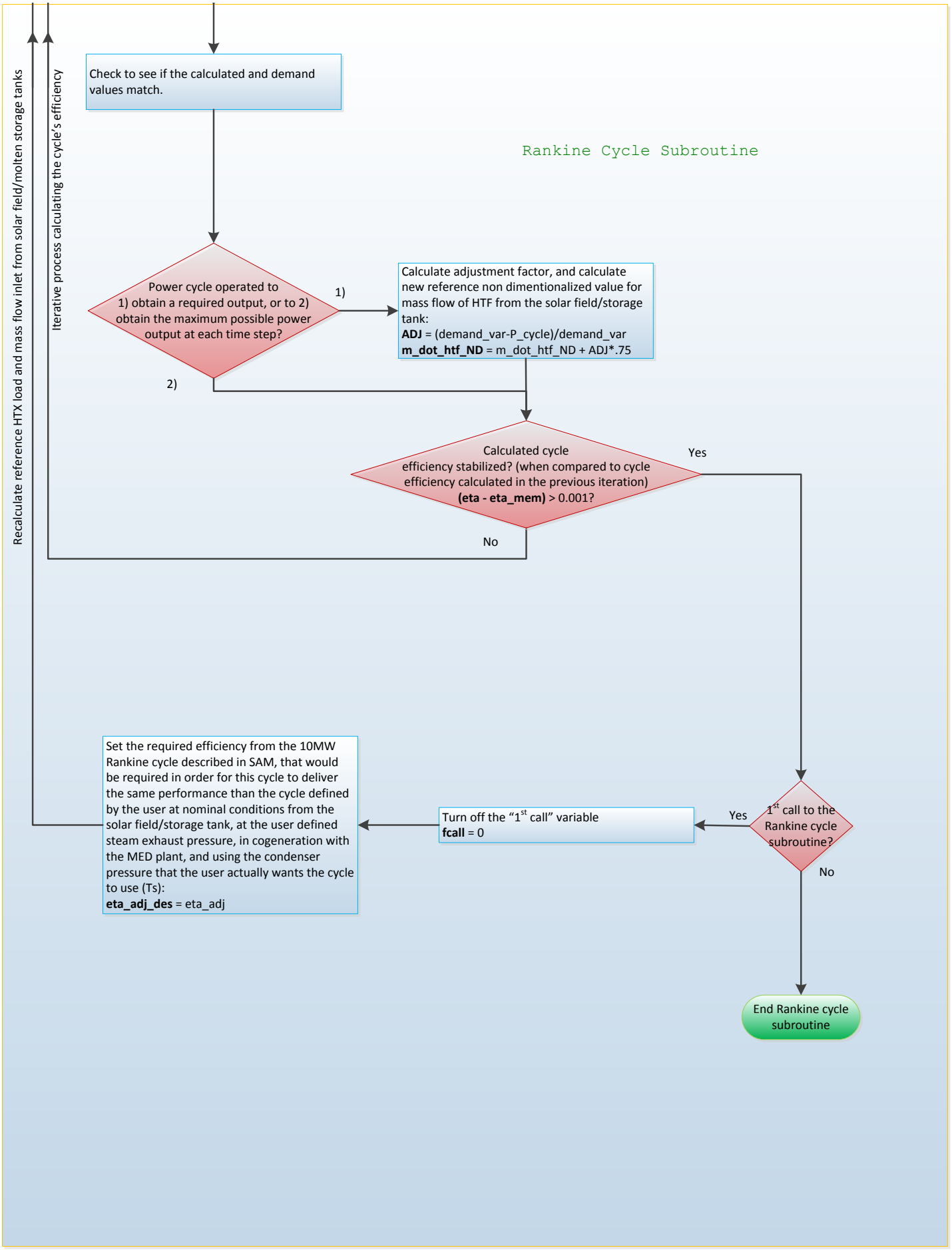
Rankine Cycle Subroutine
Recalculate reference HTX load and mass flow inlet from solar field/molten storage tanks
Iterative process calculating the cycle's efficiency
Check to see if the calculated and demand values match.
Power cycle operated to 1) obtain a required output, or to 2) obtain the maximum possible power output at each time step?
1)
2)
Calculate adjustment factor, and calculate new reference non dimentionalized value for mass flow of HTF from the solar field/storage tank:
ADJ = (demand_var-P_cycle)/demand_var
m_dot_htf_ND = m_dot_htf_ND + ADJ*.75
Calculated cycle efficiency stabilized? (when compared to cycle efficiency calculated in the previous iteration)
(eta - eta_mem) > 0.001?
Yes
No
1st call to the Rankine cycle subroutine?
Yes
No
Turn off the "1st call" variable
fcall = 0
Set the required efficiency from the 10MW Rankine cycle described in SAM, that would be required in order for this cycle to deliver the same performance than the cycle defined by the user at nominal conditions from the solar field/storage tank, at the user defined steam exhaust pressure, in cogeneration with the MED plant, and using the condenser pressure that the user actually wants the cycle to use (Ts):
eta_adj_des = eta_adj
End Rankine cycle subroutine

Annex 5 – Main Inputs and Outputs to/from SAM's New Solar Desalination Add-on

Table 37 - List of main inputs into SAM's new solar desalination Add-on

Parameter/Variable	Units	Description
CSP plant:		
Cool_type	-	Flag indicating which type of Cooling technology is set to be used
demand_var	-	Control signal indicating operational mode
m_dot_htf	kg/s	HTF mass flow rate from solar field / molten storage tank
mode	-	Cycle part load control, from plant controller
P_amb	Pa	Ambient pressure
standby_control	-	Control signal indicating standby mode
T_db	ºC	Ambient dry bulb temperature
T_htf_hot	ºC	Hot HTF inlet temperature, from solar field/ molten storage tank
T_wb	ºC	Ambient wet bulb temperature
MED Plant:		
d_Cross_flow_flag	-	Flag indicating the existance of CROSS-FLOW for the distillate routing.
E_mass_concentr_NCG	g/m3	Concentration of NCG in the seawater
E_mass_safe_NCG	-	Safety Factor of total mass of NCG to be ejected
E_Pcw_2	Pa	Pressure at which the cooling water is pumpued through the 2nd intercondenser
E_Pm	Pa	Pressure of Motive steam extracted from the turbine to power the steam
E_T_approach_cond	ºC	Temperature approach between Feedwater outlet temperature and saturated vapor pressure inside condenser receiving gases from the 1st NCG steam ejector
E_Tcw_out_2	ºC	Temperature outlet of the cooling water used in the 2nd intercondenser.
eph_flag	-	Flag indicating if the plant has feedwater preheaters, and if so, were are they
IN_Plant_distance	m	Distance between MED plant and intake of the tube bringing seawater into the
IN_velocity_sw	m/s	Velocity of the seawater inside the tube bringing seawater into the MED plant
MC_only_Ts	°C	Temperature of Steam powering the SWCC system.
MC_T_approach	°C	Temperature approach between Steam temperature and cooling water outlet in
MED_max_Qdes_frac	-	Maximum fraction of the design rejected steam produced by the steam turbine
MED_min_Qdes_frac	-	Minimum fraction of the design rejected steam produced by the steam turbine allowed to power the MED plant (comparing to the load at 100% of design for the
MED_Mm	kg/s	Mass flow of steam powering the MED plant, except steam used for NCG steam ejectors (entering the TVC if one exists, or entering directly the 1st effect if not
MED_Qdes_frac	-	Fraction of the rejected heat by the steam turbine from which the MED plant
MED_ReStart_t	h	Time taken by the MED plant to restart
MED_Tf	°C	Temperature of Feedwater leaving the down condenser.
MED_Ts_sat	ºC	Temperature of Saturated Steam from the turbine (if no TVC) or from the TVC
n	-	number of effects in the desalination MED system (used as cooling for the
n_ph_NCG	-	Number of the effect from where it is assumed that the external preheating of
OUT_Plant_distance	m	Distance between MED plant and end of the tube taking the brine back into the
OUT_velocity_sw	m/s	Velocity of the brine inside the tube taking brine back to the sea
plant_elev_sea_level	m	Site elevation (where MED plant is installed) compared with sea level
pre_PlateHTX_flag	-	Flag indicating if the plate heat exchanger preheaters of the feedwater entering
pre_Tsw_out	ºC	Temperature of the seawater leaving the plate heat exchangers
Q_Loss	-	Ratio of the total heat load loss in average per effect with extra thermodynamic losses compared with heat load from first effect (surroundings, demister,
Qs_Loss_frac_iph_1st	-	Ratio of the total heat load necessary to preheat the feed water inside the first effect up to saturation conditions (compared with heat load delivered by
STOR_distance	m	Storage tank distance to the MED plant
STOR_tank_height	m	Distillate Storage tank height
T_cond_ref	ºC	Condenser temperature related to the "Rated cycle conversion efficiency" set as
Tsw_Jan	°C	Temperature of Seawater during begining of January (assumed to be either the
Tsw_Jul	°C	Temperature of Seawater during middle of July (assumed to be either the max or

Tv_Loss	°C	Average temperature Loss with pressure losses assumed to occur when the vapour formed inside each effects flows into the HTX tubes of the next effect
Tv1	ºC	Vapor temperature in the first effect (input cannot be an array)
TVC_pct_steam_ext	%	Ratio of steam extracted from an intermediate point from the turbines of the rankine cycle, relative to the total mass of steam that enters the high pressure
TVC_Pm	Pa	Pressure at which steam powering the MED-TVC plant is extracted from the
TVC_Strategy	-	Flag indicating how the TVC is to be dimensioned considering the compression
Tvn	°C	Temperature of Vapor in the last effect
Xb1	wt%	Salinity concentration predefined to be assumed when starting iterations to
Xbn	wt%	Salinity of brine leaving the last effect
Xbn_max	wt%	Maximum allowed Salinity concentration of the brine produced in the last effect
Xsw	wt%	Salinity concentration of the seawater entering the MED plant

Table 38 - List of main outputs from SAM's new solar desalination Add-on

Parameter/Variable	Units	Description
m_dot_htf_ref	kg/h	Calculated reference htf flow rate
m_dot_htf	kg/h	Heat transfer fluid flow rate
Am	m2	Average heat transfer area per MED effect
Calc_NCG_ej	-	Flag indicating if any of the ratios available to calculate the performance of NCG was applicable to the current simulation
Cool_type	-	Type of Cooling technology is set to use
CSP Tank anti-freeze	MWe	Parasitics with CSP tank anti freeze protection system
CSP_operating_time	h	Fraction of the time step operated in which the CSP plant was online
CSP_Startup	-	Total number of startups in one year by the CSP plant
E_net	MWe	Net Power Output
EJ_Mp_tot	t/h	mass flow rate of motive steam used to power NCG steam ejectors
eta	-	Rankine Cycle efficiency at each time step
eta_adj_des	-	Rankine cycle efficiency at design point adjusted to the curves available to SAM's database
eta_adj_ref	-	Rankine cycle efficiency at reference point adjusted to the curves available to SAM's database
Mb	m3/h	Brine Total Mass flow rate flowing out of the MED plant
MC_Mcw	m3/h	Cooling water used by the SWCC
MC_Ms	t/h	Mass flow of steam condensed by the SWCC
MC_Qs	MWt	Heat load absorbed by the SWCC
MC_Total_pump_elect	MWe	Total electrical consumption with pumping just with the SWCC Main Condenser
MC_W_dot_pump	MWe	Total electrical consumption necessary to pump water inside the SWCC main condenser ONLY
Md	m3/h	Distillate Total Mass flow rate flowing out of the MED plant
Md_w_Rank_Blowdown_loss	m3/h	Losses of distillate with blowdown from the rankine cycle
MED_max_Qdes	MWt	Maximum fraction of the design rejected steam produced by the steam turbine allowed to power the MED plant
MED_Mcw	m3/h	Mass flow rate of cooling water REJECTED directly into the sea after passing through the MED down condenser
MED_min_Qdes	MWt	Minimum fraction of the design rejected steam produced by the steam turbine allowed to power the MED plant
MED_Ms	t/h	Mass flow of steam used to power the first MED effect
MED_operating_time	h	Fraction of the time step operated in which the CSP plant was online
MED_Qs	MWt	Heat load delivered by the motive steam powering the MED plant
MED_Qs_design	MWt	Heat load used to dimention the MED plant for nominal conditions
MED_Startup	-	Total number of startups in one year by the MED plant
MED_SWCC_Total_pump_e	MWe	Total electrical consumption with water pumping using both MED and SWCC systems combined
MED_Total_pump_e	MWe	Total pumping wihin the MED plant (excluding pumping from and back to the sea)
Mf	m3/h	Mass flow rate of feedwater into the MED
Ms_Total(MED_Ms+MC_Ms)	t/h	Total mass flow of steam used to power the CSP+MED/SWCC system
P_cond	Pa	Condenser pressure
P_Cycle	MWe	Gross Power output
Parasitics_CSP_only	MWe	Parasitics consumption for the CSP plant only
PR	(-)	Performance Ratio for the MED plant
Q_cycle	MWt	Heat load entering the high pressure turbine at each time step
q_pb_reject_design	MWt	Total amount of heat rejected by the rankine cycle for nominal conditions
q_reject	MWt	Total amount of heat rejected by the rankine cycle at each time step
sA	m2/(kg/	Specific heat transfer area of the MED plant
sMcw	(-)	Specific cooling water flow rate of the MED plant
T_htf_cold	ºC	Cold HTF outlet temperature to solar field/ molten from storage tank
Tsw	ºC	Seawater temperaure
Tsw_average	ºC	Average seawater temperature
W_cool_par	MWe	Parasitic electrical consumption with the standar cooling processes

Annex 6 – Correlations Describing the Performance of a Rankine Cycle for a CSP Plant in Cogeneration with a MED Unit

Table 39 - List of Rankine cycle performance curves for the high temperature Rankine cycle

HT_Eta					
f(X)=a_1*LN(T_htf_hot^2)+a_2*LN(Pc^2)+a_3*LN(T_ret^2)+a_4*j_ext+a_5*LN(P_ext_j)/P_ext_j+a_6/(T_htf_hot^3)+a_7*Pc^0.5+a_8/(m_dot_htf^3)+a_9*exp(m_dot_htf^2)+a_10/m_dot_htf+a_11/(1-(k_ext^2))+a_12*k_ext^k_ext+a_13/(1-(j_ext^2))+a_14*2^T_htf_hot+a_15*(1-T_htf_hot)^2+a_16*(1-j_ext)^2+a_17*LN(P_ext_k+1)+a_18*(1-k_ext)^2+a_19*LN(P_ext_j^2)+a_20/P_ext_j+a_21*2^j_ext+a_22/(P_ext_j^0.5)+a_23					
a(1)	5.976172596687E-02	a(10)	-3.259064733789E-02	a(19)	8.460007049803E-02
a(2)	-1.707674977008E-02	a(11)	-1.771050225951E-01	a(20)	1.220596173903E+06
a(3)	2.700695736842E-02	a(12)	-2.790883097041E-02	a(21)	2.454666848915E+01
a(4)	-2.703608672997E+01	a(13)	-1.464979848874E+00	a(22)	1.406093451312E+03
a(5)	-1.336850662537E+05	a(14)	-1.986675325649E-02	a(23)	-1.984945989169E+01
a(6)	3.587463693492E-04	a(15)	2.887094324073E-02	a(24)	0.000000000000E+00
a(7)	-1.542139503858E-04	a(16)	-4.843935878300E+00	a(25)	0.000000000000E+00
a(8)	5.875311037267E-04	a(17)	-4.004273822488E-02		
a(9)	-3.983660454218E-04	a(18)	2.957616478910E-01		

HT_Q					
f(X)=a_1/(m_dot_htf^2)+a_2*m_dot_htf^2+a_3*2^T_htf_hot+a_4*exp(T_htf_hot)+a_5*exp(m_dot_htf)+a_6*m_dot_htf^3+a_7/(T_ret^3)+a_8/(1-k_ext)+a_9/(T_ret^0.5)+a_10*2^k_ext+a_11*LN(Pc-1)+a_12/(1-j_ext)+a_13*exp(k_ext-1)+a_14*2^(-T_htf_hot)+a_15/(P_ext_k^0.5)+a_16*exp(m_dot_htf)/m_dot_htf+a_17*exp(k_ext^2)+a_18*exp(-(k_ext^2))+a_19*LN(T_htf_hot^2)+a_20/(m_dot_htf^3)+a_21/(m_dot_htf^0.5)+a_22*T_htf_hot^2+a_23					
b(1)	-6.503679531875E+01	b(10)	4.167774648671E+01	b(19)	-2.406457668944E-01
b(2)	-9.609212770272E+01	b(11)	-6.859706129893E-03	b(20)	6.370412031716E+00
b(3)	-3.212525016859E+02	b(12)	2.248976147010E-03	b(21)	-6.619809011045E+02
b(4)	6.437201855366E+01	b(13)	-3.039234318430E+01	b(22)	9.497789930944E+01
b(5)	-1.323176927143E+02	b(14)	-2.362002266819E+02	b(23)	3.625780697701E+02
b(6)	3.689153604106E+01	b(15)	2.193224965593E+00	b(24)	0.000000000000E+00
b(7)	-8.938184395619E+05	b(16)	4.195723333885E+02	b(25)	0.000000000000E+00
b(8)	-1.786075595606E+01	b(17)	6.579866774681E+01		
b(9)	2.457346904463E+00	b(18)	4.958969906331E+01		

HT_W					
f(X)=a_1/(Pc^3)+a_2/(P_ext_j^2)+a_3*j_ext^2+a_4*LN(1/P_ext_j)+a_5*LN(Pc+1)+a_6/T_htf_hot+a_7*m_dot_htf^m_dot_htf+a_8*T_htf_hot^0.5+a_9*LN(P_ext_k-1)+a_10/(1-(k_ext^2))+a_11/(T_htf_hot^0.5)+a_12*exp(m_dot_htf-1)+a_13/(1-j_ext)+a_14*sin(k_ext)+a_15/T_ret+a_16*exp(j_ext-1)+a_17*LN(1/m_dot_htf)+a_18*exp(-(j_ext^2))+a_19/(1-k_ext)+a_20*LN(Pc)/Pc+a_21*LN(1/T_htf_hot)+a_22/(1-P_ext_k)+a_23					
h(1)	2.809508350898E+08	h(10)	-5.472759216346E-01	h(19)	2.926632055021E-01
h(2)	-7.050305064292E+08	h(11)	-1.313556591549E+01	h(20)	-1.557138910909E+01
h(3)	7.778082124195E+01	h(12)	3.796811413949E-01	h(21)	9.660897514451E+00
h(4)	3.113622530360E-02	h(13)	-1.071874901658E+01	h(22)	1.860546620882E+03
h(5)	-5.006553723810E-02	h(14)	-6.912250849022E-01	h(23)	-6.778989432007E+01
h(6)	1.516115371853E+00	h(15)	-1.693470198766E+01	h(24)	0.000000000000E+00
h(7)	-1.018484045992E-01	h(16)	2.831822928542E+01	h(25)	0.000000000000E+00
h(8)	1.068282169117E+01	h(17)	-2.442695988225E-01		
h(9)	-3.539297506352E-02	h(18)	7.135592934800E+01		

HT_m_j_A

f(X)=a_1/j_ext+a_2*exp(1/T_htf_hot)+a_3*LN(T_htf_hot)/T_htf_hot+a_4*sin(k_ext)+a_5*exp(m_dot_htf)/m_dot_htf+a_6*m_dot_htf^m_dot_htf+a_7*LN(1/j_ext)+a_8/(k_ext^2)+a_9*j_ext^0.5+a_10/(j_ext^2)+a_11/(T_htf_hot^2)+a_12/(Pc^0.5)+a_13*LN(1/k_ext)+a_14*Pc^2+a_15/k_ext+a_16*exp(j_ext-1)+a_17/(T_htf_hot^3)+a_18*exp(T_htf_hot-1)+a_19*exp(-(m_dot_htf^2))+a_20*2^(-k_ext)+a_21*sin(m_dot_htf)+a_22*j_ext^j_ext+a_23

c(1)	-1.421272739778E-05	c(10)	2.734140188075E-10	c(19)	2.255687487570E+00
c(2)	-2.963575465988E-02	c(11)	-4.797863541434E-01	c(20)	-2.756373641729E-01
c(3)	-7.544217036287E-01	c(12)	-3.330501241504E-01	c(21)	3.037630071876E+00
c(4)	-3.214584252173E-01	c(13)	5.377669386379E-04	c(22)	8.437298938120E-01
c(5)	2.719647567643E-01	c(14)	4.671776899171E-13	c(23)	-4.157539475747E+00
c(6)	1.107832572090E-01	c(15)	-1.110505567956E-06	c(24)	0.000000000000E+00
c(7)	2.975816419364E-02	c(16)	-9.449610482035E-01	c(25)	0.000000000000E+00
c(8)	7.865894515946E-12	c(17)	6.940657885156E-02		
c(9)	1.297320492951E+00	c(18)	2.298637716140E-02		

HT_m_j_B

f(X)=a_1*LN(j_ext+1)+a_2*exp(1/T_htf_hot)+a_3*sin(j_ext)+a_4*j_ext^3+a_5*exp(1/m_dot_htf)+a_6*exp(-(j_ext^2))+a_7*LN(T_htf_hot+1)+a_8*LN(Pc+1)+a_9*LN(k_ext)/k_ext+a_10*k_ext^k_ext+a_11*2^(-k_ext)+a_12*exp(m_dot_htf^2)+a_13*j_ext^0.5+a_14*exp(k_ext)/k_ext+a_15*LN(j_ext)+a_16*T_htf_hot^T_htf_hot+a_17*(1-T_htf_hot)^2+a_18*LN(T_htf_hot)/T_htf_hot+a_19*(1-j_ext)^2+a_20/(T_htf_hot^2)+a_21*exp(m_dot_htf-1)+a_22/(T_htf_hot^3)+a_23

c(1)	2.663708156492E+03	c(10)	-4.036931163576E-02	c(19)	2.072046867602E+03
c(2)	5.544935057828E-02	c(11)	2.537554460235E-01	c(20)	1.628004056231E+00
c(3)	1.483635412685E+03	c(12)	-4.307156265505E-03	c(21)	1.175965743502E-01
c(4)	-5.536671106181E+02	c(13)	-8.209941470609E-01	c(22)	-1.852978272950E-01
c(5)	-2.905115212195E-03	c(14)	1.430148538614E-05	c(23)	-2.830708111475E+03
c(6)	7.564558256867E+02	c(15)	1.273174962516E-02	c(24)	0.000000000000E+00
c(7)	1.515714928664E+00	c(16)	-6.134948759903E-01	c(25)	0.000000000000E+00
c(8)	2.247705899589E-03	c(17)	1.041796588826E+00		
c(9)	1.475116414614E-06	c(18)	2.817415690581E+00		

HT_m_j_C

f(X)=a_1*LN(j_ext+1)+a_2*exp(-(j_ext^2))+a_3*T_htf_hot^0.5+a_4*LN(Pc)+a_5*exp(-(m_dot_htf^2))+a_6*sin(m_dot_htf)+a_7*k_ext^k_ext+a_8*exp(m_dot_htf-1)+a_9*exp(m_dot_htf)/m_dot_htf+a_10*exp(k_ext-1)+a_11*exp(j_ext)/j_ext+a_12/T_htf_hot+a_13

c(1)	5.750392133373E-01	c(10)	-3.007449897308E-01	c(19)	0.000000000000E+00
c(2)	-2.629789660656E-01	c(11)	-6.059766774246E-07	c(20)	0.000000000000E+00
c(3)	2.545617189163E-01	c(12)	1.163964037015E-02	c(21)	0.000000000000E+00
c(4)	8.438696950448E-04	c(13)	-2.221421609319E+00	c(22)	0.000000000000E+00
c(5)	1.242589625954E+00	c(14)	0.000000000000E+00	c(23)	0.000000000000E+00
c(6)	1.640350528962E+00	c(15)	0.000000000000E+00	c(24)	0.000000000000E+00
c(7)	1.854159986523E-02	c(16)	0.000000000000E+00	c(25)	0.000000000000E+00
c(8)	1.381144260742E-01	c(17)	0.000000000000E+00		
c(9)	1.403637937220E-01	c(18)	0.000000000000E+00		

HT_m_k_A

f(X)=a_1*j_ext^3+a_2*k_ext^2+a_3*2^(-k_ext)+a_4*LN(T_htf_hot)/T_htf_hot+a_5*LN(m_dot_htf+1)+a_6*exp(m_dot_htf)/m_dot_htf+a_7/m_dot_htf+a_8*LN(T_htf_hot+1)+a_9*(1-T_htf_hot)^2+a_10*LN(Pc)+a_11*exp(1/m_dot_htf)+a_12*m_dot_htf+a_13*exp(-m_dot_htf)+a_14*j_ext^0.5+a_15*2^(-T_htf_hot)+a_16*LN(1/T_htf_hot)+a_17*m_dot_htf^3+a_18*LN(j_ext)+a_19*2^(-m_dot_htf)+a_20/(m_dot_htf^0.5)+a_21*j_ext^2+a_22*(1-m_dot_htf)^2+a_23

d(1)	-4.222417133579E-01	d(10)	1.625897365536E-03	d(19)	-2.324796345505E+07
d(2)	2.251586995726E-01	d(11)	7.190317774754E+01	d(20)	1.581307778620E+05
d(3)	-1.060996421630E+00	d(12)	-5.879626307453E+06	d(21)	2.456312751357E-01
d(4)	-5.658771528178E-03	d(13)	9.543317588165E+06	d(22)	1.960534326567E+06
d(5)	3.409344046653E+06	d(14)	-4.266083581612E-02	d(23)	1.117252245587E+07
d(6)	3.160163812372E+05	d(15)	4.705533092992E+01	d(24)	0.000000000000E+00
d(7)	-3.471757503225E+05	d(16)	5.729974636771E-01	d(25)	0.000000000000E+00
d(8)	3.407125170669E+01	d(17)	-2.131000938135E+05		
d(9)	-1.712230733091E+00	d(18)	2.620545638759E-03		

HT_m_k_B

f(X)=a_1*LN(k_ext)/k_ext+a_2/(T_htf_hot^0.5)+a_3*k_ext^k_ext+a_4*exp(T_htf_hot)/T_htf_hot+a_5*Pc*LN(Pc)+a_6*k_ext^3+a_7*exp(k_ext)/k_ext+a_8*k_ext^0.5+a_9*LN(Pc)+a_10*2^m_dot_htf+a_11*2^(-m_dot_htf)+a_12/(k_ext^0.5)+a_13*LN(k_ext)+a_14/(k_ext^2)+a_15/T_htf_hot+a_16*T_htf_hot^3+a_17*T_htf_hot^T_htf_hot+a_18*k_ext*LN(k_ext)+a_19*m_dot_htf^2+a_20*2^(-T_htf_hot)+a_21*sin(T_htf_hot)+a_22*(1-k_ext)^2+a_23

d(1)	6.327827669011E-04	d(10)	9.199533292319E-02	d(19)	-2.686023918206E-02
d(2)	6.109361814476E+00	d(11)	-1.541463419314E-01	d(20)	-6.648013341018E+02
d(3)	5.671428023576E+01	d(12)	-2.764348506825E-01	d(21)	-7.521738195481E+02
d(4)	6.463143531644E+02	d(13)	-2.664272851108E+00	d(22)	3.106857598671E+01
d(5)	6.466357160953E-09	d(14)	7.063422079454E-09	d(23)	-1.312058809465E+02
d(6)	-1.704636699509E+01	d(15)	-6.483239524502E+02	d(24)	0.000000000000E+00
d(7)	7.462608585370E-03	d(16)	-1.743107723570E+02	d(25)	0.000000000000E+00
d(8)	6.495746722085E+01	d(17)	5.380256862237E+01		
d(9)	5.694063726778E-04	d(18)	-2.751284585322E+01		

HT_m_k_C

f(X)=a_1*k_ext^0.5+a_2*sin(Pc)+a_3*T_htf_hot+a_4*k_ext^3+a_5*2^(-m_dot_htf)+a_6/Pc+a_7*exp(-(k_ext^2))+a_8*2^(-k_ext)+a_9*k_ext^k_ext+a_10*exp(T_htf_hot)/T_htf_hot+a_11/(1-Pc)^2+a_12*2^k_ext+a_13*LN(k_ext+1)+a_14*k_ext*LN(k_ext)+a_15*exp(k_ext-1)+a_16/(1-(Pc^2))+a_17*exp(1/T_htf_hot)+a_18/(1-k_ext)^2+a_19*exp(-(m_dot_htf^2))+a_20*exp(-k_ext)+a_21*LN(m_dot_htf)/m_dot_htf+a_22*LN(k_ext)+a_23

d(1)	-3.959553276965E+01	d(10)	-9.091649384131E-03	d(19)	1.514153135814E-01
d(2)	-6.380357006461E-04	d(11)	-4.635012652328E+07	d(20)	6.659540228532E+07
d(3)	1.445085240063E-01	d(12)	-5.529477778568E+06	d(21)	-2.392688417053E-02
d(4)	5.821562396494E+06	d(13)	3.089862307334E+06	d(22)	1.162229438402E-01
d(5)	-7.957211068640E-01	d(14)	-1.477963695984E+03	d(23)	6.054723702613E+07
d(6)	-4.973618523825E+01	d(15)	-2.607517487014E+07	d(24)	0.000000000000E+00
d(7)	-1.034884786877E+06	d(16)	-4.648865779465E+07	d(25)	0.000000000000E+00
d(8)	-1.109869033461E+08	d(17)	5.215576641776E-05		
d(9)	1.269723768583E+03	d(18)	-1.207466645568E+02		

HT_Ts

f(X)=a_1/(P_ext_j^0.5)+a_2*exp(1/m_dot_htf)+a_3*T_htf_hot^2+a_4*k_ext+a_5*LN(k_ext+1)+a_6*LN(T_htf_hot+1)+a_7*sin(m_dot_htf)+a_8*T_htf_hot^T_htf_hot+a_9/(1-(j_ext^2))+a_10*exp(-T_htf_hot)+a_11*k_ext^3+a_12*Pc^0.5+a_13*LN(P_ext_j)/P_ext_j+a_14*exp(1-m_dot_htf)+a_15*Pc+a_16*(1-m_dot_htf)^2+a_17*exp(-(T_htf_hot^2))+a_18*exp(1/Pc)+a_19*LN(T_htf_hot)+a_20/T_htf_hot+a_21*exp(m_dot_htf)/m_dot_htf+a_22*Pc*LN(Pc)+a_23

e(1)	-4.426673645478E+02	e(10)	-1.836762615680E+04	e(19)	3.920835240496E+02
e(2)	-4.689472236615E-01	e(11)	1.230509520613E+01	e(20)	4.003437123628E+01
e(3)	1.590388371533E+03	e(12)	7.031092269297E-01	e(21)	6.729147955662E+00
e(4)	-1.754064131248E+01	e(13)	1.387684971592E+04	e(22)	3.949828258969E-04
e(5)	1.941529402875E+01	e(14)	-8.110684565302E+00	e(23)	3.353352267477E+04
e(6)	-2.049271086250E+04	e(15)	-5.738669780991E-03	e(24)	0.000000000000E+00
e(7)	-1.831564231884E+01	e(16)	-1.054765740512E+01	e(25)	0.000000000000E+00
e(8)	-4.162811992603E+02	e(17)	-5.097701964102E+02		
e(9)	9.133436274288E-01	e(18)	-1.332224923396E+04		

HT_Xs_A

f(X)=a_1*m_dot_htf+a_2*(1-k_ext)^2+a_3/(Pc^0.5)+a_4*LN(1/P_ext_k)+a_5*LN(k_ext^2)+a_6/Pc+a_7*T_htf_hot^T_htf_hot+a_8*Pc^0.5+a_9/(P_ext_k^0.5)+a_10*exp(k_ext)+a_11*2^j_ext+a_12*k_ext^3+a_13*2^k_ext+a_14*2^(-m_dot_htf)+a_15*LN(j_ext)/j_ext+a_16*exp(m_dot_htf)+a_17*P_ext_j*LN(P_ext_j)+a_18*j_ext+a_19*Pc*LN(Pc)+a_20*LN(T_htf_hot^2)+a_21*exp(T_htf_hot)+a_22*LN(1/P_ext_j)+a_23

g(1)	1.183337680000E-01	g(10)	-1.134539150000E+01	g(19)	-1.486743340000E-08
g(2)	9.712274980000E-01	g(11)	3.341860270000E-02	g(20)	6.099994690000E-03
g(3)	-2.115717370000E+00	g(12)	1.144948020000E+00	g(21)	6.596088500000E-02
g(4)	-1.299875830000E-02	g(13)	1.921260210000E+01	g(22)	4.917753320000E-03
g(5)	-1.496757860000E-04	g(14)	3.072234170000E-01	g(23)	-8.405108520000E+00
g(6)	2.710952200000E+01	g(15)	-7.977395420000E-09	g(24)	0.000000000000E+00
g(7)	-1.156538830000E-01	g(16)	-1.198760790000E-02	g(25)	0.000000000000E+00
g(8)	2.551275970000E-04	g(17)	5.854726090000E-10		
g(9)	3.737588040000E+01	g(18)	-1.303203790000E-02		

HT_Xs_B

f(X)=a_1*2^(-k_ext)+a_2/(m_dot_htf^2)+a_3*LN(P_ext_j)+a_4*m_dot_htf+a_5/P_ext_j+a_6*LN(1/P_ext_k)+a_7*k_ext^0.5+a_8/m_dot_htf+a_9*exp(T_htf_hot)/T_htf_hot+a_10*m_dot_htf^0.5+a_11*T_htf_hot+a_12/(Pc^0.5)+a_13*LN(Pc-1)+a_14/(1-Pc)+a_15*2^k_ext+a_16*LN(P_ext_k)/P_ext_k+a_17*exp(-m_dot_htf)+a_18*2^j_ext+a_19/(1-P_ext_k)+a_20*T_htf_hot^T_htf_hot+a_21*exp(m_dot_htf^2)+a_22*exp(1-T_htf_hot)+a_23

g(1)	-1.616538431989E-02	g(10)	-1.856301044634E+02	g(19)	2.878732516873E+04
g(2)	7.633146439955E-01	g(11)	2.286475517437E-01	g(20)	-6.581211894575E-02
g(3)	2.674696771208E-03	g(12)	3.422492419442E+00	g(21)	-1.512463393348E-02
g(4)	5.316695983993E+01	g(13)	3.036107644168E-02	g(22)	8.469847114296E-02
g(5)	1.019434883387E+03	g(14)	5.658432642592E+01	g(23)	1.732244596886E+02
g(6)	-7.279164965893E-03	g(15)	1.468392151031E-02	g(24)	0.000000000000E+00
g(7)	-5.288404342060E-03	g(16)	2.692545854060E+03	g(25)	0.000000000000E+00
g(8)	-9.477821486979E+00	g(17)	-8.633294952555E+01		
g(9)	-9.814191705118E-03	g(18)	1.409051298364E-02		

HT_Xs_C					
f(X)=a_1/(m_dot_htf^0.5)+a_2*m_dot_htf*LN(m_dot_htf)+a_3/(m_dot_htf^2)+a_4*2^j_ext+a_5*LN(P_ext_k+1)+a_6*exp(-k_ext)+a_7*2^T_htf_hot+a_8*j_ext+a_9*LN(P_ext_j+1)+a_10*exp(j_ext^2)+a_11/(1-k_ext)+a_12*LN(P_ext_k)+a_13*exp(1/Pc)+a_14/(1-(Pc^2))+a_15*exp(T_htf_hot)/T_htf_hot+a_16*T_htf_hot*exp(T_htf_hot)+a_17/(Pc^3)+a_18*LN(Pc)+a_19*m_dot_htf^2+a_20*(1-k_ext)^2+a_21/(P_ext_k^0.5)+a_22*j_ext^j_ext+a_23				
g(1)	7.083738572001E-02	g(10)	8.499455350898E-02	g(19)	-1.524819563881E-02
g(2)	3.631305285821E-02	g(11)	3.572958096025E-02	g(20)	-2.867333744774E-01
g(3)	-3.815832866384E-03	g(12)	2.475012560311E+04	g(21)	8.962052131145E+01
g(4)	-2.648176259751E-01	g(13)	9.032929931771E+01	g(22)	9.574607710586E-04
g(5)	-2.475010649793E+04	g(14)	2.345440457762E+05	g(23)	-9.039269583068E+01
g(6)	5.959033698029E-01	g(15)	-7.301036867416E-03	g(24)	0.000000000000E+00
g(7)	1.436727648229E-01	g(16)	-2.292814585152E-02	g(25)	0.000000000000E+00
g(8)	2.006284839589E-01	g(17)	2.471702857341E+08		
g(9)	1.178894981167E-03	g(18)	2.399819972790E-02		

Table 40 - List of Rankine cycle performance curves for the low temperature Rankine cycle

LT_Eta					
f(X)=a_1*2^k_ext+a_2*j_ext^0.5+a_3/(1-P_ext_j)+a_4*exp(-(j_ext^2))+a_5*exp(m_dot_htf)/m_dot_htf+a_6*LN(T_ret+1)+a_7*LN(k_ext+1)+a_8*LN(m_dot_htf+1)+a_9*LN(P_ext_j)/P_ext_j+a_10*LN(1/T_htf_hot)+a_11*LN(P_ext_k-1)+a_12/(P_ext_j^0.5)+a_13*exp(1/P_ext_k)+a_14*P_ext_j^0.5+a_15*k_ext^3+a_16*exp(j_ext-1)+a_17*T_htf_hot*LN(T_htf_hot)+a_18*T_htf_hot^3+a_19*Pc^0.5+a_20/(T_htf_hot^3)+a_21*LN(Pc-1)+a_22*k_ext^2+a_23					
a(1)	-1.573902190000E+01	a(10)	-7.299507970000E-02	a(19)	-1.515372010000E-04
a(2)	2.839287600000E-02	a(11)	-4.035338380000E-02	a(20)	2.989269480000E-04
a(3)	-1.137712330000E+06	a(12)	1.056901890000E+03	a(21)	-3.909563740000E-02
a(4)	-4.118844450000E-01	a(13)	3.018841210000E+03	a(22)	8.605338290000E+00
a(5)	-1.840988680000E-02	a(14)	1.179422750000E-04	a(23)	-3.001319440000E+03
a(6)	6.667615920000E-02	a(15)	-1.049821300000E+00	a(24)	0.000000000000E+00
a(7)	1.035518080000E+01	a(16)	-1.341750200000E+00	a(25)	0.000000000000E+00
a(8)	6.837559450000E-02	a(17)	-5.172151400000E-02		
a(9)	-1.217886510000E+05	a(18)	8.402079830000E-03		

LT_Q					
f(X)=a_1*2^j_ext+a_2*sin(m_dot_htf)+a_3*(1-T_htf_hot)^2+a_4*exp(1-T_htf_hot)+a_5/(T_htf_hot^2)+a_6*(1-j_ext)^2+a_7*LN(T_htf_hot)+a_8/(m_dot_htf^0.5)+a_9*exp(T_htf_hot)/T_htf_hot+a_10/(1-(j_ext^2))+a_11*LN(Pc+1)+a_12*LN(m_dot_htf)/m_dot_htf+a_13*2^T_htf_hot+a_14*2^(-T_htf_hot)+a_15*sin(T_htf_hot)+a_16*LN(1/m_dot_htf)+a_17*(1-k_ext)^2+a_18*exp(1-m_dot_htf)+a_19*T_htf_hot*LN(T_htf_hot)+a_20*exp(1/m_dot_htf)+a_21*exp(j_ext)+a_22*exp(m_dot_htf^2)+a_23					
b(1)	-7.268852567256E+01	b(10)	-4.400986693084E+00	b(19)	1.804113114380E+04
b(2)	-4.735455690147E+01	b(11)	-9.091481882607E-03	b(20)	1.373364834847E+00
b(3)	-1.872500578792E+04	b(12)	3.208004745543E+01	b(21)	4.601803256686E+01
b(4)	-3.046537191284E+04	b(13)	7.399867352838E+03	b(22)	-1.649398616037E-01
b(5)	-1.952157107257E+01	b(14)	1.812275496167E+05	b(23)	-7.256271441154E+04
b(6)	-2.235901973374E+00	b(15)	-4.967168747516E+03	b(24)	0.000000000000E+00
b(7)	6.689406924737E+03	b(16)	6.414518594127E+01	b(25)	0.000000000000E+00
b(8)	1.858370757955E+02	b(17)	3.546757238942E-03		
b(9)	6.823217964205E+02	b(18)	-1.558895844290E+02		

LT_W

f(X)=a_1*2^(-k_ext)+a_2*LN(1/P_ext_j)+a_3*2^k_ext+a_4*j_ext^2+a_5*exp(T_htf_hot)+a_6*(1-k_ext)^2+a_7*(1-m_dot_htf)^2+a_8*LN(T_ret-1)+a_9*LN(Pc-1)+a_10*exp(m_dot_htf^2)+a_11/(1-j_ext)+a_12/(1-(P_ext_k^2))+a_13*sin(T_ret)+a_14/(1-Pc)+a_15/(Pc^2)+a_16/(1-j_ext^2)+a_17*LN(1/P_ext_k)+a_18*exp(j_ext^2)+a_19/(1-P_ext_j)^2+a_20*m_dot_htf^m_dot_htf+a_21*LN(T_htf_hot)+a_22*exp(1-T_htf_hot)+a_23

h(1)	-7.444336246143E+00	h(10)	-2.020549268012E-02	h(19)	-6.050652185742E+08
h(2)	3.059446327702E-02	h(11)	-2.099190941723E-01	h(20)	5.814641499593E-01
h(3)	-2.042836012857E+00	h(12)	-3.003748823143E+08	h(21)	-4.215313514932E-02
h(4)	-3.381911745546E+01	h(13)	-6.447964964554E-04	h(22)	-3.309168599634E-01
h(5)	1.225501098411E-01	h(14)	1.743031480399E+02	h(23)	-2.448718625993E+01
h(6)	2.072477668419E+00	h(15)	2.365914969861E+05	h(24)	0.000000000000E+00
h(7)	-4.653257657904E-01	h(16)	-2.239869214313E+01	h(25)	0.000000000000E+00
h(8)	5.597616358531E-02	h(17)	3.184479710011E-02		
h(9)	-5.206520909156E-02	h(18)	5.585171412293E+01		

LT_m_j_A

f(X)=a_1/(1-(k_ext^2))+a_2*LN(T_htf_hot)/T_htf_hot+a_3*m_dot_htf^2+a_4*Pc^0.5+a_5/(T_htf_hot^2)+a_6/(j_ext^2)+a_7*exp(k_ext-1)+a_8*LN(m_dot_htf+1)+a_9*2^(-m_dot_htf)+a_10/(T_htf_hot^0.5)+a_11*exp(j_ext)/j_ext+a_12*LN(1/j_ext)+a_13*Pc+a_14*exp(-m_dot_htf)+a_15*LN(1/T_htf_hot)+a_16*j_ext^j_ext+a_17*exp(1/T_htf_hot)+a_18*exp(m_dot_htf)/m_dot_htf+a_19*exp(-j_ext)+a_20*sin(Pc)+a_21*Pc*LN(Pc)+a_22/(j_ext^0.5)+a_23

c(1)	5.288186780000E-02	c(10)	3.763298120000E+00	c(19)	-6.060600980000E-01
c(2)	9.057300520000E-01	c(11)	-2.821994860000E-05	c(20)	4.892091090000E-04
c(3)	-3.178657690000E+00	c(12)	-1.658840520000E-02	c(21)	3.569838530000E-07
c(4)	2.673572920000E-04	c(13)	-4.768693270000E-06	c(22)	2.930026680000E-03
c(5)	2.645866890000E-01	c(14)	1.065521960000E+00	c(23)	-1.257394970000E+02
c(6)	3.925597500000E-10	c(15)	-1.575421040000E+00	c(24)	0.000000000000E+00
c(7)	-3.828118850000E-01	c(16)	1.897309210000E-01	c(25)	0.000000000000E+00
c(8)	9.425938800000E+01	c(17)	-1.322626820000E-02		
c(9)	1.162649880000E+02	c(18)	6.124782940000E-01		

LT_m_j_B

f(X)=a_1/(m_dot_htf^2)+a_2*exp(j_ext)/j_ext+a_3/(T_htf_hot^2)+a_4*LN(T_htf_hot+1)+a_5*LN(Pc)/Pc+a_6*sin(k_ext)+a_7*LN(k_ext)/k_ext+a_8*LN(k_ext^2)+a_9*exp(m_dot_htf-1)+a_10*j_ext*LN(j_ext)+a_11*sin(Pc)+a_12/(k_ext^2)+a_13/(j_ext^0.5)+a_14/(k_ext^0.5)+a_15*2^j_ext+a_16*Pc+a_17*m_dot_htf^2+a_18/(1-(j_ext^2))+a_19*LN(1/T_htf_hot)+a_20*LN(1/j_ext)+a_21*exp(1/T_htf_hot)+a_22*T_htf_hot+a_23

c(1)	-9.345863580000E-03	c(10)	-2.249412040000E-01	c(19)	7.435672720000E-01
c(2)	1.417060900000E-06	c(11)	4.608033070000E-04	c(20)	1.496204320000E-02
c(3)	-3.794667040000E-02	c(12)	8.409228240000E-11	c(21)	6.257430430000E-03
c(4)	2.329702280000E+00	c(13)	-1.054299310000E-03	c(22)	-3.628445270000E-01
c(5)	-1.603924080000E+00	c(14)	9.002912060000E-04	c(23)	-1.721849870000E+00
c(6)	-1.507507470000E-01	c(15)	4.359978370000E-01	c(24)	0.000000000000E+00
c(7)	7.281923310000E-07	c(16)	4.199881330000E-08	c(25)	0.000000000000E+00
c(8)	2.334126180000E-03	c(17)	2.012512830000E-01		
c(9)	-3.243969150000E-01	c(18)	1.789920510000E-01		

LT_m_j_C

f(X)=a_1*(1-T_htf_hot)^2+a_2*T_htf_hot^T_htf_hot+a_3*k_ext^0.5+a_4*2^k_ext+a_5*LN(T_htf_hot)/T_htf_hot+a_6*exp(j_ext-1)+a_7*LN(Pc+1)+a_8/(1-(j_ext^2))+a_9/j_ext+a_10*LN(m_dot_htf+1)+a_11*T_htf_hot^3+a_12*2^(-m_dot_htf)+a_13

c(1)	-1.667179510000E-01	c(10)	8.254153320000E-01	c(19)	0.000000000000E+00
c(2)	-4.205301860000E-01	c(11)	1.876672110000E-01	c(20)	-2.756373641729E-01
c(3)	-1.217687760000E-02	c(12)	8.807932600000E-01	c(21)	3.037630071876E+00
c(4)	-1.587712860000E-01	c(13)	-8.850921320000E-01	c(22)	8.437298938120E-01
c(5)	-1.164995520000E-02	c(14)	0.000000000000E+00	c(23)	-4.157539475747E+00
c(6)	1.480141920000E+00	c(15)	0.000000000000E+00	c(24)	0.000000000000E+00
c(7)	6.687253190000E-04	c(16)	0.000000000000E+00	c(25)	0.000000000000E+00
c(8)	-2.300336280000E-01	c(17)	0.000000000000E+00		
c(9)	-6.120203900000E-07	c(18)	0.000000000000E+00		

LT_m_k_A

f(X)=a_1*j_ext*exp(j_ext)+a_2*Pc^0.5+a_3*exp(1-T_htf_hot)+a_4*T_htf_hot^0.5+a_5*LN(T_htf_hot+1)+a_6*LN(j_ext^2)+a_7*j_ext^0.5+a_8*k_ext^2+a_9*m_dot_htf^m_dot_htf+a_10*m_dot_htf*LN(m_dot_htf)+a_11*LN(m_dot_htf+1)+a_12/(m_dot_htf^3)+a_13*2^m_dot_htf+a_14*m_dot_htf+a_15*exp(1/m_dot_htf)+a_16/(1-(j_ext^2))+a_17*exp(1-k_ext)+a_18*T_htf_hot*LN(T_htf_hot)+a_19*m_dot_htf^2+a_20/m_dot_htf+a_21*2^T_htf_hot+a_22/(m_dot_htf^0.5)+a_23

d(1)	1.427614940000E-01	d(10)	-4.148213040000E+06	d(19)	5.087979640000E+05
d(2)	1.884650640000E-05	d(11)	-1.013889320000E+07	d(20)	-3.012620460000E+05
d(3)	1.776068520000E+01	d(12)	6.018056330000E+02	d(21)	1.096588630000E+00
d(4)	-1.909596720000E+01	d(13)	-1.423862810000E+05	d(22)	1.762290680000E+06
d(5)	6.610330560000E+01	d(14)	8.975318160000E+06	d(23)	-3.636558340000E+06
d(6)	2.165693810000E-03	d(15)	-9.929292740000E+01	d(24)	0.000000000000E+00
d(7)	-1.090100300000E-01	d(16)	-2.248555460000E-01	d(25)	0.000000000000E+00
d(8)	3.057642320000E-01	d(17)	-2.628409370000E-01		
d(9)	3.553825210000E+03	d(18)	-7.098101460000E+00		

LT_m_k_B

f(X)=a_1*sin(k_ext)+a_2*sin(T_htf_hot)+a_3*k_ext*LN(k_ext)+a_4*T_htf_hot*LN(T_htf_hot)+a_5/(k_ext^2)+a_6*Pc+a_7*exp(1-k_ext)+a_8*exp(-m_dot_htf)+a_9*(1-k_ext)^2+a_10*k_ext^0.5+a_11*k_ext^k_ext+a_12*2^m_dot_htf+a_13

d(1)	-3.599859939786E+02	d(10)	5.754350103678E+00	d(19)	0.000000000000E+00
d(2)	1.483848231318E-01	d(11)	-1.630085129195E+02	d(20)	0.000000000000E+00
d(3)	1.965915172230E+02	d(12)	4.893406305554E-02	d(21)	0.000000000000E+00
d(4)	6.216516785231E-02	d(13)	6.235993262670E+02	d(22)	0.000000000000E+00
d(5)	2.906312381603E-11	d(14)	0.000000000000E+00	d(23)	0.000000000000E+00
d(6)	8.570960981543E-08	d(15)	0.000000000000E+00	d(24)	0.000000000000E+00
d(7)	-1.612437853318E+02	d(16)	0.000000000000E+00	d(25)	0.000000000000E+00
d(8)	-1.416377615145E-01	d(17)	0.000000000000E+00		
d(9)	-2.249042227319E+01	d(18)	0.000000000000E+00		

LT_m_k_C

f(X)=a_1/(m_dot_htf^3)+a_2*k_ext^2+a_3*k_ext*LN(k_ext)+a_4*sin(Pc)+a_5*m_dot_htf*LN(m_dot_htf)+a_6*LN(m_dot_htf)/m_dot_htf+a_7*k_ext^0.5+a_8*LN(T_htf_hot+1)+a_9*LN(Pc)/Pc+a_10*T_htf_hot*LN(T_htf_hot)+a_11*T_htf_hot+a_12/(1-(k_ext^2))+a_13*exp(m_dot_htf)+a_14*LN(k_ext)/k_ext+a_15/(Pc^2)+a_16*LN(k_ext+1)+a_17/(1-k_ext)+a_18*LN(k_ext)+a_19*2^(-k_ext)+a_20*exp(k_ext)/k_ext+a_21*sin(k_ext)+a_22/(1-Pc)+a_23

d(1)	7.127753439893E-03	d(10)	-3.357363958681E-01	d(19)	-1.033348334316E+05
d(2)	3.965133992248E+03	d(11)	1.151748598143E+00	d(20)	-9.366945591516E-05
d(3)	4.248671325796E+01	d(12)	-4.974546591676E+04	d(21)	-5.342833429652E+03
d(4)	-6.764903179224E-04	d(13)	-2.052307048772E-02	d(22)	1.204610109590E+02
d(5)	1.487910668564E-01	d(14)	-7.474276942535E-06	d(23)	1.282906697121E+05
d(6)	6.261576422397E-02	d(15)	1.086515854647E+05	d(24)	0.000000000000E+00
d(7)	2.530616011799E+01	d(16)	-9.101221711375E+04	d(25)	0.000000000000E+00
d(8)	-1.311865865734E+00	d(17)	2.478719807970E+04		
d(9)	8.931247924437E+00	d(18)	-2.517069729253E-01		

LT_Ts

f(X)=a_1/(T_htf_hot^2)+a_2*Pc+a_3*T_ret^2+a_4*exp(1/Pc)+a_5*LN(P_ext_j+1)+a_6*LN(Pc-1)+a_7*T_ret*LN(T_ret)+a_8/P_ext_k+a_9*exp(m_dot_htf^2)+a_10*LN(1/T_ret)+a_11*exp(k_ext-1)+a_12*exp(1/T_htf_hot)+a_13/(Pc^0.5)+a_14/(T_htf_hot^3)+a_15*LN(T_htf_hot)/T_htf_hot+a_16/(1-(k_ext^2))+a_17*T_htf_hot*LN(T_htf_hot)+a_18*LN(Pc)/Pc+a_19*LN(P_ext_j^2)+a_20*Pc^0.5+

e(1)	4.533456320000E-01	e(10)	1.862672400000E+02	e(19)	7.341069180000E+01
e(2)	-1.224352160000E-05	e(11)	-1.798927130000E-02	e(20)	6.707708340000E-02
e(3)	7.728267710000E-04	e(12)	2.051014990000E-02	e(21)	1.253346340000E-04
e(4)	2.061816380000E+04	e(13)	1.343560330000E+03	e(22)	7.355202250000E+00
e(5)	-1.468218000000E+02	e(14)	-5.787325280000E-02	e(23)	-1.987946870000E+04
e(6)	2.028620620000E+01	e(15)	7.475373980000E-01	e(24)	0.000000000000E+00
e(7)	-1.073789640000E+00	e(16)	1.742893110000E-02	e(25)	0.000000000000E+00
e(8)	2.957537720000E+02	e(17)	4.139831270000E-02		
e(9)	3.346072820000E-05	e(18)	-5.867935930000E+03		

LT_Xs_A

f(X)=a_1*LN(Pc+1)+a_2*LN(P_ext_j)+a_3*j_ext*LN(j_ext)+a_4/(T_htf_hot^2)+a_5*LN(1/T_htf_hot)+a_6*LN(1/j_ext)+a_7*P_ext_j^0.5+a_8*exp(1/T_htf_hot)+a_9*Pc^0.5+a_10*exp(-(T_htf_hot^2))+a_11*exp(m_dot_htf)/m_dot_htf+a_12*LN(P_ext_k^2)+a_13*LN(1/k_ext)+a_14*P_ext_k^0.5+a_15*exp(k_ext^2)+a_16*exp(j_ext-1)+a_17/(T_htf_hot^3)+a_18/(Pc^2)+a_19*exp(-m_dot_htf)+a_20*k_ext^3+a_21/P_ext_k+a_22*exp(k_ext)+a_23

g(1)	1.241352620000E-02	g(10)	4.143848100000E-03	g(19)	5.226468970000E-02
g(2)	-5.694811270000E-03	g(11)	4.322290610000E-03	g(20)	3.195643900000E-02
g(3)	2.070629340000E-03	g(12)	-6.071047990000E-03	g(21)	-3.888139750000E+03
g(4)	7.692962940000E-03	g(13)	1.066176240000E-04	g(22)	1.706555760000E-02
g(5)	-4.207065440000E-02	g(14)	1.436147870000E-05	g(23)	8.800702470000E-01
g(6)	-8.879496690000E-05	g(15)	-5.704337620000E-03	g(24)	0.000000000000E+00
g(7)	1.610205350000E-05	g(16)	3.043135810000E-02	g(25)	0.000000000000E+00
g(8)	1.679686940000E-03	g(17)	-2.638725800000E-03		
g(9)	4.531839870000E-05	g(18)	2.436644060000E+03		

LT_Xs_B

f(X)=a_1*2^(-k_ext)+a_2*P_ext_k+a_3/(1-k_ext)+a_4*exp(1/m_dot_htf)+a_5*m_dot_htf^m_dot_htf+a_6/(m_dot_htf^3)+a_7*exp(j_ext)+a_8*LN(T_htf_hot^2)+a_9/(T_htf_hot^3)+a_10*exp(k_ext^2)+a_11*2^(-m_dot_htf)+a_12*2^(-T_htf_hot)+a_13*LN(1/Pc)+a_14/(1-k_ext)^2+a_15*P_ext_k^0.5+a_16*exp(1/T_htf_hot)+a_17*Pc^0.5+a_18*T_htf_hot^3+a_19*LN(1/P_ext_j)+a_20*sin(k_ext)+a_21/(1-P_ext_j)+a_22*LN(m_dot_htf)+a_23

g(1)	-9.641568740000E+01	g(10)	4.224090870000E+01	g(19)	-1.792884650000E-03
g(2)	2.198092150000E-09	g(11)	-2.328421440000E-01	g(20)	-4.491209780000E+01
g(3)	-2.840751800000E+01	g(12)	-3.756277680000E-01	g(21)	-5.684655870000E+02
g(4)	2.011559220000E-02	g(13)	-1.233415890000E-02	g(22)	-7.843354320000E-02
g(5)	-1.403390030000E-03	g(14)	3.238634750000E+00	g(23)	8.029860420000E+01
g(6)	-1.222681730000E-02	g(15)	-2.754956970000E-06	g(24)	0.000000000000E+00
g(7)	9.123409380000E-03	g(16)	1.927651220000E-03	g(25)	0.000000000000E+00
g(8)	-4.646902420000E-02	g(17)	4.598383750000E-05		
g(9)	-1.950114730000E-03	g(18)	-2.819072690000E-03		

LT_Xs_C

f(X)=a_1*2^(-m_dot_htf)+a_2/(P_ext_j^0.5)+a_3*sin(j_ext)+a_4*exp(m_dot_htf-1)+a_5/(Pc^0.5)+a_6*LN(Pc)+a_7*LN(Pc+1)+a_8*LN(T_htf_hot+1)+a_9/(k_ext^0.5)+a_10*T_htf_hot*LN(T_htf_hot)+a_11/(T_htf_hot^2)+a_12*sin(k_ext)+a_13*P_ext_j^0.5+a_14/(1-k_ext)+a_15*2^(-j_ext)+a_16*P_ext_k^0.5+a_17/(1-Pc)+a_18*LN(j_ext+1)+a_19*exp(1-m_dot_htf)+a_20*LN(P_ext_j+1)+a_21/(1-(j_ext^2))+a_22*LN(P_ext_k)+a_23

g(1)	-1.907464100000E-01	g(10)	1.775601520000E-03	g(19)	8.015727990000E-02
g(2)	-3.697033700000E+01	g(11)	-3.3939204200E-04	g(20)	-2.448896170000E-02
g(3)	-2.861604120000E-01	g(12)	4.1007991300E-03	g(21)	3.776551680000E-02
g(4)	-5.397508050000E-03	g(13)	1.7342701700E-05	g(22)	-2.525455880000E-03
g(5)	3.140817100000E+00	g(14)	1.3519048800E-02	g(23)	2.454474330000E+00
g(6)	3.118017840000E+04	g(15)	-1.5096652600E+00	g(24)	0.000000000000E+00
g(7)	-3.118015650000E+04	g(16)	3.986145510000E-06	g(25)	0.000000000000E+00
g(8)	4.637929900000E-02	g(17)	-3.108783880000E+04		
g(9)	5.263462970000E-06	g(18)	-7.477196700000E-01		

Annex 7 – Case Study: CSP+MED Extra Information

Table 41 – CSP+MED case study: Total Net Electrical Production

1 - Total Net Electrical Production										
	CT 8			CT 1		CT 2		CT 4		CT 5
	MED+SWCC			Wet Cooling		Dry Cooling		Wet Cooling		SWCC
	MWhe	%	m3/month	MWh_e	%	MWh_e	%	MWh_e	%	MWh_e	%
Jan	4 843	0%	73 924	6 143	26.9%	5 743	18.6%	6 145	26.9%	6 119	26.4%
Feb	17 181	0%	250 433	19 387	12.8%	18 321	6.6%	19 392	12.9%	19 364	12.7%
Mar	34 515	0%	550 123	39 229	13.7%	37 143	7.6%	39 239	13.7%	39 196	13.6%
Apr	31 983	0%	528 378	37 229	16.4%	35 015	9.5%	37 237	16.4%	37 176	16.2%
May	49 159	0%	882 955	60 007	22.1%	56 177	14.3%	60 019	22.1%	59 971	22.0%
Jun	43 765	0%	825 169	56 291	28.6%	52 478	19.9%	56 301	28.6%	56 104	28.2%
Jul	48 980	0%	906 889	62 716	28.0%	58 112	18.6%	62 731	28.1%	62 532	27.7%
Aug	43 398	0%	753 274	53 087	22.3%	49 303	13.6%	53 101	22.4%	53 470	23.2%
Sep	24 981	0%	402 339	28 646	14.7%	26 743	7.1%	28 653	14.7%	28 808	15.3%
Oct	20 289	0%	309 692	23 053	13.6%	21 514	6.0%	23 059	13.7%	23 158	14.1%
Nov	2 568	0%	40 670	3 444	34.1%	3 162	23.1%	3 444	34.1%	3 341	30.1%
Dec	1 688	0%	31 485	2 294	35.9%	2 106	24.7%	2 295	35.9%	2 191	29.8%
Total	323 351	0%	5 555 331	391 526	21%	365 817	13%	391 616	21%	391 430	21%

Table 42 - CSP+MED case study: Total GROSS Electrical Production

2 - Total GROSS Electrical Production										
	CT 8			CT 1		CT 2		CT 4		CT 5
	MED+SWCC			Wet Cooling		Dry Cooling		Wet Cooling		SWCC
	MWhe	%	m3/month	MWh_e	%	MWh_e	%	MWh_e	%	MW_e	%
Jan	6 429	0%	73 924	7 375	14.7%	7 067	9.9%	7 376	14.7%	7 300	13.5%
Feb	19 786	0%	250 433	20 614	4.2%	19 775	-0.1%	20 618	4.2%	20 478	3.5%
Mar	40 173	0%	550 123	41 610	3.6%	40 002	-0.4%	41 620	3.6%	41 394	3.0%
Apr	37 796	0%	528 378	39 539	4.6%	37 781	0.0%	39 547	4.6%	39 325	4.0%
May	59 752	0%	882 955	63 983	7.1%	60 948	2.0%	63 997	7.1%	63 698	6.6%
Jun	55 936	0%	825 169	60 190	7.6%	57 389	2.6%	60 204	7.6%	59 929	7.1%
Jul	62 349	0%	906 889	66 948	7.4%	63 751	2.2%	66 963	7.4%	66 587	6.8%
Aug	52 865	0%	753 274	57 060	7.9%	54 493	3.1%	57 073	8.0%	56 925	7.7%
Sep	29 595	0%	402 339	30 659	3.6%	29 382	-0.7%	30 666	3.6%	30 538	3.2%
Oct	23 592	0%	309 692	24 598	4.3%	23 527	-0.3%	24 603	4.3%	24 500	3.8%
Nov	3 643	0%	40 670	4 343	19.2%	4 115	13.0%	4 344	19.2%	4 194	15.1%
Dec	2 838	0%	31 485	3 415	20.3%	3 283	15.7%	3 415	20.3%	3 246	14.4%
Total	394 754	0%	5 555 331	420 333	6.5%	401 514	2%	420 425	7%	418 114	6%

Table 43 - CSP+MED case study: Number of Startups

3 - Number of Startups											
	CT 8				CT 1		CT 2		CT 4		CT 5
	MED+SWCC				Wet Cooling		Dry Cooling		Wet Cooling		SWCC
	CSP #	%	MED #	%	Startup #	%	Startup #	%	Startup #	%	Startup #	%
Jan	26	0%	14	-46.2%	27	3.8%	27	3.8%	27	3.8%	28	7.7%
Feb	27	0%	22	-18.5%	27	0.0%	27	0.0%	27	0.0%	27	0.0%
Mar	31	0%	30	-3.2%	33	6.5%	33	6.5%	33	6.5%	33	6.5%
Apr	29	0%	24	-17.2%	30	3.4%	30	3.4%	30	3.4%	30	3.4%
May	20	0%	18	-10.0%	22	10.0%	22	10.0%	22	10.0%	22	10.0%
Jun	16	0%	16	0.0%	18	12.5%	18	12.5%	18	12.5%	18	12.5%
Jul	24	0%	23	-4.2%	23	-4.2%	23	-4.2%	23	-4.2%	23	-4.2%
Aug	29	0%	28	-3.4%	30	3.4%	30	3.4%	30	3.4%	30	3.4%
Sep	28	0%	24	-14.3%	30	7.1%	30	7.1%	30	7.1%	30	7.1%
Oct	32	0%	23	-28.1%	34	6.3%	34	6.3%	34	6.3%	34	6.3%
Nov	18	0%	9	-50.0%	20	11.1%	20	11.1%	20	11.1%	20	11.1%
Dec	21	0%	8	-61.9%	22	4.8%	22	4.8%	22	4.8%	23	9.5%
Total	301	0%	239	-20.6%	316	5.0%	316	5.0%	316	5.0%	318	5.6%

Table 44 - CSP+MED case study: Capacity Factor (using NET Electric Output)

4 - Capacity Factor (using >>NET<< Electric Output)	CT 8 MED+SWCC				CT 1 Wet Cooling		CT 2 Dry Cooling		CT 4 Wet Cooling		CT 5 SWCC	
	CSP %	%	MED %	%	%	%	%	%	%	%	%	%
Jan	7%	0%	7%	0.5%	8%	26.9%	8%	18.6%	8%	26.9%	8%	26.4%
Feb	26%	0%	25%	-4.0%	29%	12.8%	28%	6.6%	29%	12.9%	29%	12.7%
Mar	47%	0%	49%	5.0%	53%	13.7%	50%	7.6%	53%	13.7%	53%	13.6%
Apr	45%	0%	49%	8.8%	52%	16.4%	49%	9.5%	52%	16.4%	52%	16.2%
May	67%	0%	79%	18.3%	81%	22.1%	76%	14.3%	81%	22.1%	81%	22.0%
Jun	61%	0%	76%	24.2%	79%	28.6%	74%	19.9%	79%	28.6%	79%	28.2%
Jul	66%	0%	81%	22.0%	85%	28.0%	79%	18.6%	85%	28.1%	85%	27.7%
Aug	59%	0%	67%	14.3%	72%	22.3%	67%	13.6%	72%	22.4%	73%	23.2%
Sep	35%	0%	37%	6.1%	40%	14.7%	38%	7.1%	40%	14.7%	40%	15.3%
Oct	28%	0%	28%	0.5%	31%	13.6%	29%	6.0%	31%	13.7%	31%	14.1%
Nov	4%	0%	4%	4.3%	5%	34.1%	4%	23.1%	5%	34.1%	5%	30.1%
Dec	2%	0%	3%	22.8%	3%	35.9%	3%	24.7%	3%	35.9%	3%	29.8%
Total	37.3%	0%	42.2%	13.2%	45.1%	21.1%	42.2%	13%	45.2%	21.1%	45.1%	21.1%

Table 45 - CSP+MED case study: Capacity Factor (using GROSS Electric Output)

5 - Capacity Factor (using >>GROSS<< Electric Output)	CT 8 MED+SWCC				CT 1 Wet Cooling		CT 2 Dry Cooling		CT 4 Wet Cooling		CT 5 SWCC	
	CSP %	%	MED %	%	%	%	%	%	%	%	%	%
Jan	9%	0%	7%	-24.3%	10%	14.7%	10%	9.9%	10%	14.7%	10%	13.5%
Feb	30%	0%	25%	-16.6%	31%	4.2%	30%	-0.1%	31%	4.2%	31%	3.5%
Mar	55%	0%	49%	-9.8%	56%	3.6%	54%	-0.4%	57%	3.6%	56%	3.0%
Apr	53%	0%	49%	-7.9%	55%	4.6%	53%	0.0%	55%	4.6%	55%	4.0%
May	81%	0%	79%	-2.7%	87%	7.1%	83%	2.0%	87%	7.1%	86%	6.6%
Jun	78%	0%	76%	-2.8%	84%	7.6%	81%	2.6%	84%	7.6%	84%	7.1%
Jul	85%	0%	81%	-4.2%	91%	7.4%	87%	2.2%	91%	7.4%	90%	6.8%
Aug	72%	0%	67%	-6.1%	77%	7.9%	74%	3.1%	77%	8.0%	77%	7.7%
Sep	42%	0%	37%	-10.5%	43%	3.6%	41%	-0.7%	43%	3.6%	43%	3.2%
Oct	32%	0%	28%	-13.5%	33%	4.3%	32%	-0.3%	33%	4.3%	33%	3.8%
Nov	5%	0%	4%	-26.5%	6%	19.2%	6%	13.0%	6%	19.2%	6%	15.1%
Dec	4%	0%	3%	-26.9%	5%	20.3%	4%	15.7%	5%	20.3%	4%	14.4%
Total	45.5%	0%	42.2%	-7.3%	48.5%	6.5%	46.3%	2%	48.5%	6.5%	48.2%	5.9%

Table 46 - CSP+MED case study: Rankine Cycle Efficiency

6 - Rankine Cycle Efficiency	CT 8 MED+SWCC			CT 1 Wet Cooling		CT 2 Dry Cooling		CT 4 Wet Cooling		CT 5 SWCC	
	MWhe	%	m3/month	MWhe	%	MWhe	%	MWhe	%	MWhe	%
Jan	37.59%	0%	73 924	37.62%	0.1%	36.50%	-2.9%	37.62%	0.1%	37.21%	-1.0%
Feb	37.88%	0%	250 433	38.13%	0.7%	36.83%	-2.8%	38.13%	0.7%	37.91%	0.1%
Mar	37.87%	0%	550 123	38.17%	0.8%	36.86%	-2.7%	38.18%	0.8%	37.95%	0.2%
Apr	37.86%	0%	528 378	38.17%	0.8%	36.70%	-3.1%	38.18%	0.8%	37.97%	0.3%
May	37.87%	0%	882 955	38.19%	0.8%	36.57%	-3.4%	38.20%	0.9%	38.01%	0.4%
Jun	37.88%	0%	825 169	38.23%	0.9%	36.59%	-3.4%	38.23%	0.9%	38.01%	0.3%
Jul	37.88%	0%	906 889	38.21%	0.9%	36.55%	-3.5%	38.22%	0.9%	37.98%	0.3%
Aug	37.87%	0%	753 274	38.10%	0.6%	36.60%	-3.3%	38.10%	0.6%	37.99%	0.3%
Sep	37.85%	0%	402 339	38.01%	0.4%	36.60%	-3.3%	38.02%	0.4%	37.88%	0.1%
Oct	37.85%	0%	309 692	38.00%	0.4%	36.57%	-3.4%	38.01%	0.4%	37.86%	0.0%
Nov	37.64%	0%	40 670	37.83%	0.5%	36.58%	-2.8%	37.84%	0.5%	37.48%	-0.4%
Dec	37.59%	0%	31 485	37.55%	-0.1%	36.64%	-2.5%	37.56%	-0.1%	37.38%	-0.5%
Total	37.80%	0%	5 555 331	38.02%	1%	36.63%	-3%	38.02%	1%	37.80%	0%

Table 47 - CSP+MED case study: Design Rankine Cycle Efficiency

7 - Design Rankine Cycle Efficiency	CT 8 MED+SWCC			CT 1 Wet Cooling		CT 2 Dry Cooling		CT 4 Wet Cooling		CT 5 SWCC	
	MWhe	%	m3/month	MWhe	%	MWhe	%	MWhe	%	MWhe	%
Jan	37.99%	0%	73 924	37.74%	-0.6%	37.74%	-0.6%	37.74%	-0.6%	38.06%	0.2%
Feb	37.99%	0%	250 433	37.74%	-0.6%	37.74%	-0.6%	37.74%	-0.6%	38.06%	0.2%
Mar	37.99%	0%	550 123	37.74%	-0.6%	37.74%	-0.6%	37.74%	-0.6%	38.06%	0.2%
Apr	37.99%	0%	528 378	37.74%	-0.6%	37.74%	-0.6%	37.74%	-0.6%	38.06%	0.2%
May	37.99%	0%	882 955	37.74%	-0.6%	37.74%	-0.6%	37.74%	-0.6%	38.06%	0.2%
Jun	37.99%	0%	825 169	37.74%	-0.6%	37.74%	-0.6%	37.74%	-0.6%	38.06%	0.2%
Jul	37.99%	0%	906 889	37.74%	-0.6%	37.74%	-0.6%	37.74%	-0.6%	38.06%	0.2%
Aug	37.99%	0%	753 274	37.74%	-0.6%	37.74%	-0.6%	37.74%	-0.6%	38.06%	0.2%
Sep	37.99%	0%	402 339	37.74%	-0.6%	37.74%	-0.6%	37.74%	-0.6%	38.06%	0.2%
Oct	37.99%	0%	309 692	37.74%	-0.6%	37.74%	-0.6%	37.74%	-0.6%	38.06%	0.2%
Nov	37.99%	0%	40 670	37.74%	-0.6%	37.74%	-0.6%	37.74%	-0.6%	38.06%	0.2%
Dec	37.99%	0%	31 485	37.74%	-0.6%	37.74%	-0.6%	37.74%	-0.6%	38.06%	0.2%
Total	37.99%	0%	5 555 331	37.74%	-1%	37.74%	-1%	37.74%	-1%	38.06%	0%

Table 48 - CSP+MED case study: Total Parasitics

8 - Total Parasitics	CT 8 MED+SWCC			CT 1 Wet Cooling		CT 2 Dry Cooling		CT 4 Wet Cooling		CT 5 SWCC	
	MWhe	%	m3/month	MWhe	%	MWhe	%	MWhe	%	MWhe	%
Jan	1 587	0%	73 924	1 232	-22.4%	1 325	-16.5%	1 232	-22.4%	1 182	-25.5%
Feb	2 604	0%	250 433	1 227	-52.9%	1 454	-44.2%	1 226	-52.9%	1 114	-57.2%
Mar	5 657	0%	550 123	2 381	-57.9%	2 859	-49.5%	2 381	-57.9%	2 197	-61.2%
Apr	5 813	0%	528 378	2 310	-60.3%	2 767	-52.4%	2 310	-60.3%	2 149	-63.0%
May	10 593	0%	882 955	3 977	-62.5%	4 771	-55.0%	3 978	-62.4%	3 727	-64.8%
Jun	12 171	0%	825 169	3 899	-68.0%	4 911	-59.7%	3 903	-67.9%	3 825	-68.6%
Jul	13 368	0%	906 889	4 232	-68.3%	5 639	-57.8%	4 231	-68.3%	4 055	-69.7%
Aug	9 468	0%	753 274	3 973	-58.0%	5 189	-45.2%	3 972	-58.0%	3 456	-63.5%
Sep	4 615	0%	402 339	2 013	-56.4%	2 639	-42.8%	2 013	-56.4%	1 730	-62.5%
Oct	3 302	0%	309 692	1 544	-53.2%	2 014	-39.0%	1 544	-53.2%	1 341	-59.4%
Nov	1 075	0%	40 670	899	-16.4%	953	-11.3%	900	-16.3%	853	-20.7%
Dec	1 150	0%	31 485	1 121	-2.5%	1 177	2.4%	1 121	-2.6%	1 055	-8.3%
Total	71 403	0%	5 555 331	28 806	-60%	35 697	-50%	28 809	-60%	26 684	-63%

Table 49 - CSP+MED case study: Cooling Parasitics

9 - Cooling Parasitics	CT 8 MED+SWCC			CT 1 Wet Cooling		CT 2 Dry Cooling		CT 4 Wet Cooling		CT 5 SWCC	
	MWhe	%	m3/month	MWhe	%	MWhe	%	MWhe	%	MWhe	%
Jan	425	0%	73 924	77	-81.8%	169	-60.3%	77	-81.8%	27	-93.6%
Feb	1 471	0%	250 433	200	-86.4%	426	-71.0%	199	-86.5%	87	-94.1%
Mar	3 406	0%	550 123	394	-88.4%	861	-74.7%	393	-88.5%	212	-93.8%
Apr	3 677	0%	528 378	412	-88.8%	857	-76.7%	412	-88.8%	252	-93.1%
May	6 995	0%	882 955	795	-88.6%	1 566	-77.6%	797	-88.6%	551	-92.1%
Jun	8 765	0%	825 169	884	-89.9%	1 871	-78.6%	887	-89.9%	814	-90.7%
Jul	9 806	0%	906 889	1 076	-89.0%	2 458	-74.9%	1 075	-89.0%	905	-90.8%
Aug	6 190	0%	753 274	1 006	-83.8%	2 204	-64.4%	1 004	-83.8%	494	-92.0%
Sep	2 867	0%	402 339	475	-83.4%	1 090	-62.0%	475	-83.4%	196	-93.2%
Oct	1 977	0%	309 692	328	-83.4%	790	-60.0%	328	-83.4%	125	-93.7%
Nov	261	0%	40 670	49	-81.2%	104	-60.0%	49	-81.2%	18	-93.1%
Dec	182	0%	31 485	37	-79.8%	84	-53.9%	37	-79.8%	12	-93.4%
Total	46 021	0%	5 555 331	5 732	-88%	12 480	-73%	5 734	-88%	3 695	-92%

Table 50 - CSP+MED case study: CSP Parasitics (Except Cooling)

10 - CSP Parasitics (Except Cooling)	CT 8			CT 1		CT 2		CT 4		CT 5	
	MED+SWCC			Wet Cooling		Dry Cooling		Wet Cooling		SWCC	
	MWhe	%	m3/month	MWhe	%	MWhe	%	MWhe	%	MWhe	%
Jan	1 162	0%	73 924	1 154	-0.6%	1 325	14.0%	1 154	-0.6%	1 155	-0.6%
Feb	1 133	0%	250 433	1 027	-9.4%	1 454	28.3%	1 027	-9.4%	1 027	-9.4%
Mar	2 251	0%	550 123	1 987	-11.7%	2 859	27.0%	1 987	-11.7%	1 986	-11.8%
Apr	2 136	0%	528 378	1 898	-11.1%	2 767	29.5%	1 898	-11.1%	1 897	-11.2%
May	3 598	0%	882 955	3 182	-11.6%	4 771	32.6%	3 182	-11.6%	3 176	-11.7%
Jun	3 406	0%	825 169	3 016	-11.5%	4 911	44.2%	3 016	-11.5%	3 011	-11.6%
Jul	3 563	0%	906 889	3 156	-11.4%	5 639	58.3%	3 156	-11.4%	3 150	-11.6%
Aug	3 277	0%	753 274	2 967	-9.5%	5 189	58.3%	2 967	-9.5%	2 962	-9.6%
Sep	1 748	0%	402 339	1 537	-12.0%	2 639	51.0%	1 537	-12.0%	1 533	-12.3%
Oct	1 325	0%	309 692	1 216	-8.2%	2 014	52.0%	1 216	-8.2%	1 216	-8.2%
Nov	815	0%	40 670	850	4.3%	953	17.0%	851	4.4%	835	2.4%
Dec	968	0%	31 485	1 084	12.0%	1 177	21.6%	1 084	12.0%	1 043	7.7%
Total	25 383	0%	5 555 331	23 075	-9.1%	35 697	40.6%	23 075	-9%	22 989	-9%

Table 51 - CSP+MED case study: CSP Anti-Freezing Parasitics

11 - CSP Anti-Freezing Parasitics	CT 8			CT 1		CT 2		CT 4		CT 5	
	MED+SWCC			Wet Cooling		Dry Cooling		Wet Cooling		SWCC	
	MWhe	%	m3/month	MWhe	%	MWhe	%	MWhe	%	MWhe	%
Jan	372	0%	73 924	369	-0.7%	371	-0.3%	369	-0.7%	370	-0.6%
Feb	74	0%	250 433	33	-55.8%	31	-57.5%	33	-55.8%	33	-55.3%
Mar	0	0%	550 123	1	195.9%	1	303.6%	1	195.8%	1	241.6%
Apr	12	0%	528 378	10	-13.6%	10	-12.0%	10	-13.6%	11	-8.0%
May	16	0%	882 955	8	-51.7%	7	-55.7%	8	-51.7%	8	-51.7%
Jun	0	0%	825 169	0	0.0%	0	0.0%	0	0.0%	0	0.0%
Jul	0	0%	906 889	0	0.0%	0	0.0%	0	0.0%	0	0.0%
Aug	27	0%	753 274	51	89.9%	51	89.9%	51	89.9%	51	89.9%
Sep	86	0%	402 339	60	-29.8%	63	-27.3%	60	-29.8%	59	-31.9%
Oct	19	0%	309 692	19	3.2%	20	5.1%	19	3.1%	20	5.7%
Nov	196	0%	40 670	232	18.5%	231	18.1%	233	19.0%	220	12.5%
Dec	333	0%	31 485	444	33.5%	454	36.3%	444	33.5%	408	22.5%
Total	1 134	0%	5 555 331	1 227	8.3%	1 238	9.2%	1 228	8.3%	1 179	4.0%

Table 52 - CSP+MED case study: Specific Parasitic consumption (while CSP is ON)

12 - Specific Parasitic consumption (while CSP is ON)	CT 8			CT 1		CT 2		CT 4		CT 5	
	MED+SWCC			Wet Cooling		Dry Cooling		Wet Cooling		SWCC	
	%	%	m3/month	%	%	%	%	%	%	%	%
Jan	9.8%	0%	9.8%	4.0%	-58.9%	5.5%	-43.9%	4.0%	-58.9%	3.4%	-65.3%
Feb	11.0%	0%	11.0%	4.1%	-62.8%	5.4%	-50.7%	4.1%	-62.8%	3.6%	-67.5%
Mar	13.5%	0%	13.5%	5.1%	-61.9%	6.5%	-51.5%	5.1%	-61.9%	4.7%	-64.9%
Apr	14.7%	0%	14.7%	5.2%	-64.7%	6.6%	-54.9%	5.2%	-64.7%	4.8%	-67.3%
May	17.5%	0%	17.5%	6.0%	-65.5%	7.6%	-56.4%	6.0%	-65.5%	5.7%	-67.6%
Jun	21.6%	0%	21.6%	6.3%	-70.8%	8.4%	-61.2%	6.3%	-70.8%	6.2%	-71.3%
Jul	21.3%	0%	21.3%	6.2%	-70.9%	8.7%	-59.1%	6.2%	-71.0%	6.0%	-72.0%
Aug	17.5%	0%	17.5%	6.6%	-62.5%	9.1%	-48.0%	6.6%	-62.5%	5.7%	-67.6%
Sep	14.3%	0%	14.3%	5.4%	-62.4%	7.7%	-45.9%	5.4%	-62.4%	4.5%	-68.7%
Oct	12.4%	0%	12.4%	4.8%	-61.6%	7.0%	-43.8%	4.8%	-61.6%	4.0%	-68.1%
Nov	10.6%	0%	10.6%	4.3%	-59.0%	5.9%	-43.8%	4.3%	-59.0%	3.7%	-65.2%
Dec	10.2%	0%	10.2%	4.4%	-56.4%	6.1%	-40.5%	4.4%	-56.4%	3.8%	-62.9%
Total	14.5%	0%	14.5%	5.2%	-64.2%	7.1%	-51.5%	5.2%	-64.2%	4.7%	-67.9%

Table 53 - CSP+MED case study: Specific Parasitic consumption (while CSP is ON or OFF)

13 - Specific Parasitic consumption (while CSP is ON or OFF)											
	CT 8			CT 1		CT 2		CT 4		CT 5	
	MED+SWCC			Wet Cooling		Dry Cooling		Wet Cooling		SWCC	
	%	%	m3/month	%	%	%	%	%	%	%	%
Jan	24.7%	0%	24.7%	16.7%	-32.3%	18.7%	-24.1%	16.7%	-32.3%	16.2%	-34.4%
Feb	13.2%	0%	13.2%	6.0%	-54.8%	7.4%	-44.2%	5.9%	-54.8%	5.4%	-58.7%
Mar	14.1%	0%	14.1%	5.7%	-59.4%	7.1%	-49.3%	5.7%	-59.4%	5.3%	-62.3%
Apr	15.4%	0%	15.4%	5.8%	-62.0%	7.3%	-52.4%	5.8%	-62.0%	5.5%	-64.5%
May	17.7%	0%	17.7%	6.2%	-64.9%	7.8%	-55.8%	6.2%	-64.9%	5.9%	-67.0%
Jun	21.8%	0%	21.8%	6.5%	-70.2%	8.6%	-60.7%	6.5%	-70.2%	6.4%	-70.7%
Jul	21.4%	0%	21.4%	6.3%	-70.5%	8.8%	-58.7%	6.3%	-70.5%	6.1%	-71.6%
Aug	17.9%	0%	17.9%	7.0%	-61.1%	9.5%	-46.8%	7.0%	-61.1%	6.1%	-66.1%
Sep	15.6%	0%	15.6%	6.6%	-57.9%	9.0%	-42.4%	6.6%	-57.9%	5.7%	-63.7%
Oct	14.0%	0%	14.0%	6.3%	-55.1%	8.6%	-38.9%	6.3%	-55.2%	5.5%	-60.9%
Nov	29.5%	0%	29.5%	20.7%	-29.9%	23.2%	-21.5%	20.7%	-29.8%	20.3%	-31.1%
Dec	40.5%	0%	40.5%	32.8%	-19.0%	35.9%	-11.5%	32.8%	-19.0%	32.5%	-19.8%
Total	20.5%	0.0%	20.5%	10.5%	-48.5%	12.7%	-38.2%	10.5%	-48.5%	10.1%	-50.9%

Table 54 - CSP+MED case study: Pressures in the Condenser

14 - Pressures in the Condenser											
	CT 8			CT 1		CT 2		CT 4		CT 5	
	MED+SWCC			Wet Cooling		Dry Cooling		Wet Cooling		SWCC	
	mbar	%	m3/month	mbar	%	mbar	%	mbar	%	mbar	%
Jan	50	0%	73 924	46	-9.1%	72	42.8%	46	-9.1%	50	0.0%
Feb	50	0%	250 433	53	4.6%	82	62.2%	53	4.6%	50	0.0%
Mar	50	0%	550 123	54	6.5%	82	62.9%	54	6.5%	50	0.0%
Apr	50	0%	528 378	54	6.8%	88	74.2%	54	6.8%	50	0.0%
May	50	0%	882 955	55	9.1%	93	84.5%	55	9.1%	50	0.0%
Jun	50	0%	825 169	55	8.4%	91	81.6%	55	8.4%	50	0.0%
Jul	50	0%	906 889	54	7.7%	92	83.4%	54	7.7%	50	0.0%
Aug	50	0%	753 274	57	12.4%	92	81.8%	57	12.4%	50	0.0%
Sep	50	0%	402 339	55	9.6%	89	76.4%	55	9.6%	50	0.0%
Oct	50	0%	309 692	55	8.3%	90	79.0%	55	8.3%	50	0.0%
Nov	50	0%	40 670	46	-9.3%	79	57.0%	46	-9.3%	50	0.0%
Dec	50	0%	31 485	46	-7.9%	73	45.3%	46	-7.9%	50	0.0%
Total	50	0%	5 555 331	52	4%	85	69%	52	4%	50	0%

Table 55 - CSP+MED case study: Temperatures in the Condenser

15 - Temperatures in the Condenser											
	CT 8			CT 1		CT 2		CT 4		CT 5	
	MED+SWCC			Wet Cooling		Dry Cooling		Wet Cooling		SWCC	
	ºC	%	m3/month	Temp.	%	Temp.	%	Temp.	%	Temp.	%
Jan	33	0%	73 924	31.2	-5.1%	39.5	19.8%	31.2	-5.1%	32.9	0.0%
Feb	33	0%	250 433	33.7	2.4%	41.9	27.1%	33.7	2.4%	32.9	0.0%
Mar	33	0%	550 123	34.1	3.4%	41.9	27.3%	34.1	3.4%	32.9	0.0%
Apr	33	0%	528 378	34.1	3.6%	43.2	31.2%	34.1	3.6%	32.9	0.0%
May	33	0%	882 955	34.5	4.7%	44.3	34.6%	34.5	4.7%	32.9	0.0%
Jun	33	0%	825 169	34.4	4.4%	44.0	33.6%	34.4	4.4%	32.9	0.0%
Jul	33	0%	906 889	34.3	4.0%	44.2	34.2%	34.3	4.0%	32.9	0.0%
Aug	33	0%	753 274	35.0	6.4%	44.0	33.7%	35.0	6.4%	32.9	0.0%
Sep	33	0%	402 339	34.6	5.0%	43.5	31.9%	34.6	5.0%	32.9	0.0%
Oct	33	0%	309 692	34.4	4.3%	43.7	32.8%	34.4	4.3%	32.9	0.0%
Nov	33	0%	40 670	31.2	-5.2%	41.2	25.2%	31.2	-5.2%	32.9	0.0%
Dec	33	0%	31 485	31.5	-4.4%	39.8	20.7%	31.5	-4.4%	32.9	0.0%
Total	33	0%	5 555 331	33.6	2%	42.6	29%	33.6	2%	32.9	0%

Table 56 - CSP+MED case study: Cutback on the Potential Electric Production per amount of fresh water produced (Considering Net electrical Production)

16 - Cutback on the Potential Electric Production per amount of fresh water produced (Considering NET Elect. Product						
	CT 8		CT 8 vs. WetCool CT1	CT 8 vs. DryCool CT2	CT 8 vs. WetCool CT4	CT 8 vs. SWCC CT 5
	MED+SWCC		Wet Cooling	Dry Cooling	Wet Cooling	SWCC
	%	m3/month	kWh/m3	kWh/m3	kWh/m3	kWh/m3
Jan	0%	73 924	17.59	12.18	17.61	17.26
Feb	0%	250 433	8.81	4.55	8.83	8.72
Mar	0%	550 123	8.57	4.78	8.59	8.51
Apr	0%	528 378	9.93	5.74	9.94	9.83
May	0%	882 955	12.29	7.95	12.30	12.25
Jun	0%	825 169	15.18	10.56	15.19	14.95
Jul	0%	906 889	15.15	10.07	15.16	14.94
Aug	0%	753 274	12.86	7.84	12.88	13.37
Sep	0%	402 339	9.11	4.38	9.13	9.51
Oct	0%	309 692	8.93	3.95	8.94	9.26
Nov	0%	40 670	21.54	14.61	21.55	19.01
Dec	0%	31 485	19.24	13.26	19.26	15.96
Total	0%	5 555 331	12.27	7.64	12.29	12.25

Table 57 - CSP+MED case study: Cutback on the Potential Electric Production per amount of fresh water produced (Considering Gross Elect. Production)

17 - Cutback on the Potential Electric Production per amount of fresh water produced (Considering GROSS Elect. Prod						
	CT 8		CT 8 vs. WetCool CT 1	CT 8 vs. DryCool CT 2	CT 8 vs. WetCool CT 4	CT 8 vs. SWCC CT 5
	MED+SWCC		Wet Cooling	Dry Cooling	Wet Cooling	SWCC
	%	m3/month	kWh/m3	kWh/m3	kWh/m3	kWh/m3
Jan	0%	73 924	12.79	8.63	12.81	11.78
Feb	0%	250 433	3.31	-0.04	3.32	2.77
Mar	0%	550 123	2.61	-0.31	2.63	2.22
Apr	0%	528 378	3.30	-0.03	3.31	2.89
May	0%	882 955	4.79	1.35	4.81	4.47
Jun	0%	825 169	5.16	1.76	5.17	4.84
Jul	0%	906 889	5.07	1.55	5.09	4.67
Aug	0%	753 274	5.57	2.16	5.59	5.39
Sep	0%	402 339	2.64	-0.53	2.66	2.34
Oct	0%	309 692	3.25	-0.21	3.27	2.93
Nov	0%	40 670	17.20	11.61	17.22	13.53
Dec	0%	31 485	18.31	14.13	18.33	12.94
Total	0%	5 555 331	4.60	1.22	4.62	4.20

Table 58 - CSP+MED case study: Cutback on the Potential Electric Production per amount of fresh water produced (Considering Cooling Parasitics Only)

18 - Cutback on the Potential Electric Production per amount of fresh water produced (Considering COOLING PARASIT						
	CT 8		CT 8 vs. WetCool CT 1	CT 8 vs. DryCool CT 2	CT 8 vs. WetCool CT 4	CT 8 vs. SWCC CT 5
	MED+SWCC		Wet Cooling	Dry Cooling	Wet Cooling	SWCC
	%	m3/month	kWh/m3	kWh/m3	kWh/m3	kWh/m3
Jan	0%	73 924	4.70	3.47	4.70	5.38
Feb	0%	250 433	5.07	4.17	5.08	5.52
Mar	0%	550 123	5.48	4.63	5.48	5.81
Apr	0%	528 378	6.18	5.34	6.18	6.48
May	0%	882 955	7.02	6.15	7.02	7.30
Jun	0%	825 169	9.55	8.35	9.55	9.63
Jul	0%	906 889	9.63	8.10	9.63	9.81
Aug	0%	753 274	6.88	5.29	6.88	7.56
Sep	0%	402 339	5.94	4.42	5.94	6.64
Oct	0%	309 692	5.33	3.83	5.33	5.98
Nov	0%	40 670	5.20	3.84	5.20	5.96
Dec	0%	31 485	4.61	3.11	4.61	5.40
Total	0%	5 555 331	7.25	6.04	7.25	7.62

Annex 8 - List of Main Variables Used in SAM's New Solar Desalination Code

Table 59 - List of the main variables used in the solar desalination add on in SAM, with corresponding units and description

Parameter/Variable	Units	Description
Adc	m2	Heat transfer area used at the down condenser
Ae	m2	Heat transfer area used for evaporation in each effect
Am	m2	Average heat transfer area per effect
B	kg/s	Total Mass flow of Brine inside EACH effect (sum of the produced brine +the brine entering from the previous effects - the mass of brine that originated vapor by flashing when the brine enters each effect)
B_b_flash_remain	kg/s	Mass flow of Brine flowing into the NEXT effect that REMAINS after part of it flashed due to the pressure difference.
B_evap	kg/s	Mass flow of Brine produced inside each effect as a result of the evaporation process (not the flashing)
B_Total	kg/s	Total Mass flow of Brine produced in the System
BaseLoad_ref	-	Ratio used for an assume dbase load profile for comparison purposes between Rankine cycle and/or MED outputs using solar or Natural Gas burning
BaseLoad_ref	-	Ratio used for an assume dbase load profile for comparison purposes between Rankine cycle and/or MED outputs using solar or Natural Gas burning
C_a	-	Exponent used in the calculation of the viscosity ratio correction factor (page 176 and 185, Heat Exchangers Selection, Design and Construction, E.A.D. Saunders, 1988)
C_A_pipes_out	m2	Total heat transfer area used in the MED down condenser (assuming the external area of the tubes)
C_Delta_P_Headers	Pa	Pressure loss in the headers on the MED Down condenser
C_Delta_P_nozzle_in	Pa	Pressure loss with Channel inlet to the HTX tubes in the MED down condenser (means at the entrance of the HTX tubes. Tube side nozzles in)
C_Delta_P_nozzle_out	Pa	Pressure loss with Channel outlet from the HTX tubes in the MED down condenser (means at the exit of the HTX tubes. Tube side nozzles out)
C_Delta_P_pipe_in	Pa	Pressure loss inside cylindrical tubes of the MED down condenser
C_Delta_P_total	Pa	Total pressure losses that will need to be surpassed inside the MED down condenser
C_dens_sw	kg/m3	Densisity of the seawater inside the MED down condenser (average between inlet and outlet of cooling water: C_Tbulk = (MED_Tf_dc_out +Tsw) / 2)
C_Dyn_Visc_Tbulk	N.s/m2	Dynamic viscosity of the seawater at average temperature reached inside the HTX tubes of the MED down condenser
C_Dyn_Visc_Twall	N.s/m2	Dynamic viscosity of the seawater at at the wall of the HTX tubes of the MED down condenser (C_Twall assumed to be equal to steam temperature in shell side (TV(n)))
C_Friction_c	-	Friction factor inside the HTX tubes of the down condenser.
C_h_pbrine_in	J/kg	Specific enthalpy of the seawater in the MED down condenser (at C_Tbulk)
C_h_pbrine_out	J/kg	Outlet enthalpy of seawater leaving the feedwater pump, accounting for irreversibility
C_h_pbrine_out_s	J/kg	Isentropic outlet specific enthalpy of seawater (incompressible fluid)
C_HTX_area_tot_section	m2	Total Section area of the heat transfer tubes (does not account pitch space between tubes)
C_Kh	-	Number of velocity heads lost in headers (depends on the number of tube-side passes).Page 184 and 186, Heat Exchangers Selection, Design and Construction, E.A.D. Saunders, 1988)
C_Knt_in	-	Number of velocity heads lost in tube side nozzles inlet. Page 184 and 186, Heat Exchangers Selection, Design and Construction, E.A.D. Saunders, 1988)
C_Knt_out	-	Number of velocity heads lost in tube side nozzles Outlet. Page 184 and 186, Heat Exchangers Selection, Design and Construction, E.A.D. Saunders, 1988)
C_LMTD	ºC	Logarithmic Mean Temperature Difference between vapor temperature (sheel side) and cooling water at down condenser of the MED plant
C_M_dot_pipe	kg/s	Mass flow rate of seawater passing through each tube of the tube bundle of the MED down condenser
C_mass_veloc_pipe	kg/s/m2	Mass velocity of the seawater inside each tube of the HTX of the MED down condenser
C_number_of_pipes	-	Number of pipes used in the tube bundle of the down condenser
C_pipe_diameter_in	m	Inside diameter of each pipe used in tube bundle of the MED down condenser
C_pipe_diameter_out	m	Outside diameter of each pipe used in tube bundle of the MED down condenser
C_pipe_lenght	m	Pipe lenght of tubes in HTX of the MED down condenser
C_pipe_radious_in	m	Inside Radious of each pipe used in tube bundle of the MED down condenser
C_pipe_radius_out	m	Outside Radious of each pipe used in tube bundle of the MED down condenser
C_Pipe_roughness	m	Pipe roughness used in tube bundle of the MED down condenser
C_pipe_Section_in	m2	Inside Section of each pipe used in tube bundle of the MED down condenser
C_Q	kJ/s	Heat load transfered into the MED down condenser
C_Re	-	Reynolds number for seawater flowing inside tube bundle of MED down condenser
C_Tbulk	ºC	Average temperature of seawater inside tube bundle of MED down condenser
C_tot_pipe_lenght	m	Total pipe lenght inside MED down condenser (sum of the lenght of all the tubes inside)
C_tube_side_passes	-	Number of tube side passes inside the MED down condenser
C_Twall	ºC	Temperature at the inner wall in the HTX tubes of MED down condenser
C_U	kW/m2.ºC	Overall Heat transfer coefficient at the MED down condenser
C_vel_nozzle_pipe	m/s	Velocity of seawter at HTX tube nozzles
C_veloc_sw_pipes	m/s	Velocity of seawater inside HTX tubes at MED down condenser
C_visc_corr_fact	-	Viscosity correction factor of seawter flowing inside HTX tubes
C_Vol_dot_sw	m3/s	Volumetric Flow Rate of the cooling water passing through the MED down condenser
C_W_dot_pump	We	Total electrical consumption necessary to pump water inside the MED down condenser ONLY (excludes pumping from and to the sea)
Calc_NCG_ej	-	Flag indicating if any of the ratios for the 1st NCG ejector available in the database to calculate the performance of the NCG ejection was applicable to the current simulation.
Calc_NCG_extreme	-	Flag indicating if entrainment ratio for the 1st NCG ejector is being calculated having into account a limit on the extremes defined by the maximum compression rates available in the database given by Koerting.
Calc_TVC_ej	-	Flag indicating if any of the ratios for the TVC available in the database to calculate the performance of the TVC was applicable to the current simulation.
Calc_TVC_extreme	-	Flag indicating if entrainment ratio for the TVC is being calculated having into account a limit on the extremes defined by the maximum compression rates available in the database given by Koerting.
CSP_tstep_frac_ON	-	Fraction of the time step in which the CSP plant is ON
CSP_tstep_t_ON	hours	Amount of time in each time step in which the CSP plant is ON
CT	-	Flag indicating the Cooling technology used with the Rankine cycle: 7) MED-Parallel Low temp ; 8) MED-Parallel TVC; 9) MED-FF Low temp; 10) MED-FF TVC
D	kg/s	Total Mass flow of Distillate flowing out from EACH effect (includes the distillate acutally produced inside the effect, but also the distillate flowing in from previous effects, and the distillate flowing in from the condensate collected from the NCG ejector surface-condensers. The are also called here as intercondensers)
D_created	kg/s	Mass flow of Distillate added to each distillate box compared to the mass flow flowing IN from the last effect

d_Cross_flow_flag	-	Flag indicating the existance of CROSS-FLOW for the distillate routing. If the configuration is set to have the distillate: 1) flowing between effects (and so flashing when entering the distillate boxes, representing CROSS-FLOW configuration); 0) if it is routed directly into a collecting pipe, and sent for storage (this in practice represents a Parallel configuration without a CROSS-FLOW).
d_Cross_flow_flag	-	Flag indicating the existance of CROSS-FLOW for the distillate routing. If the configuration is set to have the distillate: 1) flowing between effects (and so flashing when entering the distillate boxes, representing CROSS-FLOW configuration); 0) if it is routed directly into a collecting pipe, and sent for storage (this in practice represents a Parallel configuration without a CROSS-FLOW).
d_Cross_flow_flag	-	Flag indicating the existance of CROSS-FLOW for the distillate routing. If the configuration is set to have the distillate: 1) flowing between effects (and so flashing when entering the distillate boxes, representing CROSS-FLOW configuration); 0) if it is routed directly into a collecting pipe, and sent for storage (this in practice represents a Parallel configuration without a CROSS-FLOW).
D_d_flash_remain	kg/s	Mass flow of Distillate remaining from the flashing process referent ONLY to the mass of D(i-1) flowing into each effect.
D_d_flash_remain_cond	kg/s	Mass flow of distillate remaining in the down condenser from the flashing process referent ONLY to the mass of D(n) flowing into it.
D_d_flash_remain_Ej_1	kg/s	Mass flow of condensate from the 1st intercondenser of the NCG ejection system remaining from the flashing process. If an MED low temperature configuration is used this flashing process will take place inside the distillate box of effect number (n_ph_NCG + 1); if a TVC configuration is used this flashing process will take place inside the distillate box of the 3rd effect.
D_d_flash_remain_Ej_2	kg/s	Mass flow of condensate from the 2nd intercondenser of the NCG ejection system remaining from the flashing process. If an MED low temperature configuration is used this flashing process will take place inside the distillate box of effect number (n_ph_NCG + 1); if a TVC configuration is used this flashing process will take place inside the distillate box of the 2nd effect.
D_enter_next	kg/s	Mass flow of distillate produced in each effect that is routed into the next downstream effect, and actually used to produce fresh water This is equal to D_d_flash_remain(i) + Vd_flash(i) (the Vd_flash ends up being condensed inside the 2nd pass of each effect).
D_Total	kg/s	Total Mass flow of Distillate produced in the System (sum of D produced in all effects)
Delta_H_dc	kJ/kg	Difference between the Specific enthalpy of the inlet and outlet Feedwater + Cooling water inside the Down Condenser.
Delta_H_eph	kJ/kg	Difference between the Specific enthalpy of the inlet and outlet Feedwater inside the preheaters, which is being externally preheated 9outside the effects) by the vapor created inside each effect (In case preheaters are defined to be installed in every other effect (eg. 3, 5, 7), this variable will be zero for effects that do not have preheaters between them). It is assumed that the last effect will not have feedwater preheaters (as the down condenser is already its "feedwater preheater", and so Delta_H_eph (n) will always be zero.
Delta_H_iph	kJ/kg	Difference between the Specific enthalpy of the Brine and Feedwater entering each effect for the purpose of internal preheating ("iph"). For FF configurations this variable will be equal to zero for effects (2:n), as the feedwater enters at a higher temperature then the brine outlet from the same effect).
Delta_Qdc	kW	Difference between thermal load 1) passed into the feedwater (necessary >>only<< to run the effects) at the down condenser and 2)released by the vapor entering and formed in the down condenser.
Delta_T_b_NEA	ºC	Non Equilibrium Allowance between the hotter brine (and not the feedwater) entering each effect and the colder brine after flashing.
Delta_T_d_NEA_cond	ºC	Non Equilibrium Allowance between the hotter distillate (and not the feedwater) entering the DOWN condenser and the colder distillate after flashing.
Delta_T_d_NEA_ej_1	ºC	Non Equilibrium Allowance between the hotter distillate (and not the feedwater) from the 1st intercondenser of the NCG ejection system, and the colder distillate produced in the HTX bundle of the effect. If an MED low temperature configuration is used this flashing process will take place inside the distillate box of effect number (n_ph_NCG + 1); if a TVC configuration is used this flashing process will take place inside the distillate box of the 3rd effect.
Delta_T_d_NEA_ej_2	ºC	Non Equilibrium Allowance between the hotter distillate (and not the feedwater) from the 2nd intercondenser of the NCG ejection system, and the colder distillate produced in the HTX bundle of the effect. If an MED low temperature configuration is used this flashing process will take place inside the distillate box of effect number (n_ph_NCG + 1); if a TVC configuration is used this flashing process will take place inside the distillate box of the 2nd effect.
Delta_T_htx	ºC	Mean temperature difference (MTD) between the inside and outside fluids of the HTX tube bundle in each effect: (Tv(i) - Tv_Loss) - Tb(i+1)
Delta_Tb	ºC	Average value for the Delta Tb between effects
Delta_Tf_iph	ºC	Difference between Tb and Tf inside the effects
Delta_Ts_Super	ºC	Delta Temperature between Superheated steam and saturated steam from the turbine
Delta_Tv	ºC	Approximated value for the Delta Tv between effects
E_Cr_1	-	Compression ratio of the gases discharged by the 1st NCG ejector (Pc/Pe). The maximum compression ratio possible to be achieved by each ejector is ~10 (info given by Koerting and Kinetic Therm).
E_Cr_2	-	Compression ratio of the gases discharged by the 2nd NCG ejector (Pc/Pe). The maximum compression ratio possible to be achieved by each ejector is ~10 (info given by Koerting and Kinetic Therm).
E_Hc_Vap_1	kJ/kg	Specific enthalpy of Compressed gases leaving 1st ejector (assuming a 2 stage steam ejector system) >> the vapor that was not condensed
E_Hcond_Tc_Vap_1	kJ/kg	Specific enthalpy of the condensate formed in the 1st intercondenser at the temperature that the vapor condensed (saturated conditions)
E_Hcond_Tc_Vap_2	kJ/kg	Specific enthalpy of the condensate formed in the 2nd intercondenser at the temperature that the vapor condensed (saturated conditions)
E_Hcond_Tcw_in_1	kJ/kg	Specific enthalpy of the condensate formed in the 1st intercondenser at the temperature that it leaves the intercondenser (equal to the cooling water inlet temperature into the intercondenser)
E_Hcond_Tcw_in_2	kJ/kg	Specific enthalpy of the condensate formed in the 2nd intercondenser at the temperature that it leaves the intercondenser (equal to the cooling water inlet temperature into the intercondenser)
E_Hcond_Tcw_out_2	kJ/kg	Specific enthalpy of the cooling water leaving the 2nd intercondenser.
E_Hcw_in_2	kJ/kg.C	Specific enthalpy of the cooling water entering the 2nd intercondenser
E_Hcw_out_1	kJ/kg	Specific enthalpy of the cooling water leaving the 1st intercondenser.
E_Hcw_out_2	kJ/kg.C	Specific enthalpy of the cooling water leaving the 2nd intercondenser
E_He_Vap_2	kJ/kg	Specific enthalpy of vapor Entrained into the 2nd ejector (assuming a 2 stage steam ejector system) >> the vapor that was not condensed
E_Hv_Tc_Vap_2	kJ/kg	Specific enthalpy of vapor Entrained into the atmosphere (after extra energy by reaching the same temperature as the cooling water inlet (E_Tcw_in_2)
E_Hv_Tcw_Vap_2	kJ/kg	Specific enthalpy of the vapor that did not condens in the 2nd intercondenser at its hottest temperature (it is assumed that the 2nd intercondenser has a secondary section, where the saturated steam cools down further until reaching the same temperature that the E_Tcw_in_2)
E_LHc_Vap_1	kJ/kg	Specific enthalpy of the Compressed vapor being condensed at the 1st intercondenser (assuming all the energy released by the vapor discharged by the first ejector in the 1st intercondenser was in saturated steam conditions)

E_LHc_Vap_2	kJ/kg	Specific enthalpy of the Compressed vapor being condensed at the 2nd intercondenser (assuming all the energy released by the vapor discharged by the second ejector in the 2nd intercondenser was in saturated steam conditions)
E_M_NCG_1	kg/s	Mass flow of NCG being extracted out of the whole MED plant system
E_M_NCG_2	kg/s	Mass flow of NCG used to dimension the 2nd NCG ejector. If not enough heat load is possible to be provided by the 2nd ejector into the system, then a higher amount of NCG is considered for this ejector only (which wont represent in practice a higher amount of NCG ejected from the plant). The amount of NCG ejected from the plant will be actually E_M_NCG_1
E_mass_concentr_NCG	g/m3	Concentration of NCG in the seawater
E_mass_safe_NCG	-	Safety Factor of total mass of NCG to be ejected: "1" means that the mass of NCG to be extracted will be 100% more than the mass initially calculated only with "E_mass_concentr_NCG")
E_Mc_1	kg/s	Total Mass flow of gases discharged by the 1st steam ejector
E_Mc_2	kg/s	Total Mass flow of gases discharged by the 2nd steam ejector
E_Mc_Vap_1	kg/s	Total Mass flow of Vapor (only vapor) discharged by the 1st steam ejector (it does not include the mass of NCG)
E_Mc_Vap_2	kg/s	Total Mass flow of vapor (only vapor) discharged by the 2nd steam ejector (it does not include the mass of NCG)
E_Mcond_Vap_1	kg/s	Mass flow rate of vapor CONDENSED in the 1st intercondenser
E_Mcond_Vap_2	kg/s	Mass flow rate of vapor CONDENSED in the 2nd intercondenser
E_Mcw_1	kg/s	Mass flow of cooling water that is preheated by the 1st intercondenser of the NCG ejection system (in this case will be the feedwater fed into the first MED effects).
E_Mcw_2	kg/s	Mass flow rate of the cooling water used in the 2nd intercondenser.
E_Me_1	kg/s	Mass flow rate of gases entrained into the 1st ejector, which consist of steam and NCG, >>BEFORE<< calculating equivalence to Air
E_Me_2	kg/s	Mass flow rate of gases entrained into the 2nd ejector, which consist of steam and NCG, >>BEFORE<< calculating equivalence to Air (the mass of NCG accounted here is the potentially oversized from the 2nd ejector)
E_Me_air_equiv_1	kg/s	Mass flow of air equivalent entrained gases into the 1st ejector (input to this subroutine)
E_Me_air_equiv_2	kg/s	Mass flow of air equivalent entrained gases into the 2nd ejector (input to this subroutine)
E_Me_atm	kg/s	Mass flow rate of gases actually released into the atmosphere (it accounts E_M_NCG_1instead of the oversized E_M_NCG_2)
E_Me_cf_NCG	-	Gas Molecular Weight Correction for NCG. The 109 conversion factor between Air and NCG comes from experimental tables published in the book "Standards for Steam Jet Vacuum systems" from the Heat Exchange Institute (2000), 5th edition. It is a correction factor for Molecular Weight Entrainment Ratio, accounting that NCG have a molecular weight of 36kg/kmol. See figure figure 16, page 31from the mentioned HEI book, or freely on the second table, page 9, from "JRG/TC Models for Pumping gases" made by "Northeast Controls", or page 7 from "Jet Pumping Technical data, pumping gases", from Tyco.
E_Me_cf_Vap	-	Gas Molecular Weight Correction for Steam. The 0.81conversion factor between Air and Steam comes from experimental tables published in the book "Standards for Steam Jet Vacuum systems" from the Heat Exchange Institute (2000), 5th edition. It is a correction factor for Molecular Weight Entrainment Ratio, accounting that Steam has a molecular weight of 18kg/kmol. See figure figure 16, page 31from the mentioned HEI book, or freely on the second table, page 9, from "JRG/TC Models for Pumping gases" made by "Northeast Controls", or page 7 from "Jet Pumping Technical data, pumping gases", from Tyco.
E_Me_Vap_1	kg/s	Mass flow rate of vapor Entrained into the 1st ejector
E_Me_Vap_2	kg/s	Mass flow rate of vapor Entrained into the 2nd ejector
E_Me_Vap_atm	kg/s	Mass flow rate of vapor being released to the atmosphere by the NCG ejection system
E_Mm_1	kg/s	Mass flow of motive steam powering the 1st ejector (output from this subroutine)
E_Mm_2	kg/s	Mass flow of motive steam powering the 2nd ejector (output from this subroutine)
E_Mm_adj	kg/s	Total Mass flow rate of motive steam powering the NCG ejectors, that would actually be demanded from the actual output that would be required from the rankine cycle that User described
E_Mm_Tot	kg/s	Total Mass flow rate of motive steam powering all the ejectors
E_Molar_f_e_NCG_2	-	Molar fraction of the NCG from the total amount of gases entrained into the 2nd ejector
E_Molar_f_e_NCG_atm	-	Molar fraction of the NCG from the total amount of gases entrained into the atmosphere
E_Molar_f_e_Vap_2	-	Molar fraction of the vapor from the total amount of gases entrained in the 2nd ejector
E_Molar_f_e_Vap_atm	-	Molar fraction of the vapor from the total amount of gases entrained in the atmosphere
E_moles_e_Tot_2	kmol	Total number of moles of gas entrained into the 2nd ejector (before adjusting with corretion factors for air equivalence, needed to be able to use the given entrainment ratios).
E_moles_e_Tot_atm	kmol	Total number of moles of gas entrained into the atmosphere.
E_moles_e_Vap_2	kmol	Moles of Vapor entrained gas into the 2nd ejector (before adjusting with corretion factors for air equivalence, needed to be able to use the given entrainment ratios).
E_moles_e_Vap_atm	kmol	Moles of Vapor entrained gas into the atmosphere.
E_moles_NCG	kmol	Moles of NCG gases passing through both ejectors (before adjusting with corretion factors for air equivalence, needed to be able to use the given entrainment ratios).
E_optim_2	-	Flag indicating the optimization strategy for the 2nd NCG ejector
E_Pc_1	Pa	Pressure of compressed gas from 1st ejector (input to this subroutine)
E_Pc_2	Pa	Pressure of compressed gas from 2nd ejector (input to this subroutine)
E_Pc_NCG_2	Pa	Partial Pressure of NCG in the compressed gases leaving the 2nd ejector
E_Pc_Vap_1	Pa	Partial pressure of Vapor in the Compressed gases leaving the 1st ejector
E_Pc_Vap_1_ref	Pa	Reference Partial pressure of Vapor in the Compressed gases leaving the 1st ejector (obtained from the E_Tc_Vap_1_ref). This is the variable used in the iteration loop to find the correct E_Pc_1
E_Pc_Vap_2	Pa	Partial pressure of Vapor in the Compressed gases leaving the 2nd ejector. This is the variable that is used for the remaining calculations of the performance of the 2nd ejector, and the E_Pc_Vap_2_ref is the pressure aimed when reaching the equilibirum in the ejector calculations.
E_Pc_Vap_2_ref	Pa	Reference Partial pressure of Vapor in the Compressed gases leaving the 2nd ejector. This is the variable used in the iteration loop to find the correct E_Pc_2.
E_Pcw_2	Pa	Pressure at which the cooling water is pumpued through the 2nd intercondenser of the NCG ejection system. This value is not mentioned for the 1st intercondenser as it uses seawater, and this code does not have a formula available to calculate enthalpies of saltwater having difference pressure as an input. If the 2nd intercondenser uses also saltwater as cooling water, this parameter will not be used
E_Pe_1	Pa	Pressure of Entrained gases into the 1st ejector (input to this subroutine)
E_Pe_2	Pa	Pressure of Entrained gases into the 2nd ejector (input to this subroutine)
E_Pe_NCG_1	Pa	Partial pressure of NCG entrained into the 1st ejector
E_Pe_NCG_2	Pa	Partial pressure of NCG entrained into the 2nd ejector
E_Pe_NCG_atm	Pa	Partial pressure of NCG when discharged into the atmosphere by the 2nd intercondenser
E_Pe_Vap_1	Pa	Partial pressure of vapor entrained into the 1st ejector

E_Pe_Vap_2	Pa	Partial pressure of vapor entrained into the 2nd ejector
E_Pe_Vap_atm	Pa	Partial pressure of vapor when discharged from the 2nd intercondenser into the atmosphere
E_Pm	Pa	Motive steam pressure used to power both steam ejectors
E_Qcw_1	kW	Heat load transferred into the feedwater cooling the gases leaving the 1st ejector
E_Qcw_2	kW	Heat load transferred into the distillate cooling the gases leaving the 2nd ejector
E_Qcw_Tot	kW	Heat load added by the NCG ejection system to the MED (with 1st ejector) and Rankine system (with 2nd ejector)
E_Ra_1	-	Ratio between "Motive flow rate (steam)" / "Suction flow rate (air equivalent)" on the 1st effect (it is equal to "1/Entrainment ratio")
E_Ra_2	-	Ratio between "Motive flow rate (steam)" / "Suction flow rate (air equivalent)" on the 2nd effect (it is equal to "1/Entrainment ratio")
E_ratio_delta_Pe_2	-	Ratio Pressure difference between Entrained gas into ejector 2 compared with the Discharge pressure of Ejector 1)
E_Size_1	inches	Size of the ejector to cope with the pretended Pe, Pc, Pm and Me (output from this subroutine). Only referent to the 1st ejector
E_subcool_deltaT_1	ºC	Subcooling temperature assumed for the vapor being entrained into the 1st ejector compared to the temperature at which it is extracted from the last MED effect. Using this subcooling, a partial pressure of vapor can be calculated within the whole amount of gases being entrained into the 1st ejector. The toal pressure is the pressure at which the last effect operates. These calculations are industry practice.
E_T_approach_cond	ºC	Temperature approach between Feedwater outlet temperature and saturated vapor pressure inside condenser receiving gases from the 1st NCG steam ejector (Assuming a 2 stage NCG steam ejection system)
E_T_approach_cond_1	ºC	Temperature approach at the 1st intercondenser
E_T_approach_cond_2	ºC	Temperature approach at the 2nd intercondenser
E_T_Limit_air_equiv	ºC	Temperature limit for air equivalent correction factor to be applied. Below 70ºF there are no correction factors (at least from the literature used)
E_Tc_Vap_1	ºC	Calculated temperature of Vapor that actually leaves in the Compressed gases discharged by the 1st ejector
E_Tc_Vap_1_ref	ºC	Reference temperature aimed for the vapor in the Compressed gases leaving the 1st ejector (calculated assuming saturated conditions)
E_Tc_Vap_2	ºC	Temperature of vapor discharged by the 2nd ejector (calculated assuming saturated conditions). Thsi is the temperature actually used in the remaining calculations on the code.
E_Tc_Vap_2_max	ºC	Maximum teoretical temperature of vapor in the Compressed gases leaving the 2nd ejector (calculated assuming saturated conditions)
E_Tc_Vap_2_ref	ºC	Reference temperature of vapor discharged by the 2nd ejector (calculated assuming saturated conditions). This temperature is the one that is being aimed at accounting the temperature approach predefined for the 1st intercondenser between the feedwater temperature outlet and vapor condensation temperature.
E_Tcw_in_2	ºC	Temperature inlet of the cooling water used in the 2nd intercondenser
E_Tcw_out_1	ºC	Temperature outlet of the cooling water used in the 1st intercondenser
E_Tcw_out_2	ºC	Temperature outlet of the cooling water used in the 2nd intercondenser (only set by the user in TVC configurations: CT(8,10). In Low tempemperature configurations the input set here is disregarded).
E_Te_cf_DryAir_1	-	Temperature correction factor applicable to NCG being entrained into the 1st ejector (the ratios obtained from the industry imply the assumption of gases being entrained at 70F, and consisting of dry air)
E_Te_cf_DryAir_2	-	Temperature correction factor applicable to NCG being entrained into the 2nd ejector (the ratios obtained from the industry imply the assumption of gases being entrained at 70F, and consisting of dry air)
E_Te_cf_Vap_1	-	Temperature correction factor applicable to vapor being entrained into the 1st ejector (the ratios obtained from the industry imply the assumption of gases being entrained at 70F, and consisting of dry air)
E_Te_cf_Vap_2	-	Temperature correction factor applicable to vapor being entrained into the 2nd ejector (the ratios obtained from the industry imply the assumption of gases being entrained at 70F, and consisting of dry air)
E_Te_tot_2	ºC	Temperature used to make an approximation of the total pressure of the gases entrained into the 2nd ejector
E_Te_Vap_1	ºC	Temperature of vapor in the Entrained gases entering the 2nd ejector (calculated assuming saturated conditions)
E_Te_Vap_2	ºC	Temperature of entrained vapor into the s2nd ejector
E_Te_Vap_atm	Pa	Temperature of vapor when discharged from the 2nd intercondenser into the atmosphere
E_Wr_1	-	Entrainment Ratios used in 1st ejector (Suction flow rate(air equivalent) / Motive flow rate (steam))
E_Wr_2	-	Entrainment Ratios used in 2nd ejector (Suction flow rate(air equivalent) / Motive flow rate (steam))
E_Wr_acc_High_1	-	Ratio between between the Pressures actually used in the model, and the pressures used to find an applicable entrainment ratio to describe the steam consumption with NCG extraction with the 1st ejector (upper boundary).
E_Wr_acc_High_2	-	Ratio between between the Pressures actually used in the model, and the pressures used to find an applicable entrainment ratio to describe the steam consumption with NCG extraction with the 2nd ejector (upper boundary).
E_Wr_acc_Low_1	-	Ratio between between the Pressures actually used in the model, and the pressures used to find an applicable entrainment ratio to describe the steam consumption with NCG extraction with the 1st ejector (lower boundary).
E_Wr_acc_Low_2	-	Ratio between between the Pressures actually used in the model, and the pressures used to find an applicable entrainment ratio to describe the steam consumption with NCG extraction with the 2nd ejector (lower boundary).
Ej_num	-	Ejector number (indicating the code which block to chose in the code to perform the "Linear Interpolation" (_Lip)
eph_flag	-	Flag indicating if the plant has feedwater preheaters, and if so, if they are placed between every effect or between every 2 effects. 0) there are NO preheaters; 1) preheaters beetween every effect (with NCG ejectors); 2) preheaters between every 2 effects (with NCG ejectors); 3) preheaters beetween every effect (>> without << NCG ejectors); 4) preheaters between every 2 effects (>> without << NCG ejectors). It is always assumed in both configurations 1) and 2) that: A) there are no preheaters beetween effects that receive feedwater preheated by the NCG ejectors system intercondensers, B) that the effect just after the 1st NCG intercondenser will have no preheater also, and C) that the last effect will not have a feedwater preheater (as the down condenser acts as its own dedicated preheater).
eta_adj_des	-	Rankine cycle efficiency at design point adjusted to the curves available to SAM's database (this is the value of the efficiency of the cycle when using the Ts value set by the user, which probably will be different than the temperature related to the efficiency given as input for the cycle).
eta_adj_mem	-	Memory for the eta_adj_ref calculation.
eta_des	-	Rankine cycle efficiency at design point for the actual rankine cycle described by the user at Ts temperature (and not the efficiency of the cycle described in the SAM curves), with the intermediate steam extractions to power the MED process.
eta_mem	-	Memory used for the eta calculated at each time step (including in the first call)

eta_ND	-	Non dimensional value of Eta (its a ratio of a ratio). It represents the ratio between the Eta at design point >>OF THE CYCLE DESCRIBED IN SAM<< (and not the cycle described by the user), and the eta under the conditions defined for design (basically with the design conditions the user set for P_cond, P_ext_k and j, pct_ext_k and j, and T_med_ret. The T_htf_hot_ND and m_dot_htf_ND remain = 1).
eta_ND_mem	-	Memory variable to check if the model reaches always the same values for Eta_ND, avoiding an infinite loop.
F	kg/s	Mass flow of Feedwater entering each effect
F_flash_remain	kg/s	Mass flow of feedwater that remains after it flashed when it entered each effect (this variable is actually only used when CT(9,10) MED-FF as feedwater is actually the brine from the last effect; and when CT(7,8) this variable has a value of zero).
F_Total	kg/s	Total mass flow of feedwater used at the MED plant
fcall_MED_or_SWCC	-	Flag indicating if the MED/SWCC system is being called for the first time (0 - for first call; 1- Not the first call)
flag_myMessage(500)	-	Flag array to indicate which messages should be mentioned to the user regarding the MED and SWCC systems. Messages originated from conditions in: Type 224 (1-200); MED (201-300); SWCC (301-400); NCG (401-500) Note: some messages from Type 224 may be repeated on MED, SWCC or NCG
FORCE_SWCC_flag	-	Flag that forces the usage of the SWCC system only (discarding the MED), when it is assumed that an MED plant also is installed. Indicates if the SWCC is being force to operate alone during part of the time step that the MED plant was still starting up.
h_transfered	kJ/kg	Specific enthalpy transferedto the heat rejection mechanisms (MED and/or SWCC)
h_Turb_cond_sat	kJ/kg	Specific enthalpy of the condensed steam (at saturation temperature)
h_Turb_cond_sub	kJ/kg	Specific enthalpy of the condensed steam at subcooled temperature
h_Turb_Steam	kJ/kg	Specific enthalpy of the steam from the Rankine cycle Steam turbine powering the MED and/or SWCC systems. Quality of 100% assumed.
Hb_b_flash_remain	kJ/kg	Specific Enthalpy of the brine entering each effect AFTER part of it has flashed
Hb_Tb	kJ/kg	Specific Enthalpy of the Brine formed by evaporation inside each effect
Hb_Tb_out	kJ/kg	Specific Enthalpy of the brine leaving each effect (it is a mixture of the brine from the previous effect plus the brine formed in the current effect)
Hd_d_flash_remain	kJ/kg	Specific Enthalpy after flashing of the distillate (Hd) that has previously entered each effect.
Hd_d_flash_remain_cond	kJ/kg	Specific Enthalpy after flashing of the distillate (Hd) that entered the down condenser.
Hd_d_flash_remain_Ej_1	kJ/kg	Specific Enthalpy after flashing of the condensate (Hd) that come from the 1st intercondenser. If an MED low temperature configuration is used this flashing process will take place inside the distillate box of effect number (n_ph_NCG + 1); if a TVC configuration is used this flashing process will take place inside the distillate box of the 3rd effect.
Hd_d_flash_remain_Ej_2	kJ/kg	Specific Enthalpy after flashing of the condensate (Hd) that come from the 2nd intercondenser. If an MED low temperature configuration is used this flashing process will take place inside the distillate box of effect number (n_ph_NCG + 1); if a TVC configuration is used this flashing process will take place inside the distillate box of the 2nd effect.
Hd_out	kJ/kg	Specific Enthalpy of the distillate (Hd) actually routed into the next effect.
Hd_Td_out_cond	kJ/kg	Specific Enthalpy of the distillate leaving the down codenser at the pressure defined by the NPSHr.
Hd_Tv_out	kJ/kg	Specific Enthalpy of the distillate (Hd) formed by the condensation at Tv_out of the vapor formed in the previous effect
Hf_f_flash_remain	kJ/kg	Specific Enthalpy after flashing of the feedwater entering each effect (this variable is actually only used when CT(9,10) MED-FF as feedwater is actually the brine from the last effect; and when CT(7,8) this variable has a value of zero).
Hf_Tf	kJ/kg	Specific Enthalpy of the Feedwater entering each effect
Hf_Tf_dc_out	kJ/kg	Specific Enthalpy of the preheated Feedwater leaving the down condenser.
Hf_Tf_eph	kJ/kg	Specific Enthalpy of the Feedwater OUTLET from each external feedwater preheater (existing between effects). In the parallel configuration CT(7,8) part of the feedwater leaving the preheaters goes into the effect(i+1); in the forward feed configuration CT(9,10) all the feedwater preaheated goes directly into the next effect, until reaching the 1st effect where it finally enters the effects.
High_1	-	Used only with CT6: Ratio between between the Pressures actually used in the model, and the pressures used to find an applicable entrainment ratio to describe the steam consumption with NCG extraction with the 1st ejector (upper boundary).
High_2	-	Used only with CT6: Ratio between between the Pressures actually used in the model, and the pressures used to find an applicable entrainment ratio to describe the steam consumption with NCG extraction with the 2nd ejector (upper boundary).
Hs_dry_out	kJ/kg	Specific enthalpy of the steam leaving the low pressure turbine in case it is in a superheated state.
Hs_dry_out_sat	kJ/kg	Specific enthalpy of the steam at Saturated conditions (but 100% steam, quality of 1) leaving the low pressure turbine.
Hs_sat	kJ/kg	Specific Enthalpy of the SATURATED steam powering the MED plant
Hs_sub	kJ/kg	Specific Enthalpy of the saturated condensate after coming from the 1st effect
Hs_super	kJ/kg	Specific Enthalpy of the SUPERHEATED steam powering the MED plant
Hs_wet_out	kJ/kg	Specific enthalpy of the steam leaving the low pressure turbine in case it is in a saturated state.
Hsw_Tsw	kJ/kg	Specific Enthalpy of the seawater entering the down condenser of the MED plant
Hv_b_flash	kJ/kg	Specific Enthalpy of the vapor produced when the brine flashed after enering each effect (MED parallel config only)
Hv_d_flash	kJ/kg	Specific Enthalpy of the vapor formed by flashing in the distillate box when the distillate from the previous effect enters the current effect
Hv_d_flash_cond	kJ/kg	Specific Enthalpy of the vapor formed by flashing when the distillate from the last effect enters the down condenser.
Hv_d_flash_Ej_1	kJ/kg	Specific Enthalpy of the vapor formed by flashing when the condensate from the 1st intercondenser of the NCG ejection system enters the distillate box. If an MED low temperature configuration is used this flashing process will take place inside the distillate box of effect number (n_ph_NCG + 1); if a TVC configuration is used this flashing process will take place inside the distillate box of the 3rd effect.
Hv_d_flash_Ej_2	kJ/kg	Specific Enthalpy of the vapor formed by flashing when the condensate from the 2nd intercondenser of the NCG ejection system enters the distillate box. If an MED low temperature configuration is used this flashing process will take place inside the distillate box of effect number (n_ph_NCG + 1); if a TVC configuration is used this flashing process will take place inside the distillate box of the 2nd effect.
Hv_f_flash	kJ/kg	Specific Enthalpy of the vapor formed by flashing when the feedwater enters each effect when using the MED Forward Feed configuration (except in the first effect).
Hv_Super_b_flash	kJ/kg	Specific Enthalpy of steam formed at Tv_b_flash inside each effect
Hv_Tv	kJ/kg	Specific Enthalpy of steam formed at Tv inside each effect
Hw_out	kJ/kg	Specific enthalpy of the condensate returning into the Rankine cycle (liquid water and not steam).
IN_Delta_P_all	Pa	Pressure differential to be surpassed in order to be able to pump water into the MED and SWCC condensers inlet (= IN_Delta_P_piezom + IN_Delta_P_friction)
IN_Delta_P_friction	Pa	Pressure loss with friction, pumping water from the Sea intake up to the condenser
IN_Delta_P_piezom	Pa	Piezometric delta in Pressure: Seawater from the sea surface (not the underwater intake indepth) up to the condenser intake height
IN_delta_piez_head	m	Piezometric head between seawater intake and inlet of the condensers

IN_Delta_pres_head	m	Difference between pressure head (not the piezometric head) considering the pressure at which the seawater must leave the condensers and the atmospheric pressure (the pressure at which the seawater must leave the condensers is variable depending if the MED plant is on or off). Th pressure leaving the condensers is assumed here and not the pressure entering them, because the extra pressure necessary to use to make the seawater pass through the MED down condenser and SWCC condenser is calculated in a different section (E)
IN_Feed	kg/s	Mass flow rate of seawater intake pumped from the sea up to the MED and/or the SWCC system
IN_Friction_coeff	-	Friction factor inside main tube bringing water up to the plant
IN_Gamma_Brine	N/m3	Specific weight of seawater
IN_h_brine_pump_in	J/kg	Specific enthalpy of the seawater pumped into the plant
IN_h_brine_pump_out	J/kg	Outlet enthalpy of seawater leaving feedwater pump, accounting for irreversibility
IN_h_brine_pump_out_s	J/kg	Isentropic outlet specific enthalpy of seawater (incompressible fluid)
IN_Head_friction	m	Head loss with friction, pumping water from the sea intake up to the condenser
IN_Head_piezom	m	Hydraulic head necessary to pump Seawater from the sea surface (not the underwater intake indepth) to the condenser intake height
IN_Kin_Visc_sw	m2/s	Kinetic viscosity of seawater being pumped into the plant
IN_pipe_diameter	m	Intake pipe diameter bringing seawater into the plant
IN_Pipe_roughness	m	Roughness of Intake pipe
IN_pipe_section	m2	Section of Intake pipe (transversal)
IN_Plant_distance	m	Plant Distance to the Intake (not the seashore)
IN_Re	-	Reynolds number of Seawater inside intake pipe
IN_velocity_sw	m/s	Velocity of Seawater inside intake pipe
IN_W_dot_pump	We	Electrical consumption to pump water from the sea intake up to the plant (entrance of the MED and SWCC condensers)
kcal_to_kJ	-	Conversion factor to transform kcal into kJ
Last_MED_Ready_Flag	-	Used inside type 224 only
LHs	kJ/kg	Latent Heat of the steam powering the MED plant
LHv_b_flash	kJ/kg	Latent Heat of the vapor formed by the brine flashing when entering each effect
LHv_d_flash	kJ/kg	Latent Heat of the vapor formed by the distillate flashing when entering each effect
LHv_d_flash_cond	kJ/kg	Latent Heat of the vapor formed by the distillate flashing when entering the DOWN CONDENSER
LHv_d_flash_Ej_1	kJ/kg	Latent Heat of the vapor formed by the flashing of the condensate from the 1st intercondenser of the NCG ejection system when entering the distillate box. If an MED low temperature configuration is used this flashing process will take place inside the distillate box of effect number (n_ph_NCG +1); if a TVC configuration is used this flashing process will take place inside the distillate box of the 3rd effect.
LHv_d_flash_Ej_2	kJ/kg	Latent Heat of the vapor formed by the flashing of the condensate from the 2nd intercondenser of the NCG ejection system when entering the distillate box. If an MED low temperature configuration is used this flashing process will take place inside the distillate box of effect number (n_ph_NCG +1); if a TVC configuration is used this flashing process will take place inside the distillate box of the 2nd effect.
LHV_eff	kcal/Nm3	Fossil backup boiler Low heating value efficiency
LHv_evap	kJ/kg	Latent Heat of the vapor formed in each effect
LHv_Tv_out	kJ/kg	Latent Heat at Tv_out(i) of the vapor coming from effect (i) and condensed inside the HTX of both the preheater and effect (i+1).
LMTD_dc	ºC	Log mean temperature between the cooling water inside the HTX tubes at the down condenser and the vapor condensing outside of these tubes.
Low_1	-	Ratio between between the Pressures actually used in the model, and the pressures used to find an applicable entrainment ratio to describe the steam consumption with NCG extraction with the 1st ejector (lower boundary).
Low_2	-	Ratio between between the Pressures actually used in the model, and the pressures used to find an applicable entrainment ratio to describe the steam consumption with NCG extraction with the 2nd ejector (lower boundary).
m_dot_htf_ref_10MWe_adj	kg/s	Reference mass flow of the HTX fluid flowing in the solar field that powers the Rankine cycle, for a cycle with the same characteristics as the cycle used to obtain the SAM performance curves >>BUT<< with a different size
m_dot_j	kg/s	Mass flow of steam extracted from the lowest pressure intermediate steam extraction from the rankine cycle.
m_dot_j_ND	-	Non dimensional value of m_dot_j (its a ratio of a ratio). It represents the ratio between the "m_dot_k"/"m_dot_steam_adj" at design point >>OF THE CYCLE DESCRIBED IN SAM<< (and not the cycle described by the user).
m_dot_j_ND_mem	-	Memory variable to check if the model reaches always the same values for m_dot_j_ND, avoiding an infinite loop.
m_dot_k	kg/s	Mass flow of steam extracted from the highest pressure intermediate steam extraction from the rankine cycle.
m_dot_k_ND	-	Non dimensional value of m_dot_k (its a ratio of a ratio). It represents the ratio between the "m_dot_k"/"m_dot_steam_adj" at design point >>OF THE CYCLE DESCRIBED IN SAM<< (and not the cycle described by the user).
m_dot_k_ND_mem	-	Memory variable to check if the model reaches always the same values for m_dot_k_ND, avoiding an infinite loop.
m_dot_steam_10MWe_User	kg/s	Mass flow of steam entering the high pressure turbine, calculated for a cycle with the same efficienc y than the one defined by the user,but having 10MWe output.
m_dot_steam_User	kg/s	Mass flow of steam entering the high pressure turbine using the m_dot_steam_10MWe_User data, but scalled up to the Power actually set by the user, as for cycles with the same efficiencies (meaning in this case that only the components size change and not their efficiencies) it is assumed a linear relation between mass of motive steam entering the high pressure turbine and the installed power.
Mb	kg/s	Brine Total Mass flowrate flowing out of the MED plant
Mb	kg/s	Brine Total Mass flowrate flowing out of the MED plant
MC_Mcw	kg/s	Total mass flow of cooling water used in the SWCC Main Condenser (sum of mass of cooling water used by the SWCC when the MED plant was re-starting or in standby +the mass flow of cooling water when the MED plant was ON)
MC_Mcw	kg/s	Total mass flow of cooling water used in the SWCC Main Condenser (sum of mass of cooling water used by the SWCC when the MED plant was re-starting or in standby +the mass flow of cooling water when the MED plant was ON)
MC_Mcw_withMED_ON	kJ/kg	Mass flow rate of cooling water used by the SWCC while the MED plant is operating only
MC_Mm	kg/s	Mass flow of steam powering the SWCC Main Condenser (sum of mass of steam used by the SWCC when the MED plant was re-starting or in standby +the mass flow of steam when the MED plant was ON)
MC_Mm_withMED_ON	kg/s	Mass flow rate of steam used by the SWCC while the MED plant is operating only
MC_only_Ts	ºC	Temperature of Steam powering the SWCC system. This corresponds to the steam temperature leaving the Turbine (take into account that above ~80 degC and a salinity of 70 000ppm there a big risk of irreversal deposition of salts outside the HTX tubes)
MC_Qs	kWt	Heat Load transfered into the SWCC Main Condenser
MC_Qs_withMED_ON	kWt	Heat load used by the SWCC while the MED plant is operating only

MC_T_approach	ºC	Temperature approach between Steam temperature and cooling water outlet in the SWCC Main Condenser
MC_Total_pump_e	We	Total electrical consumptiomn with pumping just with the SWCC Main Condenser (excludes pumping from and to the sea)
MC_Total_pump_e_withMED_ON	-	Total electrical consumption with water pumping with only the SWCC Main Condenser, WHEN the MED PLANT IS OPERATING also (Includes also pumping from and to the sea)
MC_tstep_frac_ON	-	Not used inside Rankince Cycle Sub. Not used inside the SW cooling subroutine, but commands it. Only used by the SW Cooling subroutine, but has implications on the usage of the SW cooling subroutine
MC_W_dot_pump	We	Total electrical consumption necessary to pump water inside the SWCC main condenser ONLY (excludes pumping from and to the sea)
Mcw_dc_in	kg/s	Total mass flow of cooling water entering the down condenser (part of it will be used as feedwater supplying the MED system, and the remaining cooling water will be rejected back into the sea)
Mcw_dc_out_reject	kg/s	Total mass flow of cooling water leaving the down condenser that is NOT used as feedwater into the MED process and >>IS<< rejected back into the sea.
Md	kg/s	Distillate Total Mass flow rate flowing out of the MED plant
Md_desuper	kg/s	Mass flow of distillate produced in the 1st effect, that is used to desuperheat the gases leaving the Thermal Vapor Compressor (TVC), if such is assumed to exist. This variable is only used for a TVC-MED configuration.
Me_1	kg/h	Internal version of E_Me_air_equiv_1(NOTE: units of Me_1are in kg/HOUR instead of kg/s)
Me_2	kg/h	Internal version of E_Me_air_equiv_2 (NOTE: units of Me_2 are in kg/HOUR instead of kg/s)
Me_Lip_A	kg/h	1st Linear interpolation (_Lip) of the Me value when obtaining curves that have the same Me value
Me_Lip_B	kg/h	2nd Linear interpolation (_Lip) of the Me value when obtaining curves that have the same Me value
Me_Lip_C	kg/h	3rd Linear interpolation (_Lip) of the Me value when obtaining curves that have the same Me value
Me_Lip_D	kg/h	4th Linear interpolation (_Lip) of the Me value when obtaining curves that have the same Me value
Me_ratio	-	Ratio between the pretended Me and nearest value available for Me in the selected range of Pm in the database (assuming now the pretended Pc). This variable is only used in the calculations for the 1st ejector of NCG.
MED_max_Qdes_frac	-	Maximum fraction of the design rejected steam produced by the steam turbine allowed to power the MED plant (assuming Design 100%, max design fraction of 10% above the design will be: MED_max_Qdes_frac = 1.1
MED_Mcw	kg/s	Mass flow rate of cooling water REJECTED directly into the sea after passing through the MED down condenser. The part not rejected is Mf.
MED_min_Qdes_frac	-	Minimum fraction of the design rejected steam produced by the steam turbine allowed to power the MED plant (comparing to the load at 100% of design for the MED)
MED_Mm	kg/s	Mass flow of motive steam powering the MED plant, >> Except << steam used for NCG steam ejectors (entering the TVC if one exists, or entering directly the 1st effect if not TVC is present).
MED_Qdes_frac	-	Fraction of the rejected heat by the steam turbine from which the MED plant should be dimentioned
MED_Qs	kWt	Heat load delivered by the motive steam powering the MED plant
MED_Qs_design	kWt	Heat load used to dimention the MED plant for nominal conditions
MED_ready_flag	-	only used by the MED subroutine, but has implications on the usage of the SW cooling subroutine (eg. if CT = 6, turbine is working but not enough heat is available for the MED plant, then the SW cooling will opoerate to condensate the full heat rejected. In this case MED_ready_flag will be "0".
MED_ReStart_frac_remain	-	Remaining fraction of each time step still missing to allow the restart of the MED plant
MED_ReStart_t	h	Amount of time that the MED plant takes to re-start
MED_ReStart_t_remain	h	Amount of time in each time step still missing to allow the restart of the MED plant
MED_SWCC_Total_pump_e	We	Total electrical consumption with water pumping using both MED and SWCC systems combined (Includes also pumping from and to the sea)
MED_SWCC_Total_pump_e_withMED_ON	We	Total electrical consumption with water pumping using both MED and SWCC systems combined WHEN the MED PLANT IS OPERATING also (Includes also pumping from and to the sea)
MED_Tf	ºC	Temperature of feedwater leaving the down condenser of the MED plant (outlet temp of cooling water)
MED_Total_pump_e	We	Total pumping wihin the MED plant (excluding pumping from and back to the sea)
MED_Ts_sat	ºC	Temperature of Saturated Steam from the turbine (if no TVC) or from the TVC discharge.
MED_tstep_frac_ON	-	Fraction of the time step in which the MED plant is ON
MED_tstep_t_ON	hours	Amount of time in each time step in which the MED plant is ON
MED_We_m3	We	Total Electric energy consumption with all the pumping related to the MED plant per m3 of distillate produced
MED_We_m3_des	We	Total Electric energy consumption at Design conditons with all the pumping related to the MED plant per m3 of distillate produced
Mf	kg/s	Total Mass flow of feedwater entering the 1st effect of the MED plant
Mm	kg/s	Mass flow of steam powering the MED plant, >> Except << steam used for NCG steam ejectors (entering the TVC if one exists, or entering directly the 1st effect if not TVC is present).
Mm_0	kg/h	Internal version of TVC_Mm (NOTE: units of Mm_0 are in kg/HOUR instead of kg/s)
Mm_1	kg/h	Internal version of E_Mm_1(NOTE: units of Mm_1are in kg/HOUR instead of kg/s)
Mm_Lip_A	kg/h	1st Linear interpolation (_Lip) of the Mm value when obtaining curves that have the same Pc value
Mm_Lip_B	kg/h	2nd Linear interpolation (_Lip) of the Mm value when obtaining curves that have the same Pc, and same Me value
Mm_Lip_C	kg/h	3rd Linear interpolation (_Lip) of the Mm value when obtaining curves that have the same Pc, same Me, and same Pe value
Mm_Lip_D	kg/h	4th Linear interpolation (_Lip) of the Mm value when obtaining the curve that have the same Pc, same Me, same Pe, and same Pm value
Mm_out	kg/s	Total mass flow of steam leaving the low pressure steam turbine
Mm_out	kg/s	Total mass flow of steam leaving the low pressure steam turbine
Mm_ratio	-	Ratio between the pretended Mm and nearest value available for Mm in the selected range of Pm in the database (assuming now the pretended Pc). This variable is only used in the calculations for the TVC.
Ms	kg/s	Total mass flow of steam actually entering the 1st effect (if a TVC is present it will be sum of TVC_Mc_Total+TVC_Mcw_deSuper, and if no TVC is present it will be equal to Mm)
Msw_Total	kg/s	Total mass flow of cooling water needed
n	-	Number of Effects
n_ph	-	Total number of feedwater preheaters considered in the MED plant
n_ph_marker	-	Array containing the flag indicating if for the selected effect there is a preheater of not. (e.g. if n_ph_marker(5)=1, it means that between effect 5 and 6 there is a preheater). It is assumed that between the first 2 effects and between the last effect and the down condenser there are no feedwater preheaters.
n_ph_NCG	-	Number of >> the effect << from where it is assumed that the external preheating of the feedwater will be suported by NCG steam extraction. The rest of the code will adapt automatically.
OUT_B	kg/s	Mass flow of brine/seawater leaving the plant (Brine +MED cooling water rejected that did not entered the effects +cooling water from the SWCC system)
OUT_Bn_tot_salt_mass	g/kg	Mass concentration of salt in the brine output from the last effect of the MED plant

OUT_Delta_head	m	Hydraulic head to be surpassed in order to be able to pump water back into the sea (if the hydraulic head is high enough, than no pumping costs will be incurred)
OUT_Delta_P_pump	Pa	Hydraulic head aiding the discharge of seawater/brine back into the sea (assuming the MED plant is above sea level)
OUT_delta_piez_head	m	Piezometric head between seawater Outlet and outlet from the condensers
OUT_Delta_pres_head	m	Difference between pressure head (not the piezometric head) considering the pressure at which the brine/cooling water must leave the condensers and the atmospheric pressure (the pressure at which the seawater must leave the condensers is variable depending if the MED plant is on or off). The pressure leaving the condensers is assumed here and not the pressure entering them, because the extra pressure necessary to use to make the seawater pass through the MED down condenser and SWCC condenser is calculated in a different section (E)
OUT_Friction_c	-	Friction factor inside the tube taking brine/seawater back to the ocean.
OUT_Gamma_Brine	N/m3	Specific weight of Brine/seawater leaving the plant
OUT_h_pbrine_in	J/kg	Specific enthalpy of the brine/seawater sent back into the sea
OUT_h_pbrine_out	J/kg	Outlet enthalpy of brine/seawater leaving the pumps taking this mass back into the sea, accounting for irreversibility (energy to remove brine from last MED effect is not taken into account here).
OUT_h_pbrine_out_s	J/kg	Isentropic outlet specific enthalpy of brine/seawater (incompressible fluid)
OUT_Head_friction	m	Head loss with friction, pumping water from the plant back into the sea
OUT_Head_friction_Bn	m	Maximum height assumed to compensate the head friction losses in the whole piping from the MED plant down to the sea by a first brine pump next to the MED plant.
OUT_Kin_Visc_B	m2/s	Kinetic Viscosity of brine/seawater sent back into the sea.
OUT_Mcw_tot_salt_mass	g	Mass concentration of salt in the brine output from the last effect of the MED plant
OUT_P_Cond_outlet	Pa	Cooling water outlet pressure in both MED and SWCC condensers
OUT_P_Cond_outlet_MED	Pa	Cooling water outlet pressure in both MED and SWCC condensers when the MED plant is working (the pressure can be lower if the MED is not operating. This variable is used as memory for the pressure needed to operate with the MED working, so that the model does not have to calculate this every in every iteration)
OUT_P_ph	Pa	Pressure losss in average in each preheater used for the feedwater in the MED plant.
OUT_pipe_diameter	m	Outlet pipe diameter bringing seawater back to the sea
OUT_Pipe_roughness	m	Roughness of Outlet pipe
OUT_pipe_section	m2	Section of Outlet pipe (transversal)
OUT_Plant_distance	m	Plant Distance to the Outlet (not the seashore)
OUT_Re	-	Reynolds number of Seawater inside outlet pipe
OUT_T	ºC	Outlet temperature (considering the different mass flows and temperatures of seawter and brine)
OUT_velocity_sw	m/s	Velocity of Seawater/brine inside outlet pipe
OUT_W_dot_pump	We	Total consumption of electricity to pump Seawater/brine back into the sea (excludes pumping costs inside both MED and SWCC condensers)
OUT_X	wt%	Salinity of Seawater/brine leaving the plant (considering the different mass flows and temperatures of seawater and brine)
P_ext_j	Pa	Second intermediate steam extraction that it's possible to assume from the rankine cycle to a co-generation system, like the MED. It has be to assumed to be at a higher pressure than the "j" extraction.
P_ext_k	Pa	First intermediate steam extraction that it's possible to assume from the rankine cycle to a co-generation system, like the MED. It has be to assumed to be at a lower pressure than the "k" extraction.
P_out	Pa	Pressure of the vapor that enters the HTX tubes of the next effect assuming energy losses in this path (the distillate produced from the condensation of this vapor is assumed to condense at the this P_out pressure also).
Pc_0	mbar	Internal version of TVC_Pc (units in mbar)
Pc_0_max	mbar	Maximum value of Pc allowed in the selected curves for the TVC
Pc_1	mbar	Internal version of E_Pc_1(units in mbar)
Pc_1_max	mbar	Maximum value of Pc allowed in the selected curves for the 1st NCG ejector
Pc_2	mbar	Internal version of E_Pc_2 (units in mbar)
Pc_High	Bars	Array that marks the Upper value for Pc available in the database that is nearest to the selected Pm, Pe and Pc.
Pc_Lip_A	mbar	1st Linear interpolation (_Lip) of the Pc value when obtaining curves that have the same Pc value
Pc_Lip_B	mbar	
Pc_Lip_C	mbar	
Pc_Lip_D	mbar	
Pc_Low	Bars	Array that marks the Lower value for Pc available in the database that is nearest to the selected Pm, Pe and Pc.
Pc_ratio	-	Ratio between the pretended Pc and nearest value available for Pc in the database for the selected range of Pm in the database
Pc_sat	Pa	Pressure at which the condensate formed inside the HTX of the 1st effect exits into the corresponding distillate box
pct_ext_j	%	Ratio of steam extracted from an intermediate point from the turbines of the rankine cycle (the lowest pressure of the extractions), relative to the total mass of steam that enters the high pressure turbine at design conditions
pct_ext_k	%	Ratio of steam extracted from an intermediate point from the turbines of the rankine cycle (the highest pressure of the extractions), relative to the total mass of steam that enters the high pressure turbine at design conditions.
Pe_0	mbar	Internal version of TVC_Pe (units in mbar)
Pe_1	mbar	Internal version of E_Pe_1(units in mbar)
Pe_2	mbar	Internal version of E_Pe_2 (units in mbar)
Pe_High	mbar	Entrainment pressure available in the database nearest and above to the pretended Pe (if it does not match the pretending Pe by coincidence), using the selected Pm_High and Pm_Low (this variable value is calculated when Pm_Low is considered, and recalculated when Pm_High is recalculated).
Pe_Lip_A	mbar	Linear interpolation (_Lip) of the Pe value when obtaining curves that have the same Pe value
Pe_Low	mbar	Entrainment pressure available in the database nearest and bellow to the pretended Pe (if it does not match the pretending Pe by coincidence), using the selected Pm_High and Pm_Low (this variable value is calculated when Pm_Low is considered, and recalculated when Pm_High is recalculated).
Pe_ratio	-	Ratio between the pretended Pe and nearest value available for Pe in the database for the selected range of Pm in the database (assuming now the pretended Pc and Me)
plant_elev_sea_level	m	Site elevation (where MED plant is installed) compared with sea level
Pm_0	Bars	Internal version of TVC_Pm (units in Bars)
Pm_12	Bars	Internal version of E_Pm (units in Bars) used in both NCG steam ejectors (1and 2)
Pm_High	Bars	Highest value for Pm available in the database that is nearest to the pretended Pm
Pm_Lip	mbar	Linear interpolation (_Lip) of the Pm value when obtaining curves that have the same Pm value
Pm_Low	Bars	Lower value for Pm available in the database that is nearest to the pretended Pm
Pm_ratio	-	Ratio between the pretended Pm and nearest value available for Pm in the database for the selected range of Pm in the database
PR	-	Performance Ratio of the MED plant
pre_Hb_in	kJ/kg	Enthalpy of brine entering the plate HTXnger that receives brine
pre_Hb_out	kJ/kg	Enthalpy of brine leaving the plate HTXnger that receives brine

pre_Hd_in	kJ/kg	Enthalpy of distillate entering the plate HTXnger that receives distillate
pre_Hd_out	kJ/kg	Enthalpy of distillate leaving the plate HTXnger that receives distillate
pre_Hsw_in	kJ/kg	Enthalpy of seatwater entering the plate HTXngers
pre_Hsw_out	kJ/kg	Enthalpy of seatwater leaving the plate HTXngers
pre_LMTD_b	ºC	Log mean temperature between seawater and brine, inside the preheater that receives brine
pre_LMTD_d	ºC	Log mean temperature between seawater and distillate, inside the preheater that receives distillate
pre_Mcw_b	kg/s	Mass flow of seawater that is preheated inside the preheater that receives brine
pre_Mcw_d	kg/s	Mass flow of seawater that is preheated inside the preheater that receives distillate
pre_PlateHTX_flag	-	Flag indicating if the plate heat exchanger preheaters of the feedwater entering the down condenser are present or not. 0 - The Plate Heat Exchangers are NOT present; 1- The Plate Heat Exchangers ARE present.
pre_Q	kW	Total heat load necessary to be transfered by the two preheaters
pre_Q_b	kW	Heat load necessary to be transfered by the preheater that receives brine
pre_Q_d	kW	Heat load necessary to be transfered by the preheater that receives distillate
pre_T_approach_b	ºC	Temperature approach in the preheater that receives brine, between the distillate input and the seawater preheated
pre_T_approach_d	ºC	Temperature approach in the preheater that receives distillate, between the distillate input and the seawater preheated
pre_Tb_in	ºC	Temperature of brine input into the preheater that receives brine
pre_Tb_out	ºC	Temperature of brine output from the preheater that receives brine
pre_Td_in	ºC	Temperature of distillate input into the preheater that receives distillate
pre_Td_out	ºC	Temperature of distillate output into the preheater that receives distillate
pre_Tsw_in	ºC	Temperature of the seawater entering the plate heat exchangers
pre_Tsw_out	ºC	Temperature of the seawater leaving the plate heat exchangers
pre_UA_b	kW.ºC	UA value for the plate heat exchanger that receives brine
pre_UA_d	kW.ºC	UA value for the plate heat exchanger that receives distillate
Ps	Pa	Pressure at which the steam from the LPT of the CSP plant condenses (assuming Saturated conditions)
Ps_sat	Pa	Pressure of the Saturated steam powering the MED plant
Psat_des	kPa	Exaust steam pressure from the Rankine Cycle turbine when running coupled with an SWCC or MED system (this is different than the "Psat_ref", as this Psat_ref indicates the pressure at factory nominal performance, which is at another temperature. "Psat_des" is the pressure at Ts)
Q	kW	Thermal Load in each effect
Q_cycle	kW	Heat load entering the high pressure turbine at each time step (including during the first call) using the cycle described in SAM (and not the cycle described by the user)
Q_cycle_User	kW	Heat load entering the high pressure turbine at each time step (including during the first call) but using the cycle described by te user and not the cycle described in SAM.
q_dot_ref_User	kW	Heat load entering the high pressure turbine at nominal conditions for the cyle defined by the >>USER<< at nominal conditions for the Cond temp that it was defined for operation of the low pressure turbine.
Q_eph	kW	Thermal Load used in the external feedwater preheater at each stage.
Q_eph_total	kW	Sum of all Thermal Load used in from the steam not condensed in each effect to preheat the feedwater at the preheaters of each stage.
Q_iph	kW	Thermal Load used in each effect o preheat the feedwater entering each effect
Q_iph_total	kW	Sum of all Thermal Load used in each effect o preheat the feedwater entering each effect
Q_iter	kW	Variable used in the iteration process to obtain the correct Xb in each effect (used to define the evaporation ratio).
Q_Loss	-	Fraction of the thermal losses incurred in average in each effect (compared to the calculated heat load that each effect would receive). A value of "1" represents 100% and a value of 0.05 for example represents 5%.
Q_ND_tot_mem	-	Memory variable to check if the model reaches always the same values for Q_ND_tot, avoiding an infinite loop.
q_pb_reject_design	kWt	Total amount of heat rejected by the rankine cycle for nominal conditions (that is received by the MED and/or the SWCC)
Q_ph	kW	Thermal Load that is used in EACH effect for preheating purposes: Q_iph(i) +Q_eph(i)
Q_ph_total	kW	Thermal Load available for preheating in the entire system
q_reject	W	Total amount of heat rejected by the rankine cycle at each time step (that is received by the MED and/or the SWCC)
q_reject_est	W	1st estimation of the total amount of heat rejected by the rankine cycle at each time step (that is received by the MED and/or the SWCC)
q_reject_User	W	Total amount of heat rejected by the cycle that was described >>BY THE USER<< and not the cycle described in SAM
Qd_flash	kW	Thermal Load released from the flashing occuring when distilate moved from effect to effect (condensed distillate and not vapor).
Qd_flash_cond	kW	Thermal Load released from the flashing occuring when distilate moved from effect (n) into the down condenser
Qd_flash_Ej_1	kW	Thermal Load released from the flash occuring when condensate from the 1st NCG ejection system intercondenser enters the distillate box. If an MED low temperature configuration is used this flashing process will take place inside the distillate box of effect number (n_ph_NCG +1); if a TVC configuration is used this flashing process will take place inside the distillate box of the 3rd effect.
Qd_flash_Ej_2	kW	Thermal Load released from the flash occuring when condensate from the 2nd NCG ejection system intercondenser enters the distillate box. If an MED low temperature configuration is used this flashing process will take place inside the distillate box of effect number (n_ph_NCG +1); if a TVC configuration is used this flashing process will take place inside the distillate box of the 2nd effect.
Qd_flash_Ej_2_mem	kW	Memory to verify when Qd_flash_Ej_2 stabilizes, and Q(1) can be considered constant, as it is known the amount of mass of steam that will need to be discounted from the Distillate flowing from the 1st to the 2nd effect (it is assumed that the mass of steam used by the 2nd intercondenser will be replenished into the rankine cycle by extraction of distillate leaving the 1st effect distillate box (and so this will depend on the amount of steam used by the 2nd NCG ejector).
Qdc_Feed	kW	Thermal Load passed into the feedwater at the down condenser
Qdc_Vapor	kW	Thermal Load released by the vapor entering and formed in the down condenser
Qs_Loss_frac_iph_1st	-	Ratio of the total heat load necessary to preheat the feed water inside the first effect up to saturation conditions (compared with heat load delivered by condensation of Steam from turbine)
Qs_sat	kW	Heat load of the Saturated Steam entering the MED plant
Qual_s_out	-	Quality of the steam leaving the low pressure steam turbine (value between 0 and 1)
Qv	kW	Total sum of the heat load of vapor formed inside each effect
Qv_b_flash	kW	Thermal Load released from the flashing occurring when brine moves from effect to effect (temperature before and after flash are due to the NEA).
Qv_b_flash_super	kW	Thermal Load released from the flashing occuring when brine moves from effect to effect in the form of superheated steam. It is assumed that the steam formed with flashing will end up being superheated, as it will be released in a chamber with a lower pressure. This superheated load is assumed to be transfered into the feedwater (UNLIKE what is assumed for the majority of the vapor formed with brine flashing: that is going to power only the next effect, and will NOT add energy into the feedwater of the effect where it is produced)
Qv_evap	kW	Heat load of vapor formed inside each effect by evaporation process alone

Qv_evap_remain	kW	Heat load of vapor formed inside each effect by evaporation process only, that actually is used to power the next effect. It is the remain of the Qv_evap after Q_eph is deducted.
Qv_f_flash	kW	Heat load of vapor formed when the feedwater enters each effect and >> flashes << (when CT(7,8) this variable will be equal to zero, as only preheated seawater enters the effect, but when CT(9.10) Qv_f_flash will be higher than zero because what is sprayed on the top of the tube bundle is brine from the last effect.
Qv_remain_out	kW	Total sum of the heat load of vapor transfered into the next effect condensed at "Tv_out" (it assumed therefore the temperature of vapor after energy losses have occured).
Ra_1	-	Inverted Entrainment Ratio in 1st ejector: Motive Flow rate(steam) / Suction flow rate (air equivalent)
Ra_2	-	Inverted Entrainment Ratio in 2nd ejector: Motive Flow rate(steam) / Suction flow rate (air equivalent)
Rank_Md_return	kg/s	Mass of distillate returning from the MED plant into the Rankine cycle (that compensate the input of motive steam)
Rank_Pd_return	Pa	Pressure of distillate returning from the MED plant into the Rankine cycle (compensating the input of motive steam)
Rank_Td_return	ºC	Temperature of distillate returning from the MED plant into the Rankine cycle (compensating the input of motive steam)
Rank_Td_return	ºC	Temperature of distillate returning from the MED plant into the Rankine cycle (compensating the input of motive steam)
Ratio_Qdc	-	Ratio evaluating the amount of power provided by the last effect to the down condenser vs the power required to preheat the feedwater to the set feedwater temperature.
ratio_Tf_NCG	-	Ratio that can decrease the Tf(n_ph_iph), and so increase the Delta_Tf_iph, in case the Heat load to be provided by the NCG extraction is to high comparatively to the Compression ratios possible to be achieved using a 2 stage steam ejector system for NCG (max is 10 for Pc/Pe), and assuming always the same mass flow of NCG to be ejected (the heat load can be increased if a higher NCG mass flow is assumed, which will in practice result in the extraction of more low pressure vapor formed in the last effect).
RC_Delta_P_all	Pa	Pressure differential to be surpassed in order to be able to pump condensate from the MED plant back into the 1st feedwater preheater of the Rankine Cycle (includes NPSHr to remove distillate from the MED plant)
RC_Delta_P_friction	Pa	Pressure loss with friction, pumping distillate from the MED plant back into the 1st feedwater preheater of the Rankine Cycle
RC_distance	m	Distance between MED down condenser and 1st feedwater preheater of the Rankine Cycle
RC_friction_c	-	Friction factor inside the tube taking condensate from the MED down condenser and the 1st feedwater preheater of the Rankine Cycle
RC_Gamma_Distillate	N/m3	Specific weigh of condensate being returned into the Rankine cycle
RC_h_distl_pump_in	J/kg	Specific enthalpy of the distillate sent back into the 1st feedwater preheater of the Rankine Cycle
RC_h_distl_pump_out	J/kg	Outlet enthalpy of condensate leaving the pumps taking this mass into the 1st feewater preheater of the Rankine cycle, accounting for irreversibility
RC_h_distl_pump_out_s	J/kg	Isentropic outlet specific enthalpy of condensate (incompressible fluid)
RC_Hd_Td_out	kJ/kg	Specific enthlapy of the condensate being sent back into the Rankine cycle (1st feedwater preheater)
RC_Head_friction	m	Head loss with friction, pumping water from the MED down condenser back into the 1st feedwater preheater of the Rankine Cycle
RC_Kin_Visc	m2/s	Kinetic viscosity of condensate sent back into the 1st feedwater preheater of the Rankine Cycle
RC_pipe_diameter	m	Pipe diameter taking condensate back into the 1st feedwater preheater of the Rankine Cycle
RC_Pipe_roughness	m	Roughness of pipe taking condensate back into the 1st feedwater preheater of the Rankine Cycle
RC_pipe_section	m2	Section of storage pipe (transversal)
RC_Re	-	Reynolds number of condensate inside storage pipe
RC_velocity	m/s	Velocity of condensate inside pipe taking it back into the 1st feedwater preheater of the Rankine Cycle
RC_W_dot_pump	We	Total consumption of electricity to pump condensate back into the 1st feedwater preheater of the Rankine Cycle
S	kg/s	Mass flow rate of salt contained in the brine produced by evaporation in each effect
S_out	g	Mass of Salt in the brine output leaving each effect (sum of the salt in the brine formed in the current effect by evaporation +salt of the brine from the previous effects that enters the current effect)
sA	m2/kg.s	Specific HTX Area at the MED plant
Size_High	inches	Ejector size that matches the upper bound available in the database for mass of gases entrained and/or discharged by the 1st ejector
Size_Lip_A	inches	1st Liner interpolation (_Lip) of the Size that would be needed for an ejector to operate with the pretended Pc and pretended Me. This value uses still the database nearest Pe and Pm (this variable only applies to the 1st ejector, as the provided database from Koerting does not indicate different sizes of ejectors)
Size_Lip_B	inches	2nd Liner interpolation (_Lip) of the Size that would be needed for an ejector to operate with the pretended Pc, Me and Pe. This value uses still the database nearest Pm (this variable only applies to the 1st ejector, as the provided database from Koerting does not indicate different sizes of ejectors)
Size_Lip_C	inches	3rd Liner interpolation (_Lip) of the Size that would be needed for an ejector to operate with the pretended Pc, Me and Pe and Pm (this variable only applies to the 1st ejector, as the provided database from Koerting does not indicate different sizes of ejectors)
Size_Lip_D	inches	3rd Liner interpolation (_Lip) of the Size that would be needed for an ejector to operate with the pretended Pc, Me and Pe and Pm (this variable only applies to the 1st ejector, as the provided database from Koerting does not indicate different sizes of ejectors)
Size_Low	inches	Ejector size that matches the lower bound available in the database for mass of gases entrained and/or discharged by the 1st ejector
sMcw	-	Specific cooling water flow rate of the MED plant
STOR_Delta_P_all	Pa	Pressure differential to be surpassed in order to be able to pump distillate from the MED plant into the top of the storage tank (includes NPSHr to remove distillate from the MED plant)
STOR_Delta_P_friction	Pa	Pressure loss with friction, pumping distillate from the MED plant into the top of the storage tank
STOR_Delta_P_piezom	Pa	Piezometric head: Distillate from the down condenser up to the top of the storage tank
STOR_distance	m	Distance between MED down condenser and distillate Storage tank
STOR_final_T	ºC	Distillate temperature when entering storage tank
STOR_friction_c	-	Friction factor inside the tube taking distillate from the MED down condenser up to the storage tank
STOR_Gamma_Distillate	N/m3	Specific weigh of distillate (at final temperature before getting stored)
STOR_h_distl_pump_in	J/kg	Specific enthalpy of the distillate sent into the storage tank
STOR_h_distl_pump_out	J/kg	Outlet enthalpy of distillate leaving the pumps taking this mass into the storage tank, accounting for irreversibility
STOR_h_distl_pump_out_s	J/kg	Isentropic outlet specific enthalpy of distillate (incompressible fluid)
STOR_Head_friction	m	Head loss with friction, pumping water from the MED down condenser up to the storage tank
STOR_Kin_Visc	m2/s	Kinetic viscosity of distillate sent to storage
STOR_pipe_diameter	m	Pipe diameter taking distillate into storage
STOR_Pipe_roughness	m	Roughness of pipe taking distillate to storage
STOR_pipe_section	m2	Section of storage pipe (transversal)
STOR_Re	-	Reynolds number of distillate inside storage pipe
STOR_T_Subcooling	ºC	Subcooling assumed to exist in the distillate before getting stored
STOR_tank_height	m	Heigh of storage tank (taking as reference the MED plant elevation and not the sea level)
STOR_velocity	m/s	Velocity of distillate inside pipe taking it to the storage tank
STOR_W_dot_pump	We	Total consumption of electricity to pump distillate into the storage tank

T_cond_ref	ºC	Condenser temperature related to the "Rated cycle conversion efficiency" set as input (The SAM code has curves describing the Rankine cycle efficiency for one specific configuration (with a condenser pressure at 20ºC saturated). The user will say how much is the efficiency at design point for a determined temperature. The code will adjust the performance of the cycle it has in the database to the performance of the cycle described by the user. E.g.: the user says the cycle has an efficiency of 30% at 50ºC in the condenser, which will imply that it will have a higher performance at a lower temperature in the condenser (lets say 40% at 20ºC in the condenser). To simulate this rankine cycle defined by the user defined, the SAM code will assume a higher performance of the curves in the database for the temperatures that it has described as design point: 20ºC. So the cycle defined by the user is equivalent to the performance of the cycle SAM has in the database multiplied by an X factor larger than 1in the case of this example (would be the oposite if the performance given by the user would be lower than the reference at a lower temperature than 20ºC). This is why the eta_adj is calculated as eta_adj = eta_ref/(Interpolate(TT,12,2,Psat_ref)/Interpolate(TT,22,2,Psat_ref)) instead of eta_adj = eta_ref * (Interpolate(TT,12,2,Psat_ref)/Interpolate(TT,22,2,Psat_ref)) >> eta_adj = eta_ref / (Power_cycle / HeatLoad_cycle)).
T_Loss	ºC	Average temperature reduction due to thermodynamic losses with Boiling Point Elevation
Tb	ºC	Boiling temperature inside the effects
Tb_b_flash	ºC	Final temperature of the brine (and not the feedwater) after flashing inside the effect when passing from effect i-1to effect i. Temperature difference between Tb(i) and Tb_b_flash(i) is due to the Non Equilibrium Allowance.
Tb_out	ºC	Temperature of the brine leaving each effect (it will be a balance between accounting the Temperature and mass of the brine formed by evaporation and the brine remaining after flashing (that came from the previous effect).
Tb1	ºC	Brine temperature in the first effect (input cannot be an array)
Tbn	ºC	Temperature of Brine in the last effect (input cannot be an array)
Td_out	ºC	Final temperature of the Distillate leaving each distillate box from each effect.
Td_out_1_mem	ºC	Memory to verify when Td_out stabilizes, as it has an impact on the amount of cooling water used on the desuperheater (TVC_Mcw_deSuper), and therefore on the amount of heating steam powering the whole MED plant, with a direct impact on the MED plant's performance. When Td_out(1) is set to be found, then that will also imply that the TVC_Mcw_deSuper is theoretically also found (stable).
Td_out_cond	ºC	Final temperature of the Distillate leaving the down condenser
Tf	ºC	Temperature of Feedwater entering each effect
Tf_dc_out	ºC	Temperature of Feedwater leaving the down condenser.
Tf_eph	ºC	Temperature of Feedwater leavig each feedwater preheater
Tf1	ºC	Feedwater temperature entering the first effect
tolerance	-	Tolerance used to verify if the ratios calculated inside this module are correct
tolerance	-	Tolerance used to reach an equilibrium with the MED model from El-Dessouky (CT=6)
Ts	ºC	Saturated Temperature of steam assumed to run the simulations (there are 2 entrances to define steam for CT=5 and CT=6 respectively. In order to make the code uniform, depending on which cooling option is used, the Ts variable then is equalized to the correct variable (MED_Ts_sat or MC_only_Ts)
Ts_delta_super	ºC	Temperature difference assumed to exist between the Saturated steam entering the 1st effect (and which is User defined in SAM) and the slightly superheated steam leaving the desuperheater (only applies for MED-TVC configurations), or the low pressure steam turbine if a low temperature configuration is used.
Ts_out	ºC	Temperature of steam actualy leaving the low pressure steam turbine. Keep in mind that the pressure is defined by the Ts_sat.
Ts_out_mem	ºC	Memory variable to check if the model reaches always the same values for Ts_out_mem, avoiding an infinite loop.
Ts_sat	ºC	Temperature of Saturated Steam from the turbine (if no TVC) or from the TVC discharge.
Ts_sub	ºC	Temperature of the condensed steam in the 1st effect leaving the HTX tubes in into the distillate box of that same effect (if a TVC exists then the output temperature will be slightly higher as it will be mixed with the warmer water from the 2nd intercondenser of the NCG ejection system).
Ts_super	ºC	Temperature of Superheated steam from the turbine
Tsw	ºC	Temperature of Seawater used in MED plant at each iteration
Tsw_avg	ºC	Average temperature of the seawater during the year, used to dimention the MED plant
Tsw_Jan	ºC	Temperature of Seawater during begining of January (assumed to be either the max or min Tsw during the year, depending on the the hemisphere)
Tsw_Jul	ºC	Temperature of Seawater during middle of July (assumed to be either the max or min Tsw during the year, depending on the the hemisphere))
Tsw_step	ºC	Increase or decrease absolute temperature step used to calculate the intermediate seawater temperatures for the months of (Feb, Mar, Apr, May) and (Ago, Sep, Oct, Nov)
turbine_ready_flag	-	Not used inside Rankince Cycle Sub. Used by both MED and SW Cooling subroutine
Tv	ºC	Temperature of vapor formed inside each effect
Tv_b_flash	ºC	Temperature of vapor produced with the flashing of brine at each effect
Tv_d_flash	ºC	Temperature of vapor produced at effect (i) with the flashing of distillate coming from the previous effect(i-1)
Tv_d_flash_cond	ºC	Temperature of vapor produced at the DOWN CONDENSER with the flashing of distillate coming from the last effect(n)
Tv_d_flash_Ej_1	ºC	Temperature of vapor produced with the flashing of condensate coming from the 1st intercondenser of the NCG ejection system into the distillate box. If an MED low temperature configuration is used this flashing process will take place inside the distillate box of effect number (n_ph_NCG +1); if a TVC configuration is used this flashing process will take place inside the distillate box of the 3rd effect.
Tv_d_flash_Ej_2	ºC	Temperature of vapor produced with the flashing of condensate coming from the 2nd intercondenser of the NCG ejection system into the distillate box. If an MED low temperature configuration is used this flashing process will take place inside the distillate box of effect number (n_ph_NCG +1); if a TVC configuration is used this flashing process will take place inside the distillate box of the 2nd effect.
Tv_Loss	ºC	Average temperature Loss with pressure losses assumed to occur when the vapour formed inside each effects flows into the HTX tubes of the next effect until it reaches the distillate box of the next effect (heat transfer inside each effect assumed to be at Tv - Tv_Loss).
Tv_out	ºC	Temperature of the vapor that enters the HTX tubes of each effect assuming energy losses in this path (the distillate produced from the condensation of this vapor is assumed to have the same temperature). This variable does not apply to the 1st effect.
Tv1	ºC	Vapor temperature in the first effect (input cannot be an array)
TVC_Cr	-	Compression ratio of the gases discharged by the TVC (Pc/Pe). The maximum compression ratio possible to be achieved by each ejector is ~10 (info given by Koerting and Kinetic Therm).
TVC_Cr_1	-	Compression ratio of the gases discharged by the TVC (Pc/Pe) in case only a 1stage ejector system is considered for the TVC, or the first ejector in case a 2 stage ejector systems is required to be considered. The maximum compression ratio possible to be achieved by each ejector is ~10 (info given by Koerting and Kinetic Therm).

TVC_Cr_2	-	Compression ratio of the gases discharged by the TVC (Pc/Pe) when using a 2 stage ejector system. The maximum compression ratio possible to be achieved by each ejector is ~10 (info given by Koerting and Kinetic Therm).
TVC_Cr_Total	-	Total compression ratio of the TVC system (depending on the models chosen to be used, the TVC system can have 1or 2 ejectors, and this ratio show the compression ratio accounting the discharge pressure of the 2nd ejector and the entrainment pressure of the 1st ejector (if two ejectors are considered, otherwise if only 1ejector is considered then TVC_Cr_total = TVC_Cr_1)
TVC_ext_flag	-	Flag indicating if: the user specifies the mass flow of motive steam extracted from the turbine to power the TVC; 2 - the user specifices a percentage of motive steam extracted from the turbine (to power the TVC) relative to the nominal entering the high pressure turbine.
TVC_Hc_Super	kJ/kg	Specific enthalpy of the superheated steam discharged (compressed) by the TVC
TVC_Hc_Vap	kJ/kg	Specific enthalpy of the discharged ("c"ompressed) vapor by the TVC
TVC_Hcw_deSuper	kJ/kg	Specific enthalpy of the cooling water entering the desuperheater
TVC_Hs_deSuper	kJ/kg	Specific enthalpy of the superheated steam after passing throught the desuperheater
TVC_Mc_1	kg/s	Mass flow rate of steam discharged (compressed) by the 1st ejector of the TVC system (in case only a 1stage ejector system is considered for the TVC, or the first ejector in case a 2 stage ejector systems is required to be considered)
TVC_Mc_2	kg/s	Mass flow rate of steam discharged (compressed) by the 2nd ejector of the TVC system (when using a 2 stage ejector system)
TVC_Mc_Total	kg/s	Total mass flow rate of steam discharged (compressed) by the TVC (sum of TVC_Mm_Total +TVC_Me_1+TVC_Me_2). It does not include the TVC_Mcw_deSuper
TVC_Mcw_deSuper	kg/s	Mass of distillate used to desuperheat the steam discharged by the TVC
TVC_Me_1	kg/s	Mass of vapor from the last effect entrained into the TVC in case only a 1stage ejector system is considered for the TVC, or the first ejector in case a 2 stage ejector systems is required to be considered
TVC_Me_2	kg/s	Mass of vapor from the last effect entrained into the TVC when using a 2 stage ejector system
TVC_Me_air_equiv	kg/s	Mass flow of air equivalent entrained gases into the TVC (input to this subroutine)
TVC_Me_air_equiv	kg/s	Mass flow rate of air equivalent vapor entrained into the TVC
TVC_Me_cf_Vap	-	Gas Molecular Weight Correction for Steam. The 0.81conversion factor between Air and Steam comes from experimental tables published in the book "Standards for Steam Jet Vacuum systems" from the Heat Exchange Institute (2000), 5th edition. It is a correction factor for Molecular Weight Entrainment Ratio, accounting that Steam has a molecular weight of 18kg/kmol. See figure figure 16, page 31from the mentioned HEI book, or freely on the second table, page 9, from "JRG/TC Models for Pumping gases" made by "Northeast Controls", or page 7 from "Jet Pumping Technical data, pumping gases", from Tyco.
TVC_Mm	kg/s	Motive steam mass flow rate used in the TVC (input variable into this module)
TVC_Mm_1	kg/s	Mass flow rate of Motive steam used to power the TVC in case only a 1stage ejector system is considered for the TVC, or the first ejector in case a 2 stage ejector systems is required to be considered (what will enter the MED plant with a TVC configuration will be Ms = TVC_Mc_Total +TVC_Mcw_deSuper)
TVC_Mm_2	kg/s	Mass flow rate of Motive steam used to power the TVC (what will enter the MED plant with a TVC configuration will be Ms = TVC_Mc_Total +TVC_Mcw_deSuper)
TVC_Mm_des	kg/s	Mass flow of motive steam extracted from the turbine to power the TVC at design (option 1on the TVC_ext_flag)
TVC_Mm_Total	kg/s	Total mass flow rate of Motive steam used to power all the ejectors used to feed low pressure steam into the first effect (depending on the TVC model used, 1or 2 ejectors may be considered for the "TVC" system: TVC_Mm_Total = TVC_Mm_1+TVC_Mm_2).
TVC_Model	-	Flag indicating the Ejector model to be used. The options are: 1-Empirical model using ratios obtained from Koerting; 2-El Dessouky empirical model adapted from Power 1994 (ref 1); 3-El Dessouky semi-empiric model (ref 2) >>> ref 1: El-Dessouky, H.T., Modelling and Simulation of Thermal Vapor Compression Desalination Process, Proceedings of International Atomic Energy Agency, Symposium on Desalination of Seawater with Nuclear Energy, Taujon, Korea, 26-30 May (1997); ref 2: El-Dessouky, H.T., Ettouney, H.M., Alatiqi, I., and Al-Nuwaibit, G., Steam jet ejectors: Modeling and analysis, Chem. Eng. Proc, in print, 2001)
TVC_Pc	Pa	Compression pressure of the steam leaving the TVC (input variable into this module)
TVC_Pc_1	Pa	Pressure of the steam discharged by the TVC in case only a 1stage ejector system is considered for the TVC, or the first ejector in case a 2 stage ejector systems is required to be considered (Assuming saturated conditions on the outlet, which in reality wont happen, as there is no intercondenser just after the TVC because. The intercondenser could be the 1st MED effect but as a security measure the steam is desuperheated before entering the 1st effect, lowring its temperature, to avoid hard scalling of CaSO4 - Calcium sulfate).
TVC_Pc_2	Pa	Pressure of the steam discharged by the TVC when using a 2 stage ejector system (Assuming saturated conditions on the outlet, which in reality wont happen, as there is no intercondenser just after the TVC because. The intercondenser could be the 1st MED effect but as a security measure the steam is desuperheated before entering the 1st effect, lowring its temperature, to avoid hard scalling of CaSO4 - Calcium sulfate).
TVC_Pc_mem	Pa	Memory to verify if the calculation of TVC_Pc_1reached an infinite loop.
TVC_PCF	-	Motive steam pressure correction factor (from El Dessouky's formula, page 59 Fundamentals of Salt Water desalination).
TVC_pct_steam_ext		Ratio of steam extracted from an intermediate point from the turbines of the rankine cycle, relative to the total mass of steam that enters the high pressure turbine at design conditions
TVC_Pe	Pa	Entrainement pressure used in the TVC (input variable into this module)
TVC_Pe_1	Pa	Pressure of the vapor entrained by the TVC from the last effect of the MED plant, in case only a 1stage ejector system is considered for the TVC (being the first ejector in case a 2 stage ejector systems is required to be considered).
TVC_Pe_2	Pa	Pressure of the vapor entrained by the TVC from the 1st TVC ejector (in case a 2 stage TVC ejector system is considered, which is dependent on the type of ejector model selected by the user).
TVC_Pm	Pa	Motive steam pressure used in the TVC (input variable into this module)
TVC_Ra_1	-	Ratio between mass of motive steam used in the TVC per unit mass of entrained vapor in case only a 1stage ejector system is considered for the TVC, or the first ejector in case a 2 stage ejector systems is required to be considered (from El Dessouky's formula, page 59 Fundamentals of Salt Water desalination).
TVC_Ra_2	-	Ratio between mass of motive steam used in the TVC per unit mass of entrained vapor when using a 2 stage ejector system (from El Dessouky's formula, page 59 Fundamentals of Salt Water desalination).
TVC_Size	inches	Size of the ejector to cope with the pretended TVC_Pe, TVC_Pc, TVC_Pm and TVC_Mm (output from this subroutine). Only referent to the TVC
TVC_Strategy	-	Flag indicating how the TVC is to be dimensioned considering the compression ratio or a fixed Ts_sat input (it will force a specific Pc and a compression ratio)). Values: 1- TVC uses the lowest possible commpression ratio; 2 - Ts_sat is a user defined (defines the saturated pressure leaving the TVC and compression ratio); 3 - TVC uses the highest possible compression ratio.
TVC_Tc_super	ºC	Temperature of the superheated steam discharged by the TVC.
TVC_TCF_1	-	Entrained vapor temperature correction factor in case only a 1stage ejector system is considered for the TVC, or the first ejector in case a 2 stage ejector systems is required to be considered (from El Dessouky's formula, page 59 Fundamentals of Salt Water desalination).
TVC_TCF_2	-	Entrained vapor temperature correction factor when using a 2 stage ejector system (from El Dessouky's formula, page 59 Fundamentals of Salt Water desalination).

TVC_Te_1	ºC	Temperature of the entrained vapor into the TVC system (in case only a 1stage ejector system is considered for the TVC, or the first ejector in case a 2 stage ejector systems is required to be considered)
TVC_Te_2	ºC	Temperature of the entrained vapor into the 2nd ejector of the TVC system (if a 2 stage TVC ejector system is considered, depending on the ejector model selected, which is chosen by the user).
TVC_Te_cf_Vap	-	Temperature correction factor applicable to the vapor being entrained into the TVC (the ratios obtained from the industry imply the assumption of gases being entrained at 70F, and consisting of dry air)
TVC_Tm_sat	ºC	Theoretical saturated temperature of the motive steam powering the TVC >>and not the MED<< (in practice it will be higher as it will be superheated).
TVC_Ts_deSuper	ºC	Temperature of the compressed steam by the TVC after passing through the desuperheater (it will still be slightly superheated).
TVC_Ts_Super_ratio	-	Ratio between "the saturated temperature" (corresponding to the discharge pressure of the TVC) and "the temperature of the superheated steam actually leaving the TVC" (which will be at the same pressure than the saturated Ts). Basically the steam leaving the TVC will be superheated, and this variable indicates the ratio of delta T between this saturated temperature and the superheated temperature: how higher in % is the Temp superheated compared to the saturated temperature.
TVC_Wr	-	Entrainment Ratios used in TVC (Suction flow rate(air equivalent) / Motive flow rate (steam))
TVC_Wr_1	-	Entrainment Ratios used in TVC (Suction flow rate(air equivalent) / Motive flow rate (steam)), in case only a 1stage ejector system is considered for the TVC, or the first ejector in case a 2 stage ejector systems is required to be considered
TVC_Wr_2	-	Entrainment Ratios used in TVC (Suction flow rate(air equivalent) / Motive flow rate (steam)), when using a 2 stage ejector system
Tvn	ºC	Temperature of Vapor in the last effect (input cannot be an array)
Tvn_ratio	ºC	Ratio that can increase or decrease the temperature of the vapor in the last effect, to match the allowed entrainment pressures available in the database used to calculate the ejection of NCG.
U	kW/m2.C	Overall heat transfer coefficient in each effect
U_reduction	-	Reduction ratio of the overall heat transfer coefficient that is assumed to occur between adjacent effects
U1	kW/m2.ºC	Overall Heat transfer coeficient at the first effect of the MED plant
Udc	kW/m2.C	Overall heat transfer coefficient at the down condenser
V	kg/s	Total Mass of Vapour produced inside the effect. Evaporation +flashing of distillate and brine from previous effect + flashing of condensate from preheater from previous effect
V_b_flash	kg/s	Mass flow of Vapour produced inside the effect from the flashing process ocurring when the brine enters it.
V_d_flash	kg/s	Mass flow of Vapour produced inside the effect through flashing when distillate (not the vapour) moves between effects.
V_d_flash_cond	kg/s	Mass flow of Vapor produced inside the down condenser through flashing when the distillate (not the vapour) entered it.
V_d_flash_Ej_1	kg/s	Mass flow of Vapour produced through flashing when condensate from the 1st NCG ejector enters the distillate box. If a MED low temperature is used this flashing process takes place inside the distillate box of effect number (n_ph_NCG +1); if a TVC configuration is used this flashing process takes place in the 3rd effect.
V_d_flash_Ej_2	kg/s	Mass flow of Vapour produced through flashing when condensate from the 2nd NCG ejector enters the distillate box. If a MED low temperature is used this flashing process takes place inside the distillate box of effect number (n_ph_NCG +1); if a TVC configuration is used this flashing process takes place in the 2nd effect.
V_eph	kg/s	Mass flow of Vapor produced by evaporation inside the effect, that will be used for external preheating of the feedwater passing through that effects related preheater: will preheat SUM(F(1:i)). This vapor is assumed to be condensed by the feedwater preheater and sent to the distillate box of the next effect, where theoretically the distillate produced inside the HTX will be at the same temperature than V_eph.
V_evap	kg/s	Mass flow of Vapor produced by evaporation (not flashing) inside the effect.
V_evap_remain	kg/s	Mass flow of Vapor produced by evaporation (not flashing) inside the effect that >>REMAINS<< after part of this vapor is assumed to be used for external preheating: Q_eph(i).
V_f_flash	kg/s	Mass flow of Vapor produced by flash when the feedwater enters each effect (this variable is actually only used when CT(9,10) MED-FF as feedwater is actually the brine from the last effect; and when CT(7,8) this variable has a value of zero).
Wr_avg_rate	-	Average rate of change of the limit that defines the maximum Wr possible for ejectors with sizes between Size_Lip_C(1) and Size_Lip_C(2) (basically the left extremes with higher Pc from the two D curves). If the pretended Mm_0 returns a value of Wr too low for the Pc_0, then a new Pc should be assumed
Wr_limit	-	Lowest possible entrainment ratio in the calculated linear interpolated D curve with the selected Pc_0. If (for the selected Pc_0 in the D curve) the selected Mm_0 is too high or Me_0 too low, Wr will be lower than this limit, and a lower Pc has to be assumed if maintaining the same Mm_0 or Me_0 (depending if calculations will be for the TVC or the 1st NCG ejector, one of these mass flows will be the input and the other one the output).
Wr_Lip_B	-	Entrainment Ratios obtained from the linear interpolated C curves (in fact this ratio was not realy obtained directly from linear interpolation :P but is the ratio between Me_Lip_B and Mm_Lip_B. It was named "_Lip_" not to be confused with user defined inputs etc.
Wr_Lip_C	-	Entrainment Ratios obtained from the linear interpolated D curves (in fact this ratio was not realy obtained directly from linear interpolation :P but is the ratio between Me_Lip_C and Mm_Lip_C. It was named "_Lip_" not to be confused with user defined inputs etc.
Wr_Lip_D	-	Entrainment Ratios obtained from the linear interpolated E curve (in fact this ratio was not realy obtained directly from linear interpolation :P but is the ratio between Me_Lip_D and Mm_Lip_D. It was named "_Lip_" not to be confused with user defined inputs etc.
Xb	wt%	Salinity concentration of the brine produced in each effect by evaporation
Xb_out	wt%	Salinity concentration of the brine leaving each effect (balance between salinity of brine formed by evaporation in the current effect and brine from the previous effects)
Xb1	wt%	Salinity concentration predefined to be assumed when starting iterations to calculate mass flow rate of feedwater needed for the 1st effect (input cannot be an array)
Xb1_mem	wt%	Mememory used to verify if no infinite loops occur when Xb(1) is being adjusted with the Forward Feed configuration. If wrong inputs are used, there is the possibility that one part of the code tries to increase the Xb(1) value, and then another part of the code tries to decrease it, creating an infinite loop.
Xbn	wt%	Brine maximum allowed salinity
Xbn_max	wt%	Maximum allowed Salinity concentration of the brine produced in the last effect
Xf	wt%	Salinity concentration of the feedwater entering each effect
Xf_f_flash_remain	wt%	Salinity concentration of the feedwater that remains after it flashes when entering the effect (this variable is actually only used when CT(9,10) MED-FF as feedwater is actually the brine from the last effect; and when CT(7,8) this variable has a value of zero).
Xsw	wt%	Salinity concentration of the seawater entering the MED plant